Molecular Characterization of Genes Involved in Hearing Loss

……..

Dissertation zur Erlangung des
naturwissenschaftlichen Doktorgrades
der Julius-Maximilians-Universität Würzburg

Submitted by

Barbara C. Vona

Born in Edmonton, Alberta, Canada

Würzburg, May 2014

Submitted on:

Members of the *Promotionskommission*:

Dean: Univ.-Prof. Dr. rer. nat. Markus Engstler

Primary Supervisor: Univ.-Prof. Dr. med. Thomas Haaf

Secondary Supervisor: Prof. Dr. rer. nat. Dr. h.c. Manfred Schartl

Date of Public Defense:

Date Dr. rer. nat. Awarded:

The presented work was completed from January 2011 to May 2014 in the Department of Human Genetics at the University of Würzburg under the supervision of Univ.-Prof. Dr. med. Thomas Haaf.

I hereby declare that I have written this dissertation independently and exclusively using the specified resources.

The dissertation has not been previously submitted, either in the same or in a similar form in another examination.

The work has not been previously acquired for another academic degree.

Würzburg, May 2014 _____

Barbara Vona

Table of Contents

1. Summary

The auditory system is an exquisitely complex sensory organ dependent upon the synchronization of numerous processes for proper function. The molecular characterization of hereditary hearing loss is complicated by extreme genetic heterogeneity, wherein hundreds of genes dispersed genome-wide play a central and irreplaceable role in normal hearing function. The present study explores this area on a genome-wide and single gene basis for the detection of genetic mutations playing critical roles in human hearing.

This work initiated with a high resolution SNP array study involving 109 individuals. A 6.9 Mb heterozygous deletion on chromosome 4q35.1q35.2 was identified in a syndromic patient that was in agreement with a chromosome 4q deletion syndrome diagnosis. A 99.9 kb heterozygous deletion of exons 58-64 in *USH2A* was identified in one patient. Two homozygous deletions and five heterozygous deletions in *STRC* (DFNB16) were also detected. The homozygous deletions alone were enough to resolve the hearing impairment in the two patients. A Sanger sequencing assay was developed to exclude a pseudogene with a high percentage sequence identity to *STRC* from the analysis, which further solved three of the six heterozygous deletion patients with the hemizygous, *in silico* predicted pathogenic mutations c.2726A>T (p.H909L), c.4918C>T (p.L1640F), and c.4402C>T (p.R1468X). A single patient who was copy neutral for *STRC* and without pathogenic copy number variations had compound heterozygous mutations [c. 2303_2313+1del12 (p.G768Vfs*77) and c.5125A>G (p.T1709A)] in *STRC*. It has been shown that *STRC* has been previously underestimated as a hearing loss gene. One additional patient is described who does not have pathogenic copy number variation but is the only affected member of his family having hearing loss with a paternally segregating translocation t(10;15)(q26.13;q21.1).

Twenty-four patients without chromosomal aberrations and the above described patient with an *USH2A* heterozygous deletion were subjected to a targeted hearing loss gene next generation sequencing panel consisting of either 80 or 129 hearing-relevant genes. The patient having the *USH2A* heterozygous deletion also disclosed a second mutation in this gene [c.2276G>T (p.C759F)]. This compound heterozygous mutation is the most likely cause of hearing loss in this patient. Nine mutations in genes conferring autosomal dominant hearing loss [*ACTG1* (DFNA20/26); *CCDC50* (DFNA44); *EYA4* (DFNA10); *GRHL2* (DFNA28); *MYH14* (DFNA4A); *MYO6* (DFNA22); *TCF21* and twice in *MYO1A* (DFNA48)] and four genes causing autosomal recessive hearing loss were detected [*GJB2* (DFNB1A); *MYO7A* (DFNB2); *MYO15A* (DFNB3),

and *USH2A*]. Nine normal hearing controls were also included. Statistical significance was achieved comparing controls and patients that revealed an excess of mutations in the hearing loss patients compared to the control group. The family with the *GRHL2* c.1258-1G>A mutation is only the second family published worldwide with a mutation described in this gene to date, supporting the initial claim of this gene causing DFNA28 hearing loss. Audiogram analysis of five affected family members uncovered the progressive nature of DFNA28 hearing impairment. Regression analysis predicted the annual threshold deterioration in each of the five family members with multiple audiograms available over a number of years.

2. Zusammenfassung

Das Gehör als komplexes Sinnesorgan ist für eine einwandfreie Funktion abhängig von der Synchronisation zahlreicher Prozesse. Durch die extreme genetische Heterogenität wird die molekulare Charakterisierung einer erblich bedingten Schwerhörigkeit erschwert, da hunderte genomweit verteilter Gene eine zentrale und unersetzliche Rolle beim Hören spielen. Die vorliegende Studie untersucht dieses Forschungsgebiet auf genomweiter Ebene und auf der Basis von Einzelgenen, um genetische Mutationen zu ermitteln, die eine entscheidende Rolle bei der menschlichen auditiven Wahrnehmung besitzen.

Diese Arbeit beginnt mit einer Studie an 109 Personen unter Zuhilfenahme von hochauflösenden SNP-Arrays. In dieser Studie wurde eine 6,9 Mb heterozygote Deletion auf Chromosom 4q35.1q35.2 bei einem syndromalen Patienten identifiziert, die eine Übereinstimmung mit einem Chromosom 4q-Deletionssyndrom aufwies. Bei einem weiteren Patienten wurde eine 99,9 kb heterozygote Deletion der Exons 58-64 in *USH2A* nachgewiesen. Zwei homozygote Deletionen und fünf heterozygote Deletionen in *STRC* (DFNB16) wurden ebenfalls detektiert. Die homozygoten Deletionen waren ausreichend, um die Schwerhörigkeit bei beiden Patienten zu klären. Ein Sanger-Sequenzierungs-Assay wurde entwickelt, um ein Pseudogen mit einer hohen prozentualen Sequenzidentität zu *STRC* von der Analyse auszuschließen. Dadurch konnten drei der sechs heterozygoten Deletionspatienten mit hemizygot *in silico* vorhergesagten pathogenen Mutationen, c.2726A>T (p.H909L), c.4918 C>T (p.L1640F) und c.4402C>T (p.R1468X), aufgeklärt werden. Ein Patient, der eine kopieneutrale *STRC* Variation und keine pathogenen Kopienzahlvariationen besaß, zeigte eine compound heterozygote Mutation [c.2303_2313+1del12 (p.G768Vfs*77) und c.5125A>G (p.T1709A)] in *STRC*. Es wurde gezeigt, daß die Beurteilung von *STRC* als Hörstörungsgen bisher unterschätzt wurde. Zusätzlich wird ein Patient beschrieben, der keine pathogenen Kopienzahlvariationen aufwies, aber das einzige Familienmitglied mit einer Schwerhörigkeit und einer paternalen segregierten Translokation t(10;15)(q26.13;q21.1) war.

Vierundzwanzig Patienten ohne Chromosomenstörungen und der oben beschriebene Patient mit einer *USH2A* heterozygoten Deletion wurden mit einem Next Generation Sequencing Panel bestehend aus entweder 80 oder 129 für das Hören relevanter Gene untersucht. Der Patient mit einer *USH2A* heterozygoten Deletion zeigte eine zweite Mutation in diesem Gen [c.2276G>T (p.C759F)]. Diese compound heterozygote Mutation ist die wahrscheinlichste Ursache für die

Schwerhörigkeit des Patienten. Neun Mutationen in Genen, die zu einem autosomal dominanten Hörverlust führen [*ACTG1* (DFNA20/26); *CCDC50* (DFNA44); *EYA4* (DFNA10); *GRHL2* (DFNA28); *MYH14* (DFNA4A); *MYO6* (DFNA22); *TCF21*], sowie zwei *MYO1A* (DFNA48) Mutationen und Mutationen in vier weiteren Genen, verantwortlich für autosomal rezessive Schwerhörigkeit [*GJB2* (DFNB1A); *MYO7A* (DFNB2); *MYO15A* (DFNB3) und *USH2A*], konnten identifiziert werden. Neun normal hörende Kontrollen waren ebenfalls in diese Studie einbezogen worden. Durch einen Vergleich der Kontrollen mit den Patienten konnte eine statistische Signifikanz erreicht werden, die einen Überschuss an Mutationen bei der Patientengruppe gegenüber der Kontrollgruppe aufzeigte. Die Familie mit einer *GRHL2* c.1258-1G>A Mutation ist die erst zweite Familie weltweit, die mit einer Mutation in diesem Gen publiziert worden ist. Dies unterstützt die initiale Behauptung, dass dieses Gen für eine DFNA28 Schwerhörigkeit verantwortlich ist. Die Audiogrammanalyse von fünf der betroffenen Familienmitglieder lässt eine voranschreitende Natur der DFNA28 Hörschädigung erkennen. Eine jährliche Verschlechterung der Hörschwelle bei jedem der fünf Familienmitglieder konnte eine Regressionsanalyse anhand von Audiogrammen, die über eine Anzahl von Jahren zur Verfügung standen, vorhersagen.

3. Introduction

3.1 Global burden of hearing loss

According to the World Health Organization (WHO), hearing loss (HL) is listed as one of the top three most common causes of disability and among the three most prevalent conditions affecting the global population [1]. In a worldwide survey of six major and 14 sub-regions, the WHO estimated that as of 2004, there were approximately 360.8 million individuals with mild HL (defined by audiometric thresholds in the better ear between 26-40 decibels (dB)), and 275.7 million individuals with moderate to profound HL (with hearing thresholds in the better ear greater than 40 dB) totaling 636.5 million people affected with mild to profound HL [1]. As the most recent WHO report surveying the global impact of HL is ten years old, these numbers will certainly increase as surveying methodologies improve and cohesive selection rationale are applied across individual epidemiological studies. A German survey that conservatively excluded children under the age of 14 and adhered to the WHO audiometric threshold for defining HL beginning at 26 dB for epidemiological inclusion, which is a higher threshold than customarily accepted, disclosed there are over 13 million people living in Germany with HL fitting these criteria, with many more under recognized or unaccounted for individuals [2]. These troubling statistics are expected to increase in coming years reflecting an aging and increasing world population, with a growing proportion of the younger generation leisurely exposing themselves to prolonged excessive sound in the form of mp3s and iPods.

While there is no question that those living with even mild HL can face personal disadvantages throughout everyday life, the intensified effects of HL can be observed on a macroscale. Non-communicable diseases including HL have a profound impact on healthcare expense, prolonged disability, and national gross domestic product (GDP) [3]. For instance, in 2005, Australia had reported an annual loss of earnings equivalent to 1.4% of GDP representing $11.75 billion (Australian dollars), with the largest expense being reported loss in productivity [4]. When further broken down, this means that per annum, each Australian with HL paid $3,314, or every Australian, regardless of hearing status, paid $578 [4]. This figure does not account for the additional $11.3 billion required for disease burden with disability-adjusted life years [4]. Such tremendous financial hardship is often compounded by other negative consequences not only affecting employment with reduced work force and early retirement due to HL, but also introduces potential co-morbidities such as depressive symptoms, decreased quality of life, social isolation, reduced independence, and increased risk of mortality [5].

Although the precise global impact of HL is presently unclear, HL is undoubtedly a major public health concern that deserves considerable attention [6].

3.2 Etiologies of hearing loss

HL is one of the most common birth defects in the developed world stemming from both environmental and genetic components [7]. While the environmental spectrum includes premature birth, infection, physical trauma, and pharmacologic ototoxicity, these contribute to an etiology of less than 50 percent of HL cases [8]. The genetic contribution, including both syndromic and non-syndromic forms of HL, account for between 50-60 percent of cases, yielding an approximate incidence rate of one to two per one thousand newborns with bilateral permanent sensorineural HL at the time of newborn hearing screening [8]. Figure 1 depicts a schematic overview of the different causes of HL with the approximate percentage comprising each major category of HL.

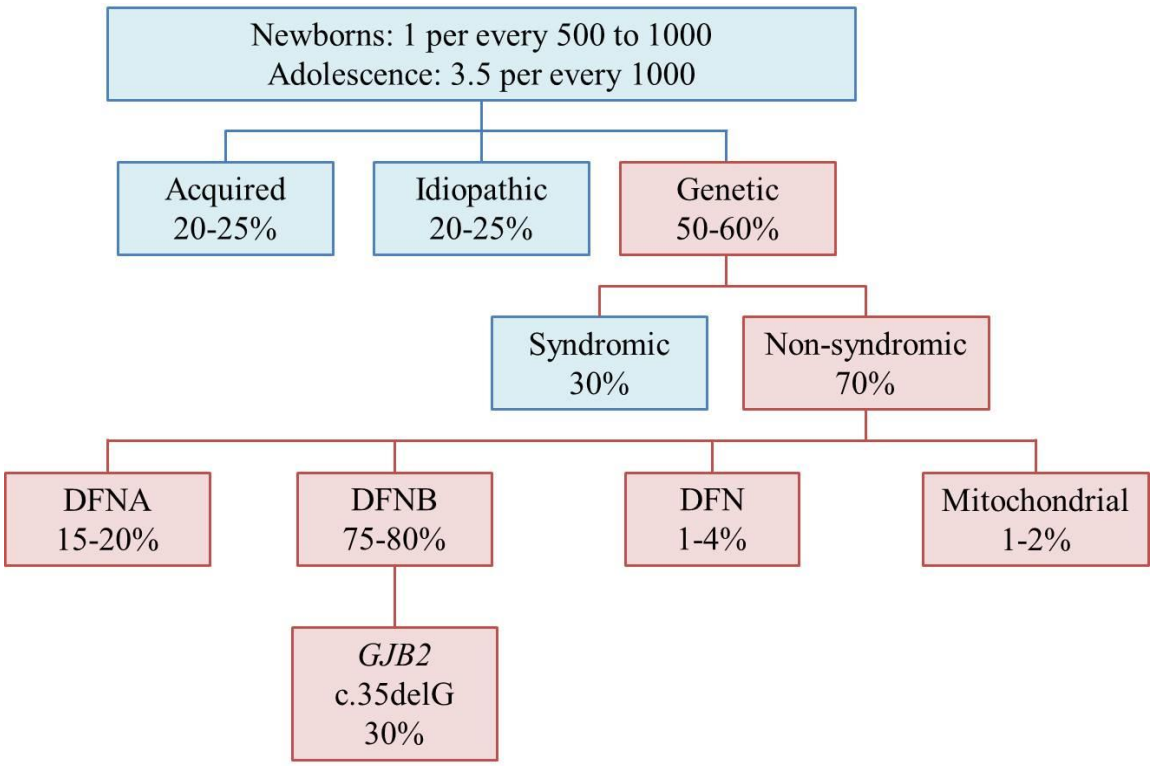

Figure 1. Classifications of hearing loss. A schematic diagram illustrates the different forms of hearing loss with the approximate percentages of occurrence. The primary focus of this study is highlighted in the red section. DFN and *GJB2* descriptions are included in sections 3.2.2.1 and 3.2.2.4.1, respectively.

3.2.1 Syndromic hearing loss

Syndromic hearing loss (SHL) is the presence of HL in the context of one or more secondary clinical features, usually involving at least one additional organ system. In some syndromes, HL is a mild or irregular clinical feature of the larger phenotypic picture, while in others, HL is a consistent, predictable and clinically significant feature [9]. Some SHL cases are erroneously assumed as non-syndromic because of very mild secondary, missed, or overlooked phenotypes. Furthermore, the development of additional phenotypes may occur long after HL is diagnosed [10]. All types of autosomal, X-linked, and mitochondrial mutation inheritance are possible, as well as the possibility of arising sporadically or *de novo*. There are between 300 and 400 known syndromes with HL in combination with other clinical indications [9]. Syndromes that include HL comprise approximately 30% of all HL with a genetic etiology. Twenty examples of syndromes with brief information about inheritance and phenotypes associated with HL are listed in the following Table 1.

Syndrome name	Gene(s), chr bands	Inheritance and additional phenotypes	References
Alport	*COL4A3*, *COL4A4*, *COL4A5*	X-linked (*COL4A5*), autosomal dominant and recessive; renal failure, hematuria, ocular lesions	[11]
Alström	*ALMS1*	Autosomal recessive; juvenile blindness, cardiomyopathy, endocrinology disorders, and metabolic dysfunction	[12]
Brachio-Oto-Renal	*EYA1*, *SIX1*	Autosomal dominant; auricular malformations, brachial arch closure defects, renal abnormalities	[13]
CHARGE	*CHD7*	Autosomal dominant; Colobomba, Heart detects, Atresia of the choanae, Retarded growth and development, Genital hypoplasia and Ear anomalies and/or deafness	[13]
DiGeorge/ Velocardiofacial	*TBX1*	Autosomal dominant; chronic otitis media, hyperactive behaviour, middle and inner ear malformations, craniofacial anomalies (including cleft palate), cardiovascular defects, thymus hypoplasia, and learning disabilities	[14]
Down	Trisomy 21	Sporadic; mental retardation, malformations of the heart and gastrointestinal tract, increased risk of leukemia	[15,16]
Ehlers-Danlos	*FKBP14*	Autosomal recessive; progressive kyphoscoliosis, myopathy, joint hypermobility, and hyperplastic skin	[17]
Friedreich ataxia	*FXN*	Autosomal dominant; ataxia of gait, limb weakness, loss of tendon reflexes, nystagmus, kyphoscoliosis, cardiac complications are a frequent cause of mortality	[18,19]
Goldenhar/ Hemifacial microsomia	14q32; multifactorial	Autosomal recessive/sporadic; craniofacial anomalies (facial asymmetry, mandibular hypoplasia, preauricular tags), with vertebral, renal, cardiovascular and central nervous system defects	[20]
Hunter-MacDonald	Unknown	Autosomal dominant; short stature, skeletal dysplasia, cardiac abnormalities, pectus carinatum, cranial nerve palsies, hand and foot abnormalities	[21]
Hurler	*IDUA*	Autosomal recessive; coarse facial features, corneal clouding, mental retardation, mucopolysaccharidosis type IH	[22]
Jarvell and Lange-Nielsen	*KCNE1*, *KCNQ1*	Autosomal recessive; prolonged QT intervals often causing syncope, high risk of sudden death	[23]
Neurofibromatosis II	*NF2*	Autosomal dominant; vestibular schwannoma with tinnitus, balance dysfunction, facial weakness, and risk of early death from brainstem compression	[24]

Noonan	*BRAF*, *KRAS*, *NRAS*, *PTPN11*, *RAF1*, *SOS1*	Autosomal dominant; short stature, congenital heart defects, facial dysmorphology, broad thorax/pectus carinatum, undescended testes, recurrent otitis media	[25]
Norrie	*NDP*	X-linked; eye disorders, mental retardation	[26]
Pendred	*SLC26A4*	Autosomal recessive; euthyroid goiter, vestibular aqueduct enlargement, absence of interscalar septum between upper and middle cochlear turns	[13]
Pfeiffer	*FGFR1*, *FGFR2*	Autosomal dominant; craniosynostosis with hand and foot abnormalities	[27]
Stickler	*COL2A1*, *COL9A1*, *COL9A2*, *COL11A1*, *COL11A2*	Autosomal dominant and recessive; retinal detachment, myopia, cataract, midfacial underdevelopment (as part of Pierre Robin sequence)	[28]
Usher	*CDH23*, *CIB2*, *GPR98*, *HARS*, *MYO7A*, *PCDH15*, *PDZD7*, *SANS*, *USH1C*, *USH2A*, *USH3A*	Autosomal recessive; retinitis pigmentosa; there are three types arranged according to severity and onset of HL and retinal degeneration	[26,29-32]
Waardenburg	*EDN3*, *EDNRB*, *MITF*, *PAX3*, *SNAI2*, *SOX10*	Autosomal dominant; white forelock, heterochromia of iris, congenital leukoderma; there are four different types (I-IV) characterized by severity; HL can be unilateral	[13]

Table 1. Syndromes commonly associated with hearing loss. Chr is the abbreviation for chromosome.

3.2.2 Non-syndromic hearing loss

3.2.2.1 The history of non-syndromic deafness locus mapping and identification

Identification of the genes involved in non-syndromic hearing loss (NSHL) contributes to a larger understanding of the processing of auditory functions. Historically, linkage analysis involving large multigenerational families was the only way to map statistically significant loci to a physical or genetic position with the goal of subsequently identifying a genetic variant responsible for the described HL. This led to the annotation of deafness (DFN) loci that are numbered according to the order in which they were mapped, with several loci merging into one locus over a number of years as the causative gene is eventually disclosed. As the search for new HL genes is on-going, it is not yet possible to determine the exact number of genes that are involved in proper hearing function; however, estimates of the total number of genes with important hearing function puts this number around 1% of coding genes in the human genome or just over 200 genes [33]. As depicted in Figure 1, it is estimated that autosomal dominant hearing

loss (ADHL: represented by DFNA) comprises 15-20%, autosomal recessive hearing loss (ARHL: represented by DFNB) characterizes 75-80%, X-linked (DFN) constitutes 1-4%, and mutations in the mitochondria represent 1-2% of all NSHL [34]. To date, there are 48, 28 and 3 DFNB, DFNA and DFN loci with 52, 31 and 4 genes identified, respectively (Table 2), including a fraction of these genes exhibiting both dominant and recessive modes of inheritance. Many loci are mapped and numbered without a causative gene presently identified. The scope of this dissertation extends to the analysis of autosomal and X chromosomal mutational fallout in HL patients.

Recessive Hearing Loss		Dominant Hearing Loss		X-linked Hearing Loss	
DFNB	Gene	DFNA	Gene	DFN	Gene
DFNB1A	*GJB2*	DFNA1	*DIAPH1*	DFN2	*PRPS1*
DFNB1B	*GJB6*	DFNA2A	*KCNQ4*	DFN3	*POU3F4*
DFNB2	*MYO7A*	DFNA2B	*GJB3*	DFN6	*SMPX*
DFNB3	*MYO15A*	DFNA3A	*GJB2*	-	*COL4A6*
DFNB5	*SLC26A4*	DFNA3B	*GJB6*		
DFNB6	*TMIE*	DFNA4	*MYH4/CEACAM16*		
DFNB7/11	*TMC1*	DFNA5	*DFNA5*		
DFNB8/10	*TMPRSS3*	DFNA6/14/38	*WFS1*		
DFNB9	*OTOF*	DFNA8/12	*TECTA*		
DFNB12	*CDH23*	DFNA9	*COCH*		
DFNB15/72/95	*GIPC3*	DFNA10	*EYA4*		
DFNB16	*STRC*	DFNA11	*MYO7A*		
DFNB18	*USH1C*	DFNA13	*COL11A2*		
DFNB21	*TECTA*	DFNA15	*POU4F3*		
DFNB22	*OTOA*	DFNA17	*MYH9*		
DFNB23	*PCDH15*	DFNA20/26	*ACTG1*		
DFNB24	*RDX*	DFNA22	*MYO6*		
DFNB25	*GRXCR1*	DFNA23	*SIX1*		
DFNB28	*TRIOBP*	DFNA25	*SLC17A8*		
DFNB29	*CLDN14*	DFNA28	*GRHL2*		
DFNB30	*MYO3A*	DFNA36	*TMC1*		
DFNB31	*WHRN*	DFNA41	*P2RX2*		
DFNB35	*ESRRB*	DFNA44	*CCDC50*		
DFNB36	*ESPN*	DFNA48	*MYO1A*		
DFNB37	*MYO6*	DFNA50	*MIRN96*		
DFNB39	*HGF*	DFNA51	*TJP2*		
DFNB42	*ILDR1*	DFNA56	*TNC*		
DFNB44	*ADCY1*	DFNA64	*DIABLO*		
DFNB48	*CIB2*	-	*CRYM*		
DFNB49	*MARVELD2*	-	*TBC1D24*		
DFNB49	*BDP1*				
DFNB53	*COL11A2*				
DFNB59	*PJVK*				
DFNB61	*SLC26A5*				
DFNB63	*LRTOMT*				
DFNB66/67	*LHFPL5*				
DFNB70	*PNPT1*				
DFNB74	*MSRB3*				
DFNB77	*LOXHD1*				
DFNB79	*TPRN*				
DFNB82	*GPSM2*				
DFNB84	*PTPRQ*				
DFNB84	*OTOGL*				
DFNB86	*TBC1D24*				
DFNB88	*ELMOD3*				
DFNB89	*KARS*				
DFNB91	*GJB3*				
DFNB93	*CABP2*				
DFNB98	*TSPEAR*				
DFNB101	*GRXCR2*				
DFNB102	*CLIC5*				
-	*SERPINB6*				
-	*OTOG*				
	EPS8				

Table 2. Non-syndromic hearing loss gene list. A current list of NSHL loci with causative genes obtained from the Hereditary Hearing Loss Homepage.

3.2.2.2 Pedigree analysis and family history

Pedigree analysis, wherein the hearing and clinical statuses of multiple generations of family members are disclosed, provides a critical source of information for genetic analysis. HL is described as a Mendelian, or single gene, trait that is caused by inheritance of a mutation(s) in a single gene that can be autosomal dominant, autosomal recessive or X-linked. Intrafamilial variability, variable expressivity, and incomplete penetrance can occasionally describe specific genes or mutations within particular genes, but is atypical for NSHL. For example, the homozygous mutations c.35delG, c.167delT, and c.235delC in *GJB2* have demonstrated complete penetrance with variable expressivity [35], and mutations in *MYO1A* are believed to demonstrate reduced penetrance and/or expressivity explaining normal hearing in individuals with damaging mutations [36].

Autosomal dominant. In an autosomal dominant disorder, an affected individual is heterozygous for the disease allele and has a 50% chance of having children with the same allelic configuration. A pedigree from a family affected with autosomal dominant HL would most likely show multiple generations affected with a similar type of HL, with the exception of a founder, *de novo* mutation, or a family with few members. Mutational segregation analysis would require all clinically affected individuals to have the mutation and clinically healthy individuals to be mutation negative.

Autosomal recessive. Autosomal recessive inheritance is especially important in HL, since between 75-80% of HL is described as recessive. Each affected individual is either homozygous or compound heterozygous for mutations in a single gene and unaffected individuals can either be homozygous wild type or heterozygous carriers. The children of heterozygous carrier parents have a 25% chance of inheriting a combination of alleles conducive to a recessive disease status. The pedigrees of recessive families are typically limited to one generation or oftentimes the children of the nuclear family, sometimes appearing as sporadic cases if a limited number of children are present. This can lead to unexpectedly affected children if there is no prior family history of a genetic disorder. One exception to this is seen in consanguineous kinships where multiple generations can be affected. Large consanguineous families have provided a powerful source of pedigree information by means of recessive loci mapping via linkage analysis and disease gene identification. Mutational segregation analysis would require clinically affected individuals to be either homozygous or compound heterozygous. In either case, parents would be heterozygous asymptomatic carriers.

Consanguineous marriage is common in many parts of the world, such as the Middle East, parts of South Asia, sub-Saharan Africa and South East Asia [37]. The high rate of consanguinity in Pakistan makes it an ideal population to study a recessive trait such as HL. It is estimated that 60% of marriages in Pakistan are consanguineous, of which, over 80% are between first degree cousins [38]. These marriages result in an increased prevalence of children harbouring a homozygous recessive variant in recessive genes [37]. Genetic studies involving the Pakistani population alone has led to the identification of a combined 31 recessive genes and loci. The discovery of these loci highlights the extensive genetic heterogeneity of NSHL and also reinforces the advantages of certain population types in a candidate gene study.

X-linked. In autosomal dominant and recessive inheritance, males and females have an equal probability of inheriting a disorder. Antagonistically, X-linked inherited disorders affect males either exclusively or more severely than affected females. Fifty percent of the male children from a carrier female mother will be affected. The pedigrees of X-linked families show only affected males and unaffected females, or females with a later onset and/or with a milder phenotype. The presence of a milder phenotype could be explained by a skewed X inactivation mechanism during early embryonic life, allowing for an imbalance or skew deviating from a typical 50:50 ratio of maternally:paternally originating X chromosome expression [79].

3.2.2.3 Gene and protein classes involved in hearing loss

Genes demonstrate a broad and dynamic expression in various tissue types at distinctive developmental stages and after exposure to a variety of environmental conditions. Furthermore, certain transcript types are exclusively expressed in specific tissues [80]. Because of this transcriptional complexity, mutations in genes can have seemingly unconnected outcomes such as NSHL exclusively despite exhibiting a wide tissue distribution, since ear-specific functions are irreplaceably lost.

Although there are hundreds of genes localizing to the auditory system, there are typically three main categories of genes/proteins that share central features to the ear and brain (Table 3). These categories are genes involved in: (1) homeostasis of the cochlea, (2) structure and function of the hair cell, and (3) cytoskeletal formation [81]. There are many unknown genes remaining to be elucidated, as well as already identified genes with poorly or limited understood function.

Category	Description	Examples of genes
Ion homeostasis	Circulation and recycling of ions through ion channels	*CLDN14*, *GJB2*, *GJB3*, *GJB6*, *KCNQ4*, *SLC26A4*
Structure and function of auditory components	Adhesion molecules that compose tip links in hair cells, scaffolding proteins with organizational involvement and myosins that maintain cell shape	*CDH23*, *MYH14*, *MYO6*, *MYO7A*, *MYO15A*, *PCDH15*
Cytoskeleton formation	Regulate cell shape, transport and motility: broken down into extracellular matrix components, attachment of otoconial membrane to sensory hair bundles, and transcription factors that ensure normal growth and development	*ACTG1*, *COL11A2*, *COCH*, *ESPN*, *GRHL2*, *OTOA*, *STRC*

Table 3. Summary of gene classes involved in non-syndromic hearing loss [81].

3.2.2.4 Non-syndromic hearing loss genes

The extensive genetic heterogeneity elucidating HL adds to the already complex picture of sensory disorders. Non-syndromic cases constitute the majority of genetic HL with the only described abnormality being reduced hearing capability. There are several genes that are important to highlight in the context of this dissertation.

3.2.2.4.1 The primary recessive genes *GJB2* and *STRC*

***GJB2* (DFNB1A).** Despite the highly diverse genetic nature of HL, *GJB2* (chr13q11q12), the gene encoding a gap junction ion channel required for hair cell cortilymph homeostasis [82], accounts for a disproportionately high number of HL cases in the European population than would be expected. One single mutation in *GJB2* (c.35delG) (Figure 1) is responsible for roughly one out of every three HL cases in Germany and manifests as profound prelingual HL [81]. The presence of this mutation has been evaluated in a number of diverse populations wherein a one in 31 carrier rate was disclosed in Mediterranean individuals with an estimated causative involvement to be between 28 to 63% of HL cases [83]. However, the implication of *GJB2* mutations is not consistent across all populations. In the African American [84], Pakistani [85] and Indonesian [86] populations, *GJB2* mutations contribute very little to the diagnosis of HL.

Although *GJB2* is largely regarded as a recessive NSHL gene, specific mutations confer progressive ADHL (DFNA3A), as well as syndromic HL with distinctive skin phenotypes [87]. DFNA3A HL typically begins in childhood with high tones initially affected progressing to include middle tones by the sixth decade of life [88].

***STRC* (DFNB16).** The structure, function and expression of stereocilin (*STRC*) have formerly been investigated in animal models that indicate the presence of various stereocilia links running laterally between and across each of the rows, joining adjacent stereocilia within the outer hair cell's hair bundle. These links are proposed as providing varying longitudinal rigidity in response to mechanical stimuli that result in the opening of stereociliary mechano-electrical transduction channels [89,90]. During all stages of mouse embryonic development extending into postnatal day (P) 19, there is a rapid development and refinement of stereocilin link architecture that is important for full maturation [91].

STRC has emerged as an increasingly important gene for recessive NSHL [92]. The mutational fallout of *STRC* is complicated by a non-processed pseudogene adjacently positioned in a 100 kilobase pair (kb) segmental duplication on chr15q15.3 with 98.8% genomic and 99.6% coding sequence identity [93,94]. Two independent studies estimate the deletion carrier frequency between 1.0 and 1.6% in the general population, with an extrapolated incidence of *STRC* HL up to 1 in 16,000 individuals [92,93,95]. Given the high carrier frequency for copy number variations (CNVs) in *STRC*, CNV detection via multiplex ligation-dependent probe amplification (MLPA), high resolution whole-genome microarray (single nucleotide polymorphism, or SNP array, and array CGH, or comparative genomic hybridization), quantitative polymerase chain reaction (qPCR) and Sanger sequencing are important for determining the copy number and mutation status of this gene in HL patients. Due to the presence of a closely linked pseudogene, accurate next generation sequencing (NGS) data acquisition of this gene is not possible, making the only currently available method for mutational analysis the Sanger sequencing assay described in Attachment 3.

Individuals with HL as the result of *STRC* have uniquely sloping audiograms such as the audiogram depicted in Figure 3C. This aspect will be described in greater detail in the Audiometry section.

3.2.2.4.2 The autosomal dominant gene *GRHL2* (DFNA28)

Grainyhead-like 2 (*GRHL2*) is a highly conserved transcription factor with a role in the development and function of certain tissues. The same developmental pathways that are activated during embryogenesis can also be activated in cancer during tumour progression [96]. Presently, *GRHL2* (chr8q22) has implication in the tumour progression of colorectal, gastric, breast, oral squamous cell and hepatocellular carcinomas [97-103], as well as idiopathic pulmonary fibrosis [96].

Despite a strong link to cancer, *GRHL2* is associated with age-related hearing impairment [104] and is an ADHL (DFNA28) NSHL gene [105]. Expression has been documented in the mouse cochlear duct at embryonic day (E) 18.5 and P5 [105,106]. Zebrafish studies involving *Tol2* transposon-mediated insertional mutagenesis revealed abnormal anatomical development of the otocysts, otoliths and semi-circular canals [107]. *GRHL2* was initially mapped for DFNA28 NSHL from a five-generation North American family affected with HL [105]. Prior to the family described in Attachment 4, this was the only family with a *GRHL2* mutation causing NSHL described in the literature. The family in Attachment 4 is the second family with a *GRHL2* mutation confirming the importance of this gene in normal hearing function.

3.3 Types of hearing loss

The ear is comprised of three main components: the outer, middle, and inner ear (Figure 2). Defects in any of these areas yield a uniquely identifiable HL, namely conductive, sensorineural, mixed, and central auditory dysfunction. In order to distinguish the different types of HL, direct measurements that separate the conduction of the sound through the external and middle ear components (by air conduction measurement) and the response of the inner ear (by bone conduction measurement) are performed through audiogram measurements that are discussed in greater detail in the Audiogram section. The precise determination of HL is important for follow-up treatment and therapy options, since not all remedial alternatives are the same for all types of HL.

A patient with conductive HL would demonstrate normal bone conduction, since the inner ear is unaffected, but would have increased air conduction thresholds indicative of a defect in the external of middle ear. This differs from a patient with sensorineural HL wherein both air and bone conduction are uniformly increased and overlap at each frequency. Mixed HL is present when both air and bone conduction thresholds are increased, but the thresholds are not overlapping [108].

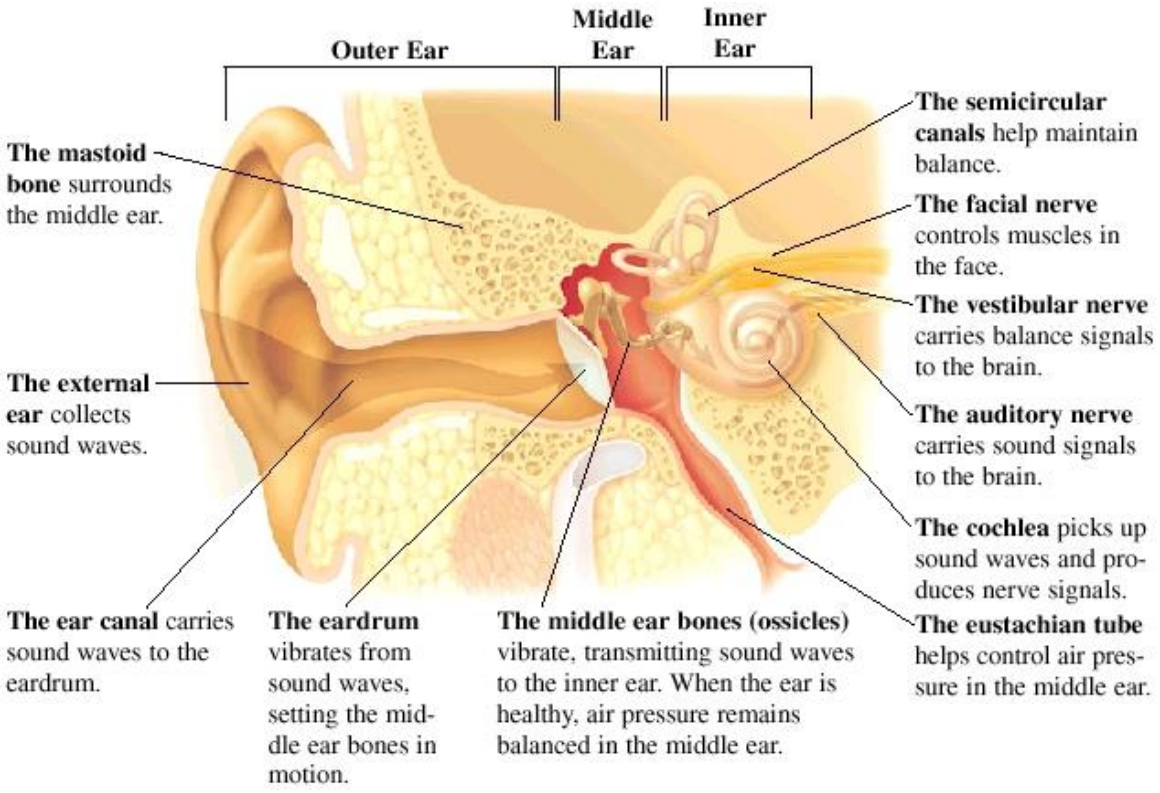

Figure 2. Anatomy of the ear. Source: http://www.fairview.org/healthlibrary/Article/83594

Onset of HL relative to the critical period for speech and language acquisition is another aspect that can be assessed for HL delineation. Prelingual HL begins before the age of five years, when language is typically acquired [8]. Postlingual HL begins any time after the age of five years until the fourth or fifth decades of life, with later onset being most likely due to age-related HL (presbycusis) [34].

3.4 Audiometry

Audiometry measures air and bone conduction components to assess how well sound is processed in individuals. Initial identification of HL is based upon increased audiometric thresholds beyond the normal range of sound perception in the 0-20 dB intensity range across the commonly measured frequencies of 0.25, 0.50, 1.0, 2.0, 4.0, and 8.0 kilohertz (kHz). The difference between the plotted patient thresholds in each ear against normal range thresholds determines the severity of HL that can be categorized as mild, moderate, moderately severe, severe and profound, accordingly (Figure 3A). HL is considered mild when hearing thresholds increase to 21-40 dB, moderate from 41-55 dB, moderately severe from 56-70 dB, severe from 71-90 dB, and thresholds > 91 dB are indicative of profound HL (Figure 3A). A normal hearing person can hear all frequencies between 0 and 20 dB intensities (Figure 3B).

Apart from measuring severity of HL, audiograms provide additional supporting information that aid with the proper diagnosis of HL. An aspect of HL that can be audiometrically assessed is the progressive or stable character by assessing threshold measurements. For this determination, a collection of patient audiograms over a number of years are analyzed per frequency measurement over time. Furthermore, lateralization or sidedness of HL can be easily seen by the increasing threshold differences across ears. Though not always the case, unilateral HL is more commonly seen in syndromes compared to classical NSHL [34].

Audiometric profiles can be conducive to a diagnostic hypothesis as the genotype-phenotype correlation of NSHL is constantly expanding with every new HL gene revealed and every case report going into further depths about the audiological spectrum of HL genes. High frequency HL is commonly seen in mutations in *STRC* (DFNB16) [41], *KCNQ4* (DFNA2) [109], *DFNA5* (DFNA5) [110], and *COCH* (DFNA9) [111] (Figure 3C) lower frequency HL is characteristic of *DIAPH1* (DFNA1) [112] and *WFS1* (DFNA6/14/38) [113] (Figure 3D), middle frequency, or "cookie bite" hearing loss is seen in *COL11A2* (DFNA13) [114], *TECTA* (DFNA8/12) [115] (Figure 3E), or flat with all frequencies having roughly the same threshold as seen with *MYO6* (DFNA22) [116] (Figure 3G). On extremely rare occasions, a "tent" audiogram profile (Figure 3F) with low and high frequencies acutely affected and middle frequencies in the normal to moderate HL range appear. However, this is likely the result of a combination of low frequency HL such as *WFS1* and either presbycusis or acoustic trauma [117].

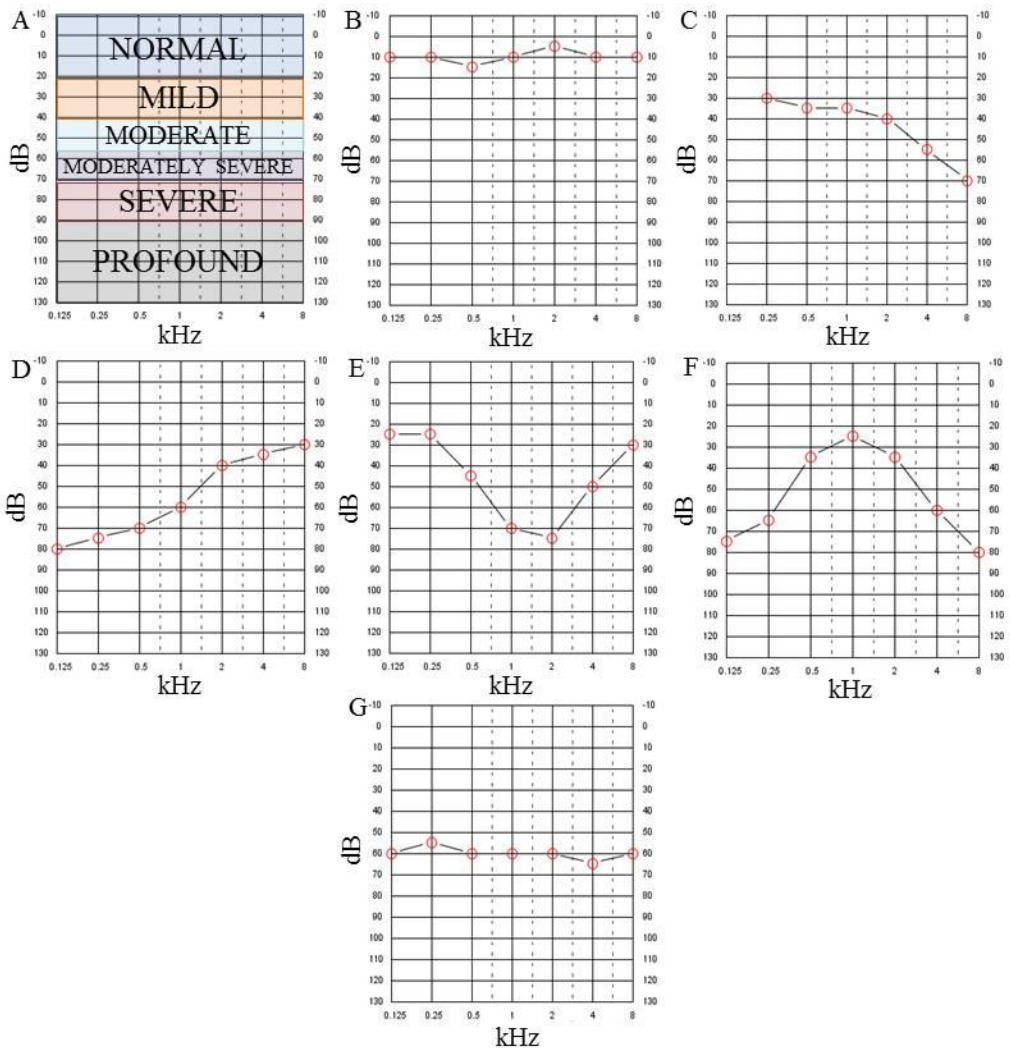

Figure 3. Example audiograms. A. Hearing loss can be categorized according to threshold plotting as mild, moderate, moderately severe, severe or profound. **B.** Example of an audiogram measurement from a normal hearing person. **C.** Sloping audiogram indicating HL is more acute in the high frequencies. **D.** Reverse sloping audiogram with lower frequencies acutely affected. **E.** Cookie bite profile with low and high frequencies better than middle frequency tones. **F.** Tent profile with low and high frequencies more severely affected compared to middle frequencies. **G.** Flat audiogram where all frequencies are affected to roughly the same degree.

3.5 Current overview of hearing loss clinical diagnosis

The diagnosis of HL is often challenging and involves a multidisciplinary team of professionals for holistic investigation [118], and to the credit of decade-long work and international collaboration, numerous diagnostic improvements have been met with great success. Firstly, in the context of pediatric HL, implementation of universal newborn hearing screening programs have reduced the average time of diagnosis in infants from 24 to 30 months to two to three

months [119]. Furthermore, and not limited to pediatric cases, once HL is observed, a complete clinical work-up is ordered for the patient to distinguish genetic from acquired, as well as to rule out the presence of HL in the context of a syndrome. This clinical work-up includes: kidney and thyroid sonography, urinalysis, electrocardiogram (ECG), neurological examination, blood profile (including, liver (alanine aminotransferase and aspartate aminotransferase), thyroid (thyroid stimulating hormone and thyroxine), cholesterol, kidney (creatinine) and free fatty acid values), serological analysis for toxoplasmosis, cytomegalovirus, herpes simplex virus and rubella, as well as ophthalmological examination and magnetic resonance imaging of brain, inner ear and temporal bones. Simultaneously, genetic testing routinely begins with *GJB2* and MLPA (P163 GJB-WFS1 probe mix, MRC-Holland) testing, that detects CNVs and single nucleotide variants (SNVs) in *GJB2*, *GJB3*, *GJB6*, *POU3F4*, and *WFS1*. Additional genes are also included in testing when further clinical indications in addition to HL are present. For example, *SLC26A4* is tested with goiter or enlarged vestibular aqueduct and *OTOF* is tested when recessive auditory neuropathy is present. Recent improvements in genetic testing, including the advent of high throughput NGS technologies are able to translate into improved patient care as many mutations in HL genes demonstrate a characteristic age of onset, progression, and pattern of inheritance. Particularly of interest to clinicians is target capture NGS involving only a sub-set of disease relevant genes in the form of gene panels that generate sequencing data for dozens or hundreds of genes in parallel that has the advantage over conventional polymerase chain reaction (PCR)-based direct sequencing approaches in that it is able to achieve faster results at a fraction of the price [120].

3.6 Strategies for mutation detection

Each of the methods subsequently described have resolution limitations for the detection of sequence or chromosomal aberrations. For example, the SNP arrays employed in this study can detect deletions and duplications with a 5-6 kb resolution. The ability to detect large chromosomal aberrations emphasizes the importance of SNP arrays, which is not currently a reliable aspect of NGS bioinformatics. Sequencing methods can easily detect indels that reside below the resolution of microarrays in the base pair (bp) size range. The methodology described in subsequent sections combines methods to reduce the resolution limitations of each method.

3.6.1 Whole-genome SNP array analysis

Whole-genome SNP arrays provide a number of informative benefits as a research and diagnostic tool. There are two types of probes on the SNP arrays yielding different data: (1) genotyping probes allow for SNP genotyping making the determination of SNP heterozygosity or homozygosity possible and (2) intensity only probes fill in providing a higher resolution for CNV calling giving hint to chromosomal aberration. Together, these probes allow for the detection of CNV, loss of heterozygosity (LOH), mosaicism, and uniparental disomy (UPD). In the context of this project, the detection or exclusion of large CNVs is important with the decision to either proceed to the next method for investigation or make a concrete diagnosis. In addition, the genotyping data can be used for haplotype analysis such as parent-of-origin in the context of a large deletion, determination of percent identity by descent, homozygosity mapping (HomozygosityMapper), or linkage analysis, since the genotyping quality on SNP arrays is consistently excellent.

The Illumina Omni1-Quad arrays were used in this study to yield Log R Ratio and B allele frequency data per chromosomal aberration that was detected using cnvPartition and QuantiSNP [121] CNV algorithms and visualized in GenomeStudio. Figure 4 shows a visual overview of the different call types.

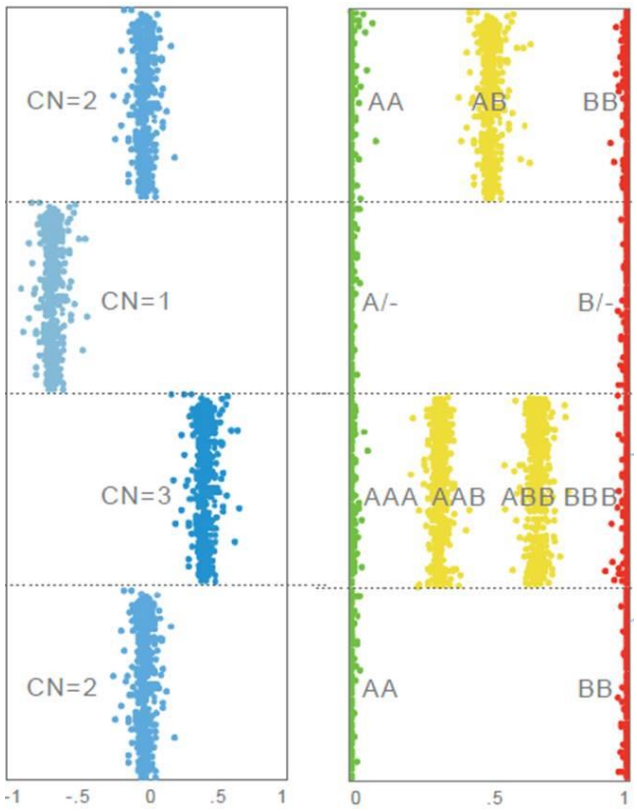

Figure 4. SNP array interpretation. Illustration of normal copy number (CN = 2), heterozygous deletion (CN = 1) heterozygous duplication (CN = 3) and copy neutral LOH (CN = 2), from top to bottom. The left plot shows the Log R Ratio that calculates copy number intensities. The right plot shows the B allele frequency that indicates genotyping results. Heterozygous SNPs plot along the AB central line, whereas homozygous SNPs plot on either the zero or one axis as AA or BB [122].

The Illumina Omni1-Quad arrays provide over 1.1 million 60mer probe markers with a median spacing of 1.2 kb for whole-genome coverage including 98% of RefSeq genes (hg19) [122]. The SNP markers originate from the HapMap and 1000 Genomes projects and > 600,000 markers are positioned within 10 kb of a gene providing informative CNV coverage [122].

Microarrays were performed on a total of 109 individuals for research. Of those, 90 were classified as non-syndromic, ten had syndromes that could not be excluded at the time of clinical data collection and nine had various syndromic features. CNVs that were disclosed from the arrays were validated via PCR when homozygous deletions or qPCR when heterozygous deletions or duplications were detected.

3.6.2 Next generation sequencing

While Sanger sequencing has long been regarded as the gold standard of molecular genetic testing, it has tremendous limitations that make it an unfeasible approach for detecting mutations in a large subset of genes, which is a practical approach for a disorder such as HL that has

hundreds of genes with implication in HL. In contrast to Sanger sequencing, NGS platforms allow for the massively parallel sequencing of single deoxyribonucleic acid (DNA) amplicons that permit the scaling up of data output by orders of magnitude [123]. NGS can take the form of targeted gene panels of clinically relevant genes, whole exome sequencing (WES) of the entire protein-coding fraction of the genome or whole genome sequencing. In the context of this dissertation, only panel NGS is of relevance. Potentially significant mutations that were of interest given the clinical background of the patient were Sanger sequence validated for confirmation of the mutation via a second method.

3.7 Multiple approaches to hearing loss diagnostics

One of the goals from this work was to understand the types of mutations that underlie HL. To initiate this process, *GJB2* negative patients were screened in stages, beginning with a whole-genome Illumina Omni1-Quad microarray study comprising 109 individuals and followed by a targeted deafness gene NGS analysis of 25 hearing impaired individuals. Patients positive for mutations that either segregate or are in agreement with clinical histories when parents are unavailable for genetic testing are regarded as solved cases and are no longer queued for further investigation. Figure 5 illustrates the schematic overview of the study.

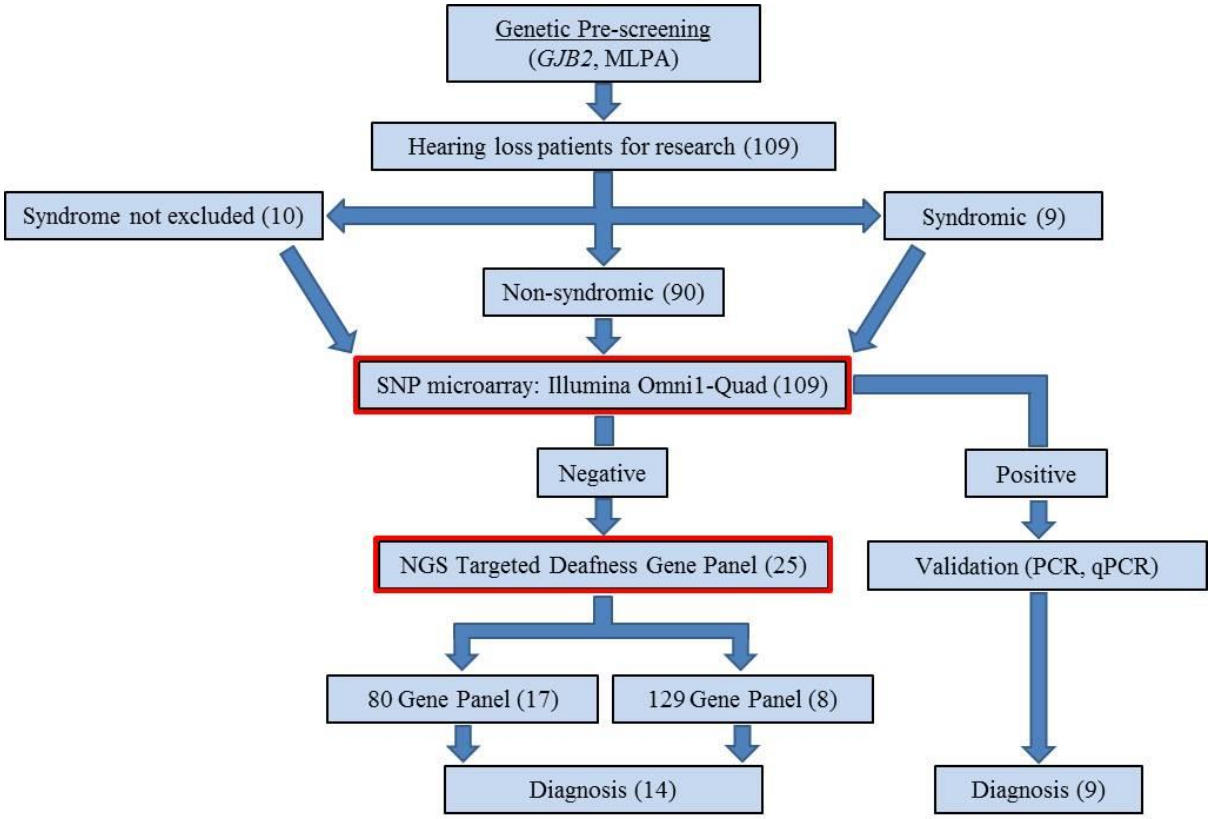

Figure 5. Schematic overview of the study. The two different methods are boxed in red. The number of patients included in each of the different methods is indicated in parenthesis.

CNVs that encompass a large number of genes are analyzed on a gene-by-gene basis for gene content and implication that a change in gene dosage would have on HL. Similarly, when a SNV or indel affecting a gene is uncovered, a number of different databases and resources are exploited for interpretation: dbSNP, Exome Variant Server (EVS), MutationTaster, PolyPhen-2, SIFT, ClinVar, SwissVar, HGMD, 1000 Genomes Project, STRING, as well as location of SNV relative to protein domain coding sequence, and amino acid and nucleotide (nt) conservation. For all variation, regardless of size, resources that are used for ascertainment of gene information are: OMIM, GeneCards, UniGene, UCSC Genome Browser, DECIPHER, DGV, Ensembl, MGI, Zfin, and PubMed. The pathogenicity clues yielded from this work either support or reject the likelihood a mutation or gene being a new NSHL candidate gene or implicated as a causative mutation in a known HL gene.

4. Objectives

The present work has several aims. One goal is using molecular methods to realize the basis of the genetic heterogeneity of HL without *GJB2* involvement, wherein diverse subsets of genes play critical roles in hearing, and to determine whether the mutational spectrum of patients is disclosed by mutations in the same gene or different genes. In order to accomplish this, patients need to be tested in stages at different resolutions, beginning with a SNP array and following with targeted deafness gene NGS with appropriate *in silico* analysis. Apart from analyzing the potential effects of several genes, this study focuses on the phenotypic spectrum of *GRHL2* and the mutational spectrum of *STRC*. To this end, the establishment of a *STRC* Sanger sequencing assay is a paramount objective for accurately assessing mutations in *STRC* to avert pseudogene influence.

5. Materials and Methods

One hundred nine individuals with suspected genetic HL who were pre-screened and negative for genetic mutations in commonly affected genes were recruited for the NSHL research study. Parental and/or patient consent was obtained from all patients. Patients were recruited mainly from the Universities of Würzburg and Mainz. Clinical, audiological and familial information were obtained to assist mutation analysis.

5.1 Copy number variation analysis

5.1.1 Illumina Omni1-Quad SNP array (See Attachment 1, Materials and Methods)

The Illumina Omni1-Quad SNP array is used for the detection of chromosomal structural aberrations such as duplications and deletions in genomic DNA (gDNA). They also generate genotypes that can determine which parental allele is involved in the chromosomal abnormality. Copy-neutral LOH, UPD and mosaicism can also be disclosed from SNP arrays. The genotypes produced from these arrays can be used for homozygosity mapping and linkage analysis.

5.1.2 Cytogenetic analysis (See Attachment 1, Materials and Methods)

Metaphase chromosomes were prepared from the short term culture of peripheral blood lymphocytes of the patient stimulated with phytohaemagglutinin according to standard procedures. Chromosomes were subjected to G-banding with trypsin-Giemsa (GTG Banding). Structural analysis of chromosomes of the proband was performed routinely at the 500 band level and at the specific region involved in chromosomal aberrations was assigned based on ISCN 2013 criteria.

5.1.3 Fluorescent *in situ* hybridization (See Attachment 1, Materials and Methods)

Fluorescent *in situ* hybridization (FISH) is a technique used for the localization of chromosomal breakpoints. It can also disclose aberrations such as deletions, duplications, as well as chromosomal translocations and inversions. FISH is an especially important method in the presence of a balanced translocation, since array CGH or SNP array cannot detect such events.

5.1.4 Quantitative PCR (See Attachment 1, Materials and Methods)

qPCR is a method that quantitates the copies of a DNA input. The test and control samples are diluted to a 10 ng/µl concentration. The result of the test sample is compared against four total

controls, with two having normal DNA concentrations and two with a 1:2 dilution simulating a heterozygous deletion. The sample is normalized against the controls for the calculation of a copy number, as well as a percent variation value as a quality control indicator. All valid qPCRs must have a percent variation value ≤ 2% to be considered a valid investigation.

5.1.5 Parent-of-origin determination (See Attachment 1, Materials and Methods)

Maternal and paternal SNP genotypes from the Illumina Omni1-Quad array were compared to the configuration in the child proband. This analysis is especially important when a large deletion or duplication is detected.

5.2 Expression of *ATE1* and *SLC12A1* during zebrafish development

5.2.1 Zebrafish *in situ* hybridization (See Attachment 5, Materials and Methods)

Zebrafish (*Danio rerio*) are a model organism to study the spatiotemporal gene expression pattern during embryonic development using *in situ* hybridization. At desired time points, labeled nucleic acid hybridizes specific messenger RNA (mRNA) sequences, if expressed, that localizes and depicts the gene expression patterns in developing tissues.

5.2.2 Positional cloning of translocation breakpoints (See Attachment 5, Materials and Methods)

Positional cloning is a method to refine breakpoints in a translocation to delineate the precise bp breakpoint position or to narrow the interval of interest harbouring the breakpoint to a smaller region. It also directly illustrates the plausible gene disruption within the breakpoint region allowing for functional evaluation.

5.3 Sanger sequencing

5.3.1 Long-range PCR (See Attachment 2, Materials and Methods)

Long-range PCR (LR-PCR) is required for the amplification of PCR products over 5 kb using a mixture of DNA polymerases that remain stable for the amplification of a long target.

5.3.2 Sanger sequencing (See Attachment 2, Materials and Methods)

Sanger sequencing determines the nt order of an amplicon using a chain termination method. This entails the separation of the double stranded DNA, the annealing of a sequence primer, a chain termination sequencing step essentially using four separate reactions for each of the four

nucleotides that bind to the single DNA strand, and then the release of the template and separation on a high resolution denaturing gel electrophoresis.

5.4 *GRHL2* splice site analysis

5.4.1 mRNA isolation (See Attachment 4, Materials and Methods)

mRNA isolation methods involve the sampling of a tissue, such as saliva, with a stability reagent to protect mRNA degradation for follow-up extraction, whereby mRNA is purified for complementary DNA (cDNA) synthesis.

5.4.2 cDNA synthesis (See Attachment 4, Materials and Methods)

cDNA synthesis begins with an mRNA template that is converted to a stable DNA form. The enzyme reverse transcriptase is required for cDNA synthesis. This method is important for the confirmation of a splice mutation because splicing has already occurred in the mature mRNA strand.

5.5 Next Generation Sequencing

5.5.1 Target enrichment NGS (See Attachment 5, Materials and Methods)

Target enrichment NGS design selects genes or gene regions through the selective capture and enrichment of gene exons and flanking intronic sequence during library preparation. Libraries are massively parallel sequenced on an Illumina HiSeq2000 that generates 100 bp paired-end reads.

5.5.2 Bioinformatic analysis (See Attachment 5, Materials and Methods)

Sequencing reads are aligned to the hg19 genome build. Quality and sequence depth are analyzed after alignment and variant calling are performed using DNAnexus. The analysis filtering pipeline used in this study are described in Attachments 4 and 5.

6. Summary and Discussion of Published Results

6.1 Terminal chromosome 4q deletion syndrome: a case report and mapping of critical intervals for associated phenotypes

Chromosome 4q deletion syndrome is subdivided into two classifications based on the delineation of the location of the long arm of chromosome 4q that is deleted (Figure 6). With an incidence rate of 1 in 100,000, chromosome 4q deletion syndrome is a rare event. The high degree of variability in presentation among patients complicates the clinical diagnosis. To date, there are over 150 cases presented in the literature for large deletions involving any part of the long arm of chromosome 4, many of which were characterized using traditional techniques such as GTG banding only, making the genotype-phenotype delineation complicated [124].

Terminal chromosome 4q syndrome is characterized by a broad spectrum of phenotypes including intellectual disability (ID), craniofacial dysmorphism, rotated or low-set ears, cleft palate, micrognathia, congenital heart defects, craniofacial, skeletal and digital abnormalities, and occasionally autism spectrum disorder, behavioural disorders and developmental delay [125,126]. Distal deletions in 4q34q35 are associated with an especially extensive presentation of characteristic features, making prognostic outcome extremely challenging [127]. HL is a rarely reported phenotype of this syndrome; however, in addition to the case presented in this dissertation, two other cases, one *de novo* deletion case [128] and a single DECIPHER case (#256186) have been diagnosed with terminal chromosome 4q deletion syndrome, but had a variety of unrelated phenotypes making a phenotypic delineation difficult.

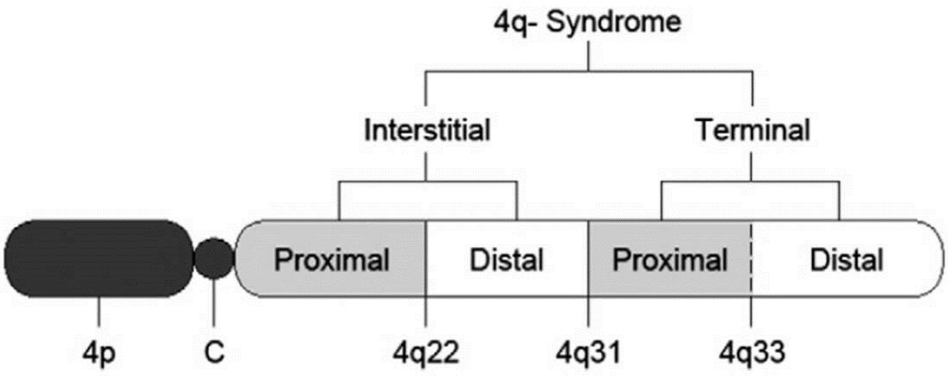

Figure 6. Chromosome 4q deletion syndrome classifications. The 4q interstitial classification is the presence of heterozygous deletions spanning from the centromere (C) to 4q28.3 and the 4q terminal division spans from 4q31.1 to 4qter (q terminus) [126].

Syndromes with HL as part of a larger multi-system phenotypic picture represent approximately 30% of HL cases with a genetic etiology. A male patient with initial presentation of NSHL at four months of age was included as part of the microarray study that disclosed a large 6.9 megabase (Mb) (chr4:184,046,156-190,901,117, hg19) heterozygous deletion that included 18 OMIM genes on chromosome 4q35.1q35.2 (Attachment 1, Figure 1B). Upon acquisition and thorough analysis of medical records, a number of phenotypes in line with the diagnosis of terminal chromosome 4q deletion syndrome were discovered. The proband's phenotypes include: aortic isthmus stenosis that was corrected with balloon angioplasty and patent foramen ovale in the first year of life, submucous cleft palate and velopharyngeal insufficiency surgically corrected at the age of five years, chronic Eustachian tube dysfunction that was operated several times with myringomy tubes throughout life, as well as bifid uvula and bilateral cryptorchidism requiring a right testicular orchiopexie. An abdominal sonogram assessing kidney physiology could not rule out the possibility of a left duplex kidney malformation. He had an abnormally small thyroid but tested euthyroid. As he has required multiple surgeries throughout childhood, a record with deficiencies of blood coagulation factors IX (56%), XI (48%), and XII (38%) was available. He had elevated prothrombin time of 46.5 s (normal: 25-39 s) and lupus anticoagulant confirmatory test of 1.26 (normal: 0.91-1.07). Further coagulation testing was negative for von Willebrand disease. Shortened cardiac PQ wave intervals on an ECG indicated atrioventricular node irregularity. Neurological evaluation at the age of five showed a deficiency in age-appropriate coordination. Mild developmental delay of approximately six months at the age of three to four years was detected, but follow-up testing has shown that this deficiency has since been remediated. A reported speech and language development delay was present that is believed to be a compounded effect from both HL and extensive hospitalization history. He currently attends a regular school and does not demonstrate a learning disability.

Genetic testing on record included *GJB2*, *GJB3*, and *GJB6* sequencing that could not be attributed to the HL in the patient, as he had a c.94C>T heterozygous mutation in *GJB3*, with a minor allele frequency (MAF) of 0.015 (rs1805063) which by itself does not cause HL. A targeted NGS panel including 129 deafness genes was performed after the microarray chromosome 4 aberration was detected. The NGS panel was negative for mutations that could explain the HL in the proband. qPCR confirmed the deletion in *FRG1* exons 1 and 8, as well as that the deletion in *DUX4L6* extends beyond the terminally defined breakpoint disclosed from the microarray to at least chr4:190,939,252 bp. Cytogenetic analyses of the mother and father, did not reveal any detectable gross abnormalities (Attachment 1, Figure 1A). However, a

4q35.1q35.2 deletion was evident in the proband from GTG banding. FISH analysis on metaphases from the three family members labelled with selected bacterial artificial chromosomes (BACs) hybridized to the expected 4q35.1 region in the parental metaphases labelling both homologs but confirmed the deletion on one of the proband's chromosome 4 metaphases. The FISH results did not indicate a cytogenetically cryptic subtelomeric translocation in the parental karyotypes. The proband's mother and father were also included on the SNP array to determine from which parental allele the deletion arose (Attachment 1, Figure C). This analysis concluded an absence of maternal genotypes in the proband. The child appeared "homozygous" in the deletion interval because of the presence of genotypes only from one parental allele, namely the father. For example, at rs12643595, the mother is BB, the father is AB, and the child is AA, with the only possibility for inheritance of the A genotype from the father. With an incidence rate of 1 in 100,000, it is possible that a common underlying mechanism results in the large deletion in the chromosome 4q28.3qter region. An analysis of crossover recombination hotspots (Attachment 1, Figure 2, bottom section) shows enrichment in both male and female gametes in otherwise recombination cold chromosomal intervals.

A literature review mapping and correlating the overlapping deletion intervals and phenotypes for a total of 36 patients with 4q terminal deletion syndrome was performed (Attachment 1, Figure 2 upper section, Attachement 1, Table S2). The genes contained in this interval (Attachment 1, Figure 2 middle section) were analyzed for possible roles in phenotypic presentation. Each of the deletion cases were plotted to determine common and overlapping phenotypes (Attachment 1, Figure 2 upper section). Emphasis on genes with an important link to the phenotypic spectrum of 4q deletion syndrome are described (Attachment 1, Table S1). From a review of the literature, cleft palate, ID, autism spectrum disorder, and two congenital heart defect critical interval loci were mapped. Further analysis of the gene content in this region allowed for the proposal of candidate genes for the various loci. The gene with possible implication in cleft palate is the maternally imprinted gene *PDGFC* that is linked with lethal clefting phenotypes in knockout mice [129], and non-syndromic orofacial clefting [130]. Furthermore, this gene is predicted to exhibit moderate haploinsufficiency (HI). The ID locus remains without a clearly linked candidate gene; however, the gene *SCRG1* is of interest due to high brain expression and differential regulation in schizophrenia and bipolar disorder [131]. Heterozygous deletions in the gene *FAT1* have implication in autism from two independent studies [132,133]. Behavioural disorders are also closely linked with this gene [134]. The large first congenital heart defect locus (Attachment 1, Figure 2 upper part, light green) overlaps with

two cardiac-important genes *TLL1* and *HAND2* with likely HI. *Tll1* demonstrates importance for normal septation and blood circulation in the mouse [135]. Similarly, *hand2* plays a role in zebrafish cardiac morphogenesis, as well as angiogenesis, right ventricle and aortic arch artery development [136]. The second congenital heart defect locus comprises a smaller region with two genes residing in the critical interval (*PDLIM3* and *SORBS2*). *Pdlim3* is involved in mouse right ventricular formation and thought to reinforce mechanical stability of cardiac muscle during development [137]. *SORBS2* demonstrates a high expression in cardiac tissue after acute myocardial infarction [138].

It is well known that SNP arrays are poorly covered in telomeric and centromeric chromosomal regions because these regions are especially rich in repetitive sequences [139,140]. The qPCR distal to the telomeric breakpoint was performed to test the terminal limit of the deletion. It is not surprising that this was not ultimately resolved since arrays are uninformative in this region.

This case highlights the necessity for patients to undergo medical evaluation at regular intervals to monitor not only hearing status, but also to document syndromic progression. This is especially important for patients having a large chromosomal aberration that is known to demonstrate a broad phenotypic spectrum, with the primary interest being better clinical management and prognosis.

6.2 Disruption of the *ATE1*and *SLC12A1* genes by balanced translocation in a boy with non-syndromic hearing loss

Balanced reciprocal translocations affect approximately 0.1% of newborns [141]. In many cases, balanced reciprocal translocations do not have a phenotypic outcome; however, they can be associated with a number of consequences, which are thought to be attributed to gene disruption, cryptic imbalances, unmasking of a recessive mutation, or disruption in gene regulation. The majority of balanced translocations are inherited and about one in five is a *de novo* event [142]. When balanced translocations are associated with a disease, they are a powerful tool for the identification of the causative genes [143].

A family with a balanced reciprocal translocation t(10;15)(q26.13;q21.1) in three generations had no reported clinical indications apart from sensorineural HL in one of the children that started at six years of age. The proband developed normally in early childhood and achieved all

developmental milestones as expected. Clinical evaluations including thyroid function test, ECG, and kidney sonography were all normal.

The proband was tested and negative for mutations in *GJB2* and *GJB6* and underwent subsequent cytogenetic analysis beginning with GTG banding that disclosed translocations between chromosomes 10 and 15 (Attachment 2, Figure 1A and 1B). The proband's brother, parents, and paternal grandparents were recruited to determine possible segregation of the translocation in normal hearing family members. The GTG banding of the paternal grandfather and father disclosed the same chromosome 10 and 15 translocation. Breakpoints were provisionally delinieated that continued with FISH (Attachment 2, Figure 1C). The narrowing of breakpoints disclosed two interrupted genes: *ATE1* and *SLC12A1*. The breakpoints in both of the genes were delineated to 10.1 and 8.7 kb intervals, respectively (Attachment 2, Figure 2). An Illumina SNP array was performed on all family members to exclude the involvement of large losses or gains of chromosomal material. CNVs with implication to HL were not detected. A target enrichment NGS deafness gene panel including 129 known, clinically relevant deafness genes was negative for informative SNVs. One mutation (c.1985G>A, p.G662E) in the DFNA48 gene *MYO1A* was reported as possibly pathogenic by UniProt and one previous publication [36]. Interestingly, this mutation also segregated in the proband's father and paternal grandfather, both of whom have normal hearing, complicating the assignment of this mutation as pathogenic in this family. However, we cannot exclude the formal possibility of reduced penetrance since this was previously disclosed in this gene [36].

ATE1 and *SLC12A1* were Sanger sequenced in 180 *GJB2*-mutation negative children with NSHL. Seven synonymous, two benign non-synonymous and one probably damaging, in addition to four synonymous and one non-synonymous variants were detected in *ATE1* and *SLC12A1*, respectively (Attachment 2, Table 1). The single pathogenic variant according to *in silico* prediction is the heterozygous variant c.1208A>G, p.Y403C (rs148135505: MAF = 0.001) in *ATE1*. While this mutation is rare in dbSNP and the exome variant server (EVS), limited conclusions can be made connecting this gene to the proband because secondary to HL, the patient with this mutation also suffers from chronic bilateral tinnitus, as well as reverse sloping audiogram configurations with low frequencies acutely affected and normal hearing at 6 and 8 kHz. This is contradictory to the audiogram profile from the proband, with normal hearing up to 1 kHz and then sloping in the higher thresholds to 60 dB at 8 kHz.

The expression of both genes was evaluated in the zebrafish. Major expression of *ate1* was marked at 91 hours post-fertilization (hpf) in the heart and fin bud with minor expression in the neuromasts (Attachment 2, Figure 3A). Expression of *slc12a1* is most prominent beginning with the somite (15-16 hpf), 30 hpf and 96 hpf in the distal pronephros (Attachment 2, Figure 3B). The expression pattern of both genes is not in the ear like sensory organs in the zebrafish that would support a role of "hearing." Expression in the lateral line that contains the hair cells, otic placode and otic vesicle, would provide the strongest support for either one of the genes being implicated in normal hearing function. As the proband was diagnosed with sensorineural HL, expression in the brain could also be favourable with hearing involvement.

Determining the spatiotemporal expression of genes is critical to understanding or predicting the physiological role of genes and proteins with relation to interactions forming complex networks underlying organ development and function [144]. The *in situ* hybridization data show there is pronephros (embryonic kidney) expression of *slc12a1* in wild-type zebrafish. It is interesting to note that *slc12a1* has a paralog with 64% protein identity to *slc12a2*. In the mouse, *Slc12a1* is exclusively expressed in the macula densa and thick ascending limb of the kidney, whereas *Slc12a2* is expressed in the kidney and ear [145-147]. *Slc12a2* mice demonstrated abnormal locomotor activity consistent with the shaker/waltzer phenotype and failed to respond to sound stimulus, thus illustrating that both hearing and balance are affected by the absence of *Slc12a2* [145]. However, to date *SLC12A2* is not associated with a deafness phenotype in humans.

Mutations in *SLC12A1* and *ATE1* are associated with Bartter syndrome type I and heart phenotypes (in the mouse), respectively. One noteworthy Costa Rican case study disclosed a stop mutation in *SLC12A1* in a Bartter syndrome patient who also had sensorineural HL, but the HL was not well characterized [148]. Interestingly, the analysis of genetic variation in the breakpoint regions in the Database of Genomic Variants (DGV), *ATE1* lacks genomic variation and *SLC12A1* has one indel reported in 270 HapMap controls. This implies normal copy number is important for absence of a phenotype, but no further conclusions can be drawn from this. While both these genes lack extensive genomic variation in the healthy human population, they are unlikely haploinsufficient according to DECIPHER, weakening arguments about gene dosage sensitivity as playing a critical role in the deafness seen in our patient. According to the last clinical examination, neither the index patient nor affected family members with the described translocation have renal or cardiac defects, suggesting that disruption of these genes are tolerated and not sensitive to gene dosage.

Because the balanced translocation is present not only in the index patient, but also in other normal hearing family members, the causative mutation is likely recessive. Interestingly, there are three ARHL genes located on chromosome 10: *MYO3A*, *PCDH15*, and *CDH23*. They are located approximately 97, 67, and 50 Mb proximal to *ATE1*, respectively. A fourth recessive gene, *PDZD7*, resides nearly 21 Mb proximal to *ATE1*. Although not presently recognized as a NSHL gene, there is supporting evidence whereby disruption of *PDZD7* is involved in ARHL [149]. Only one ARHL gene on chromosome 15 is (*STRC*) positioned 4.5 Mb distal to *SLC12A1*. As *ATE1* and *SLC12A1* are not genes responsible for ARHL and the aforementioned genes were sequenced via targeted gene sequencing, it is important to consider whether the translocation potentially disrupts regulation and expression of other genes associated with deafness. Regulatory elements well outside the transcription and promoter regions can influence gene expression [150]. Breakpoints and/or microdeletions that occur in a regulatory element as far away as 1 Mb from the promoter have been shown to impact gene regulation and expression. However, to date, there is a lack of evidence supporting the idea that regulation and expression can be affected by position effects at a distance exceeding 1 Mb.

There are many genes within a flanking 1 Mb region of *ATE1* and *SLC12A1* that are not associated with a HL phenotype that have moderate to strong expressed sequence tags (ESTs) in the human ear (Attachment 3, Table S4). Investigation of ear-specific ESTs within a 1 Mb region up- and downstream from the translocation breakpoints may aid in uncovering genes needed for hearing despite being indirectly affected in the translocation. Changes that occur as a result of a nearby breakpoint may affect gene regulation and/or expression and may negatively impact hearing. The possibility of disrupted gene expression or regulation as a result of being less than 1 Mb in proximity of the translocation or a recessive mutation residing in a gene that is not already associated with HL as conferring recessive HL cannot be excluded; however, this has not been evaluated in the proband.

It can be assumed from sequence analysis in the genes at the breakpoint interval and the targeted gene panel results that the patient has a pathological mutation in a gene that is not yet associated with HL. One way to further investigate these cases would be to employ WES. Sequence variation analysis comparing the index patient with the normal hearing family members also affected with the translocation may uncover a mutation explaining the phenotype.

6.3 DFNB16 is a frequent cause of congenital hearing impairment: implementation of *STRC* analysis in routine diagnostics

Biallelic mutations in the gene *STRC* (DFNB16) result in pediatric, postlingual high frequency HL [41]. A tandemly residing pseudogene complicates the detection of SNVs in this gene. The Illumina Omni1-Quad SNP array is appropriately designed in terms of both probe density with seven SNP probes covering the gene (Figure 7) and probe specificity to support the detection of CNVs in this gene. The 60mer sequence of each of the array probes was checked using UCSC BLAT for specificity to *STRC* and the pseudogene (*pSTRC*) by genomic position (Table 4). For CNV detection, five consecutive SNP probes must give a uniform increase or decrease in signal intensity as detected by the CNV calling software using a sliding window statistical calculation. Because of the limited number of divergent bases between *STRC* and *pSTRC*, it is not always possible to design a probe that is able to make this differentiation. However, three of the seven SNP probes (rs2447196, rs12050645, rs2260160) select for *STRC* and are critical for determining the gene-specific copy number status.

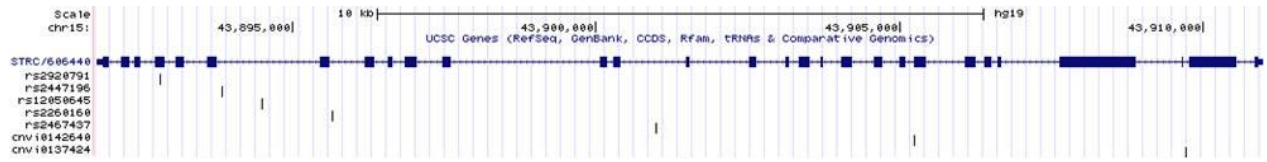

Figure 7. SNP probe coverage overview of *STRC*. This figure was designed using the UCSC Genome Browser SNP/CNV Arrays track.

SNP Probe	Start	Stop	% Identity	gDNA Start	gDNA End	*STRC* or *pSTRC*
rs2920791	1	60	100.0%	43892747	43892806	*STRC*
	1	60	100.0%	43992565	43992624	*pSTRC*
rs2447196	1	60	100.0%	43893758	43893817	*STRC*
	1	60	91.7%	43993576	43993635	*pSTRC*
rs12050645	1	60	100.0%	43894433	43894492	*STRC*
	1	60	93.4%	43994253	43994312	*pSTRC*
rs2260160	1	60	100.0%	43895644	43895703	*STRC*
	1	36	91.7%	43995147	43995182	*pSTRC*
rs2467437	1	60	100.0%	43900912	43900974	*STRC*
	1	60	100.0%	44000386	44000446	*pSTRC*
cnvi0142640	1	60	100.0%	43905185	43905244	*STRC*
	1	60	100.0%	44004647	44004706	*pSTRC*
cnvi0137424	1	60	100.0%	43909658	43909717	*STRC*
	1	60	100.0%	44009120	44009179	*pSTRC*

Table 4. ***STRC* SNP probes.** Analysis of the seven SNP probes included on the Illumina Omni1-Quad array. *STRC* (chr15:43,891,761-43,910,998; RefSeq, hg19) and *pSTRC* (chr15:43,991,686-43,010,382; ENCODE version 19) are distinguishable by SNP probes since their design targets three critical divergent regions.

The observation of recurrent deletions in *STRC* from the SNP array analysis supported the development of a Sanger sequencing assay to screen for additional sequence variants conferring ARHL. Two homozygous deletions, five heterozygous deletions (Attachment 3, Figure 1) and ten copy-neutral patients with a LOH >1 Mb overlapping with *STRC* were identified (Attachment 3, Table S3). These patients were negative for additional disease-relevant CNVs after genome-wide analysis. The homozygous and heterozygous deletions were confirmed by PCR and qPCR, respectively, using exon 22 primers that are able to discriminate *STRC* from its pseudogene counterpart. The copy-neutral LOH regions are not by themselves pathogenic; however, since a statistically significant stretch of homozygous genotypes in this region are detected, it provides a hint of a possible homozygous pathogenic mutation in overlapping genes, namely *STRC*, that could confer DFNB16 HL. One additional independent patient not included in the array study was tested via qPCR and positive for a heterozygous deletion. During the assay development, the audiograms of all patients were analyzed and 20 individuals with appropriately sloping high frequency HL (Attachment 3, Figure 2) were selected for testing. This constituted a total of 36 patients for Sanger sequencing analysis.

For pseudogene exclusion, two long-range (LR) primer pairs were designed specifically for the exclusive amplification of *STRC* (Attachment 3, Figure S1). The first and second LR primers amplified exons 1-19 and 12-29, respectively. LR amplicons were diluted 1:1000 to reduce unintended pseudogene carryover from gDNA. An overlapping region in intron 18 served as a

quality control measure whereby a three nt frameshift is present from gDNA carryover and sequencing would be re-performed to ensure clean exclusion of pseudogene sequence. Nested PCRs for each exon were performed using the corresponding LR amplicon and each exon-specific primer pair.

Sanger sequencing of the 36 patients uncovered a variety of pathogenic mutations and sequence variants. Three out of six patients with a heterozygous deletion disclosed a hemizygous pathogenic mutation [c.2726A>T (p.H909L); c.4918C>T (p.L1640F); c.4402C>T (p.R1468X)] (Attachment 3, Table 1). A LOH patient had a heterozygous pathogenic variant [c.5180A>G, (p.E1727G)]. One of the 20 patients selected on the basis of ARHL and supporting audiogram had a compound heterozygous mutation [c.2303_2313+1del12, (p.G768Vfs*77); c.5125A>G, (p.T1709A)]. A single variant that was predicted as possibly pathogenic [c.3893A>G, (p.H1298R)] by SIFT was present with a MAF of 9% of the patient cohort. This variant was detected heterozygously in four patients and homozygously in one patient. Sequencing of 100 normal hearing German controls revealed a MAF of 11% in these individuals. Despite strong conservation (Attachment 3, Figure S2) and mutation prediction algorithm outcomes, the high MAF in the normal hearing population argues against pathogenicity.

The presence of LOH with a minimum length of 1 Mb is not a strong indication for initiating *STRC* sequence analysis and unexpectedly led to the detection of one heterozygous variant. The power and confidence of LOH calling is greatly increased with parental genotypes [151]. As such, single patients in the absence of familial inclusion demonstrate a higher chance of heterozygous SNPs residing in a LOH region. As parents were rarely included in our SNP array analysis, it was not possible to interrogate LOH calls beyond analyzing gene content and size. Although only ten patients had LOH spanning *STRC*, the LOH observed is not enriched with *STRC* mutations and is not the best indication for DFNB16 HL.

MLPA is an alternative method that can be used to test for mutations in this gene [95], but is limited to few divergent sequence positions. The Sanger sequencing assay outlined in Attachment 3 in combination with an array having high SNP density coverage in *STRC* or qPCR provide the most comprehensive methods for the detection of disease causing mutations. In contrast to the Illumina Omni1-Quad arrays, recent experience has demonstrated that the 298K Illumina CytoSNP-12 arrays do not provide high enough SNP coverage in this gene. This array only has one SNP probe in the gene as opposed to the Illumina Omni1-Quad with seven. The

array type that is used for follow-up investigation should be carefully selected on the basis of density in this gene and flanking regions.

The results disclosed in this study support Sanger sequencing and qPCR copy number testing of *STRC* after mutations in *GJB2* have been excluded, especially when recessive, postlingual HL acutely affecting high frequencies is presented.

6.4 Confirmation of *GRHL2* as the gene for the DFNA28 locus

The gDNA from one individual with a well-documented family history of postlingual ADHL was submitted for 80 gene targeted NGS that disclosed a c.1258-1G>A heterozygous mutation in the gene *GRHL2*. Nine additional family members, both with HL and normal hearing, were recruited for Sanger sequencing mutation segregation analysis (Attachment 4, Figure 1). Table 5 discloses the results of mutational segregation in those who were tested with familial relationship to the index patient, as well as clinical hearing status and onset, when HL was present.

Pedigree ID	Relationship to IV:4	c.1258-1 G>A	Affected	Onset
III:1	Father	-	No	NA
III:2	Mother	+	Yes	Fifth decade of life
III:3	Maternal uncle	+	Yes	Middle of seventh decade of life
III:4	Maternal uncle	+	Yes	Fifth decade of life
IV:2	Sister	+	No[1]	NA
IV:3	Brother	+	Yes	Fifth decade of life
IV:4*	Index patient	+	Yes	Early fourth decade of life
V:1	Nephew (son of IV:2)	+	No	NA
V:2	Niece (daughter of IV:2)	-	No	NA
V:3	Daughter	-	No	NA

Table 5. Summary of gDNA testing results for the *GRHL2* c.1258-1G>A mutation. Hearing status and onset information are included. The index patient is individual IV:4, marked with an asterisk, with an earlier than typical onset. A "+" or "–" symbol indicates positive or negative mutation status, respectively. Individual IV:2 has the mutation and normal hearing apart from mild HL in the right ear (6 and 8 kHz frequencies) that is not severe enough for hearing aid intervention. The onset ranges from early fourth to middle of the seventh decade of life.

The c.1258-1G>A mutation resides in intron 9, one nt before exon 10 in the 3' splice consensus sequence region having one of two likely consequences on the splicing of exon 10: (1) with the destruction of the splice site, complete exon skipping is a possibility, or (2) in combination with the sequence change introduced by the guanine (G) to adenine (A) mutation and the first nt of exon 10 being a G, a 3' cryptic splice mutation could be activated. The large red box in figure 8 depicts the region of interest with both the wild type (upper) and mutated sequences (lower).

Two smaller red boxes show the 3' splice consensus AG sequence, which hints to a shift in the overall splice position.

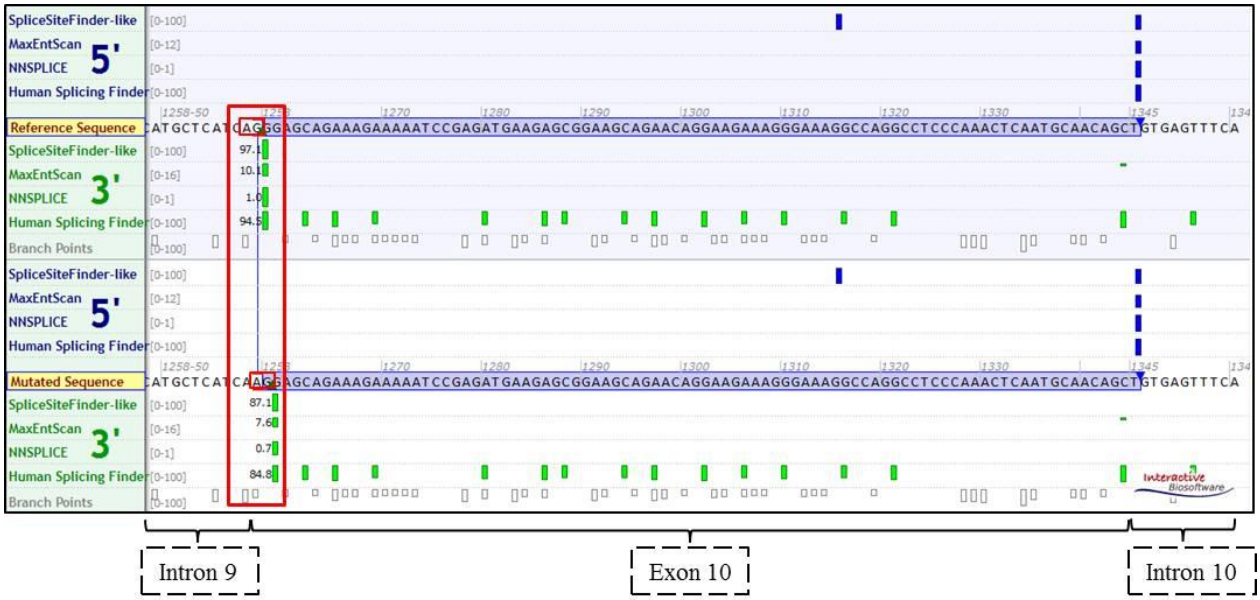

Figure 8. Splice prediction outcomes for the *GRHL2* c.1258-1G>A mutation. The long blue bars with sequence represents exon 10. The flanking unhighlighted sequences on the left and right sides illustrate introns 9 and 10, respectively. Each of the four prediction programs has a specific scale for judging splice strength shown in gray numbers to the left. The upper green bar section represents the wild type sequence with the splice scores to the left. The lower green bar section shows the impact the mutation has on the predicted splice position and splice strength scores. The image was generated using the Alamut splice window tool.

To test this splice site mutation, the expression profile of *GRHL2* was analyzed to select the best non-invasive tissue for mRNA extraction, followed by cDNA synthesis. The best non-invasive tissues are the oral mucosa, saliva, skin, and blood. Figure 9 shows the expression profile for *GRHL2* in these tissues. A two milliliter (mL) saliva sample was collected from the proband and a normal hearing control for mRNA extraction that was followed by cDNA synthesis, and target amplification for Sanger sequencing. The consequence of the splice mutation was observed in the proband sequencing chromatograms with an apparent heterozygous frameshift, illustrating that the exon is not skipped, but rather spliced incorrectly with the activation of a cryptic splice site resulting in a single nt deletion (Attachment 4, Figures 4B and 4C). Nevertheless, the cDNA sequence does not demonstrate a splicing aberration on the whole exon level. Given the cDNA sequencing data, there is a high probability that this mutation negatively impacts the protein. There are several hypothesized outcomes as a consequence of mutations leading to premature termination codons, two of which are nonsense-mediated mRNA decay and loss of protein function via protein truncation; however, this was not investigated in our present study

[152,153]. It should also be noted that apart from our index patient, other family members were not evaluated for mutations on the cDNA level, although it is expected that the same splicing effect would also be present in accordance with the cDNA results disclosed in this study.

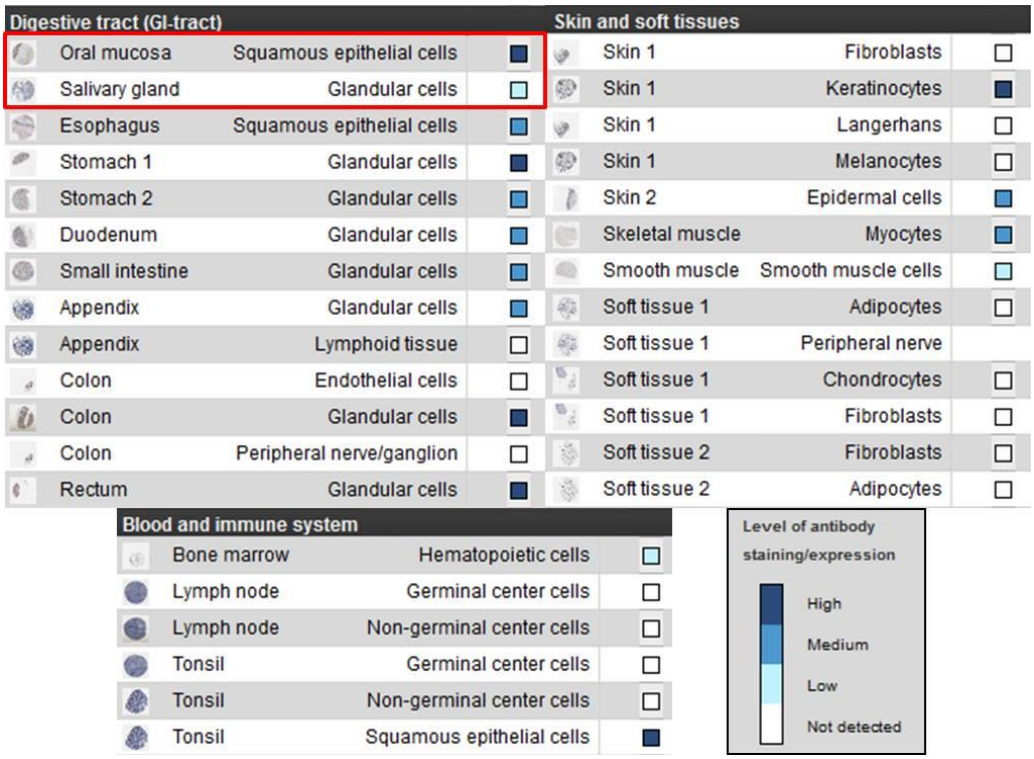

Figure 9. Human expression profile of GRHL2. Various specialized cell types of the digestive tract, skin and soft tissues, and blood and immune system were analyzed. The key indicating level of expression is in the lower right section that corresponds with expression level in each tissue type. Dark blue indicates high, middle blue shows medium, light blue illustrates low, and white depicts a lack of expression, respectively. The red box marks the tissue types obtained in the saliva sample for analysis. The GRHL2 expression profile was obtained from the Human Protein Atlas.

This mutation segregated in III:2, III:3, III:4, and IV:3 with a characteristic late onset HL diagnosed in the fifth to seventh decades of life and also segregated in individual IV:2, who was 44 years-old at the time of last acquired audiogram. She had normal hearing in the left ear and normal hearing for all frequencies in the right ear except for 50 and 30 dB threshold responses at 6 and 8 kHz, respectively. This is most likely indicative of early hearing degeneration. Individuals V:1, V:2, and V:3 were all tested with only V:1 having the mutation. All three individuals are in their first decade of life and thus well below the age of onset. This testing was performed as a predictive measure to encourage the avoidance of noisy environments in those with the mutation to prevent premature hearing decline.

The proband has an unusually early HL onset that was first diagnosed at 32 years of age and a more pronounced progression of HL compared to other nuclear family members. Annual threshold deterioration (ATD) linear regressions were calculated by averaging the audiometric thresholds across all frequencies according to age of audiogram measurement for individuals III:2, III:3, III:4, IV:2 and IV:4 and compared these values against control audiograms from normal hearing individuals in the same age range to demonstrate expected HL due to presbycusis (Attachment 4, Figure 3A). The ATD plots of the dB thresholds at each of the routinely measured frequencies across a number of years disclose the dB per year that are lost due to the progressive nature of HL from mutations in this gene. For this measurement, an extensive collection of audiograms over many years/decades were maintained (Attachment 4, Figure 2). The ATD plots clustered linearly per individual, showing a positive correlation between HL progression and advancing age exceeding that from presbycusis. The only exception was individual IV:2 having only one audiogram available and therefore not enough data for ATD plots. The proband, with an earlier than typical onset, also demonstrated a larger loss in hearing capacity with approximately 2.41 dB lost annually. His other family members have ATDs ranging between 0.76 dB and 1.69 dB per year (Attachment 4, Figure 3B). Hearing thresholds were compared across ears to determine the possibility of a lateral HL asymmetry over time. The proband showed a slight decline in hearing in the right ear. The same right-ear worsening was not observed in his other family members. The decline in hearing capacity in these individuals is predictable and has a linear relationship over time.

The explanation of a variable onset and severity in the proband could be due to the compounded impact of co-morbidities. The proband was diagnosed with type I diabetes at the age of 10 years with no further clinical phenotypes. HL is also reported to extend to more distant family members. A number of these family members have other co-morbidities noted such as epilepsy and reduced intelligence quotient, which could influence the onset and severity of HL. Some of the other family members (I:3, II:4, II:5, II:10, III:6, III:8, III:10, and III:11) in the pedigree have a postlingual childhood onset, with an unknown explanation for this variability (Attachment 4, Figure 1). Detailed medical records were not always available for all family members. Two hypotheses for this observation are the interplay of environmental and genetic factors causing earlier onset and the segregation of other mutations altering the type of HL described. As these members were unavailable for genetic testing, this is unable to be resolved.

As this is the second family described to date with a novel DFNA28 mutation, *GRHL2* is validated as having an indispensable role in normal hearing and is correctly assigned as a NSHL

gene. The reproducibility of mutations fitting a specific HL phenotype are important for confirmation of a gene being correctly associated with NSHL. The detailed audiological analysis described in Attachment 4 further expands the genotype-phenotype character of HL caused by mutations in this gene.

6.5 Targeted deafness gene next generation sequencing of hearing impaired individuals uncovers informative mutations

The advent and increased availability of NGS technologies has created new possibilities for genetic diagnostics. Targeted NGS in the form of gene panels provides a powerful approach to screening only disease relevant genes. A total of 23 probands were screened using one of two different panel types consisting of either 80 or 129 genes (Attachment 5, Table S2). These individuals were screened on the Illumina Omni1-Quad arrays and were negative for clearly pathogenic CNVs, with one exception being the heterozygous deletion of exons 58-64 in the 72 exon gene, *USH2A*. Furthermore, clinical information was collected for all patients except two (Attachment 5, Table S1). Pedigree information was obtained from all patients to aid with mutation analysis. Parents and siblings were also recruited for segregation analysis upon the detection of a mutation possibly explaining the phenotype, but it was not obtainable from all family members in every case. Based on pedigree information and variant analysis, the patients were grouped into one of three categories: (1) dominant group (abbreviated "D"), (2) recessive group (abbreviated "R"), or (3) unsolved group (abbreviated "U"). Ultimately, there were eight dominant, five recessive and ten unsolved group patients. The patients were assigned to the unsolved group if an appropriate mutation was not disclosed from the analysis. Nine subjectively normal hearing controls were included for variant filtering assistance and statistical comparison.

Quality and coverage per patient and control were analyzed for missed or poorly performing exons. Missing or poorly covered exons were uniform among patients and thus probably not due to deletion(s). Since all variants were of potential interest for statistical methods, data were filtered conservatively based on minimum depth and quality scores. Three mutation interpretation programs were used (MutationTaster, PolyPhen-2 and SIFT), with the requirement for inclusion of a variant being two out of three *in silico* predictions in agreement with judging a variant as damaging or deleterious. This resulted in a total of 89 variants in the patients and 14 variants in the controls (Attachment 5, Table S4), which include pathogenic mutations or variants

predicted to be pathogenic or damaging but not supporting the type of inheritance suggested by the clinical or pedigree information.

Strong pathogenic mutations implicative of HL were detected in 12 of the patients, yielding a success rate of 52% (Attachment 5, Figures 1 and 2). The dominant and recessive group mutations are summarized in Table 6.

Group Name	Gene	Mutation	Zygosity
D1	*MYO6*	c.884_893delGCAAAAGTCC (p.R295Lfs*13)	Heterozygous
D2	*ACTG1*	c.974T>A (p.M325K)	Heterozygous
D3	*TCF21*	c.63C>G (p.D21E)	Heterozygous
D4	*CCDC50*	c.227G>A (R76H)	Heterozygous
D5	*MYO1A*	c.2032A>T (p.I678F)	Heterozygous
D6	*MYH14*	c.5008C>T (p.R1670C)	Heterozygous
D7	*MYO1A*	c.2390C>T (p.S797F)	Heterozygous
D8	*EYA4*	c.1341-19T>A	Heterozygous
R1	*MYO15A*	c.1137delC (p.Y380Mfs*65); c.7124_7127delACAG (p.D2375Vfs*29)	Compound heterozygous
R2	*MYO7A*	c.3935T>C (p.L1312P)	Homozygous
R3	*USH2A*	c.1841-2A>G and c.2440C>T (p.Q814*)	Compound heterozygous
R4	*USH2A*	c.2776G>T (p.C759F)	Compound heteroyzgous
R5	*GJB2*	c.35delG (p.G12Vfs*2)	Homozygous

Table 6. Summary of NGS mutations.

Further comparative analysis was performed using the 80 overlapping genes between the two panel types. The 129 gene panel includes more genes with the same 80 core genes in common (Attachment 5, Table S5). The median number of variants in each of the different groups was 4.5, 3.6, 3.0, and 1.4 in the dominant, recessive, unsolved, and control groups, respectively (Attachment 5, Figure 3). Pairwise Wilcoxon tests with multiple testing correction revealed significant p-values when comparing each of the three patient groups to the control group, but not among the different case groups. Further analysis of the distribution patterns between the control and unsolved groups disclosed extensive heterogeneity between the patient groups and the control group (Attachment 5, Figure S1). The control group shows only a few variants with a higher similarity compared to the numerous and diverse mutations in the patient unsolved group.

The *EYA4* c.1341-19T>A splice site mutation (Figure 10) was tested using a two mL saliva sample from each of the two affected family members and the same method previously described and specific *EYA4* cDNA primers for splice site confirmation [154]. Other non-invasive tissues had poor expression (Figure 11). Unfortunately, this did not yield specific or adequate product, which may be because expression of this gene is too low in saliva and/or oral mucosa. Other tissues with higher expression are not possible to test, such as skeletal muscle, lung, and heart

with high *EYA4* expression. It is of possible interest that an earlier publication [155] described a c.1282-12T>A novel splice site mutation in this gene wherein the authors describe being unable to test the splice mutation due to not being able to obtain suitable patient material for mRNA analysis. The material that was tested, if any, was not disclosed in this study. The c.1341-19T>A splice mutation remains unclear; however, onset of HL and audiogram profiles were in accordance with those previously described for *EYA4* [155]. Onset in the proband was around six years of age, which is the earliest onset described from the earlier publication, and audiograms are in agreement with a "cookie bite" profile with all frequencies affected [155] .

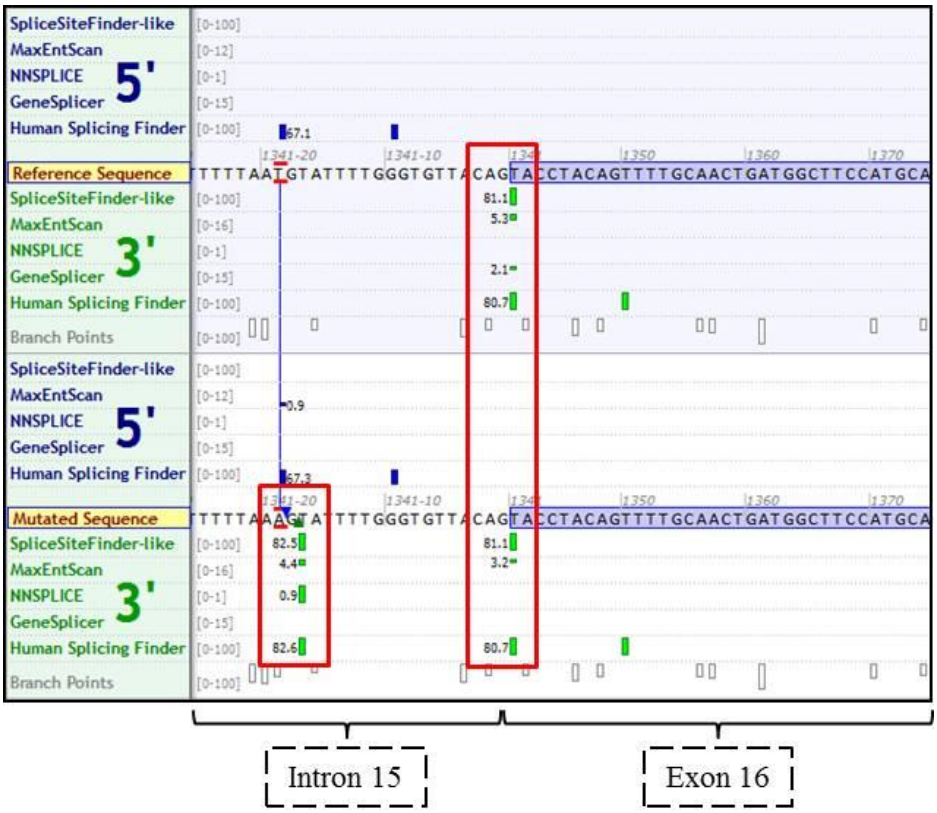

Figure 10. Splice prediction outcomes for the *EYA4* c.1341-19T>A mutation. The long blue bars with sequence represents exon 16. The unhighlighted sequence to the left side illustrates intron 15. Each of the four prediction programs has a specific scale for judging splice strength shown in gray numbers to the left. The upper green bar section represents the wild type sequence with the splice scores to the left. The lower left green bar section shows the predicted activation of a 3' cryptic splice site and splice strength scores. The new mutation (bottom left) shows an increased splice strength compared to the wild type score. The image was generated using Alamut the splice window tool.

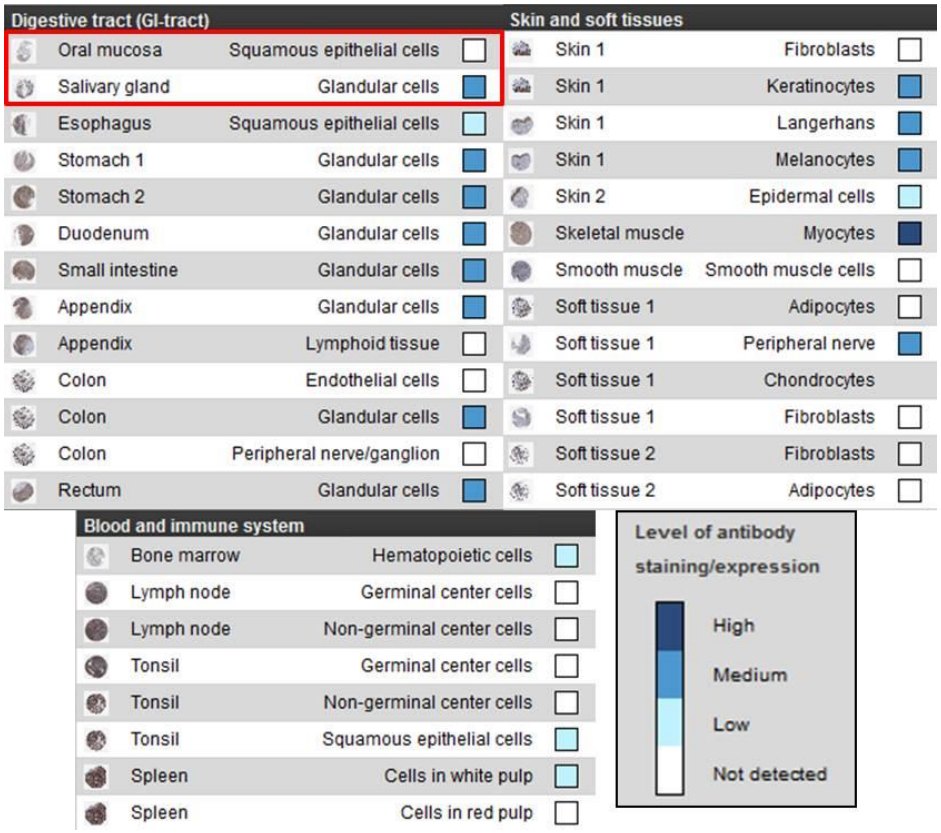

Figure 11. Human expression profile of EYA4. Various specialized cell types of the digestive tract, skin and soft tissues, and blood and immune system were analyzed. The key indicating level of expression is in the lower right section that corresponds with expression level in each tissue type. Dark blue indicates high, middle blue shows medium, light blue illustrates low, and white depicts a lack of expression, respectively. The red box marks the tissue types obtained in the saliva sample for analysis. The EYA4 expression profile was obtained from the Human Protein Atlas.

An additional patient that was included on a previous microarray indicated a heterozygous deletion in *USH2A* (Figure 12) that was not obvious from the NGS coverage on a per exon basis. This deletion has not been described in HGMD or USHbases, which is a database specifically for Usher syndrome mutations. Biallelic mutations in *USH2A* result in early onset HL and retinitis pigmentosa around puberty. The coverage of each of the exons included in the deletion, as well as exons external to the deletion were checked (Table 7). Validation was performed via qPCRs for exons 61, 63 and 64. The average sequencing depth of the *USH2A* gene is 271; however, the sequencing depth of each exon and particularly in exons that are not deleted did not show uniformity indicative of copy number status. This means that the possibility of detecting the deletion per hand is not possible since the DNAnexus bioinformatic software that was used for analysis and variant calling did not have a tool for CNV calling.

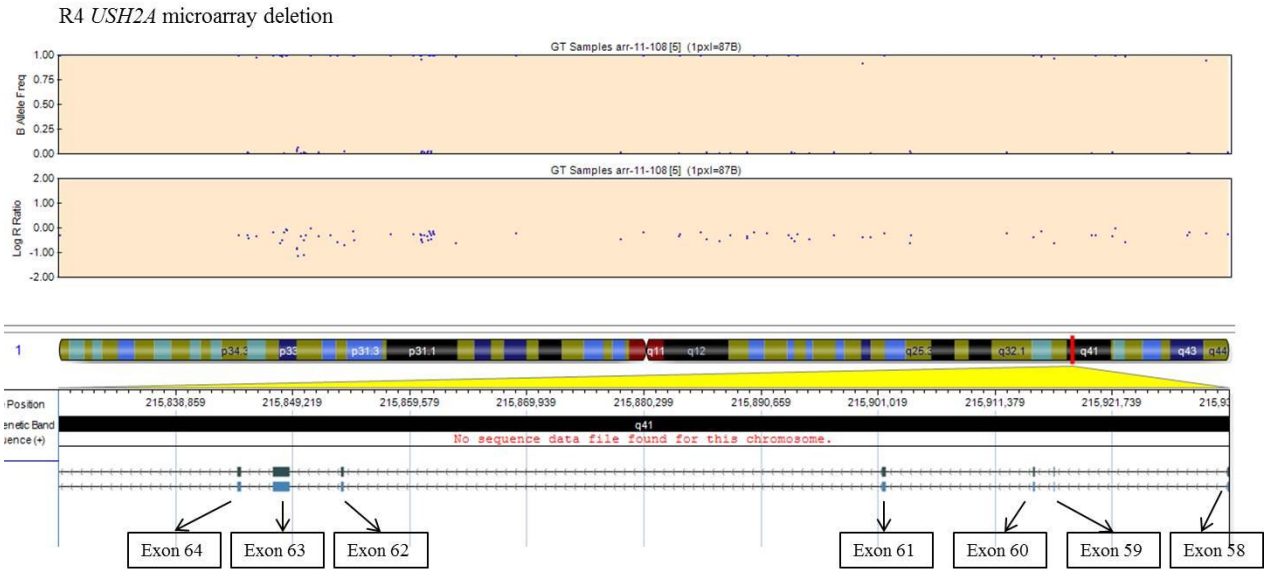

Figure 12. Illustration of the 99.9 kb *USH2A* heterozygous deletion. This deletion encompasses exons 58-64.

Exon	Depth	Exon	Depth
58	140	7	82
59	185	13	175
60	144	26	92
61	232	34	64
62	117	45	175
63	35	46	173
64	102	53	209

Table 7. *USH2A* NGS depth example. Example of exon depth for the *USH2A* heterozygous deletion and exons external to the deletion for comparison. The left side of the table represents the sequencing depth of the exons included in the deletion. The right side illustrates the coverage of exons not included in the deletion for comparison. The heterozygous deletion is not evident from the sequence coverage.

Ten patients from this cohort were negative for mutations in the known deafness genes included on the panels. These families are the most promising for candidate gene identification using WES, which is currently underway in one of these families.

The observation of an enrichment of deleterious variants in genes important for normal hearing function in the HL patients compared to controls supported a mutational load hypothesis. Deleterious variants in hearing required genes in the control group appears at a much lower frequency than in the majority of HL patients. This observation supports the formation of two hypotheses: (1) an accumulation of deleterious variants predicted to be damaging could contribute to HL, and (2) HL has a complex dimension expanding its conventional understanding. Together, these two hypotheses comprise an area for future investigation resulting from this work.

The NGS testing from this work has disclosed several clinical benefits that underscore the power stemming from this method. Firstly, reassessment of a misdiagnosis as seen in the patient with suspected auditory neuropathy later disclosing a homozygous *GJB2* c.35delG mutation was unexpected; however, this emphasizes an advantage of screening many genes in parallel, as misdiagnoses can occur or the complete clinical background of a patient may not be fully understood or at full presentation at the time of patient examination. The initial *GJB2* screen was missed in this patient because single gene *OTOF* Sanger sequencing was priority with the diagnosed auditory neuropathy, which was negative for informative mutations. Secondly, the value of providing an early diagnosis of syndromic HL supports early intervention and lifestyle modification, as well as routine monitoring from respective specialist physicians. This has potential benefit specifically for the two probands with *USH2A* mutations conferring Usher syndrome type 2 and the proband with the *TCF21* mutation associated with adult-onset cardiomyopathy. All three probands are young children and thus below the age of onset for the additional symptoms that would confirm syndromic HL.

The main limitation of this study is the small sample size; nonetheless, the statistics that were performed were conservative and disclose a result that should be replicated in an expanded study. However, the strong initial solve rate communicated from this small sample size provides a positive outlook for this method as molecular genetics is rapidly changing to NGS based approaches.

7. Conclusion and Outlook

The recent expanded availability and shift to massively parallel NGS methods is revolutionizing HL research and diagnostics and providing never before feasible tools such as the coordinated sequencing of hundreds of genes in a single experiment. NGS investigations can bridge the gap between genotype and phenotype, as there is not always a clear distinction between syndromic and non-syndromic HL, which can be particularly problematic in young children. Predictive or early diagnosis of syndromic HL, such as the Usher syndrome and cardiomyopathy cases described, may provide beneficial outcomes to these patients, since primary referral to an appropriate team of physicians can be coordinated before onset of additional symptoms occurs. This is especially relevant since Usher syndrome is more prevalent than expected. As demonstrated in this study, mutations in known deafness genes are able to solve roughly half of *GJB2* negative cases, supporting a high diagnostic yield and a practical method from which to approach the diagnostics of heterogeneous disorders such as HL.

The identification of the second autosomal dominant family worldwide with a mutation in the gene *GRHL2* provided significant support for the correct assignment of *GRHL2* as a NSHL gene. Extensive audiometric analysis systematically characterized the HL in multiple family members to expand the genotype-phenotype correlation in a gene with only one previous description of a family with DFNA28 HL.

The *STRC* assay that was developed significantly contributes to the molecular genetic assessment in pediatric onset, high frequency HL patients, since the importance of *STRC* has been grossly underestimated as the testing of this gene is complicated by *pSTRC*. Furthermore, it is recommended that for *GJB2* negative patients fulfilling clinical criteria, *STRC* is prioritized as the second gene to be sequenced.

Every method has limitations that can be reduced through a multiple approach. The SNP array that was employed in this study narrowed certain restrictions seen in NGS. Firstly, NGS bioinformatic tools, as presently demonstrated, are unable to detect heterozygous deletions. In the context of the heterozygous deletion and heterozygous damaging SNV as seen in the *USH2A* example, a missed Usher syndrome diagnosis would have resulted, had the SNP array not been employed. Secondly, the nearly identical pseudogene sequence of *STRC* interferes with clean sequence acquisition and analysis because the target enrichment methods used for NGS library preparation amplify and target both regions for massively parallel sequencing. Finally, since the

most considerable success came with NGS analysis, it is apparent that mutations causing HL are largely SNVs and not structural variants that are detected by SNP arrays. The resolution of the SNP arrays cannot detect all possible structural variants, but they are an important tool for ruling out the possibility of these variations as implicative in HL. The combination of SNP arrays with NGS explored in this study not only helps to elucidate the mutation spectrum of various deafness genes, but also bears a potential impact in a diagnostic service to HL patients.

The NGS bioinformatic tools for assessing SNVs/CNVs will continue to improve, as well as continued advancements with enrichment protocols that will aim to overcome technical limitations. In the foreseeable future, it will not be possible to exclude pseudogene sequence without a LR-PCR protocol, so the assay developed in the context of this work will not be quickly obsolete but rather employable for many years to come.

The multiple mutations that were detected in the patients through the targeted deafness gene NGS study are time consuming to follow-up. Singleton patients complicate the chances of a successful and definitive analysis, since segregation analysis of mutations in a family are essential for complete understanding of pathogenicity. There is no substitution for familial recruitment and involvement, especially in the context of HL, since this study demonstrates HL patients have a higher median number of mutations compared to normal hearing controls. For continued success of future work, the cohesive teamwork from both medical and laboratory departments is indispensable; however, the future outlook for new gene discovery and the value of NGS diagnosis for patients and their families provide an invaluable benefit for participating patients.

In conclusion, the current study identified and detailed clinical information and HL descriptions for fifteen novel mutations not described previously in the literature.

8. References

1. Organization WH (2008) The global burden of disease: 2004 update. Geneva: World Health Organization.

2. Zahnert T (2011) The differential diagnosis of hearing loss. Dtsch Arztebl Int 108: 433-443.

3. Bloom DE CE, Jané-Llopis E, Abrahams-Gessel S, Bloom LR, Fathima S, Feigl AB, Gaziano T, Mowafi M, Pandya A, Prettner K, Rosenberg L, Seligman B, Stein AZ, Weinstein C (2011) The Global Economic Burden of Noncommunicable Diseases Geneva: World Economic Forum.

4. (2006) Listen hear! The economic impact and cost of hearing loss in Australia. CRC for cochlear implant and hearing aid innovation and Vicdeaf. Victoria, Australia.

5. McMahon CM, Gopinath B, Schneider J, Reath J, Hickson L, et al. (2013) The need for improved detection and management of adult-onset hearing loss in Australia. Int J Otolaryngol 2013: 308509.

6. Stevens G, Flaxman S, Brunskill E, Mascarenhas M, Mathers CD, et al. (2013) Global and regional hearing impairment prevalence: an analysis of 42 studies in 29 countries. Eur J Public Health 23: 146-152.

7. Smith RJ, Bale JF, Jr., White KR (2005) Sensorineural hearing loss in children. Lancet 365: 879-890.

8. Morton CC, Nance WE (2006) Newborn hearing screening--a silent revolution. N Engl J Med 354: 2151-2164.

9. Nance WE (2003) The genetics of deafness. Ment Retard Dev Disabil Res Rev 9: 109-119.

10. Petersen MB, Wang Q, Willems PJ (2008) Sex-linked deafness. Clin Genet 73: 14-23.

11. Savige J, Gregory M, Gross O, Kashtan C, Ding J, et al. (2013) Expert guidelines for the management of Alport syndrome and thin basement membrane nephropathy. J Am Soc Nephrol 24: 364-375.

12. Sanyoura M, Woudstra C, Halaby G, Baz P, Senee V, et al. (2014) A novel ALMS1 splice mutation in a non-obese juvenile-onset insulin-dependent syndromic diabetic patient. Eur J Hum Genet 22: 140-143.

13. Huang BY, Zdanski C, Castillo M (2012) Pediatric sensorineural hearing loss, part 2: syndromic and acquired causes. AJNR Am J Neuroradiol 33: 399-406.

14. Funke B, Epstein JA, Kochilas LK, Lu MM, Pandita RK, et al. (2001) Mice overexpressing genes from the 22q11 region deleted in velo-cardio-facial syndrome/DiGeorge syndrome have middle and inner ear defects. Hum Mol Genet 10: 2549-2556.

15. Mazzoni DS, Ackley RS, Nash DJ (1994) Abnormal pinna type and hearing loss correlations in Down's syndrome. J Intellect Disabil Res 38 (Pt 6): 549-560.

16. Raut P, Sriram B, Yeoh A, Hee KY, Lim SB, et al. (2011) High prevalence of hearing loss in Down syndrome at first year of life. Ann Acad Med Singapore 40: 493-498.

17. Baumann M, Giunta C, Krabichler B, Ruschendorf F, Zoppi N, et al. (2012) Mutations in FKBP14 cause a variant of Ehlers-Danlos syndrome with progressive kyphoscoliosis, myopathy, and hearing loss. Am J Hum Genet 90: 201-216.

18. Sylvester PE (1958) Some unusual findings in a family with Friedreich's ataxia. Arch Dis Child 33: 217-221.

19. Evans-Galea MV, Lockhart PJ, Galea CA, Hannan AJ, Delatycki MB (2014) Beyond loss of frataxin: the complex molecular pathology of Friedreich ataxia. Discov Med 17: 25-35.

20. Martelli H, Jr., Miranda RT, Fernandes CM, Bonan PR, Paranaiba LM, et al. (2010) Goldenhar syndrome: clinical features with orofacial emphasis. J Appl Oral Sci 18: 646-649.

21. Armstrong L, Graham GE, Schimke RN, Collins DL, Kirse DJ, et al. (2008) The Hunter-MacDonald syndrome with expanded phenotype including risk of meningioma: an update and review. Am J Med Genet A 146A: 83-92.

22. Wang RY, Bodamer OA, Watson MS, Wilcox WR (2011) Lysosomal storage diseases: diagnostic confirmation and management of presymptomatic individuals. Genet Med 13: 457-484.

23. Hedley PL, Jorgensen P, Schlamowitz S, Wangari R, Moolman-Smook J, et al. (2009) The genetic basis of long QT and short QT syndromes: a mutation update. Hum Mutat 30: 1486-1511.

24. Plotkin SR, Ardern-Holmes SL, Barker FG, 2nd, Blakeley JO, Evans DG, et al. (2013) Hearing and facial function outcomes for neurofibromatosis 2 clinical trials. Neurology 81: S25-32.

25. Agarwal P, Philip R, Gutch M, Gupta KK (2013) The other side of Turner's: Noonan's syndrome. Indian J Endocrinol Metab 17: 794-798.

26. Bayazit YA, Yilmaz M (2006) An overview of hereditary hearing loss. ORL J Otorhinolaryngol Relat Spec 68: 57-63.

27. Gonzales M, Heuertz S, Martinovic J, Delahaye S, Bazin A, et al. (2005) Vertebral anomalies and cartilaginous tracheal sleeve in three patients with Pfeiffer syndrome carrying the S351C FGFR2 mutation. Clin Genet 68: 179-181.

28. Acke FR, Dhooge IJ, Malfait F, De Leenheer EM (2012) Hearing impairment in Stickler syndrome: a systematic review. Orphanet J Rare Dis 7: 84.

29. Riazuddin S, Belyantseva IA, Giese AP, Lee K, Indzhykulian AA, et al. (2012) Alterations of the CIB2 calcium- and integrin-binding protein cause Usher syndrome type 1J and nonsyndromic deafness DFNB48. Nat Genet 44: 1265-1271.

30. Puffenberger EG, Jinks RN, Sougnez C, Cibulskis K, Willert RA, et al. (2012) Genetic mapping and exome sequencing identify variants associated with five novel diseases. PLoS One 7: e28936.

31. Ebermann I, Wiesen MH, Zrenner E, Lopez I, Pigeon R, et al. (2009) GPR98 mutations cause Usher syndrome type 2 in males. J Med Genet 46: 277-280.

32. Weil D, El-Amraoui A, Masmoudi S, Mustapha M, Kikkawa Y, et al. (2003) Usher syndrome type I G (USH1G) is caused by mutations in the gene encoding SANS, a protein that associates with the USH1C protein, harmonin. Hum Mol Genet 12: 463-471.

33. Friedman TB, Griffith AJ (2003) Human nonsyndromic sensorineural deafness. Annu Rev Genomics Hum Genet 4: 341-402.

34. Hoefsloot LH, Feenstra I, Kunst HP, Kremer H (2013) Genotype-phenotype correlations for nonsyndromic hearing impairment: approaches to management. Clin Genet.

35. Kenneson A, Van Naarden Braun K, Boyle C (2002) GJB2 (connexin 26) variants and nonsyndromic sensorineural hearing loss: a HuGE review. Genet Med 4: 258-274.

36. Donaudy F, Ferrara A, Esposito L, Hertzano R, Ben-David O, et al. (2003) Multiple mutations of MYO1A, a cochlear-expressed gene, in sensorineural hearing loss. Am J Hum Genet 72: 1571-1577.

37. Modell B, Darr A (2002) Science and society: genetic counselling and customary consanguineous marriage. Nat Rev Genet 3: 225-229.

38. Hussain R, Bittles AH (1998) The prevalence and demographic characteristics of consanguineous marriages in Pakistan. J Biosoc Sci 30: 261-275.

39. Veske A, Oehlmann R, Younus F, Mohyuddin A, Muller-Myhsok B, et al. (1996) Autosomal recessive non-syndromic deafness locus (DFNB8) maps on chromosome 21q22 in a large consanguineous kindred from Pakistan. Hum Mol Genet 5: 165-168.

40. Scott HS, Kudoh J, Wattenhofer M, Shibuya K, Berry A, et al. (2001) Insertion of beta-satellite repeats identifies a transmembrane protease causing both congenital and childhood onset autosomal recessive deafness. Nat Genet 27: 59-63.

41. Verpy E, Masmoudi S, Zwaenepoel I, Leibovici M, Hutchin TP, et al. (2001) Mutations in a new gene encoding a protein of the hair bundle cause non-syndromic deafness at the DFNB16 locus. Nat Genet 29: 345-349.

42. Moynihan L, Houseman M, Newton V, Mueller R, Lench N (1999) DFNB20: a novel locus for autosomal recessive, non-syndromal sensorineural hearing loss maps to chromosome 11q25-qter. Eur J Hum Genet 7: 243-246.

43. Wilcox ER, Burton QL, Naz S, Riazuddin S, Smith TN, et al. (2001) Mutations in the gene encoding tight junction claudin-14 cause autosomal recessive deafness DFNB29. Cell 104: 165-172.

44. Ansar M, Din MA, Arshad M, Sohail M, Faiyaz-Ul-Haque M, et al. (2003) A novel autosomal recessive non-syndromic deafness locus (DFNB35) maps to 14q24.1-14q24.3 in large consanguineous kindred from Pakistan. Eur J Hum Genet 11: 77-80.

45. Collin RW, Kalay E, Tariq M, Peters T, van der Zwaag B, et al. (2008) Mutations of ESRRB encoding estrogen-related receptor beta cause autosomal-recessive nonsyndromic hearing impairment DFNB35. Am J Hum Genet 82: 125-138.

46. Naz S, Griffith AJ, Riazuddin S, Hampton LL, Battey JF, Jr., et al. (2004) Mutations of ESPN cause autosomal recessive deafness and vestibular dysfunction. J Med Genet 41: 591-595.

47. Ahmed ZM, Morell RJ, Riazuddin S, Gropman A, Shaukat S, et al. (2003) Mutations of MYO6 are associated with recessive deafness, DFNB37. Am J Hum Genet 72: 1315-1322.

48. Schultz JM, Khan SN, Ahmed ZM, Riazuddin S, Waryah AM, et al. (2009) Noncoding mutations of HGF are associated with nonsyndromic hearing loss, DFNB39. Am J Hum Genet 85: 25-39.

49. Aslam M, Wajid M, Chahrour MH, Ansar M, Haque S, et al. (2005) A novel autosomal recessive nonsyndromic hearing impairment locus (DFNB42) maps to chromosome 3q13.31-q22.3. Am J Med Genet A 133A: 18-22.

50. Borck G, Ur Rehman A, Lee K, Pogoda HM, Kakar N, et al. (2011) Loss-of-function mutations of ILDR1 cause autosomal-recessive hearing impairment DFNB42. Am J Hum Genet 88: 127-137.

51. Ansar M, Chahrour MH, Amin Ud Din M, Arshad M, Haque S, et al. (2004) DFNB44, a novel autosomal recessive non-syndromic hearing impairment locus, maps to chromosome 7p14.1-q11.22. Hum Hered 57: 195-199.

52. Santos-Cortez RL, Lee K, Giese AP, Ansar M, Amin-Ud-Din M, et al. (2014) Adenylate cyclase 1 (ADCY1) mutations cause recessive hearing impairment in humans and defects in hair cell function and hearing in zebrafish. Hum Mol Genet.

53. Mir A, Ansar M, Chahrour MH, Pham TL, Wajid M, et al. (2005) Mapping of a novel autosomal recessive nonsyndromic deafness locus (DFNB46) to chromosome 18p11.32-p11.31. Am J Med Genet A 133A: 23-26.

54. Hassan MJ, Santos RL, Rafiq MA, Chahrour MH, Pham TL, et al. (2006) A novel autosomal recessive non-syndromic hearing impairment locus (DFNB47) maps to chromosome 2p25.1-p24.3. Hum Genet 118: 605-610.

55. Ahmad J, Khan SN, Khan SY, Ramzan K, Riazuddin S, et al. (2005) DFNB48, a new nonsyndromic recessive deafness locus, maps to chromosome 15q23-q25.1. Hum Genet 116: 407-412.

56. Ramzan K, Shaikh RS, Ahmad J, Khan SN, Riazuddin S, et al. (2005) A new locus for nonsyndromic deafness DFNB49 maps to chromosome 5q12.3-q14.1. Hum Genet 116: 17-22.

57. Riazuddin S, Ahmed ZM, Fanning AS, Lagziel A, Kitajiri S, et al. (2006) Tricellulin is a tight-junction protein necessary for hearing. Am J Hum Genet 79: 1040-1051.

58. Girotto G, Abdulhadi K, Buniello A, Vozzi D, Licastro D, et al. (2013) Linkage study and exome sequencing identify a BDP1 mutation associated with hereditary hearing loss. PLoS One 8: e80323.

59. Shaikh RS, Ramzan K, Nazli S, Sattar S, Khan SN, et al. (2005) A new locus for nonsyndromic deafness DFNB51 maps to chromosome 11p13-p12. Am J Med Genet A 138: 392-395.

60. Irshad S, Santos RL, Muhammad D, Lee K, McArthur N, et al. (2005) Localization of a novel autosomal recessive non-syndromic hearing impairment locus DFNB55 to chromosome 4q12-q13.2. Clin Genet 68: 262-267.

61. Ali G, Santos RL, John P, Wambangco MA, Lee K, et al. (2006) The mapping of DFNB62, a new locus for autosomal recessive non-syndromic hearing impairment, to chromosome 12p13.2-p11.23. Clin Genet 69: 429-433.

62. Du X, Schwander M, Moresco EM, Viviani P, Haller C, et al. (2008) A catechol-O-methyltransferase that is essential for auditory function in mice and humans. Proc Natl Acad Sci U S A 105: 14609-14614.

63. Ahmed ZM, Masmoudi S, Kalay E, Belyantseva IA, Mosrati MA, et al. (2008) Mutations of LRTOMT, a fusion gene with alternative reading frames, cause nonsyndromic deafness in humans. Nat Genet 40: 1335-1340.

64. Tariq A, Santos RL, Khan MN, Lee K, Hassan MJ, et al. (2006) Localization of a novel autosomal recessive nonsyndromic hearing impairment locus DFNB65 to chromosome 20q13.2-q13.32. J Mol Med (Berl) 84: 484-490.

65. Shabbir MI, Ahmed ZM, Khan SY, Riazuddin S, Waryah AM, et al. (2006) Mutations of human TMHS cause recessively inherited non-syndromic hearing loss. J Med Genet 43: 634-640.

66. Kalay E, Li Y, Uzumcu A, Uyguner O, Collin RW, et al. (2006) Mutations in the lipoma HMGIC fusion partner-like 5 (LHFPL5) gene cause autosomal recessive nonsyndromic hearing loss. Hum Mutat 27: 633-639.

67. Santos RL, Hassan MJ, Sikandar S, Lee K, Ali G, et al. (2006) DFNB68, a novel autosomal recessive non-syndromic hearing impairment locus at chromosomal region 19p13.2. Hum Genet 120: 85-92.

68. Ain Q, Nazli S, Riazuddin S, Jaleel AU, Riazuddin SA, et al. (2007) The autosomal recessive nonsyndromic deafness locus DFNB72 is located on chromosome 19p13.3. Hum Genet 122: 445-450.

69. Rehman AU, Gul K, Morell RJ, Lee K, Ahmed ZM, et al. (2011) Mutations of GIPC3 cause nonsyndromic hearing loss DFNB72 but not DFNB81 that also maps to chromosome 19p. Hum Genet 130: 759-765.

70. Riazuddin S, Anwar S, Fischer M, Ahmed ZM, Khan SY, et al. (2009) Molecular basis of DFNB73: mutations of BSND can cause nonsyndromic deafness or Bartter syndrome. Am J Hum Genet 85: 273-280.

71. Waryah AM, Rehman A, Ahmed ZM, Bashir ZH, Khan SY, et al. (2009) DFNB74, a novel autosomal recessive nonsyndromic hearing impairment locus on chromosome 12q14.2-q15. Clin Genet 76: 270-275.

72. Ahmed ZM, Yousaf R, Lee BC, Khan SN, Lee S, et al. (2011) Functional null mutations of MSRB3 encoding methionine sulfoxide reductase are associated with human deafness DFNB74. Am J Hum Genet 88: 19-29.

73. Rehman AU, Morell RJ, Belyantseva IA, Khan SY, Boger ET, et al. (2010) Targeted capture and next-generation sequencing identifies C9orf75, encoding taperin, as the mutated gene in nonsyndromic deafness DFNB79. Am J Hum Genet 86: 378-388.

74. Ali RA, Rehman AU, Khan SN, Husnain T, Riazuddin S, et al. (2012) DFNB86, a novel autosomal recessive non-syndromic deafness locus on chromosome 16p13.3. Clin Genet 81: 498-500.

75. Rehman AU, Santos-Cortez RL, Morell RJ, Drummond MC, Ito T, et al. (2014) Mutations in TBC1D24, a gene associated with epilepsy, also cause nonsyndromic deafness DFNB86. Am J Hum Genet 94: 144-152.

76. Jaworek TJ, Richard EM, Ivanova AA, Giese AP, Choo DI, et al. (2013) An alteration in ELMOD3, an Arl2 GTPase-activating protein, is associated with hearing impairment in humans. PLoS Genet 9: e1003774.

77. Basit S, Lee K, Habib R, Chen L, Umm e K, et al. (2011) DFNB89, a novel autosomal recessive nonsyndromic hearing impairment locus on chromosome 16q21-q23.2. Hum Genet 129: 379-385.

78. Imtiaz A, Kohrman DC, Naz S (2014) A Frameshift Mutation in GRXCR2 Causes Recessively Inherited Hearing Loss. Hum Mutat 35: 618-624.

79. Chabchoub G, Uz E, Maalej A, Mustafa CA, Rebai A, et al. (2009) Analysis of skewed X-chromosome inactivation in females with rheumatoid arthritis and autoimmune thyroid diseases. Arthritis Res Ther 11: R106.

80. Brown JB, Boley N, Eisman R, May GE, Stoiber MH, et al. (2014) Diversity and dynamics of the Drosophila transcriptome. Nature.

81. (2007) Genes, Hearing, and Deafness. In: Martini A SD, Read AP, editor. London, England: Thompson Publishing Services. pp. 328.

82. Kudo T, Kure S, Ikeda K, Xia AP, Katori Y, et al. (2003) Transgenic expression of a dominant-negative connexin26 causes degeneration of the organ of Corti and non-syndromic deafness. Hum Mol Genet 12: 995-1004.

83. Mahdieh N, Rabbani B (2009) Statistical study of 35delG mutation of GJB2 gene: a meta-analysis of carrier frequency. Int J Audiol 48: 363-370.

84. Samanich J, Lowes C, Burk R, Shanske S, Lu J, et al. (2007) Mutations in GJB2, GJB6, and mitochondrial DNA are rare in African American and Caribbean Hispanic individuals with hearing impairment. Am J Med Genet A 143A: 830-838.

85. Santos RL, Wajid M, Pham TL, Hussan J, Ali G, et al. (2005) Low prevalence of Connexin 26 (GJB2) variants in Pakistani families with autosomal recessive non-syndromic hearing impairment. Clin Genet 67: 61-68.

86. Snoeckx RL, Djelantik B, Van Laer L, Van de Heyning P, Van Camp G (2005) GJB2 (connexin 26) mutations are not a major cause of hearing loss in the Indonesian population. Am J Med Genet A 135: 126-129.

87. Bazazzadegan N, Sheffield AM, Sobhani M, Kahrizi K, Meyer NC, et al. (2011) Two Iranian families with a novel mutation in GJB2 causing autosomal dominant nonsyndromic hearing loss. Am J Med Genet A 155A: 1202-1211.

88. Morle L, Bozon M, Alloisio N, Latour P, Vandenberghe A, et al. (2000) A novel C202F mutation in the connexin26 gene (GJB2) associated with autosomal dominant isolated hearing loss. J Med Genet 37: 368-370.

89. Hackney CM, Furness DN (1986) Intercellular cross-linkages between the stereociliary bundles of adjacent hair cells in the guinea pig cochlea. Cell Tissue Res 245: 685-688.

90. Tsuprun V, Santi P (2002) Structure of outer hair cell stereocilia side and attachment links in the chinchilla cochlea. J Histochem Cytochem 50: 493-502.

91. Goodyear RJ, Marcotti W, Kros CJ, Richardson GP (2005) Development and properties of stereociliary link types in hair cells of the mouse cochlea. J Comp Neurol 485: 75-85.

92. Hoppman N, Aypar U, Brodersen P, Brown N, Wilson J, et al. (2013) Genetic testing for hearing loss in the United States should include deletion/duplication analysis for the deafness/infertility locus at 15q15.3. Mol Cytogenet 6: 19.

93. Francey LJ, Conlin LK, Kadesch HE, Clark D, Berrodin D, et al. (2012) Genome-wide SNP genotyping identifies the Stereocilin (STRC) gene as a major contributor to pediatric bilateral sensorineural hearing impairment. Am J Med Genet A 158A: 298-308.

94. Poliseno L (2012) Pseudogenes: newly discovered players in human cancer. Sci Signal 5: re5.

95. Knijnenburg J, Oberstein SA, Frei K, Lucas T, Gijsbers AC, et al. (2009) A homozygous deletion of a normal variation locus in a patient with hearing loss from non-consanguineous parents. J Med Genet 46: 412-417.

96. Varma S, Cao Y, Tagne JB, Lakshminarayanan M, Li J, et al. (2012) The transcription factors Grainyhead-like 2 and NK2-homeobox 1 form a regulatory loop that coordinates lung epithelial cell morphogenesis and differentiation. J Biol Chem 287: 37282-37295.

97. Quan Y, Jin R, Huang A, Zhao H, Feng B, et al. (2014) Downregulation of GRHL2 inhibits the proliferation of colorectal cancer cells by targeting ZEB1. Cancer Biol Ther 15.

98. Werner S, Frey S, Riethdorf S, Schulze C, Alawi M, et al. (2013) Dual roles of the transcription factor grainyhead-like 2 (GRHL2) in breast cancer. J Biol Chem 288: 22993-23008.

99. Cheng L, Wang P, Yang S, Yang Y, Zhang Q, et al. (2012) Identification of genes with a correlation between copy number and expression in gastric cancer. BMC Med Genomics 5: 14.

100. Kang X, Chen W, Kim RH, Kang MK, Park NH (2009) Regulation of the hTERT promoter activity by MSH2, the hnRNPs K and D, and GRHL2 in human oral squamous cell carcinoma cells. Oncogene 28: 565-574.

101. Tanaka Y, Kanai F, Tada M, Tateishi R, Sanada M, et al. (2008) Gain of GRHL2 is associated with early recurrence of hepatocellular carcinoma. J Hepatol 49: 746-757.

102. Xiang X, Deng Z, Zhuang X, Ju S, Mu J, et al. (2012) Grhl2 determines the epithelial phenotype of breast cancers and promotes tumor progression. PLoS One 7: e50781.

103. Yang X, Vasudevan P, Parekh V, Penev A, Cunningham JM (2013) Bridging cancer biology with the clinic: relative expression of a GRHL2-mediated gene-set pair predicts breast cancer metastasis. PLoS One 8: e56195.

104. Van Laer L, Van Eyken E, Fransen E, Huyghe JR, Topsakal V, et al. (2008) The grainyhead like 2 gene (GRHL2), alias TFCP2L3, is associated with age-related hearing impairment. Hum Mol Genet 17: 159-169.

105. Peters LM, Anderson DW, Griffith AJ, Grundfast KM, San Agustin TB, et al. (2002) Mutation of a transcription factor, TFCP2L3, causes progressive autosomal dominant hearing loss, DFNA28. Hum Mol Genet 11: 2877-2885.

106. Wilanowski T, Tuckfield A, Cerruti L, O'Connell S, Saint R, et al. (2002) A highly conserved novel family of mammalian developmental transcription factors related to Drosophila grainyhead. Mech Dev 114: 37-50.

107. Han Y, Mu Y, Li X, Xu P, Tong J, et al. (2011) Grhl2 deficiency impairs otic development and hearing ability in a zebrafish model of the progressive dominant hearing loss DFNA28. Hum Mol Genet 20: 3213-3226.

108. O'Reilly O GP, Hone S, Kelly V, McGovern B, McShane D, Murphy D, Norman G, Walsh M (1998) Hearing disability assessment. Dublin, Ireland: Department of Health and Children.

109. Dominguez LM, Dodson KM (2012) Genetics of hearing loss: focus on DFNA2. Appl Clin Genet 5: 97-104.

110. Van Laer L, Vrijens K, Thys S, Van Tendeloo VF, Smith RJ, et al. (2004) DFNA5: hearing impairment exon instead of hearing impairment gene? J Med Genet 41: 401-406.

111. Robertson NG, Lu L, Heller S, Merchant SN, Eavey RD, et al. (1998) Mutations in a novel cochlear gene cause DFNA9, a human nonsyndromic deafness with vestibular dysfunction. Nat Genet 20: 299-303.

112. Lynch ED, Lee MK, Morrow JE, Welcsh PL, Leon PE, et al. (1997) Nonsyndromic deafness DFNA1 associated with mutation of a human homolog of the Drosophila gene diaphanous. Science 278: 1315-1318.

113. Goncalves AC, Matos TD, Simoes-Teixeira HR, Pimenta Machado M, Simao M, et al. (2014) WFS1 and non-syndromic low-frequency sensorineural hearing loss: a novel mutation in a Portuguese case. Gene 538: 288-291.

114. De Leenheer EM, Bosman AJ, Kunst HP, Huygen PL, Cremers CW (2004) Audiological characteristics of some affected members of a Dutch DFNA13/COL11A2 family. Ann Otol Rhinol Laryngol 113: 922-929.

115. Govaerts PJ, De Ceulaer G, Daemers K, Verhoeven K, Van Camp G, et al. (1998) A new autosomal-dominant locus (DFNA12) is responsible for a nonsyndromic, midfrequency, prelingual and nonprogressive sensorineural hearing loss. Am J Otol 19: 718-723.

116. Topsakal V, Hilgert N, van Dinther J, Tranebjaerg L, Rendtorff ND, et al. (2010) Genotype-phenotype correlation for DFNA22: characterization of non-syndromic, autosomal dominant, progressive sensorineural hearing loss due to MYO6 mutations. Audiol Neurootol 15: 211-220.

117. Bespalova IN, Van Camp G, Bom SJ, Brown DJ, Cryns K, et al. (2001) Mutations in the Wolfram syndrome 1 gene (WFS1) are a common cause of low frequency sensorineural hearing loss. Hum Mol Genet 10: 2501-2508.

118. Hilgert N, Smith RJ, Van Camp G (2009) Forty-six genes causing nonsyndromic hearing impairment: which ones should be analyzed in DNA diagnostics? Mutat Res 681: 189-196.

119. Harrison M, Roush J, Wallace J (2003) Trends in age of identification and intervention in infants with hearing loss. Ear Hear 24: 89-95.

120. Lin X, Tang W, Ahmad S, Lu J, Colby CC, et al. (2012) Applications of targeted gene capture and next-generation sequencing technologies in studies of human deafness and other genetic disabilities. Hear Res 288: 67-76.

121. Colella S, Yau C, Taylor JM, Mirza G, Butler H, et al. (2007) QuantiSNP: an Objective Bayes Hidden-Markov Model to detect and accurately map copy number variation using SNP genotyping data. Nucleic Acids Res 35: 2013-2025.

122. H V (2010) Identlfying chromosomal abnormalities using Infinium SNP BeadChips.

123. Majewski J, Schwartzentruber J, Lalonde E, Montpetit A, Jabado N (2011) What can exome sequencing do for you? J Med Genet 48: 580-589.

124. Strehle EM (2011) Dysmorphological and pharmacological studies in 4q- syndrome. Genet Couns 22: 173-185.

125. Giuffrè M, La Placa S, Carta M, Cataliotti A, Marino M, et al. (2004) Hypercalciuria and kidney calcifications in terminal 4q deletion syndrome: further evidence for a putative gene on 4q. Am J Med Genet A 126A: 186-190.

126. Strehle EM, Gruszfeld D, Schenk D, Mehta SG, Simonic I, et al. (2012) The spectrum of 4q- syndrome illustrated by a case series. Gene 506: 387-391.

127. Keeling SL, Lee-Jones L, Thompson P (2001) Interstitial deletion 4q32-34 with ulnar deficiency: 4q33 may be the critical region in 4q terminal deletion syndrome. Am J Med Genet 99: 94-98.

128. Calabrese G, Giannotti A, Mingarelli R, Di Gilio MC, Piemontese MR, et al. (1997) Two newborns with chromosome 4 imbalances: deletion 4q33-->q35 and ring r(4)(pterq35.2-qter). Clin Genet 51: 264-267.

129. Ding H, Wu X, Bostrom H, Kim I, Wong N, et al. (2004) A specific requirement for PDGF-C in palate formation and PDGFR-alpha signaling. Nat Genet 36: 1111-1116.

130. Wu D, Wang M, Wang X, Yin N, Song T, et al. (2012) Maternal transmission effect of a PDGF-C SNP on nonsyndromic cleft lip with or without palate from a Chinese population. PLoS One 7: e46477.

131. Vawter MP, Atz ME, Rollins BL, Cooper-Casey KM, Shao L, et al. (2006) Genome scans and gene expression microarrays converge to identify gene regulatory loci relevant in schizophrenia. Hum Genet 119: 558-570.

132. Youngs EL, Henkhaus RS, Hellings JA, Butler MG (2012) 12-year-old boy with a 4q35.2 microdeletion and involvement of MTNR1A, FAT1, and F11 genes. Clin Dysmorphol 21: 93-96.

133. Roberts JL, Hovanes K, Dasouki M, Manzardo AM, Butler MG (2014) Chromosomal microarray analysis of consecutive individuals with autism spectrum disorders or learning disability presenting for genetic services. Gene 535: 70-78.

134. Abou Jamra R, Becker T, Georgi A, Feulner T, Schumacher J, et al. (2008) Genetic variation of the FAT gene at 4q35 is associated with bipolar affective disorder. Mol Psychiatry 13: 277-284.

135. Stańczak P, Witecka J, Szydło A, Gutmajster E, Lisik M, et al. (2009) Mutations in mammalian tolloid-like 1 gene detected in adult patients with ASD. Eur J Hum Genet 17: 344-351.

136. Sasaki MM, Nichols JT, Kimmel CB (2013) edn1 and hand2 Interact in early regulation of pharyngeal arch outgrowth during zebrafish development. PLoS One 8: e67522.

137. Pashmforoush M, Pomies P, Peterson KL, Kubalak S, Ross J, Jr., et al. (2001) Adult mice deficient in actinin-associated LIM-domain protein reveal a developmental pathway for right ventricular cardiomyopathy. Nat Med 7: 591-597.

138. Kakimoto Y, Ito S, Abiru H, Kotani H, Ozeki M, et al. (2013) Sorbin and SH3 domain-containing protein 2 is released from infarcted heart in the very early phase: proteomic analysis of cardiac tissues from patients. J Am Heart Assoc 2: e000565.

139. Sellick GS, Longman C, Tolmie J, Newbury-Ecob R, Geenhalgh L, et al. (2004) Genomewide linkage searches for Mendelian disease loci can be efficiently conducted using high-density SNP genotyping arrays. Nucleic Acids Res 32: e164.

140. Iwamoto K, Bundo M, Ueda J, Nakano Y, Ukai W, et al. (2007) Detection of chromosomal structural alterations in single cells by SNP arrays: a systematic survey of amplification bias and optimized workflow. PLoS One 2: e1306.

141. Hook EB HJ (1977) The frequency of chromosome abnormalities detected in consecutive newborn studies - differences between studies - results by sex and by severity of the phenotypic involvement; Hook Eb PI, editor. New York: Academic Press.

142. Jacobs PA, Browne C, Gregson N, Joyce C, White H (1992) Estimates of the frequency of chromosome abnormalities detectable in unselected newborns using moderate levels of banding. J Med Genet 29: 103-108.

143. Bugge M, Bruun-Petersen G, Brondum-Nielsen K, Friedrich U, Hansen J, et al. (2000) Disease associated balanced chromosome rearrangements: a resource for large scale genotype-phenotype delineation in man. J Med Genet 37: 858-865.

144. Diez-Roux G, Banfi S, Sultan M, Geffers L, Anand S, et al. (2011) A high-resolution anatomical atlas of the transcriptome in the mouse embryo. PLoS Biol 9: e1000582.

145. Delpire E, Lu J, England R, Dull C, Thorne T (1999) Deafness and imbalance associated with inactivation of the secretory Na-K-2Cl co-transporter. Nat Genet 22: 192-195.

146. Nielsen S, Maunsbach AB, Ecelbarger CA, Knepper MA (1998) Ultrastructural localization of Na-K-2Cl cotransporter in thick ascending limb and macula densa of rat kidney. Am J Physiol 275: F885-893.

147. Schmitt R, Ellison DH, Farman N, Rossier BC, Reilly RF, et al. (1999) Developmental expression of sodium entry pathways in rat nephron. Am J Physiol 276: F367-381.

148. Kurtz CL, Karolyi L, Seyberth HW, Koch MC, Vargas R, et al. (1997) A common NKCC2 mutation in Costa Rican Bartter's syndrome patients: evidence for a founder effect. J Am Soc Nephrol 8: 1706-1711.

149. Schneider E, Marker T, Daser A, Frey-Mahn G, Beyer V, et al. (2009) Homozygous disruption of PDZD7 by reciprocal translocation in a consanguineous family: a new member of the Usher syndrome protein interactome causing congenital hearing impairment. Hum Mol Genet 18: 655-666.

150. Kleinjan DA, van Heyningen V (2005) Long-range control of gene expression: emerging mechanisms and disruption in disease. Am J Hum Genet 76: 8-32.

151. Peiffer DA, Le JM, Steemers FJ, Chang W, Jenniges T, et al. (2006) High-resolution genomic profiling of chromosomal aberrations using Infinium whole-genome genotyping. Genome Res 16: 1136-1148.

152. Ware MD, DeSilva D, Sinilnikova OM, Stoppa-Lyonnet D, Tavtigian SV, et al. (2006) Does nonsense-mediated mRNA decay explain the ovarian cancer cluster region of the BRCA2 gene? Oncogene 25: 323-328.

153. Berry FB, Tamimi Y, Carle MV, Lehmann OJ, Walter MA (2005) The establishment of a predictive mutational model of the forkhead domain through the analyses of FOXC2 missense mutations identified in patients with hereditary lymphedema with distichiasis. Hum Mol Genet 14: 2619-2627.

154. Vona B, Nanda I, Neuner C, Muller T, Haaf T (2013) Confirmation of GRHL2 as the gene for the DFNA28 locus. Am J Med Genet A 161A: 2060-2065.

155. Hildebrand MS, Coman D, Yang T, Gardner RJ, Rose E, et al. (2007) A novel splice site mutation in EYA4 causes DFNA10 hearing loss. Am J Med Genet A 143A: 1599-1604.

156. Tamura M, Hosoya M, Fujita M, Iida T, Amano T, et al. (2013) Overdosage of Hand2 causes limb and heart defects in the human chromosomal disorder partial trisomy distal 4q. Hum Mol Genet 22: 2471-2481.

157. Koumandou VL, Scorilas A (2013) Evolution of the plasma and tissue kallikreins, and their alternative splicing isoforms. PLoS One 8: e68074.

158. Duga S, Salomon O (2013) Congenital factor XI deficiency: an update. Semin Thromb Hemost 39: 621-631.

159. Bruder-Nascimento T, Chinnasamy P, Riascos-Bernal DF, Cau SB, Callera GE, et al. (2013) Angiotensin II induces Fat1 expression/activation and vascular smooth muscle

cell migration via Nox1-dependent reactive oxygen species generation. J Mol Cell Cardiol 66C: 18-26.

9. Abbreviations

A	Adenine
ACTG1	Actin, gamma-1; MIM: *102560
ADCY1	Adenylate cyclase 1; MIM: *103072
ADHL	Autosomal dominant hearing loss
ALMS1	Alstrom syndrome 1; MIM: *606844
ARHL	Autosomal recessive hearing loss
ATD	Annual threshold deterioration
ATE1	Arginyltransferase 1; MIM: *607103
BAC	Bacterial artificial chromosome
BDP1	B-double prime 1, subunit of RNA polymerase III transcription initiating factor IIIB; MIM: *607012
bp	Base pair
BRAF	V-raf murine sarcoma viral oncogene homolog B; MIM: *164757
CABP2	Calcium-binding protein 2; MIM: *607314
CCDC50	Coiled-coil domain-containing protein 50; MIM: *611051
CDH23	Cadherin 23; MIM: *605516
cDNA	Complementary DNA
CEACAM16	Carcinoembryonic antigen-related cell adhesion molecule 16; MIM: *614591
CGH	Comparative genomic hybridization
CHD7	Chromodomain helicase DNA-binding protein 7; MIM: *608892
chr	Chromosome
CIB2	Calcium and integrin binding family member 2; MIM: *605564
CLDN14	Claudin 14; MIM: *605608
CNV	Copy number variation
COCH	Cochlin; MIM: *603196
COL2A1	Collagen, type II, alpha-1; MIM: +120140

COL4A3	Collagen, type IV, alpha-3; MIM: +120070
COL4A4	Collagen, type IV, alpha-4; MIM: *120131
COL4A5	Collagen, type IV, alpha-5; MIM: *303630
COL4A6	Collagen, type IV, alpha-6; MIM: *303631
COL9A1	Collagen, type IX, alpha-1; MIM: *120210
COL9A2	Collagen, type IX, alpha-2; MIM: *120260
COL11A1	Collagen, type XI, alpha-1; MIM: *120280
COL11A2	Collagen, type XI, alpha-2; MIM: *120290
CRYM	Crystallin, mu; MIM: *123740
D	Dominant group
dB	Decibels
DFN	Deafness locus annotation (DeaFNess); also represents non-syndromic X-linked deafness locus annotation
DFNA	Autosomal dominant non-syndromic deafness
DFNA5	DFNA5 gene; MIM: *608798
DFNB	Autosomal recessive non-syndromic deafness
DIABLO	Diablo, IAP-binding mitochondrial protein; MIM: *605219
DIAPH1	Diaphanous-related formin 1; MIM: *602121
DNA	Deoxyribonucleic acid
DUX4L6	Double homeobox 4 like 6
E	Embryonic day
ECG	Electrocardiogram
EDN3	Endothelin 3; MIM: *131242
EDNRB	Endothelin receptor, type B; MIM: *133244
ELMOD3	ELMO/CED-12 domain containing 3; MIM: *615427
ESPN	Espin; MIM: *606351
ESRRB	Estrogen-related receptor, beta; MIM: *602167

ESTs	Expressed sequence tags
EYA1	Eyes absent homolog 1; MIM: *601653
EYA4	Eyes absent 4; MIM: *603550
FAT1	FAT atypical cadherin; MIM: *600976
FGFR1	Fibroblast growth factor receptor 1; MIM: *136350
FGFR2	Fibroblast growth factor receptor 2; MIM: *176943
FISH	Fluorescent *in situ* hybridization
FKBP14	FK506-binding protein 14; MIM: *614505
FRG1	FSHD region gene 1; MIM: *601278
G	Guanine
gDNA	Genomic DNA
GDP	Gross domestic product
GIPC3	GIPC PDZ domain-containing family, member 3; MIM: *608792
GJB2	Gap junction protein, beta-2; MIM: *121011
GJB3	Gap junction protein, beta-3; MIM: *603324
GJB6	Gap junction protein beta-6; MIM: *604418
GPR98	G protein-coupled receptor 98; MIM: *602851
GPSM2	G protein signaling modulator 2; MIM: *609245
GRHL2	Grainyhead-like 2 (Drosophila); MIM: *608576
GRXCR1	Glutaredoxin, cysteine-rich 1; MIM: *613283
GRXCR2	Glutaredoxin, cysteine-rich 2; MIM: *615762
GTG	G-banding with trypsin-Giemsa
HAND2	Heart and neural crest derivatives expressed transcript 2; MIM: *602407
HARS	Histidyl-tRNA synthetase; MIM: *142810
HGF	Hepatocyte growth factor; MIM: *142409
HI	Haploinsufficient/haploinsufficiency
HL	Hearing loss

hpf	Hours post-fertilization
ID	Intellectual disability
IDUA	Alpha-L-iduronidase; MIM: *252800
ILDR1	Immunoglobulin-like domain containing receptor 1; MIM: *609739
KARS	Lysyl-tRNA synthetase; MIM: *601421
kb	Kilobase pair
KCNE1	Potassium voltage-gated channel, Isk-related family, member 1; MIM: *176261
KCNQ1	Potassium voltage-gated channel, KQT-like family, member 1; MIM: *607542
KCNQ4	Potassium voltage-gated channel, KQT-like family, member 4; MIM: *603537
kHz	Kilohertz
KRAS	Kirsten rat sarcoma viral oncogene homolog; MIM: *190070
LHFPL5	Lipoma HMGIC fusion partner-like 5; MIM: *609427
LOH	Loss of heterozygosity
LOXHD1	Lipoxygenase homology domain-containing 1; MIM: *613072
LR	Long range
LR-PCR	Long-range PCR
LRTOMT	Leucine-rich transmembrane and O-methyltransferase domain containing; MIM: *612414
MAF	Minor allele frequency
MARVELD2	MARVEL domain containing 2; MIM: *610572
Mb	Megabase pair
MIM	Online Mendelian Inheritance in Man
MIRN96	Micro RNA 96; MIM: *611606
MITF	Microphthalmia-associated transcription factor; MIM: *156845
mL	Milliliter
MLPA	Multiplex ligation-dependent probe amplification
mRNA	Messenger ribonucleic acid

MSRB3	Methionine sulfoxide reductase B3; MIM: *613719
MYH4	Myosin, heavy chain 4, skeletal muscle; MIM: *160742
MYH9	Myosin, heavy chain 9, non-muscle; MIM: *160775
MYO1A	Myosin IA; MIM: *601478
MYO3A	Myosin IIIA; MIM: *606808
MYO6	Myosin VI; MIM: *600970
MYO7A	Myosin VIIA; MIM: *276903
MYO15A	Myosin XVA; MIM: *602666
NDP	Norrie disease (pseudoglioma); MIM: *300658
NF2	Neurofibromin 2; MIM: *607379
NGS	Next generation sequencing
NRAS	Neuroblastoma RAS viral oncogene homolog; MIM: *164790
NSHL	Non-syndromic hearing loss
nt	Nucleotide
OTOA	Otoancorin; MIM: *607038
OTOF	Otoferlin; MIM: *603681
OTOG	Otogelin; MIM: *604487
OTOGL	Otogelin-like protein; MIM: *614925
P	Postnatal day
p	Pseudo
P2RX2	Purinergic receptor P2X, ligand-gated ion channel 2; MIM: *600844
PAX3	Paired box 3; MIM: *606597
PCDH15	Protocadherin 15; MIM: *605514
PCR	Polymerase chain reaction
PDGFC	Platelet-derived growth factor C; MIM: *608452
PDLIM3	PDZ and LIM domain protein 3; MIM: *605889
PDZD7	PDZ domain containing 7; MIM: *612971

PJVK	Pejvakin (DFNB59 gene); MIM: *610219
PNPT1	Polyribonucleotide nucleotidyltransferase 1; MIM: *610316
POU3F4	POU domain, class 3, transcription factor 4: MIM: *300039
POU4F3	POU domain, class 4, transcription factor 3; MIM: *602460
PRPS1	Phosphoribosylpyrophosphate synthetase 1; MIM: *311850
PTPN11	Protein-tyrosine phosphatase, non-receptor type 11; MIM: *176876
PTPRQ	Protein-tyrosine phosphatase, receptor-type, Q; MIM: *603317
qPCR	Quantitative polymerase chain reaction
R	Recessive group
RAF1	V-raf-1 murine leukemia viral oncogene homolog 1; MIM: *164760
RDX	Radixin; MIM: *179410
SANS	Scaffold protein containing ankyrin repeats and SAM domain; MIM: *607696
SCRG1	Scrapie-responsive gene 1; MIM: *603163
SERPINB6	Serpin peptidase inhibitor, clade B (ovalbumin), member 6; MIM: *173321
SHL	Syndromic hearing loss
SIX1	SIX homeobox 1; MIM: *601205
SLC12A1	Solute carrier family 12 (sodium/potassium/chloride transporter), member 1; MIM: *600839
SLC17A8	Solute carrier family 17 (sodium-dependent inorganic phosphate cotransporter), member 8; MIM: *607557
SLC26A4	Solute carrier family 26, member 4; MIM: *605646
SLC26A5	Solute carrier family 26, member 5; MIM: *604943
SMPX	Small muscle protein, X-linked; MIM: *300226
SNAI2	Snail family zinc finger 2; MIM: *602150
SNP	Single nucleotide polymorphism
SNV	Single nucleotide variant
SORBS2	Sorbin and SH3 domain containing 2
SOS1	Son of sevenless homolog 1; MIM: *182530

SOX10	SRY-box 10; MIM: *602229
STRC	Stereocilin; MIM: *606440
TBC1D24	TBC1 domain family, member 24; MIM: *613577
TBX1	T-box 1; MIM: *602054
TECTA	Tectorin alpha; MIM: *602574
ter	Terminus
TJP2	Tight-junction protein 2; MIM: *607709
TLL1	Tolloid-like 1; MIM: *606742
TMC1	Transmembrane channel-like protein 1; MIM: *606706
TMIE	Transmembrane inner ear-expressed gene; MIM: *607237
TMPRSS3	Transmembrane protease, serine 3; MIM: *605511
TNC	Tenascin; MIM: *187380
TPRN	Taperin; MIM: *613354
TRIOBP	TRIO-and F actin binding protein; MIM: *609761
TSPEAR	Thrombospondin-type laminin G domain and EAR repeats; MIM: *612920
U	Unsolved group
UPD	Uniparental disomy
USH1C	Usher syndrome 1C/Harmonin; MIM: *605242
USH2A	Usher syndrome 2A; MIM: *608400
USH3A	Usher syndrome 3A/Clarin 1; MIM: *606397
WES	Whole exome sequencing
WFS1	Wolframin; MIM:*606201
WHO	World Health Organization
WHRN	Whirlin; MIM: *607928

10. Database Sources

Database	Full Database Name	URL
1000 Genomes Project	-	http://www.1000genomes.org/
ClinVar	-	http://www.ncbi.nlm.nih.gov/clinvar/
dbSNP	-	http://www.ncbi.nlm.nih.gov/SNP/
DECIPHER	Database of Chromosomal Imbalance and Phenotype in Humans Using Ensembl Resources	http://decipher.sanger.ac.uk/
DGV	Database of Genomic Variants	http://dgv.tcag.ca/dgv/app/home
Ensembl	-	http://www.ensembl.org/index.html
EVS	Exome Variant Server	http://evs.gs.washington.edu/EVS/
Hereditary Hearing loss Homepage	-	http://hereditaryhearingloss.org/
HGMD	Human Gene Mutation Database	https://portal.biobase-international.com/cgi-bin/portal/login.cgi
HomozygosityMapper	-	http://doro.charite.de/HomozygosityMapper/index.html
Human Protein Atlas	-	http://www.proteinatlas.org/
GeneCards	-	http://www.genecards.org/
MGI	Mouse Genome Informatics	http://www.informatics.jax.org/
MutationTaster	-	http://www.mutationtaster.org/
OMIM	Online Mendelian Inheritance in Man	http://omim.org/
PolyPhen-2	Polymorphism Phenotyping v2	http://genetics.bwh.harvard.edu/pph2/
PubMed	-	http://www.ncbi.nlm.nih.gov/pubmed
SIFT	Sorting Tolerant from Intolerant	http://sift.jcvi.org/
STRING		http://string-db.org/
SwissVar	-	http://swissvar.expasy.org/
UCSC BLAT	-	http://genome.ucsc.edu/cgi-bin/hgBlat?command=start
UCSC Genome Browser	-	http://genome.ucsc.edu/index.html

UniGene	-	http://www.ncbi.nlm.nih.gov/unigene/
USHbases		http://www.umd.be/usher.html
Zfin	Zebrafish Information Network	http://zfin.org/

11. List of Figures

12. List of Tables

13. List of Publications

Enclosure 1:

Terminal chromosome 4q deletion syndrome: a case report and mapping of critical intervals for associated phenotypes.

Vona B, Nanda I, Neuner C, Schröder J, Kalscheuer VM, Shehata-Dieler W, Haaf T.

In review: BMC Medical Genetics

Enclosure 2:

Disruption of the *ATE1* and *SLC12A1* genes by balanced translocation in a boy with non-syndromic hearing loss.

Vona B, Neuner C, El Hajj N, Schneider E, Farcas R, Beyer V, Zechner U, Keilmann A, Bartsch O, Nanda I, Haaf T.

Mol Syndromol. 2014 Jan;5(1):3-10. doi:10.1159/000355443.

Enclosure 3:

DFNB16 is a frequent cause of congenital hearing impairment: implementation of *STRC* mutation analysis in routine diagnostics.

Vona B, Hofrichter MAH, Neuner C, Schröder J, Gehrig A, Hennermann JB, Kraus F, Shehata-Dieler W, Klopocki E, Nanda I, Haaf T.

Clin Genet. 2014 in press. doi:10.1111/cge.12332.

Enclosure 4:

Confirmation of *GRHL2* as the gene for the DFNA28 locus.

Vona B, Nanda I, Neuner C, Müller T, Haaf T.

Am J Med Genet A. 2013 Aug;161A(8):2060-5. doi:10.1002/ajmg.a.36017.

Enclosure 5:

Targeted deafness gene next generation sequencing of hearing impaired individuals uncovers unformative mutations.

Vona B, Müller T, Nanda I, Neuner C, Hofrichter MAH, Schröder J, Bartsch O, Läßig A, Keilmann A, Schraven S, Kraus F, Shehata-Dieler W, Haaf T.

Genet Med. 2014 in press.

14. List of Presented Publications

14.1 Attachment 1

Terminal chromosome 4q deletion syndrome: a case report and mapping of critical intervals for associated phenotypes.

Terminal chromosome 4q deletion syndrome: a case report and mapping of critical intervals for associated phenotypes

Running title: Terminal 4q deletion syndrome

Barbara Vona[1], Indrajit Nanda[1], Cordula Neuner[1], Jörg Schröder[1], Vera M Kalscheuer[2], Wafaa Shehata-Dieler[3] and Thomas Haaf[1]

[1]Institute of Human Genetics, Julius Maximilians University, Würzburg, Germany

[2]Department of Human Molecular Genetics, Max Planck Institute for Molecular Genetics, Berlin, Germany

[3]Comprehensive Hearing Center, Department of ORL, Plastic, Aesthetic and Reconstructive Head and Neck Surgery, Würzburg, Germany

*Correspondence to:

Professor Thomas Haaf, Institute of Human Genetics, Julius-Maximilians-Universität Würzburg, Biozentrum, Am Hubland, 97074 Würzburg, Germany.

Tel.: +49 931 3188738; Fax: +49 931 3187398; Email: thomas.haaf@uni-wuerzburg.de

Abstract

Background: Terminal deletions of chromosome 4q are associated with a broad spectrum of phenotypes including cardiac, craniofacial, digital, and cognitive impairment. The rarity of this syndrome renders genotype-phenotype correlation difficult, which is further complicated by the widely different phenotypes observed in patients sharing similar deletion intervals.

Case presentation: Here we describe a boy with a variety of moderate syndromic features that prompted SNP array analysis disclosing a heterozygous 6.9 Mb deletion in the 4q35.1q35.2 region, which arose de novo in the maternal germ line. Chromosome banding and FISH analysis revealed normal parental karyotypes.

Conclusion: In addition to the index patient, we review cases from the literature and DECIPHER database to define intervals with recurrent phenotypic overlap, particularly for cleft palate, congenital heart defect, intellectual disability, and autism spectrum disorder. Some genes in the deleted intervals are prime candidates for the associated phenotypes. Re-evaluation of a combined 36 cases allows one to dissect different phenotypic components and will further add to the genotype-phenotype correlation for a syndrome with great phenotypic variability.

Key words: Genotype-phenotype association, Copy number variation, Parent-of origin, SNP array, Terminal 4 q deletion syndrome

Background

Terminal deletions of chromosome 4q are a rare event with an approximate incidence of 1 in 100,000 [1, 2]. While the majority are *de novo* cases, an estimated 14% are the unbalanced product of a parental reciprocal translocation. Furthermore, some pediatric cases with classical phenotypes have inherited their 4q deletion from a parent described as either normal or only mildly affected [3-6]. Although there is a high degree of phenotypic variation in those presenting overlapping deletion intervals, there is a general consensus that chromosome 4q deletion syndrome is characterized by intellectual disability (ID), craniofacial dysmorphism, rotated or low-set ears, cleft palate (CP), micrognathia, congenital heart defects (CHD), craniofacial, skeletal and digital abnormalities, and occasionally autism spectrum disorder (ASD), behavioural disorders, and developmental delay [7-9]. Chromosome 4q deletions are divided in two different subgroups depending on the region of 4q that is deleted: interstitial, spanning from the centromere through 4q28.3 and terminal, from 4q31.1 to 4qter. Although both deletion types each have highly variable phenotypic associations, terminal deletion cases present a broader phenotypic range including CHD, craniofacial and skeletal abnormalities. The 4q33 region has been proposed as a critical for ulnar deficiency, cleft lip and palate, and brain development [10].

Herein, we report on an eight year-old boy with moderate dysmorphic features and a *de novo* deletion in the 4q35.1q35.2 region. Because the case we describe presents a monosomy in the terminal 4q syndrome subgroup, we restrict our focus to this region and go into more depth analyzing the considerable phenotypic variability of terminal 4q deletion cases from the literature and attempt to delineate critical intervals for common phenotypic features.

Case presentation

Clinical report

The proband is the only child of two healthy unrelated parents of German ethnicity, born at a gestational age of 38.3 weeks, with an uncomplicated pregnancy and normal spontaneous delivery. Birth weight was 3,125 g (25th centile), APGAR scores of nine and ten at one and five minutes, respectively, cord blood pH was 7.3, and an unremarkable otoacoustic emmissions newborn hearing screening test was recorded. At four months of age, he was found to have bilateral hearing impairment in the 60 dB range and was fitted with hearing aids. We sequenced genes commonly screened for hearing loss, including *GJB2* (MIM: 121011), *GJB3* (MIM: 603324), and *GJB6* (MIM: 604418) to rule out common mutations. Sequencing disclosed a heterozygous mutation in *GJB3* c.94C>T, p.Arg32Trp (rs1805063; minor allele frequency T=0.015), which is a well-described autosomal recessive deafness gene requiring a second heterozygous mutation either *in trans* or in compound heterozygous configuration to convey hearing loss. A targeted deafness gene next generation sequencing panel was negative for other mutations that could explain his hearing impairment.

In the first year of life, he was diagnosed with aortic isthmus stenosis, corrected via balloon angioplasty, and a patent foramen ovale. He demonstrated shortened PQ intervals on an electrocardiogram indicative of an atrioventricular node irregularity. Regular pediatric cardiology follow-up was recommended. He also presented with chronic Eustachian tube dysfunction that was treated several times with myringotomy tubes, as well as a bifid uvula. In the fifth year of life, a submucous CP was detected. During the same year, he underwent corrective surgery for the CP and velopharyngeal insufficiency. Aditionally, he presented with bilateral crpytorchidism that required testicular orchiopexie. An abdominal sonogram could not

rule out the possibility of a left duplex kidney; urine analysis was within normal limits. Despite a small thyroid, he was noted to be euthyroid on lab testing. His blood profile was unremarkable apart from mild concurrent deficiencies of blood coagulation factors IX (56%), XI (48%), and XII (38%). He had an elevated prothrombin time of 46.5 s (normal: 25-39 s) and an elevated lupus anticoagulant confirmatory test of 1.26 (normal: 0.91-1.07). Further coagulation testing was negative for von Willebrand disease.

Psychological developmental evaluation at the age of three to four years showed mild general developmental delay (six months). Subsequent evaluations showed normal development. Neurological evaluation at age five showed lack of age-appropriate coordination. He also had delayed speech and language development, likely secondary at least in part to his hearing impairment and extensive hospitalization history. Now he attends regular school and does not require remedial classroom instruction.

Methods

Classical cytogenetic and fluorescence in situ hybridization (FISH) analyses

Chromosomes of the proband and his parents were prepared from peripheral blood lymphocyte cultures and analyzed by GTG-banding at the 500 band resolution. FISH was carried out using selected BAC probes from the deleted region. BAC DNA was extracted by alkaline lysis, labelled by nick translocation with either fluorescein-12-dUTP (Roche Diagnostics, Mannheim, Germany) or tetramethyl-rhodamine-5-dUTP (Roche), and hybridized overnight to denatured chromosomes. After post-hybridization washing and DAPI counterstaining, chromosomes were analyzed with a Zeiss AxioImager microscope. Image acquisition and analysis were performed using a CCD camera and FISHView 2.0 software (Applied Spectral Imaging, Edingen-

Neckarhausen, Germany). At least 20 metaphases were evaluated to verify the location of probe hybridization in the proband karyotype.

Copy number variation and genotype analyses

Genomic DNA (gDNA) of the proband and his parents was prepared from peripheral blood by standard salt extraction method. The Illumina Omni1-Quad v1.0 SNP array (Illumina, San Diego, CA, USA), with >1.1 million SNP markers, was used for whole genome genotyping and copy number variation (CNV) detection. 200 ng gDNA were utilized in an Illumina Infinium HD Ultra Assay according to the manufacturer's specifications. Data were analyzed using GenomeStudio (v2011.1) software with both cnvPartition 3.2.0 (Illumina) and QuantiSNP 2.2 copy number algorithm [11] for assessment of CNV size. Genotypes of father, mother and proband were obtained from the SNP array for parent-of-origin determination. HaploPainter [12] was used in combination with manual intervention to illustrate the absence of maternal genotypes in the deletion patient.

The terminal 4q monosomy was validated by real-time quantitative polymerase chain reaction (qPCR) of *FRG1* exons 1, 8, and *DUX4L6* using the SensiMix SYBR Green kit (Bioline, Luckenwalde, Germany). Primer sequences are available upon request.

For exome capture and targeted next generation sequencing of 129 deafness genes, gDNA from the proband was submitted to Otogenetics Corporation (Norcross, GA, USA). Paired-end reads of 90-100 bp generated on an Illumina (San Diego, CA, USA) HiSeq 2000 were analyzed for quality, exome coverage and exome-wide SNP/InDels using DNAnexus (Mountain View, CA, USA) cloud-based data analysis.

Mapping critial intervals for terminal 4q deletion syndrome phenotypes

This study makes use of data generated by the DECIPHER consortium, which is funded by the Wellcome Trust. A full list of centres who contributed relevant data is available from http://decipher.sanger.ac.uk. With the combined DECIPHER cases (nos. 278055, 248967, 249192, 249458, 249476, 249536, 249541, 249655, 251175, 253743, 254882, 256186, 257358, 264122, 264942, 267783, 269176, and 276704) and review of the literature [6-10, 13-22], phenotypic and deletion overlaps among individuals with monosomies spanning different sizes were delineated. We used the UCSC Genome Browser Custom Track (http://genome-euro.ucsc.edu/cgi-bin/hgCustom) to map these cases and target the narrowest critical interval for CP, CDH, ID, and ASD.

Results

Classical and molecular cytogenetic analyses

Conventional chromosome banding analysis of the proband revealed a 46,XY karyotpe without gross abnormalities. However, the distal G-band negative region in the long arm of chromosome 4 corresponding to q35.1q35.2 appeared to be somewhat smaller in one of the homologs, suggestive of a loss of chromosome material (Figure 1A). Both parents had normal karyotypes without evidence of deletion involving the segment of chromosome 4q.

To validate the deletion in the proband, SNP array analysis was performed which revealed a 6.9 Mb heterozygous deletion on chromosome 4q35.1q35.2 (184,046,156-190,901,117 bp from rs17074417 to rs10005101, hg19) (Figure 1B). qPCR analysis of *FRG1* exons 1, 8, and *DUX4L6* confirmed that the distal deletion breakpoint extends beyond 190,939,252 bp (data not shown),

encompassing a total of 42 annotated genes (18 OMIM genes). Based on these results, the proband's karyotype could be assigned as 46,XY,del(4)(q35.1q35.2). SNP array analyses of maternal and paternal DNA did not indicate CNV for chromosome 4q in the parental karyotypes, consistent with a *de novo* deletion in the child. Informative SNPs from the terminal 4q region for which the mother and father have divergent genotypes revealed a loss of maternal genotypes in the child (Figure 1C), consistent with maternal origin of the deleted chromosome.

FISH analysis was performed with BACs from the proximal flanking region 4q35.1 (RP11-188P17) and the deleted region 4q35.1q35.2 (RP11-775P18, RP11-118M15, and RP11-652J12). As expected, the flanking BAC probe hybridized to both chromosomes 4 in the proband's and the parents' metaphase spreads. Probes from the deleted region recognized only one chromosome 4 homolog of the patient, but were present on both chromosomes 4q35.1q35.2 copies of father and mother (Figure 1A). Obviously, the de novo deletion is not due to a cytogenetically cryptic subtelomeric translocation in a parental karyotype.

Genotype-phenotype correlation of terminal 4q deletion syndrome

We created a map of terminal 4q deletion syndrome cases through reviewing the literature and DECIPHER database. Figure 2 (upper section) presents 36 deletion cases (including our own) meeting our interval criteria and after controlling for normal copy number variation from the Database of Genomic Variants (http://dgv.tcag.ca/dgv/app/home). Although we had to estimate best fit intervals for cases describing deletions using various low-resolution methods, we were able to roughly map out five critical regions for four common 4q deletion syndrome phenotypes: CP, CHD, ID and ASD. Figure 2 (middle section) and Supplementary Table S1 show the gene content of the deletion region, with an emphasis on genes that are thought to be important for the

various associated phenotypes. Supplementary Table S2 summarizes the literature review and DECIPHER cases with approximate deletion sizes, inheritance and phenotype information.

A locus (chr. 4: 155,600,001-158,373,133 bp) for CP (Figure 2, purple interval) was mapped between the case from [10] and the DECIPHER case 264122. Two out of three cases spanning this region presented CP [7, 10]. The imprinted gene *PDGFC* in the critical interval is important for development of the palate with implication in non-syndromic orofacial clefting [23], and is predicted to exhibit moderate haploinsufficiency (Table S1). Furthermore, *Pdgfc*$^{-/-}$ knockout mice display clefting and die in the perinatal period from feeding and respiratory difficulties [24]. Thirteen cases under evaluation indicate CP, suggesting an additional critical interval or gene involved in palate formation, to be discussed later.

Congenital heart defects were mapped to two separate regions. The first region (Figure 2, light green) spans a large interval (chr. 4: 160,717,000-178,579,037 bp) unable to be further subdivided based on the cases presented, beginning with case [18] and ending with [21]. There are 17 cases with various cardiac phenotypes, 13 of which overlap with the proposed interval, with three individuals unique to this first CHD locus [10, 18, 21]. This interval contains two likely haploinsufficient genes of interest (Table S1). *TLL1* is important for mammalian heart development, specifically for septation [25]. Mice with abnormalities in this gene die from blood circulation failure [26]. From mouse and zebrafish experiments, it is apparent that *HAND2* is also involved in cardiac morphogenesis, angiogenesis, and formation of the right ventricle and aortic arch arteries and, interestingly, plays a role in limb formation [27, 28]. Although many individuals presented digital and forearm deficiencies, we were not able to clearly map these phenotypes to this region as well.

The second CHD locus (chr. 4: 184,046,156-186,997,806 bp) maps between the beginning of the case we present and the end of case #20 from [9] (Figure 2, red). Twelve out of 17 cases with cardiac phenotypes overlapped with this interval, two of whom uniquely overlap with this region (present case and case [9] #20). The critical interval contains two adjacent genes, *PDLIM3* and *SORBS2*, implicated in cardiac development. *PDLIM3* is essential for right ventricular development and thought to play a role in enhancing mechanical strength stability of cardiac muscle during mouse development [29]. *SORBS2* is highly expressed in the intercalated disk in normal cardiac tissue [30]. Additionally, *SORBS2* is thought to have implication in CP formation, since case [9] #20 with CP has a small deletion (chr. 4: 186,533,075-186,997,806 bp) exclusively affecting *SORBS2* and *TLR3* (Figure 2, upper and middle section). Ten out of 13 total individuals with CP overlapped with this region, but the proximal border was too large to map an informative locus.

A smaller region (chr. 4:171,144,641-175,897,427 bp) within the first CHD interval may account for ID, with eight of 15 individuals with ID overlapping between DECIPHER cases 276704 and 251175 (Figure 2, dark green). While no gene is presently linked to ID in this region, the gene *SCRG1* is a prime candidate due to its high expression in the brain and differential regulation in schizophrenia and bipolar disorder [31] (Table S1). Lack of genomic variation among healthy individuals in the Database of Genomic Variants and strong evolutionary conservation (data not shown) further emphasize the importance of normal copy number of this ID region.

A number of reports implicate chromosome 4q35.2 in ASD [20, 22]. While only four cases reviewed here have ASD (Table S2), all four overlap one narrow interval (chr. 4: 187,234,067-188,424,639 bp) (Figure 2, turquoise) with only three genes (*MTNR1A*, *FAT1* and *F11*), that was

first reported in a boy in a boy with ASD [22]. *FAT1* has been associated with affective disorder [32] and ASD [33]. This gene is essential for controlling cell proliferation in developmental processes [34].

Mild factor XI deficiency and elevated prothrombin time in our proband are presumably explained through deletion of *F11* [35, 36] and an adjacent coagulation gene, *KLKB1* [37]. Surprisingly, the mild bleeding tendencies that can be associated with *F11* and *KLKB1* haploinsufficiency have not been discussed in great details yet, although many children with terminal 4q deletion syndrome require multiple surgeries.

The first clinical symptom of our patient with 6.9 Mb deletion (chr. 4: 184,046,156-190,901,117 bp) was mild to severe bilateral hearing loss. Two additional cases with larger deletions, DECIPHER case 256186 and [16], were also reported with hearing impairment. In a Swiss-German kindred with autosomal-dominant non-syndromic hearing loss, an autosomal-dominant deafness locus, DFNA24 (MIM: 606282) was mapped to an 8.1 Mb region (chr. 4: 183,200,000-191,154,276 bp) (Figure 2, orange) on chromosome 4q35qter [38, 39]. However, in this context it is important to emphasize that 11 normal hearing terminal 4q deletion cases overlap completely and nine normal hearing cases overlap partially with the DFNA24 interval. Thus, DFNA24 haploinsufficiency alone does not cause deafness. Mouse knockout experiments suggest that *Casp3*, which is contained in the critical region, is required for proper functioning of the cochlea [40-42]. *Casp3*$^{-/-}$ mice indicated sensorineural hearing loss, whereas *Casp3*$^{+/-}$ mice displayed intermediate vestibular dysfunction as well as marginally increased hair cell counts.

Discussion

Since its first description [43], the genotype-phenotype delineation of chromosome 4q deletion syndrome has been complicated by extensive inconsistencies reported among individuals with similar deletion intervals. With >170 genes residing in the terminal 4q region, delineation of the phenotypes associated with such deletions presents a tremendous task toward understanding the complete spectral presentation of a syndrome with excessive phenotypic disunity. Several dozen cases with terminal 4q deletions reported in the literature and DECIPHER database aid in bridging the gap between genotype and phenotype and will prove helpful to management and therapies in years to come. The patient we present was analyzed with a high resolution SNP array to delineate the deletion interval and the parental origin of the *de novo* rearrangement. We found it especially challenging to finely map disease-relevant intervals with the various low-resolution techniques that used GTG banding [7, 10, 13-15], FISH [16], and the various resolution arrays, including BAC array CGH [18], 1 Mb aCGH [19], 44K aCGH [6, 17, 20], 105K aCGH [9, 22], and 300K SNP array [21]. Another limitation includes possible variations in the depth of clinical descriptions listed, especially those from the DECIPHER database, which were not as detailed as the published cases. Collectively, we were able to define critical regions for several distinct phenotypes, specifically CP, CDH, ID, and ASD, that have been associated with the terminal 4q deletion syndrome, with a majority of cases supporting our locus mapping. Assuming that the same gene(s) is underlying hearing impairment in terminal 4q deletion and DFNA24 patients, our case may help to further narrow down the DFNA24 locus. Hearing impairment may be caused by a dominant gain-of-function mutation in one allele (DFNA24) and, possibly, alternatively by loss of one copy in combination with a second event, i.e. a hypomorphic mutation on the second allele.

With the high degree of phenotypic variability of terminal 4q deletions of similar size and gene content, it is tempting to speculate about the role imprinted genes may play. To date, three imprinted genes (*GAB1*, *SFRP2*, and *PDGFC*) have been identified in the 4q31.1qter region (www.otago.ac.nz/IGC). *PDGFC*, which has been implicated in CP [23], is preferentially expressed from the maternal chromosome.

The overwhelming majority of cases are *de novo* possibly due to errors during meiotic recombination leading to a loss of chromosomal material from one parental allele. Structural features of a genome, such as short and long interspersed nuclear elements (SINEs and LINEs, respectively), provide the architectural substrates for recombination [44]. Mispairing between these elements is a frequent cause of intrachromosomal recombination, leading to deletions and/or duplications. The majority of crossover recombination positions are localized to non-random hotspots which have been mapped according to frequency and spatial distribution in both males and females [45]. The deCODE recombination map of the 4q31.1qter illustrates an enrichment of both male and female hotspots along the majority of this interval (Figure 2, bottom section), with each marked position meeting a standardized recombination rate strength cut-off value of ten or greater [46]. The recombination hotspots are positioned in a segment also flanked by a high density of LINE and SINE elements (data not shown), supporting mispairing during maternal meiotic recombination as a plausible mechanism for the deletion.

Consent

The study was approved by the Ethics Committee of the University of Würzburg. Full informed parental consent was obtained prior to initiating our investigation.

Abbreviations

ASD, Autism spectrum disorder; BAC, Bacterial artificial chromosome; CHD, Congenital heart defect; CNV, copy number variation; CP, Cleft palate; FISH, Fluorescence in situ hybridization; ID, Intellectual disability; PCR, polymerase chain reaction.

Competing interest

No potential conflicts of interest as well as commercial interests were disclosed.

Authors' contributions

BV, IN and CN carried out the molecular cytogenetic and data analyses. JS and WSD performed a clinical analysis of the patient. VK provided materials. BV and TH researched the literature and wrote the manuscript. All authors have critically reviewed and approved the manuscript.

Acknowlegements

The authors are grateful for the participation of the family for their willingness to engage in this study. We also thank Prof. Dr. Holger Thiele from the Cologne Center for Genomics for constructive dialogue about HaploPainter, Dr. Christopher Riley at Phoenix Children's Hospital for clinical assessment, and Andrea Hörning for assistance with karyotype analysis. This work was supported by the German Research Foundation (grant no. HA 1374/7-2).

References

1. Strehle EM, Ahmed OA, Hameed M, Russell A: **The 4q- syndrome.** *Genet Couns* 2001, **12:**327-339.
2. Strehle EM, Bantock HM: **The phenotype of patients with 4q-syndrome.** *Genet Couns* 2003, **14:**195-205.
3. Descartes M, Keppler-Noreuil K, Knops J, Longshore JW, Finley WH, Carroll AJ: **Terminal deletion of the long arm of chromosome 4 in a mother and two sons.** *Clin Genet* 1996, **50:**538-540.
4. Ravnan JB, Tepperberg JH, Papenhausen P, Lamb AN, Hedrick J, Eash D, Ledbetter DH, Martin CL: **Subtelomere FISH analysis of 11 688 cases: an evaluation of the frequency and pattern of subtelomere rearrangements in individuals with developmental disabilities.** *J Med Genet* 2006, **43:**478-489.
5. Balikova I, Menten B, de Ravel T, Le Caignec C, Thienpont B, Urbina M, Doco-Fenzy M, de Rademaeker M, Mortier G, Kooy F, van den Ende J, Devriendt K, Fryns JP, Speleman F, Vermeesch JR: **Subtelomeric imbalances in phenotypically normal individuals.** *Hum Mutat* 2007, **28:**958-967.
6. Rossi MR, DiMaio MS, Xiang B, Lu K, Kaymakcalan H, Seashore M, Mahoney MJ, Li P: **Clinical and genomic characterization of distal duplications and deletions of chromosome 4q: study of two cases and review of the literature.** *Am J Med Genet A* 2009, **149A:**2788-2794.
7. Giuffrè M, La Placa S, Carta M, Cataliotti A, Marino M, Piccione M, Pusateri F, Meli F, Corsello G: **Hypercalciuria and kidney calcifications in terminal 4q deletion syndrome: further evidence for a putative gene on 4q.** *Am J Med Genet A* 2004, **126A:**186-190.

8. Strehle EM, Gruszfeld D, Schenk D, Mehta SG, Simonic I, Huang T: **The spectrum of 4q-syndrome illustrated by a case series.** *Gene* 2012, **506:**387-391.
9. Strehle EM, Yu L, Rosenfeld JA, Donkervoort S, Zhou Y, Chen TJ, Martinez JE, Fan YS, Barbouth D, Zhu H, Vaglio A, Smith R, Stevens CA, Curry CJ, Ladda RL, Fan ZJ, Fox JE, Martin JA, Abdel-Hamid HZ, McCracken EA, McGillivray BC, Masser-Frye D, Huang T: **Genotype-phenotype analysis of 4q deletion syndrome: proposal of a critical region.** *Am J Med Genet A* 2012, **158A:**2139-2151.
10. Keeling SL, Lee-Jones L, Thompson P: **Interstitial deletion 4q32-34 with ulnar deficiency: 4q33 may be the critical region in 4q terminal deletion syndrome.** *Am J Med Genet* 2001, **99:**94-98.
11. Colella S, Yau C, Taylor JM, Mirza G, Butler H, Clouston P, Bassett AS, Seller A, Holmes CC, Ragoussis J: **QuantiSNP: an Objective Bayes Hidden-Markov Model to detect and accurately map copy number variation using SNP genotyping data.** *Nucleic Acids Res* 2007, **35:**2013-2025.
12. Thiele H, Nürnberg P: **HaploPainter: a tool for drawing pedigrees with complex haplotypes.** *Bioinformatics* 2005, **21:**1730-1732.
13. Jefferson RD, Burn J, Gaunt KL, Hunter S, Davison EV: **A terminal deletion of the long arm of chromosome 4 [46,XX,del(4)(q33)] in an infant with phenotypic features of Williams syndrome.** *J Med Genet* 1986, **23:**474-477.
14. Menko FH, Madan K, Baart JA, Beukenhorst HL: **Robin sequence and a deficiency of the left forearm in a girl with a deletion of chromosome 4q33-qter.** *Am J Med Genet* 1992, **44:**696-698.

15. Borochowitz Z, Shalev SA, Yehudai I, Bar-el H, Dar H, Tirosh E: **Deletion (4)(q33->qter): a case report and review of the literature.** *J Child Neurol* 1997, **12:**335-337.

16. Calabrese G, Giannotti A, Mingarelli R, Di Gilio MC, Piemontese MR, Palka G: **Two newborns with chromosome 4 imbalances: deletion 4q33-->q35 and ring r(4)(pterq35.2-qter).** *Clin Genet* 1997, **51:**264-267.

17. Quadrelli R, Strehle EM, Vaglio A, Larrandaburu M, Mechoso B, Quadrelli A, Fan YS, Huang T: **A girl with del(4)(q33) and occipital encephalocele: clinical description and molecular genetic characterization of a rare patient.** *Genet Test* 2007, **11:**4-10.

18. Kaalund SS, Møller RS, Teszas A, Miranda M, Kosztolanyi G, Ullmann R, Tommerup N, Tümer Z: **Investigation of 4q-deletion in two unrelated patients using array CGH.** *Am J Med Genet A* 2008, **146A:**2431-2434.

19. Kitsiou-Tzeli S, Sismani C, Koumbaris G, Ioannides M, Kanavakis E, Kolialexi A, Mavrou A, Touliatou V, Patsalis PC: **Distal del(4) (q33) syndrome: detailed clinical presentation and molecular description with array-CGH.** *Eur J Med Genet* 2008, **51:**61-67.

20. Chien WH, Gau SS, Wu YY, Huang YS, Fang JS, Chen YJ, Soong WT, Chiu YN, Chen CH: **Identification and molecular characterization of two novel chromosomal deletions associated with autism.** *Clin Genet* 2010, **78:**449-456.

21. Xu W, Ahmad A, Dagenais S, Iyer RK, Innis JW: **Chromosome 4q deletion syndrome: narrowing the cardiovascular critical region to 4q32.2-q34.3**. *Am J Med Genet A* 2012, **158A:**635-640.

22. Youngs EL, Henkhaus RS, Hellings JA, Butler MG: **12-year-old boy with a 4q35.2 microdeletion and involvement of MTNR1A, FAT1, and F11 genes.** *Clin Dysmorphol* 2012, **21:**93-96.

23. Wu D, Wang M, Wang X, Yin N, Song T, Li H, Zhang F, Zhang Y, Ye Z, Yu J, Wang DM, Zhao Z: **Maternal transmission effect of a PDGF-C SNP on nonsyndromic cleft lip with or without palate from a Chinese population.** *PLoS One* 2012, **7:**e46477.

24. Ding H, Wu X, Bostrom H, Kim I, Wong N, Tsoi B, O'Rourke M, Koh GY, Soriano P, Betsholtz C, Hart TC, Marazita ML, Field LL, Tam PP, Nagy A: **A specific requirement for PDGF-C in palate formation and PDGFR-alpha signaling.** *Nat Genet* 2004, **36:**1111-1116.

25. Stańczak P, Witecka J, Szydło A, Gutmajster E, Lisik M, Auguściak-Duma A, Tarnowski M, Czekaj T, Czekaj H, Sieroń AL: **Mutations in mammalian tolloid-like 1 gene detected in adult patients with ASD.** *Eur J Hum Genet* 2009, **17:**344-351.

26. Clark TG, Conway SJ, Scott IC, Labosky PA, Winnier G, Bundy J, Hogan BL, Greenspan DS: **The mammalian Tolloid-like 1 gene, Tll1, is necessary for normal septation and positioning of the heart.** *Development* 1999, **126:**2631-2642.

27. Sasaki MM, Nichols JT, Kimmel CB: **Edn1 and hand2 interact in early regulation of pharyngeal arch outgrowth during zebrafish development**. *PLoS One* 2013, **8:**e67522.

28. Tamura M, Hosoya M, Fujita M, Iida T, Amano T, Maeno A, Kataoka T, Otsuka T, Tanaka S, Tomizawa S, Shiroishi T: **Overdosage of Hand2 causes limb and heart defects in the human chromosomal disorder partial trisomy distal 4q.** *Hum Mol Genet* 2013, **22:**2471-2481.

29. Pashmforoush M, Pomies P, Peterson KL, Kubalak S, Ross J, Jr., Hefti A, Aebi U, Beckerle MC, Chien KR: **Adult mice deficient in actinin-associated LIM-domain protein reveal a developmental pathway for right ventricular cardiomyopathy.** *Nat Med* 2001, **7:**591-597.

30. Kakimoto Y, Ito S, Abiru H, Kotani H, Ozeki M, Tamaki K, Tsuruyama T: **Sorbin and SH3 domain-containing protein 2 is released from infarcted heart in the very early phase: proteomic analysis of cardiac tissues from patients.** *J Am Heart Assoc* 2013, 2:e000565.

31. Vawter MP, Atz ME, Rollins BL, Cooper-Casey KM, Shao L, Byerley WF: **Genome scans and gene expression microarrays converge to identify gene regulatory loci relevant in schizophrenia.** *Hum Genet* 2006, **119:**558-570.

32. Abou Jamra R, Becker T, Georgi A, Feulner T, Schumacher J, Stromaier J, Schirmbeck F, Schulze TG, Propping P, Rietschel M, Nothen MM, Cichon S: **Genetic variation of the FAT gene at 4q35 is associated with bipolar affective disorder.** *Mol Psychiatry* 2008, **13:**277-284.

33. Roberts JL, Hovanes K, Dasouki M, Manzardo AM, Butler MG: **Chromosomal microarray analysis of consecutive individuals with autism spectrum disorders or learning disability presenting for genetic services.** *Gene* 2014, **535:**70-78.

34. Bruder-Nascimento T, Chinnasamy P, Riascos-Bernal DF, Cau SB, Callera GE, Touyz RM, Tostes RC, Sibinga NE: **Angiotensin II induces Fat1 expression/activation and vascular smooth muscle cell migration via Nox1-dependent reactive oxygen species generation.** *J Mol Cell Cardiol* 2013, **66:**18-26.

35. Mitchell M, Dai L, Savidge G, Alhaq A: **An Alu-mediated 31.5-kb deletion as the cause of factor XI deficiency in 2 unrelated patients**. *Blood* 2004, **104:**2394-2396.

36. Duga S, Salomon O: **Congenital factor XI deficiency: an update.** *Semin Thromb Hemost* 2013, **39:**621-631.

37. Koumandou VL, Scorilas A: **Evolution of the plasma and tissue kallikreins, and their alternative splicing isoforms.** *PLoS One* 2013, **8:**e68074.

38. Häfner FM, Salam AA, Linder TE, Balmer D, Baumer A, Schinzel AA, Spillmann T, Leal SM: **A novel locus (DFNA24) for prelingual nonprogressive autosomal dominant nonsyndromic hearing loss maps to 4q35-qter in a large Swiss German kindred.** *Am J Human Genet* 2000, **66:**1437-1442.

39. Santos RL, Häfner FM, Huygen PL, Linder TE, Schinzel AA, Spillmann T, Leal SM: **Phenotypic characterization of DFNA24: prelingual progressive sensorineural hearing impairment.** *Audiol Neurootol* 2006, **11:**269-275.

40. Morishita H, Makishima T, Kaneko C, Lee YS, Segil N, Takahashi K, Kuraoka A, Nakagawa T, Nabekura J, Nakayama K, Nakayama KI: **Deafness due to degeneration of cochlear neurons in caspase-3-deficient mice.** *Biochem Biophys Res Comm* 2001, **284:**142-149.

41. Parker A, Hardisty-Hughes RE, Wisby L, Joyce S, Brown SD: **Melody, an ENU mutation in Caspase 3, alters the catalytic cysteine residue and causes sensorineural hearing loss in mice.** *Mamm Genome* 2010, **21:**565-576.

42. Makishima T, Hochman L, Armstrong P, Rosenberger E, Ridley R, Woo M, Perachio A, Wood S: **Inner ear dysfunction in caspase-3 deficient mice.** *BMC Neurosci* 2011, **12:**102.

43. Ockey CH, Feldman GV, Macaulay ME, Delaney MJ: **A large deletion of the long arm of chromosome no. 4 in a child with limb abnormalities.** *Arch Dis Child* 1967, **42:**428-434.

44. Emanuel BS, Shaikh TH: **Segmental duplications: an 'expanding' role in genomic instability and disease.** *Nat Rev Genet* 2001, **2:**791-800.

45. Kauppi L, Jeffreys AJ, Keeney S: **Where the crossovers are: recombination distributions in mammals.** *Nat Rev Genet* 2004, **5:**413-424.

46. Kong A, Thorleifsson G, Gudbjartsson DF, Masson G, Sigurdsson A, Jonasdottir A, Walters GB, Jonasdottir A, Gylfason A, Kristinsson KT, Gudjonsson SA, Frigge ML, Helgason A, Thorsteinsdottir U, Stefansson K: **Fine-scale recombination rate differences between sexes, populations and individuals.** *Nature* 2010, **467:**1099-1103.

FIGURE LEGENDS

Figure 1. Molecular karyptyping of the patient and his parents. (**A**) GTG-banding and FISH analysis of homologous chromosomes 4 in proband, mother and father. The proximal flanking BAC RP11-188P17 is labeled with fluorescein-dUTP (green), the deleted BAC RP11-775P18 with rhodamine-dUTP (red), and the chromosomes are counterstained with DAPI (blue). An arrowhead indicates the critical band q35.1q35.2 on the patient's derivative chromosome. (**B**) Illumina SNP array analysis (B allele frequency and log R ratio) of the 4q35.1q35.2 region in the boy with terminal 4q deletion syndrome. (**C**) Selected genotypes in the deletion interval from the Illumina array are depicted for proband (left), mother (middle) and father (right). Mendelian transmission errors (absence of maternal genotypes) in the proband are indicated in gray.

Figure 2. Genotype-phenotype correlation of terminal 4q deletions. The upper part of the figure presents the mapped deletion intervals in chromosome 4q31.1qter including the present case, marked with a box, and 35 additional cases from DECIPHER and the literature. The red bars delineate the deletion region for each case. Highlighted intervals indicate critical regions for common phenotypes among the cases. Depicted are from left to right the intervals for cleft palate (purple), congenital heart defect region 1 (light green), intellectual disability (dark green), congenital heart defect region 2 (red), and autism spectrum disorder (turquoise). Orange indicates the mapping interval of the DFNA24 locus. The middle part shows the gene content of the 4q31.1qter region. Likely disease-relevant genes overlapping with critical deletion intervals are boxed. The bottom diagram shows the deCODE recombination map, highlighting male and female recombination hotspots in the terminal 4q deletion syndrome region.

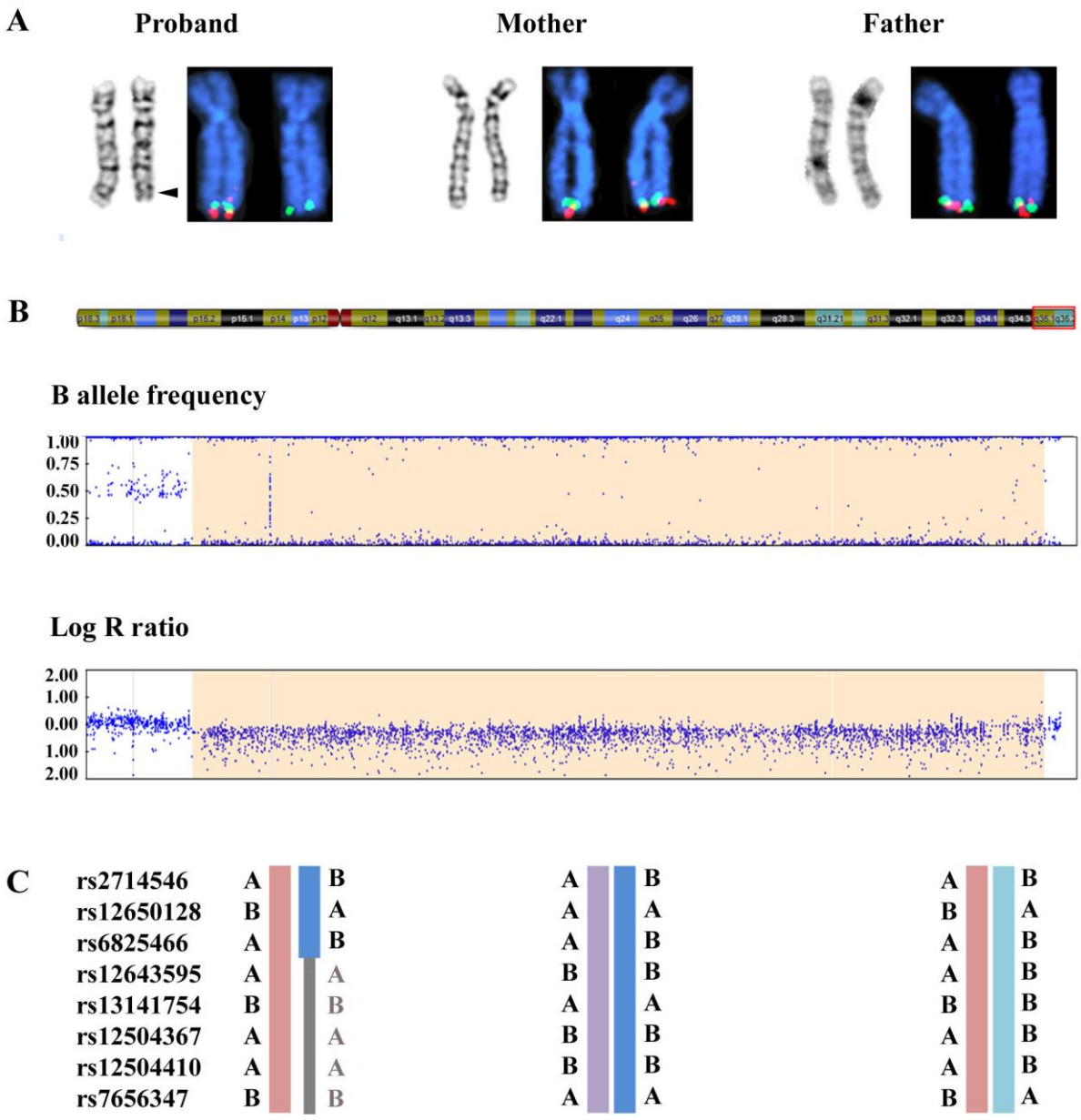
A
Proband
Mother
Father
B
B allele frequency
1.00
0.75
0.50
0.25
0.00
Log R ratio
2.00
1.00
0.00
1.00
2.00
C
rs2714546 A B
rs12650128 B A
rs6825466 A B
rs12643595 A A
rs13141754 B B
rs12504367 A A
rs12504410 A A
rs7656347 B B
A B
A A
A B
B B
A A
B B
B B
A A
A B
B A
A B
A B
B B
A B
A B
B A

Figure 1

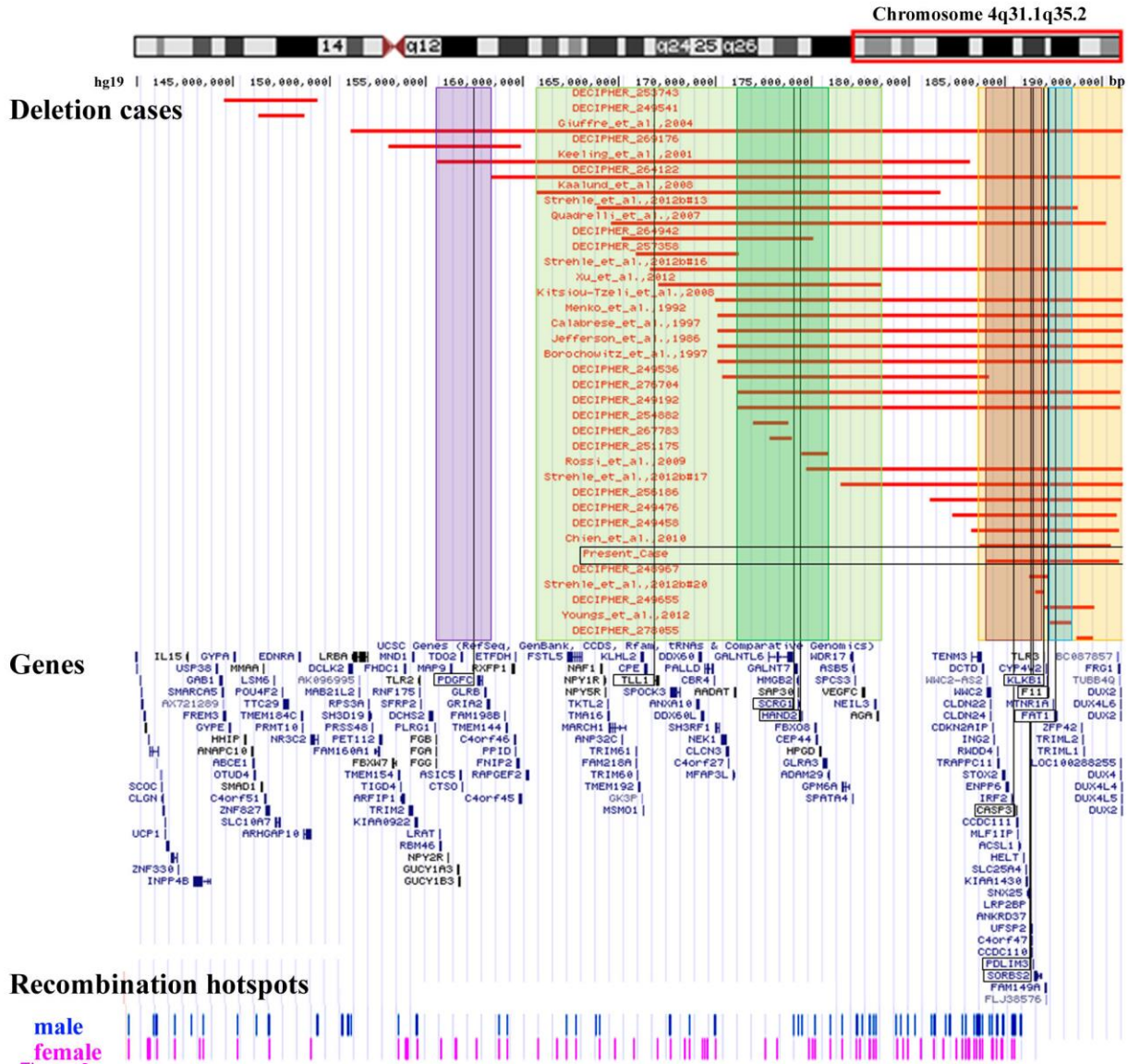
Chromosome 4q31.1q35.2
Deletion cases
Genes
Recombination hotspots
male
female
Present_Case

Figure 2

Table S1 Summary of disease-relevant genes in the deletion region with functions, phenotypes and cases with agreeable phenotypes

Gene	*Name*	*OMIM*	*Band*	*Function*	*Phenotype*	*HI (%)**	*Cases*
PDGF	Platelet-derived growth factor C	608452	q32.1	Growth factor for embryonic fusion of the palate shelf [130]	Cleft lip, cleft palate	32.2	[7], [10]
TLL1	Tolloid-like 1	606742	q32.3	Important for the development of the mammalian heart, specifically for interatrial septum [135]	Atrial septal defect	16.1	[6], [7], [9] #16 and #17, [10], [13], [15], [16], [17], [18], [19], [21], DECIPHER #276704
SCRG1	Stimulator of chondrogenesis 1	603163	q34.1	Associated with neurodegenerative changes	Bipolar disorder and schizophrenia, of possible interest for intellectual disability	-	[6], [9] case #13, DECIPHER #264122, #276704, #249192, #254882, #267783, and #251175
HAND2	Heart- and neural crest derivatives-expressed 2	602407	q34.1	Cardiac morphogenesis, angiogenesis, formation of right ventricle and aortic arch arteries; also implicated in limb development [136,156]	Congenital heart defect, aortic arch artery deformities, limb developmental defects	10.7	[6], [7], [9] #16 and #17, [10], [13], [15], [16], [17], [18], [19], [21], DECIPHER #276704
CASP3	Caspase 3	600636	q35.1	Important for maintaining spiral ganglion neurons and support of inner and outer hair cells [40]	Hearing loss	2.6	[16], DECIPHER #256186, present case
PDLIM3	PDZ and LIM domain protein 3	605889	q35.1	Cytoskeletal assembly via assembly of alpha-actin complexes, morphogenesis of the right ventricular chamber [137]	Right ventricular cardiomyopathy	45.6	[7], [9] #16, [17]
SORBS2	Sorbin and SH3 domain containing 2	-	q35.1	Subcellular localization in epithelial and cardiac tissue; though to act in cytoskeletal organization [138]	Congenital heart defect, cleft palate	22.2	[6], [9] #17 and #20, [13], [15], [16], [19], DECIPHER #276704, present
KLKB1	Kallikrein B, plasma 1	229000	q35.2	Blood coagulation pathway, regulates blood pressure [157]	Fletcher factor deficiency	23.1	Present case
F11	Coagulation factor XI	264900	q35.2	Blood coagulation pathway [158]	Factor XI deficiency	96.2	Present case
FAT1	FAT tumour suppressor 1	600976	q35.2	Developmental cell proliferation control, highly expressed during cardiac and vascular remodelling [132,159]	Implicated in affective [133] and autism spectrum disorder [134].	-	[20], [22], DECIPHER #249536 and #256186

*****HI = haploinsufficiency index, based on a scale of 0-100%, with a score of 0-10% being likely haploinsufficient and a score of 90-100% being unlikely haploinsufficient.

Table S2 Summary of our proband and cases from DECIPHER and the literature with deletions exclusively residing in the 4q31.1qter region

Case	*Sex*	*Size (Mb)*	*Origin*	*CHD*	*EA*	*HL*	*CP*	*CO*	*SD*	*GD*	*ID*	*ASD*	*BD*	*MH*	*CJF*	*HFA*	*UA*	*WID*	*UGA*	*PRS*	*SE*	*RI*
DECIPHER #253743	f	4.9	de novo	+																		
DECIPHER #249541	nd	3.4	nd		+						+				+							
[7]	f	40.1*	de novo	+	+		+			+					+	+						
DECIPHER #269176	f	6.9	de novo								+			+	+							+
[10]	f	27.6*	de novo	+			+			+					+	+	+			+		
DECIPHER #264122	f	32.6	de novo								+											
[18]	m	21.0*	de novo	+	+		+		+						+	+						+
[9] #13	m	24.9	nd		+		+		+	+	+				+	+	+		+			+
[17]	f	25.7	de novo	+	+					+					+	+			+			
DECIPHER #264942	f	10.0	nd							+						+						
DECIPHER #257358	f	5.4	inherited								+				+							
[9] #16	f	24.5	de novo	+						+					+	+						
[21]	m	11.6	de novo	+	+					+						+						
[19]	m	18.9-22.9*	de novo	+	+		+			+			+	+	+	+			+			
[14]	f	21.1*	de novo				+								+	+	+			+		
[16]	m	21.1*	de novo	+	+	+	+	+		+				+	+	+		+				
[13]	f	21.1*	de novo	+						+					+	+						
[15]	m	21.1*	de novo	+	+								+		+	+						
DECIPHER #249536	nd	nd	nd		+		+					+			+			+	+			
DECIPHER #276704	f	19.8	de novo	+	+				+	+	+				+	+						
DECIPHER #249192	f	18.0	nd				+				+						+					
DECIPHER #254882	m	1.8	nd								+				+						+	
DECIPHER #267783	m	1.1	inherited								+		+								+	
DECIPHER #251175	f	1.4	de novo								+				+							

[6]	f	16.4	de novo	+						+	+		+		+	+			+			
[9] #17	f	14.6	nd	+	+		+			+				+	+							
DECIPHER #256186	m	10.0	inherited			+		+	+		+	+			+							
DECIPHER #249476	nd	8.5	nd								+			+	+							
DECIPHER #249458	nd	7.7	nd											+	+							
[20]	m	6.8	de novo						+			+		+								
Present case	m	6.9	de novo	+		+	+	+	+													
DECIPHER #248967	f	1.0	inherited				+															
[9], #20, F	f	0.5	nd	+	+		+							+	+	+						+
DECIPHER #249655	nd	2.6	nd								+		+		+							
[22]	m	2.1	nd	+					+	+	+	+	+									
DECIPHER #278055	f	0.9	inherited										+									

Abbreviations: nd = not disclosed; f = female; m = male; CHD = congenital heart defect; EA = ear abnormalities; HL = hearing loss; CP = cleft palate; CO = cryptorchidism; SD = speech delay; GD = general delay; BD = behavioural disorder; MH = muscle hypotonia; CJF = craniofacial, jaw, facial dysmorphism; HFA = hand and/or foot abnormalities; UA = ulna absent; WID = wide intermamillary distance; UGA = urogenital abnormalities; PRS = Pierre Robin sequence; SE = seizures or epilepsy; RI = recurrent infection.

"+" sign denotes the phenotype is present.

*estimated size based on chromosomal band assignment from FISH, GTG-Banding or BAC aCGH.

14.2 Attachment 2

Disruption of the *ATE1* and *SLC12A1* genes by balanced translocation in a boy with non-syndromic hearing loss.

Original Article

Molecular Syndromology

Mol Syndromol
DOI: 10.1159/000355443

Accepted: August 5, 2013
by M. Schmid
Published online: October 4, 2013

Disruption of the *ATE1* and *SLC12A1* Genes by Balanced Translocation in a Boy with Non-Syndromic Hearing Loss

B. Vona[a] C. Neuner[a] N. El Hajj[a] E. Schneider[a] R. Farcas[b] V. Beyer[b]
U. Zechner[b] A. Keilmann[c] M. Poot[d] O. Bartsch[b] I. Nanda[a] T. Haaf[a]

[a]Institute of Human Genetics, Julius Maximilians University, Wuerzburg, [b]Institute of Human Genetics, and
[c]Division of Communication Disorders, Department of ORL, University Medical Center, Mainz, Germany;
[d]Department of Medical Genetics, University Medical Center, Utrecht, The Netherlands

Key Words
ATE1 · Disease-associated balanced chromosome rearrangement · Non-syndromic hearing impairment · Reciprocal translocation · *SLC12A1*

Abstract
We report on a boy with non-syndromic hearing loss and an apparently balanced translocation t(10;15)(q26.13;q21.1). The same translocation was found in the normally hearing brother, father and paternal grandfather; however, this does not exclude its involvement in disease pathogenesis, for example, by unmasking a second mutation. Breakpoint analysis via FISH with BAC clones and long-range PCR products revealed a disruption of the arginyltransferase 1 *(ATE1)* gene on translocation chromosome 10 and the solute carrier family 12, member 1 gene *(SLC12A1)* on translocation chromosome 15. SNP array analysis revealed neither loss nor gain of chromosomal regions in the affected child, and a targeted gene enrichment panel consisting of 130 known deafness genes was negative for pathogenic mutations. The expression patterns in zebrafish and humans did not provide evidence for ear-specific functions of the *ATE1* and *SLC12A1* genes. Sanger sequencing of the 2 genes in the boy and 180 *GJB2* mutation-negative hearing-impaired individuals did not detect homozygous or compound heterozygous pathogenic mutations. Our study demonstrates the many difficulties in unraveling the molecular causes of a heterogeneous phenotype. We cannot directly implicate disruption of *ATE1* and/or *SLC12A1* to the abnormal hearing phenotype; however, mutations in these genes may have a role in polygenic or multifactorial forms of hearing impairment. On the other hand, it is conceivable that our patient carries a disease-causing mutation in a so far unidentified deafness gene. Evidently, disruption of *ATE1* and/or *SLC12A1* gene function alone does not have adverse effects.

Autosomal reciprocal translocations affect approximately 0.1% of newborns [Hook and Hamerton, 1977]. When associated with abnormal phenotypes and/or developmental delay, apparently balanced chromosome rearrangements pose challenging situations in genetic counseling. Gene disruption by translocation or microdeletions/duplications in the breakpoint region or elsewhere in the genome may have phenotypic consequences. The latter are more frequent in de novo translocations with syndromic phenotypes, whereas gene disruption appears to occur at comparable frequencies in phenotypi-

KARGER

E-Mail karger@karger.com
www.karger.com/msy

1661–8769/13/0000–0000$38.00/0

T. Haaf
Institute of Human Genetics, Julius Maximilians University Wuerzburg
Biozentrum, Am Hubland
DE–97074 Wuerzburg (Germany)
E-Mail thomas.haaf@uni-wuerzburg.de

cally normal and abnormal translocation carriers [Baptista et al., 2008]. This argues in favor of the notion that in many cases gene disruption can be compensated for and has only mild or no phenotypic expression. It has been suggested that the breakpoints in non-syndromic patients may be associated with common and complex diseases [Bache et al., 2006]. Chromosomal rearrangements can cause haploinsufficiency not only by direct gene disruption, but also by position effects separating the coding region of a gene from regulatory elements occurring at a considerable distance as great as one megabase. This event may consequently lead to gene dysregulation [Kleinjan and van Heyningen, 2005]. Disease-associated balanced chromosome rearrangements provide a powerful tool for the identification of disease-causing genes [Bugge et al., 2000; Higgins et al., 2008].

If a balanced rearrangement is detected both in the carrier parent and offspring, then the risk for phenotypic abnormality is generally thought to be very low. Nonetheless, there are several studies reporting patients with abnormal phenotypes despite having the same balanced rearrangement as their phenotypically normal carrier parent [Warburton, 1991]. One possible explanation for discordant phenotypes in carriers of the same familial translocation or inversion is segregation of a second genetic mutation on the homologous chromosomes (compound heterozygosity) or elsewhere in the genome (digenic/polygenic inheritance). Furthermore, additional cryptic genomic imbalances may arise in the germline of balanced translocation carriers due to non-homologous recombination events.

We identified a family with a balanced reciprocal translocation t(10;15)(q26.13;q21.1) that was inherited through 3 generations. All translocation carriers were healthy with no reported abnormalities except non-syndromic sensorineural hearing loss affecting one child. Hearing impairment is estimated to affect one out of every 1,000 newborns and increases to 3.5 out of 1,000 individuals by 18 years of age [Morton and Nance, 2006]. Furthermore, it is hypothesized that up to 1% of the greater than 20,000 genes in humans are necessary for hearing [Friedman and Griffith, 2003]. If roughly 200 genes are anticipated to play various roles in hearing and given that the number of known deafness genes (http://hereditaryhearingloss.org) are fewer than the suspected number, then there are many more deafness genes remaining to be discovered. We analyzed the chromosome breakpoint regions of our proband with the idea to identify a candidate gene(s) for hearing impairment. Previous studies have already demonstrated that in a given patient/family, disease-associated balanced chromosome rearrangements can provide a visible bridge between hearing impairment and the underlying genotype [Williamson et al., 2007; Damatova et al., 2009; Schneider et al., 2009].

Material and Methods

Classic and Molecular Cytogenetic Analyses

Cytogenetic analyses were performed on the index patient as well as his parents, paternal grandparents and brother from peripheral blood lymphocyte cultures using conventional GTG-banding techniques at the 550-band level.

To delineate the breakpoint regions, FISH was carried out using selected BAC probes from the chromosomal 10q25.3q26.13 and 15q15q21.3 regions (online suppl. table 1; for all online suppl. material, see www.karger.com/doi/10.1159/000355443). The locations of these BAC clones were chosen from the Ensembl browser (GRCh37) and ordered from the Children's Hospital Oakland Research Institute (Oakland, Calif., USA). In order to amplify larger BAC subfragments ranging from 3.5 to 10.7 kb, the Expand Long Template PCR System (Roche Diagnostics, Mannheim, Germany) was used according to the manufacturer's recommendations with a series of primer pairs (online suppl. table 2) chosen from the genomic sequence of the breakpoint clones.

Detection of CNVs was performed with an Illumina CytoSNP-12 v2 microarray (Illumina Inc., San Diego, Calif., USA) according to the manufacturer's protocol. Array data were analyzed using GenomeStudio version 2011.1 and cnvPartition 3.2.0 (Illumina). A minimum cut-off value of 5 probes with a consistently aberrant signal was included in our criteria to ascertain a copy number change.

Sanger Sequencing and Targeted Next Generation Sequencing of Deafness Genes

Genomic DNA was extracted from whole blood using a standard salt extraction method. PCR was performed with an initial denaturation at 95°C for 3 min, 25 cycles of 95°C for 30 s, 60°C for 30 s, 72°C for 30 s, and a final 10 min extension using M13 primers (Metabion, Munich, Germany) (online suppl. table 3), PCR buffer, nucleotide mixture and Fast Start Taq Polymerase (Roche Diagnostics). The 12 exons of *ATE1* and 26 coding exons of *SLC12A1* were Sanger sequenced with an ABI PRISM 377 (Applied Biosystems, Life Technologies, Carlsbad, Calif., USA). The sequence reaction was completed with 5× sequencing buffer and big dye terminator (Applied Biosystems). DNA sequence analysis was performed using NCBI BLAST. In the case of non-synonymous substitutions, PolyPhen-2 [Adzhubei et al., 2010], SIFT [Ng and Henikoff, 2001] and Alamut (Interactive Biosoftware, Rouen, France) were used to predict the impact of any identified amino acid substitution on the protein structure and function and the disease-causing potential.

Genomic DNA of the proband was submitted to Otogenetics Corporation (Norcross, Ga., USA) for exome capture targeting 130 known deafness genes and sequencing on a HiSeq2000 (Illumina). Paired-end reads of 90–100 bp were analyzed for quality, exome coverage and exome-wide SNP/InDels using the platform provided by DNAnexus (Mountain View, Calif., USA).

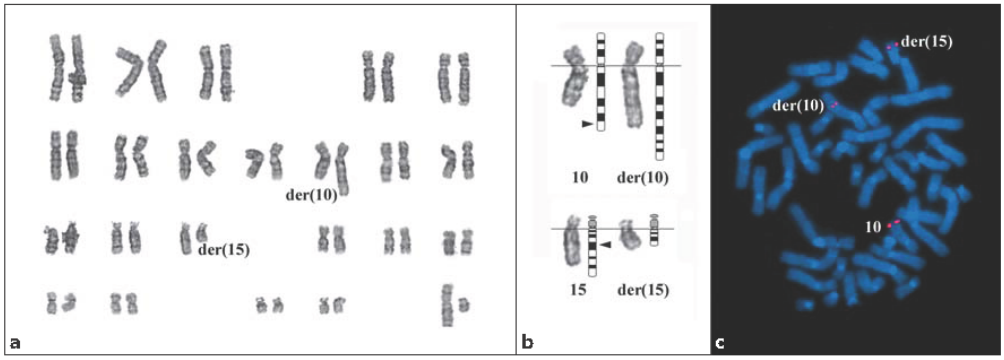

Fig. 1. Chromosome banding and FISH analysis of breakpoint regions. **a** G-banded karyotype of the index patient showing the apparently balanced derivative chromosomes. **b** G-banding pattern as well as corresponding ideograms showing the normal and derivative chromosomes resulting from the t(10;15)(q26.13;q21.1) translocation. Arrowheads indicate the translocation breakpoints. **c** DAPI-stained (blue) metaphase spread of the index patient hybridized with digoxigenin-labeled (red) BAC RP11-78A18. The breakpoint-spanning BAC highlights the *ATE1* gene on the normal chromosome 10 as well as the 2 derivative chromosomes 10 and 15.

Zebrafish Whole Mount in situ Hybridization

Whole mount in situ hybridization was done to assess *ate1* and *slc12a1* expression in wild-type developing zebrafish (*Danio rerio*, wild-type TüAB strain) embryos. Antisense riboprobes for *ate1* and *slc12a1* were prepared using the pCRII-TOPO vector (Invitrogen, Darmstadt, Germany). A 646-bp fragment of *ate1* on zebrafish chr.Zv9_NA48 was isolated from the cDNA of whole embryos (26–28 hours post fertilization, hpf) using forward primer 5′-GGCCTCCTCCTCAAGTCTCT-3′ and reverse primer 5′-GACACACAAGAGGGCAGGAT-3′ and was cloned into a pCRII-TOPO vector. For preparation of the *ate1* antisense riboprobe, pCRII-*ate1* was digested with *Bam*HI and transcribed with T7 RNA polymerase. Similarly, a 505-bp fragment of *slc12a1* on zebrafish chromosome 18 was isolated using forward primer 5′-TCTGCCTAAAGGGACTCTGC-3′ and reverse primer 5′-CGAGGCCAGAAAGAAGTTGG-3′. The fragment was cloned into a pCRII-TOPO vector. For preparation of the *slc12a1* antisense riboprobe, pCRII-*slc12a1* was digested with *Hin*dIII and transcribed with T7 RNA polymerase. In situ hybridization was performed as described in Winkler and Moon [2001]. Embryos were mounted in glycerol and photographed as whole mounts.

Results

Clinical Report

The patient is the first child of non-consanguineous German parents without a family history of hearing loss in childhood. His grandparents, parents and younger brother were healthy and normally hearing. Following an uneventful pregnancy, he was born at term with Apgar scores of 10 and 10 at 1 and 5 min, respectively. Birth weight was 5,300 g (+4 SD), length was 62 cm (+4.5 SD) and occipitofrontal circumference 39 cm (+3.7 SD). The reasons for the macrosomia and macrocephaly remained unknown; in particular, there was no evidence for an overgrowth syndrome or for gestational diabetes. Newborn hearing screening (otoacoustic emission) was not performed. Development was normal and without notable diseases, and his overgrowth gradually decreased to normal. He could sit unassisted at age 6 months, spoke first words at 12 months and walked at 13 months. At the age of 6 years, his mother noticed hearing problems and bilateral sensorineural impairment was diagnosed. Pure tone audiometry showed a nearly symmetrical loss with normal hearing up to 1 kHz and hearing thresholds of 35 dB at 2 kHz, 40 dB at 4 kHz and 60 dB at 8 kHz, respectively. Speech and language had developed normally. His achievements in school and developmental testing (German version of the Developmental Test of Visual Perception) were ahead of age. The boy was fitted with hearing aids and his problems to understand at home and in school ceased. At the age of 7½ years, height was 120.3 cm (25th percentile) and weight 24.5 kg (25–50th percentile). Clinical investigation disclosed no abnormalities apart from a mild hyperopia that was also present in his younger brother. Thyroid function test, electrocardiogram and kidney ultrasound were normal, as was mutation analysis of common hearing loss genes including *GJB2* and *GJB6*.

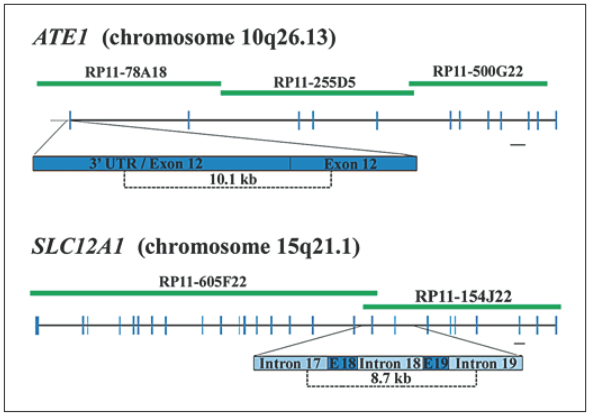

Fig. 2. Graphic illustrations showing a translocation-mediated disruption of the *ATE1* and *SLC12A1* genes. The upper part shows a BAC (green) contig covering the *ATE1* breakpoint region on chromosome 10. Bars represent 20 kb. An expanded representation of the breakpoint including exon 12 with the end of the coding region and the 3′ UTR region is shown in dark blue, and comprises a 10.1-kb interval. The bottom part shows a BAC contig covering the *SLC12A1* breakpoint on chromosome 15. An expanded representation of the breakpoint spanning introns 17–19 and exons 18 and 19 in light blue and dark blue, respectively, comprise an 8.7-kb interval.

Chromosome Banding Analysis

The patient was identified in a cytogenetic screen for disease-associated balanced chromosome rearrangements in >300 children with non-syndromic hearing impairment [Schneider et al., 2009]. GTG banding revealed an apparently balanced translocation between the long arms of chromosomes 10 and 15. At the cytogenetic level, the breakpoints were assigned to bands 10q26.11q26.13 and 15q21.1q21.2 (fig. 1a, b). Karyotyping of the parents and family (data not shown) revealed that the translocation had been inherited from the father and was also present in the proband's brother and paternal grandfather, all with normal hearing. The mother and the paternal grandmother had normal female karyotypes.

Positional Cloning of Translocation Breakpoints

Once the breakpoints were provisionally delineated, FISH experiments were used to refine the breakpoint location. Online supplementary table 1 lists the BAC clones that were selected with their corresponding mapping results. BAC RP11-78A18 (83 kb) hybridized to the normal chromosome 10 and both derivative chromosomes 10 and 15 (fig. 1c), as expected for a chromosome 10-breakpoint spanning clone. Similarly, we identified a breakpoint-spanning BAC clone, RP11-154J22 (101 kb) on chromosome 15. Based on the FISH results, the proband's karyotype was refined to 46,XY,t(10;15)(q26.13;q21.1).

To further narrow down the breakpoint regions, we generated long-range PCR products from the breakpoint-spanning clones on chromosomes 10 and 15 (online suppl. table 2). The FISH mapping of individual long-range PCR products assigned breakpoints to a 10.1-kb interval (amplicon 6 of BAC RP11-78A18) on chromosome 10 localizing to exon 12 including the end of the coding sequence and the 3′ UTR of the *ATE1* gene and an 8.7-kb interval (amplicon 2b of BAC154J22) on chromosome 15 between introns 17 and 19 of the *SLC12A1* gene. Breakpoint intervals are illustrated in figure 2.

Consistent with the UniGene database (http://www.ncbi.nlm.nih.gov/unigene), we found that *ATE1* but not *SLC12A1* is expressed in blood. Although we localized the translocation breakpoints to predicted regions within 2 genes, we were unable to successfully detect fusion gene transcripts in the proband (data not shown). However, because of the 3′–5′ orientation of *ATE1* and the 5′–3′ orientation of *SLC12A1* in the derivative chromosomes, the possibility of an *ATE1-SLC12A1* or *SLC12A1-ATE1* fusion transcript is unlikely due to the opposing transcriptional directions.

In addition to direct gene disruption, the translocation could indirectly affect the regulation of genes within a flanking one megabase region of *ATE1* and *SLC12A1*. There are several interesting candidate genes in these regions that, while not associated with a deafness phenotype, demonstrate expressed sequence tags in the human ear (online suppl. table 4).

Mutation Analyses

According to DECIPHER version 5.1 (http://decipher.sanger.ac.uk), both *ATE1* and *SLC12A1* are not thought to affect the phenotype by way of haploinsufficiency. In order to test whether gene disruption by translocation unmasks a recessive mutation in the second allele of our proband, we sequenced all 12 coding exons of *ATE1* (MIM 604103) and all 26 coding exons of *SLC12A1* (MIM 600839) and did not detect any pathogenic mutation. He was homozygous for 2 synonymous SNPs c.303A>G (rs10749435) and c.1236A>G (rs4237536) in *ATE1* and heterozygous for one non-synonymous benign SNP c.2873T>C, p.Val958Ala (rs1552311) in *SLC12A1*.

In addition, we performed a mutation screening in 180 *GJB2* mutation-negative children with non-syndromic hearing impairment. Fifteen to 20% had mild, the remaining cases moderate to profound hearing impairment. Al-

Table 1. Results for *ATE1* and *SLC12A1* mutation screening in 180 patients

Gene	Exon	Nucleotide change	Amino acid change	rdbSNP (build 13)	PolyPhen-2 prediction[a]	SIFT prediction[b]
ATE1 (exons 1–12)	1	c.9C>T	p.Phe3Phe	rs79570924		
	1	c.88T>G	p.Ser30Ala		benign (0.000)	tolerated (0.83)
	3	c.198C>T	p.Val66Val			
	4	c.303A>G[c]	p.Ala101Ala	rs10749435		
	5	c.499C>T	p.Leu167Phe	rs148095496	benign (0.000)	tolerated (0.09)
	9	c.1125G>A	p.Ser375Ser	rs139300996		
	9	c.1140C>T	p.Gly380Gly	rs150860078		
	10	c.1208A>G	p.Tyr403Cys	rs148135505	probably damaging (1.000)	deleterious (0.00)
	10	c.1236A>G	p.Ser412Ser	rs4237536		
	11	c.1371A>C	p.Pro457Pro	rs35350755		
SLC12A1 (coding exons 2–27)	7	c.828G>A	p.Val276Val	rs3825960		
	13	c.1539C>T	p.Val513Val			
	14	c.1614T>C	p.Tyr538Tyr	rs6493311		
	18	c.2067G>A	p.Gly689Gly	rs35783293		
	24	c.2873T>C	p.Val958Ala	rs1552311	benign (0.000)	tolerated (0.77)

[a] PolyPhen-2 operates on a scale from 0 to 1.0, with 1.0 having the highest probability of being a damaging substitution.
[b] SIFT values <0.05 predict substitutions that are deleterious, whereas values >0.05 predict tolerated substitutions.
[c] The NCBI SNP database listed c.303G>A and not c.303A>G. This could be the result of a manual entry error.

together, the *ATE1* gene sequencing identified 7 synonymous, 2 benign non-synonymous and 1 probably damaging or deleterious base change (table 1). The potentially pathogenic c.1208A>G (p.Tyr403Cys) mutation was present in a heterozygous state in a single individual with severe hearing impairment in the lower frequencies that improves to normal hearing at higher frequencies (particularly at 6 and 8 kHz). She also suffers from recurrent bilateral tinnitus for at least 10 years. This mutation occurs in a highly conserved nucleotide and amino acid, up to Baker's yeast (considering 12 species) and has a large physicochemical difference existing between Tyr and Cys with a Grantham distance of 194 (Alamut version 2.0). This variation is also entered in dbSNP (http://www.ncbi.nlm.nih.gov/SNP) as rs148135505, with a MAF of 0.001 (1000 Genomes) and is in the Exome Variant Server database (http://evs.gs.washington.edu) with a similar MAF of 0.002 in the European population. The *SLC12A1* sequencing detected 4 synonymous and 1 non-synonymous variant (table 1).

Targeted Next Generation Sequencing of Deafness Genes and SNP Array Analysis

Because the translocation was segregating in both affected and unaffected family members and we did not find evidence for mutations in *ATE1* and *SLC12A1* underlying hearing impairment, we used targeted deafness gene enrichment sequencing (Otogenetics) to screen for mutations in 130 known deafness genes. The analysis strategy we employed disclosed only apparently non-pathogenic variants. Notably, one non-synonymous heterozygous change, c.1985G>A, p.Gly662Glu, in myosin IA (*MYO1A*, MIM 601478), a major contributor to autosomal dominant hearing loss (DFNA48) [Donaudy et al., 2003], was reported as possibly pathogenic by UniProt through the Alamut mutation report. However, because this variant is in a position of the *MYO1A* motor domain that is not evolutionarily conserved and also listed as a SNP (rs33962952), it is unlikely to cause hearing impairment. The fact that this SNP was found in the normally

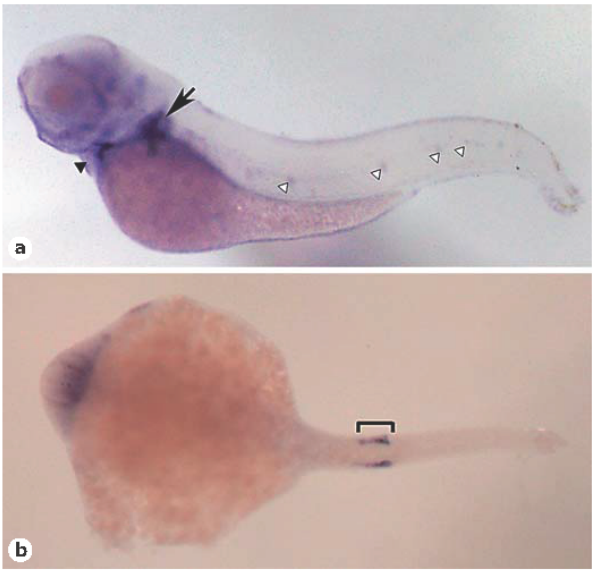

Fig. 3. Whole-mount in situ hybridization of wild-type zebrafish embryos shows the expression pattern of *ate1* and *slc12a1* during embryogenesis. **a** 91-hpf lateral view depicting strong *ate1* expression in the fin bud (arrow) and heart (filled arrowhead) with minor expression in neuromasts (open arrowheads). **b** A polar view of the 15–16-hpf somite stage with *slc12a1* expression in the distal early pronephros (bracket).

hearing father and paternal grandfather of our proband also argues against a dominant causative mutation, although the formal possibility of reduced penetrance in unaffected family members cannot be excluded.

In some cases of apparently balanced chromosome rearrangements, microdeletions and/or duplications in the vicinity of the breakpoint regions [Yue et al., 2005] or elsewhere in the genome [Baptista et al., 2008] were found to be disease-causing. The SNP array analysis did not reveal any cryptic gain or loss of chromosome material in the proband (data not shown). There was no detectable difference in the breakpoint regions between affected and unaffected tranlocation carriers. The proband displayed a 4-Mb copy neutral loss of heterozygosity on chromosome 17 (50,329,974–54,383,237 bp; NCBI 37/hg19); however, this region does not contain any strong deafness candidate genes. Interestingly, when investigating known copy number variation in the breakpoint intervals in the database of genomic variants [Zhang et al., 2006], *ATE1* lacks genomic variation and *SLC12A1* has only one indel reported in 270 HapMap controls.

Expression of ate1 and slc12a1 during Zebrafish Development

According to UniGene, neither *ATE1* nor *SLC12A1* appears to be expressed in the human ear. To evaluate the possible functional role of *ATE1* and *SLC12A1* during ear development, the expression patterns were investigated in zebrafish embryos using *ate1* and *slc12a1* cDNA probes. Major expression of *ate1* was marked at 91 hpf in the heart and fin bud, with minor expression in the neuromasts (fig. 3a). Prominent expression of *slc12a1* was observed in the distal early pronephros in all stages beginning with the somite stage at 15–16 hpf, at 30 hpf and in 96 hpf (fig. 3b). As expected, no signal was visualized with the sense riboprobes.

Discussion

The proband inherited a balanced translocation t(10; 15) from his phenotypically normal father; thus, it is unlikely that the translocation alone is by itself the cause of deafness. However, interplaying with other genetic and/or environmental factors, it could contribute to the events leading to hearing loss. Upon the identification of the 2 disrupted genes in the breakpoint regions (*ATE1* in 10q26.13 and *SLC12A1* in 15q21.2), we began a candidate gene approach involving bidirectional sequencing of all exons of each of the disrupted genes in the proband as well as a pool of 180 hearing impaired individuals.

To date, there are no disease-causing mutations or phenotypes associated with *ATE1* in humans that have been cataloged in databases such as HGMD (http://www.biobase-international.com/product/hgmd) and SwissVar (http://swissvar.expasy.org). Evidence from *Ate1*$^{-/-}$ knockout mice suggests that this gene is important for cardiovascular development [Kwon et al., 2002]. We show strong expression of the zebrafish ortholog in the developing heart (and fin bud). To the best of our knowledge, neither the proband nor affected family members with the described translocation have heart defects. An interesting point for discussion is that there was weak expression of *ate1* observed in the neuromasts of zebrafish. Neuromasts are, in morphology and functionality, similar to hair cells of the ear. Consistent with the in silico prediction (DECIPHER) that *ATE1* is not sensitive to haploinsufficiency, heterozygous disruption of *ATE1* alone can be tolerated. Posttranslational arginylation by ATE1 is an important biological regulator of protein properties and function. The tRNA-dependent addition of Arg onto proteins is essential for mammalian embryo-

genesis and tissue morphogenesis [Saha and Kashina, 2011]. In this light, it is tempting to speculate that arginylation of a potential ATE1-target protein, which is essential for normal hearing development, is altered by a second mutation that is present in the genome of the proband, but not in his healthy brother and father. Arginylation of hearing loss genes is not well investigated. However, differential arginylation of actin isoforms is well known [Zhang et al., 2010] and both beta and gamma actins have specific roles for auditory hair cells [Perrin et al., 2010].

In our cohort of hearing-impaired individuals, we found one potentially pathogenic mutation affecting a highly conserved nucleotide and amino acid (c.1208A>G, p.Tyr403Cys) in the *ATE1* gene in a heterozygous state. Together with our translocation patient, 2 of 180 studied individuals exhibit only one wild-type *ATE1* allele. However, we have not assessed the pathogenicity of the identified mutations on a functional level. The Exome Variant Server database contains 2 additional probably pathogenic frameshift mutations which are not in dbSNP v135. The c.427_430del4 deletion with a MAF of 0.004 in Europeans affects the protein by inducing a premature stop codon (p.Leu143Valfs*8). The c.93_94insC insertion (p.Ser32Glnfs*72) with a MAF of 0.04 is listed with a read depth of only 8 and, therefore, a sequencing artifact cannot be excluded.

Homozygous or compound heterozygous mutations in *SLC12A1* are associated with antenatal Bartter syndrome type I (MIM 601678), a life-threatening renal tubular disorder [Simon et al., 1996]. In this light, it is not unexpected that our zebrafish experiments showed strong *slc12a1* expression in the pronephros. None of the translocation carriers were reported to suffer from renal problems. However, it is noteworthy that 2 of 9 Costa Rican Bartter syndrome patients with a homozygous premature stop mutation in the *SLC12A1* gene exhibited sensorineural hearing loss [Kurtz et al., 1997]. Considering that the incidence of Bartter syndrome (with at least 5 different types) is approximately 1 in 800,000–1,000,000 (http://www.orpha.net), the frequency of heterozygous *SLC12A1* mutation carriers is estimated to be approximately 1 in 1,000. The risk of our index patient for a child with Bartter syndrome is then approximately 1 in 4,000.

In conclusion, heterozygous disruption of *ATE1* and/or *SLC12A1* gene function is benign in nature and does not cause a haploinsufficient state. Additionally, from sequencing data, the proband lacks a second mutation in either of these genes. Since we eliminated the contribution of another known deafness gene by performing sequencing of 130 genes associated with deafness, we can argue in favor of the notion that the proband suffers from a polygenic or multifactorial form of deafness. On the other hand, we cannot exclude the possibility that the translocation and hearing impairment are coincidental or that our proband has a pathological mutation in a gene that is not yet associated with hearing loss. Collectively, our study emphasizes the difficulty of finding causative mutations in patients with non-syndromic hearing loss. Such particularly challenging patients may become targets for novel techniques such as whole exome or genome sequencing.

Acknowledgements

The authors thank the proband and his family for participating in this study. We also thank Stefanie Kleinmichel and Katharina Eirich for help with sequencing analyses, Dr. Natalja Damatova for SNP array experiments and analysis, Dr. Jörg Schröder for clinical information, and Prof. Manfred Schartl for providing the zebrafish embryos. This work was supported by the German Research Foundation (HA 1374/7-2).

References

Adzhubei IA, Schmidt S, Peshkin L, Ramensky VE, Gerasimova A, et al: A method and server for predicting damaging missense mutations. Nat Methods 7:248–249 (2010).

Bache I, Hjorth M, Bugge M, Holstebroe S, Hilden J, et al: Systematic re-examination of carriers of balanced reciprocal translocations: a strategy to search for candidate regions for common and complex diseases. Eur J Hum Genet 14:410–417 (2006).

Baptista J, Mercer C, Prigmore E, Gribble SM, Carter NP, et al: Breakpoint mapping and array CGH in translocations: comparison of a phenotypically normal and an abnormal cohort. Am J Hum Genet 82:927–936 (2008).

Bugge M, Bruun-Petersen G, Brøndum-Nielsen K, Friedrich U, Hansen J, et al: Disease associated balanced chromosome rearrangements: a resource for large scale genotype-phenotype delineation in man. J Med Genet 37:858–865 (2000).

Damatova N, Beyer V, Galetzka D, Schneider E, Napiontek U, et al: Haploinsufficiency of 16.4 Mb from chromosome 22pter-q11.21 in a girl with unilateral conductive hearing loss. Cytogenet Genome Res 125:241–247 (2009).

Donaudy F, Ferrara A, Esposito L, Hertzano R, Ben-David O, et al: Multiple mutations of *MYO1A*, a cochlear-expressed gene, in sensorineural hearing loss. Am J Hum Genet 72:1571–1577 (2003).

Friedman T, Griffith AJ: Human nonsyndromic sensorineural deafness. Annu Rev Genomics Hum Genet 4:341–402 (2003).

Higgins AW, Alkuraya FS, Bosco AF, Brown KK, Bruns GA, et al: Characterization of apparently balanced chromosomal rearrangements from the developmental genome anatomy project. Am J Hum Genet 82:712–722 (2008).

Hook EB, Hamerton JL: The frequency of chromosome abnormalities detected in consecutive newborn studies – differences between studies – results by sex and by severity of phenotypic involvement, in Hook EB, Porter IH (eds): Population Cytogenetics – Studies in Humans, pp 63–79 (Academic Press, New York 1977).

Kleinjan DA, van Heyningen V: Long-range control of gene expression: emerging mechanisms and disruption in disease. Am J Hum Genet 76:8–32 (2005).

Kurtz CL, Karolyi L, Seyberth HW, Koch MC, Vargas R, et al: A common *NKCC2* mutation in Costa Rican Bartter's syndrome patients: evidence for a founder effect. J Am Soc Nephrol 8:1706–1711 (1997).

Kwon YT, Kashina AS, Davydov IV, Hu RGH, An JA, et al: An essential role of N-terminal arginylation in cardiovascular development. Science 297:96–99 (2002).

Morton CC, Nance WE: Newborn hearing screening – a silent revolution. N Engl J Med 354:2151–2164 (2006).

Ng PC, Henikoff S: Predicting deleterious amino acid substitutions. Genome Res 11:863–874 (2001).

Perrin BJ, Sonnemann KJ, Ervasti JM: β-actin and γ-actin are each dispensable for auditory hair cell development but required for stereocilia maintenance. PLoS Genet 6:e1001158 (2010).

Saha S, Kashina A: Posttranslational arginylation as a global biological regulator. Dev Biol 358: 1–8 (2011).

Schneider E, Märker T, Daser A, Frey-Mahn G, Beyer V, et al: Homozygous disruption of *PDZD7* by reciprocal translocation in a consanguineous family: a new member of the Usher syndrome protein interactome causing congenital hearing impairment. Hum Mol Genet 18:655–666 (2009).

Simon DB, Karet FE, Hamdan JM, DiPietro A, Sanjad SA, Lifton RP: Bartter's syndrome, hypokalaemic alkalosis with hypercalciuria, is caused by mutations in the Na-K-2Cl cotransporter *NKCC2*. Nat Genet 13:183–188 (1996).

Warburton D: De novo balanced chromosome rearrangements and extra marker chromosomes identified at prenatal diagnostics: clinical significance and distribution of breakpoints. Am J Hum Genet 49:995–1013 (1991).

Williamson RE, Darrow KN, Michaud S, Jacobs JS, Jones MC, et al: Methylthioadenosine phosphorylase (MTAP) in hearing: gene disruption by chromosomal rearrangement in a hearing impaired individual and model organism analysis. Am J Med Genet A 143A:1630–1639 (2007).

Winkler C, Moon RT: Zebrafish mdk2, a novel secreted midline, participates in posterior neurogenesis. Dev Biol 229:511–515 (2001).

Yue Y, Grossmann B, Holder SE, Haaf T: De novo t(7;10)(q33;q23) translocation and closely juxtaposed microdeletion in a patient with macrocephaly and developmental delay. Hum Genet 117:1–8 (2005).

Zhang F, Saha S, Shabalina SA, Kashina A: Differential arginylation of actin isoforms is regulated by coding sequence-dependent degradation. Science 329:1534–1537 (2010).

Zhang J, Feuk L, Duggan GE, Khaja R, Scherer SW: Development of bioinformatics resources for display and analysis of copy number and other structural variants in the human genome. Cytogenet Genome Res 115:205–214 (2006).

Supplementary Table 1. BAC clones used for breakpoint mapping by FISH

Clone name	Chromosomal position	Position (bp) on human chromosomes 10 and 15*	Results of FISH mapping
RP11-498B4	10q25.3	118,348,517-118,544,777	10, der(10)
RP11-354M20	10q26.11	119,736,145-119,927,813	10, der(10)
RP11-435O11	10q26.11	120,794,356-120,920,583	10, der(10)
RP11-781P14	10q26.12	121,775,064-121,857,461	10, der(10)
RP11-95I16	10q26.12	122,636,390-122,782,544	10, der(10)
RP11-78A18	10q26.13	123,418,495-123,577,576	10, der(10), der(15)
RP11-255D5	10q26.13	123,577,577-123,652,558	10, der(15)
RP11-105F10	10q26.13	123,774,481-123,949,157	10, der(15)
RP11-162A23	10q26.13	123,809,055-124,988,926	10, der(15)
RP11-391M7	10q26.13	125,391,503-125,586,310	10, der(15)
RP11-109A6	10q26.3	131,491,998-131,620,189	10, der(15)
RP11-90M11	15q15	43,079,476-43,207,353	15, der(15)
RP11-718O11	15q21.1	46,127,483-46,265,112	15, der(15)
RP11-501G11	15q21.1	47,182,267-47,353,026	15, der(15)
RP11-198M11	15q21.1	48,043,348-48,192,722	15, der(15)
RP11-208K4	15q21.1	48,296,809-48,447,823	15, der(15)
RP11-605F22	15q21.1	48,447,824-48,562,707	15, der(15)
RP11-154J22	15q21.1	48,562,708-48,663,776	15, der(10), der(15)
RP11-348A14	15q21.1	48,663,777-48,754,765	15, der(10)
RP11-227D13	15q21.1	48,935,522-49,049,783	15, der(10)
RP11-485O10	15q21.1	49,051,622-49,223,905	15, der(10)
RP11-96N2	15q21.2	50,233,525-50,390,039	15, der(10)
RP11-562A8	15q21.2	50,656,494-50,843,844	15, der(10)
RP11-547D13	15q21.3	55,421,271-55,542,614	15, der(10)

*according to Ensembl release 67.

Supplementary Table 2. Long-range PCR BAC fragments for FISH mapping

BAC name	Ampli-con no.	Forward primer sequence (5'-3')	Reverse primer sequence (5'-3')	Position (bp) on human chromosomes 10 and 15*
RP11-78A18	1	CCAATACCTTCCCATGTTTTGGG	GGGAAAACTATCAGCTACAGGG	chr.10: 123,540,595-123,549,965
RP11-78A18	2	GAACGAAACCAAGGCTTGGAG	CCCCTGTCAGAAAAGGAAAACC	chr.10: 123,530,464-123,541,252
RP11-78A18	3	GGTGCTCTAATCTCTGAAGAGG	GTGTGTAACTTCAGTTACCTCAGC	chr.10: 123,521,167-123,530,569
RP11-78A18	4	CTAGCCAGAAAGAACTCCAGG	CCTCTTCAGAGATTAGAGCACC	chr.10: 123,512,973-123,521,188
RP11-78A18	5	GCACAACACAGGAACTTCCC	GGCCAGTATTTACAGATCCTACC	chr.10: 123,503,159-123,513,152
RP11-78A18	6	GACAGACTGGTATTTTCCTAGG	CTGCATTATGACCTAGCCCCC	chr.10: 123,492,813-123,502,999
RP11-78A18	7	AGGTGCATGCAACATCTTGCC	GCAGAAGAGTGGTAAACGTGAGG	chr.10: 123,483,792-123,492,883
RP11-78A18	8	CCTACCCACAAGACATTGTACC	CAGTAAGGAGGGATAGCTTGC	chr.10: 123,480,111-123,483,662
RP11-154J22	1	AGCGGCAATGTTAGCTATGCC	CCTCAACCTGAAGTTATGACGG	chr.15: 48,563,475-48,572,671
RP11-154J22	2a	CCTTGAGGAGAAAGCCTTAGC	CAAAGGAAGAAACCAAGCCAGG	chr.15: 48,552,854-48,563,078
RP11-154J22	2b	GAAAAATGAGGTCCAGACACTGG	CAAAGGAAGAAACCAAGCCAGG	chr.15: 48,554,330-48,563,078

*according to Ensembl release 67.

Supplementary Table 3. Sequencing primers for *ATE1* and *SLC12A1* mutation analysis

Primer name	Sequence (5'–3')	Product size (bp)
ATE1 Exon 1 F	TGCATTGTGGGGTGGCGG	312
ATE1 Exon 1 R	AGAGTGCCCCCTCCGTCT	
ATE1 Exon 2 F	CTCCTGACCTTGTGATTTGC	311
ATE1 Exon 2 R	TTTTCTTAAACCTCTTTCCAACAG	
ATE1 Exon 3 F	TGTGCTAGGCTGTTTTGGTG	220
ATE1 Exon 3 R	GACATCTACCTAGAGCGGAAATAAAC	
ATE1 Exon 4 F	GGGCTGGGATTAGAGGCTAC	321
ATE1 Exon 4 R	TTAATGACCCTTCCCCTTCC	
ATE1 Exon 5 F	TGGAGGATGAGAATGGATTTG	447
ATE1 Exon 5 R	TTTTGGCTGATGGAAAGACC	
ATE1 Exon 6 F	GCCTAACCATTGAAACTCTTTG	473
ATE1 Exon 6 R	CAAATGTTACTTCTTCCCAGTTC	
ATE1 Exon 7 F	AATTCGAGTTCGAGCTTTGG	418
ATE1 Exon 7 R	AGAACGCATCCTGAATTTGC	
ATE1 Exon 8 F	TCTCTGGATGAATTTTATGGACAC	277
ATE1 Exon 8 R	CCACCAAAATGAGCACTCC	
ATE1 Exon 9 F	GCTGTTTGTGCCTCTGCTTT	314
ATE1 Exon 9 R	GCAACAAATCATTATAATACACTGTCA	
ATE1 Exon 10 F	CAAATGTTTACCATCAAATTACACAG	271
ATE1 Exon 10 R	AACCCATTCGTCCTTCCTTC	
ATE1 Exon 11 F	GAGCCTTGAGTCAAACGTGC	370
ATE1 Exon 11 R	TAAGAGCCACAGCCACACAC	
ATE1 Exon 12 F	GTGGATGTTGCAGTGAGGTG	399
ATE1 Exon 12 R	TGACAGTTATTTCCCCACAGG	
SLC12A1 Exon 1+2 F	AACAACCACAAAGTAGATAGCTCAGT	499
SLC12A1 Exon 1+2 R	AAGGGAGGAGACTTGCTTGTG	
SLC12A1 Exon 3+4 F	TGGAACCCTTTGTTCATTGAC	449
SLC12A1 Exon 3+4 R	GCAAAATTATTTAGGAGGGGAAA	
SLC12A1 Exon 5 F	GGGAGGTGGATCTTTCTGTG	290
SLC12A1 Exon 5 R	AGCAATATGTTACTTTCACTTCCAAT	
SLC12A1 Exon 6 F	AACACAGGATTCCTAAAATTACTGG	359
SLC12A1 Exon 6 R	CCCTTAGTGCCCTGAGAAGG	
SLC12A1 Exon 7 F	GCTGCAATAAGACTCACATGC	217
SLC12A1 Exon 7 R	CCTGACCAGCCACTGTTGAT	
SLC12A1 Exon 8 F	TCTGATTTGGTTTCCTTTTACCTT	199
SLC12A1 Exon 8 R	GAGGAGGGCAATGGAGAAGT	
SLC12A1 Exon 9 F	GGACTAGGGAAGCCAATGGT	241
SLC12A1 Exon 9 R	AGGACTGCAAAGCAGAGCAA	
SLC12A1 Exon 10 F	TGCTCTGTATTCTTCTACCTCCA	179
SLC12A1 Exon 10 R	GAACAACTGGACCCCTCGTA	
SLC12A1 Exon 11 F	GAAAACCGTAAGGGACCAGA	250
SLC12A1 Exon 11 R	AATAGCAGTGAACATTTTTGAATTT	
SLC12A1 Exon 12 F	TGTAGTTGAAAGCCGTTTGC	277
SLC12A1 Exon 12 R	AAATGATTGCCAGTGAGAACG	
SLC12A1 Exon 13 F	TGACTGTGCATAGCTATAAATGACAA	249
SLC12A1 Exon 13 R	CAAACTAAAAGGAAAGCCCTATGA	
SLC12A1 Exon 14 F	CCCCTGGTCTCATCACTCAT	187
SLC12A1 Exon 14 R	TGCTTAGGCATATTTTAGTTTGGA	
SLC12A1 Exon 15 F	TGGAAGTTTTCCTTCTGCAT	221

SLC12A1 Exon 15 R	TGGAAACGCTATTCCAGACA	
SLC12A1 Exon 16 F	TGCCAATTTCCTCCTTTATCC	155
SLC12A1 Exon 16 R	AACACCAGGATGCCTGAGAC	
SLC12A1 Exon 17 F	CCACTGGAATGGTTCTAAGGTT	249
SLC12A1 Exon 17 R	CCTCACCCAAAATAATCCAAGA	
SLC12A1 Exon 18 F	GGCATTGCTGGCTATTTTTG	284
SLC12A1 Exon 18 R	TGGAGCACTAATTGTCTTTTGC	
SLC12A1 Exon 19 F	CCCAGTACGGTAAGGATTGC	176
SLC12A1 Exon 19 R	CACGTCTTGAAAGCCATCAC	
SLC12A1 Exon 20 F	TCAAAATCCTAGAAGCAAGTGTAA	243
SLC12A1 Exon 20 R	CCATAACAATGTCAGGCACAA	
SLC12A1 Exon 21 F	TGAGTTAAGTAGGTGATTTTGTCTTC	249
SLC12A1 Exon 21 R	CGGACTCTTCATAGATGCTCAA	
SLC12A1 Exon 22+23 F	GCCCTCAAAAGCAAACAGAT	528
SLC12A1 Exon 22+23 R	GACCTAACATGTGAGTGGCAAA	
SLC12A1 Exon 24 F	TCAAACACCAACCAAAAAGC	383
SLC12A1 Exon 24 R	CCATGTCATGCTTATTTGAAGG	
SLC12A1 Exon 25 F	GCCAGTCACACCTGGAGTATC	277
SLC12A1 Exon 25 R	TCAACTACTGTTTCCTTTCTCAGC	
SLC12A1 Exon 26 F	TGGTAGAACTGTACTCAACAAATCTGA	195
SLC12A1 Exon 26 R	CCTGAAGAGTCCCAAGCTTTT	
SLC12A1 Exon 27 F	CACTTTCATTTTTAAATTTTTCCTTCA	272
SLC12A1 Exon 27 R	GGTTTGCATATCCATAGATCAGA	

Supplementary Table 4. Genes flanking *ATE1* and *SLC12A1* and showing expression in the ear

Chromosome	Gene symbol	Gene name	Expression in ear* (transcripts per million)
10	*BRWD2*	Bromodomain and WD repeat domain containing 2	62
10	*FGFR2*	Fibroblast growth factor receptor 2	621
10	*HTRA1*	HtrA serine peptidase 1 precursor	186
15	*SEMA6D*	Semaphorin 6D isoform 1 precursor	248
15	*MYEF2*	Myelin expression factor 2	62
15	*DUT*	Deoxyuridine triphosphatase	186
15	*FBN1*	Fibrillin 1 precursor	124
15	*SHC4*	Rai-like protein	62
15	*EID1*	CREBBP/EP300 inhibitor 1	124
15	*SECISBP2L*	SECIS binding protein 2-like	62

*gathered from the *Homo sapiens* UniGene database.

14.3 Attachment 3

DFNB16 is a frequent cause of congenital hearing impairment: implementation of *STRC* mutation analysis in routine diagnostics.

CLINICAL GENETICS An International Journal of Genetics, Molecular and Personalized Medicine

Clin Genet 2014
Printed in Singapore. All rights reserved

CLINICAL GENETICS
doi: 10.1111/cge.12332

Short Report

DFNB16 is a frequent cause of congenital hearing impairment: implementation of *STRC* mutation analysis in routine diagnostics

Vona B., Hofrichter M.A.H., Neuner C., Schröder J., Gehrig A., Hennermann J.B., Kraus F., Shehata-Dieler W., Klopocki E., Nanda I., Haaf T. Short Report.
Clin Genet 2014. © 2013 The Authors. *Clinical Genetics* published by John Wiley & Sons A/S. Published by John Wiley & Sons Ltd., 2013

Increasing attention has been directed toward assessing mutational fallout of stereocilin (*STRC*), the gene underlying DFNB16. A major challenge is due to a closely linked pseudogene with 99.6% coding sequence identity. In 94 *GJB2/GJB6*-mutation negative individuals with non-syndromic sensorineural hearing loss (NSHL), we identified two homozygous and six heterozygous deletions, encompassing the *STRC* region by microarray and/or quantitative polymerase chain reaction (qPCR) analysis. To detect smaller mutations, we developed a Sanger sequencing method for pseudogene exclusion. Three heterozygous deletion carriers exhibited hemizygous mutations predicted as negatively impacting the protein. In 30 NSHL individuals without deletion, we detected one with compound heterozygous and two with heterozygous pathogenic mutations. Of 36 total patients undergoing *STRC* sequencing, two showed the c.3893A>G variant in conjunction with a heterozygous deletion or mutation and three exhibited the variant in a heterozygous state. Although this variant affects a highly conserved amino acid and is predicted as deleterious, comparable minor allele frequencies (MAFs) (around 10%) in NSHL individuals and controls and homozygous variant carriers without NSHL argue against its pathogenicity. Collectively, six (6%) of 94 NSHL individuals were diagnosed with homozygous or compound heterozygous mutations causing DFNB16 and five (5%) as heterozygous mutation carriers. Besides *GJB2/GJB6* (DFNB1), *STRC* is a major contributor to congenital hearing impairment.

Conflict of interest

The authors have no conflicts of interest to disclose.

B. Vona[a], M.A.H. Hofrichter[a], C. Neuner[a], J. Schröder[a], A. Gehrig[a], J.B. Hennermann[b], F. Kraus[c], W. Shehata-Dieler[c], E. Klopocki[a], I. Nanda[a] and T. Haaf[a]

[a]Institute of Human Genetics, Julius Maximilians University, Würzburg, Germany, [b]Department of Pediatric Endocrinology, Gastroenterology and Metabolic Diseases, Charité Universitätsmedizin, Berlin, Germany, and [c]Comprehensive Hearing Center, Department of Otorhinolaryngology, Plastic, Aesthetic and Reconstructive Head and Neck Surgery, University Hospital, Würzburg, Germany

Key words: chromosome 15q15.3 – congenital hearing impairment – deafness-infertility syndrome (DIS) – DFNB16 – non-syndromic hearing loss (NSHL) – *STRC*

Corresponding author: Prof. Thomas Haaf, Institute of Human Genetics, Julius-Maximilians-Universität Würzburg, Biozentrum, Am Hubland, 97074 Würzburg, Germany.
Tel.: +49 931 3188738;
fax: +49 931 3187398;
e-mail: thomas.haaf@uni-wuerzburg.de

Received 15 October 2013, revised and accepted for publication 12 December 2013

Hearing impairment is an extremely heterogeneous disorder affecting approximately 1 of 1000 newborns (1). At present, 42 genes and 69 loci (http://hereditaryhearingloss.org) are implicated in non-syndromic autosomal recessive deafness (locus notation DFNB). In the European population, 20–40% of non-syndromic hearing loss (NSHL) is due to mutations in *GJB2* (MIM: 121011) and *GJB6* (MIM: 604418), together comprising the DFNB1 locus (2). With few exceptions, autosomal-recessive NSHL has similar manifestations, wherein hearing loss is severe to profound with prelingual onset (3).

An initial candidate gene approach assigned *STRC* (MIM: 606440) to chromosome 15q15.3 encompassing the DFNB16 locus (4). Stereocilia form crosslinks necessary for longitudinal rigidity and outer hair cell structure, and upon mechanical deflection, stereociliary transduction sensitive channels open for cellular

depolarization (5, 6). Reverse transcriptase polymerase chain reaction (RT PCR) from several mouse tissues showed strong, nearly exclusive expression in the inner ear (4) and upon knockout, these key structures were absent (7).

STRC deletion frequencies of >1% have been calculated in mixed deafness populations (8, 9) and the incidence of *STRC* hearing loss is an estimated 1 in 16,000 (10). Accumulating evidence suggests that DFNB16 constitutes a significant proportion of the otherwise genetically heterogeneous etiology comprising NSHL. One challenge impeding diagnostic implementation of *STRC* screening is the presence of a non-processed pseudogene with 98.9% genomic and 99.6% coding sequence identity (9) residing less than 100 kb downstream from *STRC* in a region encompassing a segmental duplication with four genes, *HISPPD2A* (MIM: 610979), *CATSPER2* (MIM: 607249), *STRC*, and *CKMT1A* (MIM: 613415). Apart from *CKMT1A*, these pseudogenes have mutations rendering them inactive (10). In the case of *pSTRC*, inactivity is due to a nonsense mutation in exon 20 (4). Homozygous deletions of *STRC* and *CATSPER2* result in deafness infertility syndrome (DIS; MIM: 611102), characterized by deafness in both males and females, and exclusive male infertility, as *CATSPER2* is required for sperm motility. Not only is it challenging to generate accurate sequencing data without pseudogene inclusion, it is even more difficult interpreting such data without the usual reliable resources for mutation interpretation, as these databases are 'polluted' with pseudogene data as well.

Materials and methods

The study was approved by the Ethics Committee at the Medical Faculty of Würzburg University. Informed written consent was obtained from all participants/parents.

Subjects

Our study cohort consisted of primarily pediatric individuals. Patients 1–94, with NSHL were recruited through the Comprehensive Hearing Center at Würzburg University Hospital. All patients had mild to profound sensorineural hearing loss (SNHL). Although study participants were counselled primarily for NSHL, additional symptoms were found in a limited minority. Patient 95 with syndromic SNHL was recruited through Charité Universitätsmedizin Berlin. Genomic DNA (gDNA) was extracted from whole blood using standard salt extraction methods.

STRC copy number counting

Individuals 1–93 were screened for copy number variations (CNVs) using the Omni1-Quad v1.0 array (Illumina, San Diego, CA) and analyzed using GenomeStudio version 2011.1. CNV calling was performed with QuantiSNP 2.2 (11) and cnvPartition 3.2.0 (Illumina). Syndromic patient 95 was tested by array CGH using the Agilent 4x180K (Agilent Technologies, Santa Clara, CA) platform. Individual 94 was tested for *STRC* CNVs by quantitative real-time PCR (qPCR), using unique *STRC* exon 22 primers excluding the pseudogene (Table S1, Supporting Information; exon 22 primers without M13 tags) and the SensiMix SYBR Green Kit (Bioline, Luckenwalde, Germany).

Primer design and Sanger sequencing of *STRC*

To exclude pseudogene sequences, two long-range (LR) PCR products were generated for subsequent nested PCR. Primers (Table S1) were designed using PRIMER3 (version 0.4.0) software (12) or obtained from the literature (9). The RefSeq *STRC* sequence annotation corresponds to NM_153700.2 and Ensembl ENSG00000166763 (hg 18). *STRC* and *pSTRC* sequences were aligned in UCSC Genome Browser (http://genome.ucsc.edu). *STRC*-specific sequences were verified using BLAT. Although confined to few divergent bases up- and downstream from *STRC*, we targeted these regions for LR-PCR primer design, placing the divergent nucleotides at the terminal 3′ end if possible (Fig. S1).

LR-PCR was performed with the Qiagen LongRange PCR Kit (Qiagen, Hilden, Germany) using cycling profiles in Table S2. Amplification products were diluted 1:1000 to reduce pseudogene carryover from gDNA and then used for nested PCR. A sequencing control in intron 18 overlapping with both LR products was included for pseudogene exclusion confirmation. Nested PCRs (Table S2) and sequencing continued after LR-PCR products were verified negative for a three-nucleotide frameshift, indicative of *pSTRC* sequence.

Bidirectional sequencing, performed with an ABI 3130xl 16-capillary sequencer (Applied Biosystems, Carlsbad, CA), was analyzed using Gensearch (Phenosystems, Lillois Witterzee, Belgium) and CodonCode Aligner (CodonCode, Dedham, MA). SIFT (13) and PolyPhen-2 (14) predicted amino acid substitution and disease causing potential.

Results

Individuals 1–93 were run on Illumina Omni1-Quad microarrays. We identified 2 cases with homozygous deletions, 5 with heterozygous deletions, and 10 with copy-neutral loss of heterozygosity (LOH) (Fig. 1; Table S3). Using the Agilent 4x180K array, we detected an additional homozygous deletion in syndromic patient 95. None of these individuals displayed disease-relevant CNVs elsewhere. The homozygous deletions were verified via PCR in exon 22 and the heterozygous deletions via qPCR. By qPCR, we also detected heterozygous deletions in both parents of the homozygous patients 1 and 95. Individual 94 did not have a microarray performed to simulate a diagnostic setting for NSHL patients where copy number counting is performed by qPCR. This individual showed a heterozygous

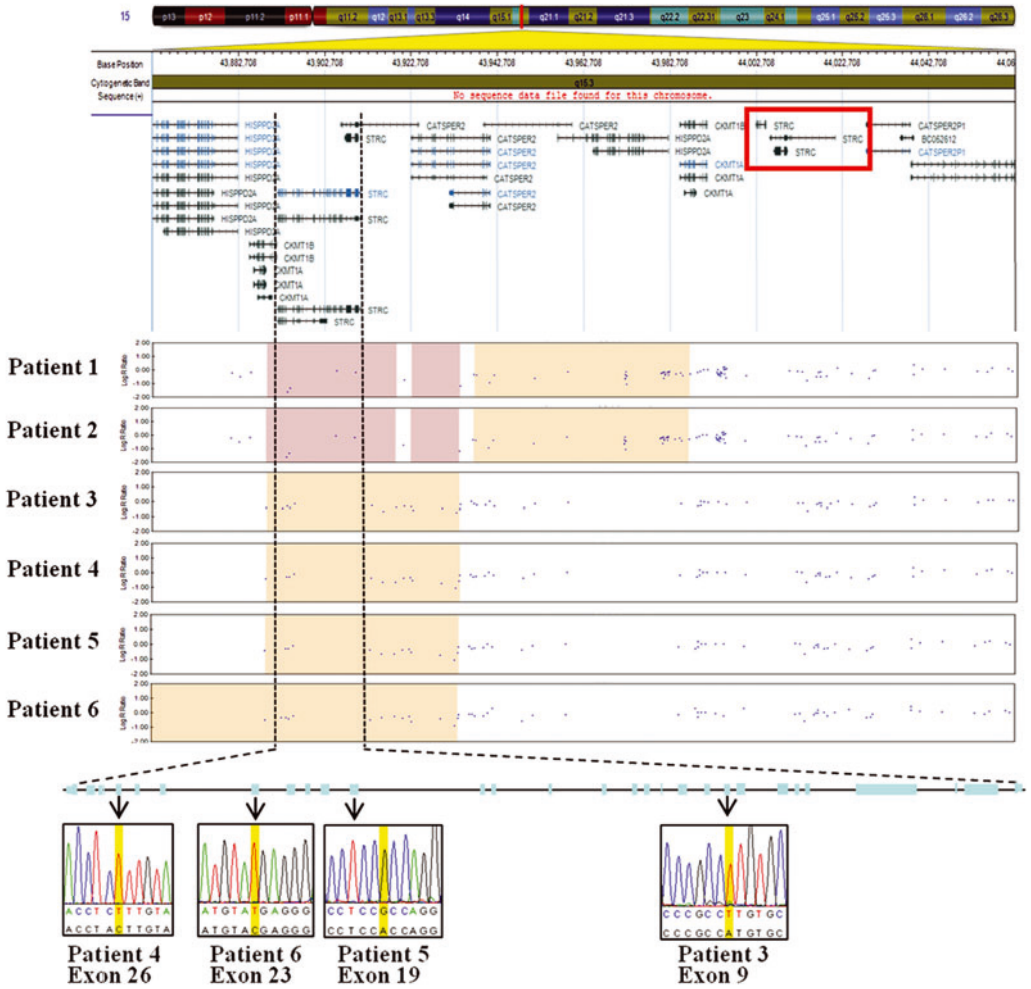

Fig. 1. Overview of patients with biallelic mutations in *STRC*. The upper part of the figure shows a map of the analyzed region. *pSTRC* transcripts are boxed in red. Illumina Omni1-Quad array data in the middle depict deletions in relation to the *STRC* and *pSTRC* genes. Regions with altered signal intensity are marked in pink representing homozygous deletions and orange indicating heterozygous deletions. The lower part of the figure shows Sanger sequencing chromatograms of the four heterozygous deletion patients with hemizygous sequence changes in relation to exonic position within the gene.

deletion, yielding a combined six heterozygous deletions (Table S3).

Thirty-six NSHL individuals, including six heterozygous deletion, 10 LOH and 20 cases without deletion or LOH, were selected for subsequent Sanger sequencing. Of the six heterozygous deletion carriers, three (nos. 3, 4, and 6) presented hemizygous pathogenic *STRC* mutations following pseudogene exclusion, with an additional patient (no. 5) exhibiting a heterozygous deletion in conjunction with a candidate mutation c.3893A>G (Fig. 1; Table 1). Table S4 summarizes PolyPhen-2 and SIFT prediction outcomes. None of the 10 individuals with copy-neutral LOH exhibited a homozygous pathogenic mutation; one (no. 16) had a heterozygous mutation. Of the 20 individuals without microdeletion or LOH, 1 (no. 24) displayed compound heterozygous pathogenic mutations, 1 (no. 25) a pathogenic mutation in conjunction with the homozygous c.3893A>G variant, and 3 (nos. 22, 23, and 26) heterozygous c.3893A>G variants (Table 1). The remaining cases were mutation negative. The minor allele frequency (MAF) of the c.3893A>G variant in our NSHL cohort is 9%. In 100 normally hearing adults, we identified 18 heterozygous and 2 homozygous

Table 1. SNHL individuals with *STRC* deletions and/or sequence changes in respective exons

No.	Allele 1	Allele 2	Exon	Interpretation
DFNB16 patients				
1, 2, 95	*STRC* gene deletion	*STRC* gene deletion		Homozygous deletions
3	*STRC* gene deletion	c.2726A>T, p.H909L	9	Heterozygous deletion and hemizygous pathogenic mutation
4	*STRC* gene deletion	c.4918C>T, p.L1640F	26	Heterozygous deletion and hemizygous pathogenic mutation
6	*STRC* gene deletion	c.4402C>T, p.R1468X	23	Heterozygous deletion and hemizygous pathogenic mutation
24	c.2303_2313+1del12, p.G768Vfs*77	c.5125A>G, p.T1709A	6, 28	Compound heterozygous pathogenic mutations
Heterozygous deletion, mutation, and variant carriers				
5	*STRC* gene deletion	c.3893A>G, p.H1298R	19	Heterozygous deletion and hemizygous variant
7, 94	*STRC* gene deletion	Normal		Heterozygous deletion
25	c.2640G>T, p.E880D; c.3893A>G, p.H1298R	c.3893A>G, p.H1298R	8, 19	Heterozygous pathogenic mutation and homozygous variant
16	c.5180A>G, p.E1727G	Normal	28	Heterozygous pathogenic mutation
22, 23, 26	c.3893A>G, p.H1298R	Normal	19	Heterozygous variant

variant carriers, corresponding to an MAF of 11%. Orthologous alignments illustrate strong evolutionary conservation in mutated positions, including the recurrent variant c.3893A>G (Fig. S2).

All patients with biallelic mutations underwent clinical evaluation and, with few exceptions, had audiogram(s) available (Fig. 2). Audiological, clinical and family history descriptions are detailed in Table 2. Besides the 7 DFNB16 patients here, 32 additional patients with biallelic *STRC* mutations (including 13 cases from four families) have been published so far (8–10, 15, 16) (Table S5). Many of these patients have sloping high-frequency audiometric profiles and together show an age of onset spectrum ranging from birth to childhood.

Discussion

We analyzed a cohort of 94 NSHL and one syndromic patient and determined three homozygous and six heterozygous *STRC* deletions. Deletions of 30 kb (two cases), 45 kb (four cases) and 82 kb (two cases) are recurrent (Fig. 1; Table S3), suggesting non-homologous recombination events (17) between highly similar short DNA elements in chromosome 15q15.3. The homozygous *STRC* deletions described here extend into *CATSPER2* and are responsible for male DIS, contributing to the limited cases in the literature (Table S5). Two of the three homozygous deletion patients are pre-pubertal boys unevaluated for fertility. One of them (no. 95) displayed congenital abnormalities and comorbidities (Table 2), which are probably independent of DFNB16. Three of the six heterozygous deletion patients exhibited hemizygous pathogenic mutations in the second allele, consistent with DFNB16. Among 10 patients with LOH >1 Mb, we identified a single heterozygous mutation, indicating that at least small stretches of LOH are not useful predictors of homozygous *STRC* mutations. Among 20 patients without heterozygous deletion or LOH, one exhibited biallelic mutations. Although microdeletions are the most frequent mutation type, Sanger sequencing for the detection of point mutations or smaller intragenic deletions/duplications is mandatory in all SNHL patients displaying appropriate DFNB16 audiogram configurations.

There are different methods for *STRC* CNV detection. Multiplex ligation-dependent probe amplification (MLPA) (10) and qPCR successfully distinguish copy numbers, but are limited to small non-homologous regions harboring divergent nucleotides. The Illumina SNP array employed here covers *STRC* with seven single-nucleotide polymorphism (SNP) probes (three of them lacking 100% identity with *pSTRC*), which is conducive to CNV detection using standard diagnostic reporting algorithms. Array CGH similarly shows adequate resolution to detect a 45 kb deletion.

One previous study (9) employed a Sanger sequence approach to detect small sequence changes, but was unable to differentiate the *STRC* gene from the pseudogene, which is a drawback we have overcome. There are limited divergent nucleotides between *STRC* and *pSTRC* toward the 3′ portion of the gene. The absence of these in our LR exon 12–29 sequences confirmed specificity. In addition, we implemented an LR-PCR control in intron 18, whereby a three-nucleotide frameshift is present if *pSTRC* is amplified. This control verifies pseudogene exclusion for each LR-PCR, since this region overlaps with both LR products. This is important because *pSTRC* amplifies with unoptimized annealing temperatures and unintended gDNA carryover.

Interpretation is especially challenging for *STRC* analysis since we cannot rely on customary mutation and allele frequency data. Thousand Genomes Project and dbSNP index variants from Next Generation

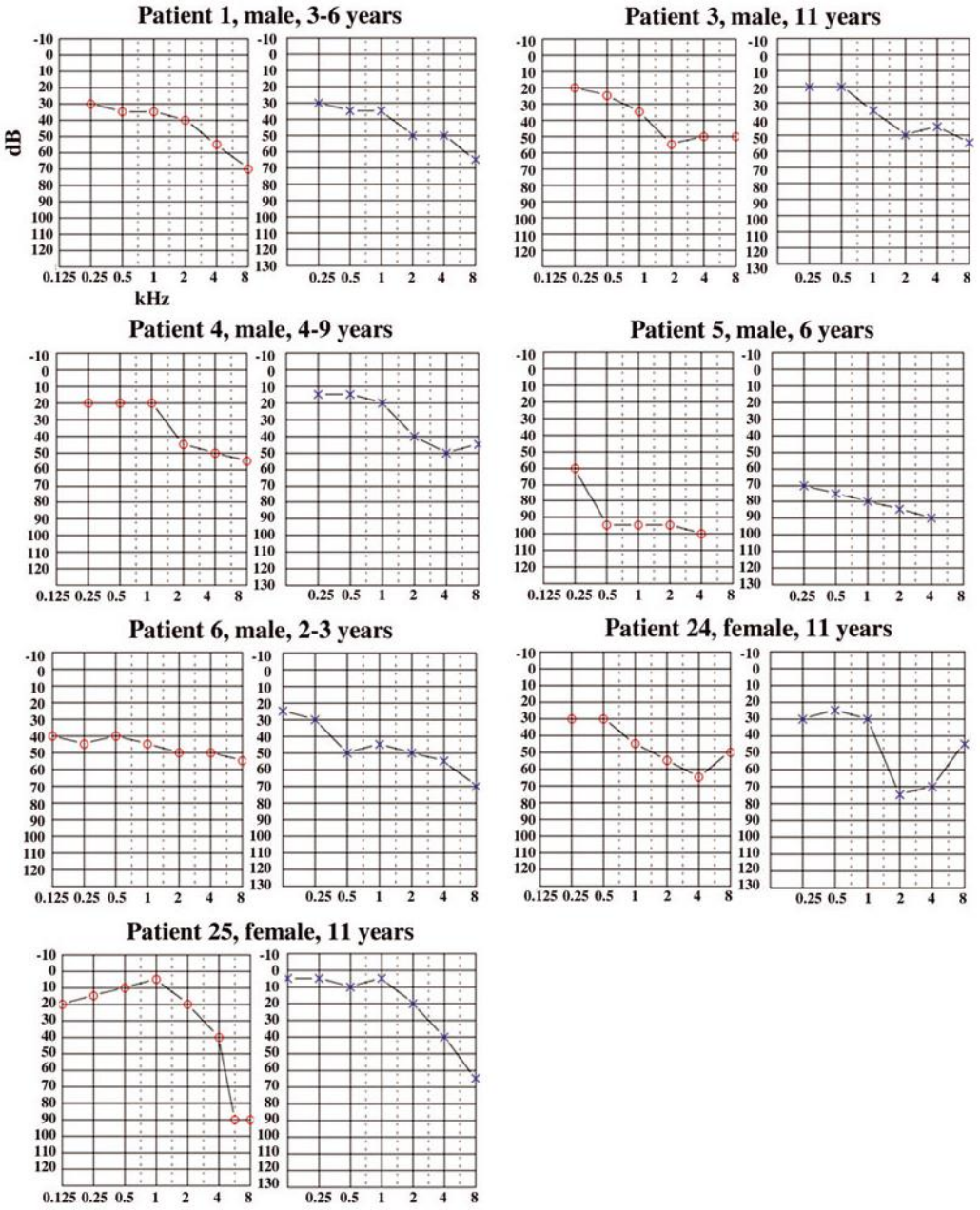

Fig. 2. Bilateral pure tone audiograms from individuals with biallelic *STRC* mutations. Above the audiograms are the patient number, sex, and age. Circles in the audiograms represent the right, and crosses, the left ear, respectively. If multiple audiograms were present, an age range is listed and the average of all thresholds is depicted. Created with AUDIOGRAMMAKER software (http://www.jacobhaskins.com/).

Table 2. Audiological, clinical and family histories of biallelic *STRC* mutation patients

No.	Onset	Audiological description[a]	Clinical description	Family history of HL
Patients with homozygous *STRC* deletions				
1	2 years	HL in all frequencies with mild HL in low- to mid-frequencies until 4 kHz, moderate to severe HL to 8 kHz	No additional symptoms	None; parents are confirmed heterozygous deletion carriers
2	Childhood	High tone HL, no further description available	Delayed speech and language development	Sister has HL since birth; two additional sisters are without HL; maternal grandmother and paternal grandfather have reported age-related HL
95	Birth	Auditory brainstem response measurements from the newborn hearing test indicated maximal thresholds of 65 dB	Born in the 35th week of gestation presenting facial dysmorphisms (long eye lashes, flat nasal bridge, and epicanthus), hypoplastic widely spaced nipples, atrial septal defect, and delayed speech development; also diagnosed with hydroxylysinuria, hydroxylysinemia, and severe recurrent infections	No family history of HL; parents are first-degree cousins and confirmed heterozygous deletion carriers; one sibling died at 3 months because of an infection of unknown etiology
Patients with *STRC* deletion and pathogenic DNA sequence mutation				
3	5 years	Audiogram from age 10 indicated moderate HL, mildly sloping at higher frequencies	Oral motor skills and vocabulary developed normally per age; bifid uvula and sigmatism interdentalis diagnosed at 5 years of age; underwent intensive ambulant therapy for 1 year for dyslalia	Family history of HL
4	3 years	High frequency HL with normal hearing thresholds until 1 kHz and mild to moderate HL from 2 to 8 kHz	None available	None
6	Birth	Mild to middle grade HL; free field and PTA between 2 and 4 years of age demonstrated mild HL in all frequencies and sloping audiometric profiles, more pronounced between 2 and 8 kHz	Hypothyroidism with HL prompted Pendred syndrome screening with *SLC26A4* mutation negative result	None
Patient with compound heterozygous DNA sequence mutations				
24	6 years	PTA with sloping high frequency configuration in the right ear and cookie bite pattern in the left ear	No additional symptoms	Father and paternal uncle have mild HL; parents are first-degree cousins with two additional normally hearing children

HL, hearing loss; PTA, pure tone audiometry.
[a]All patients are bilaterally affected.

Sequencing (NGS) platforms that generate amplicon libraries indiscriminate of pseudogene counterparts. A well-rounded approach for *STRC* mutation assessment calls for consideration of evolutionary conservation of variants (18), as well as utilizing audiograms as helpful diagnostic tools, since high-frequency sloping appears a uniting feature of DFNB16. The c.3893A>G variant, which is predicted to be deleterious, was found with comparable MAFs (around 10%) in SNHL individuals and controls. Although we cannot entirely exclude the formal possibility that c.3893A>G in conjunction with an *STRC* deletion or pathogenic mutation contributes to SNHL, it should be considered as non-pathogenic as long as functional analyses are missing.

Conclusions

Our data confirm that *STRC* biallelic mutations significantly contribute to NSHL, particularly in children with mild to moderate hearing impairment with greater affection in higher frequencies. The frequency of DFNB16 in children with NSHL may be even higher than 6%

(6 of 94), considering we did not sequence all patients without *STRC* deletion. Gathering evidence implies that in addition to *GJB2/GJB6*, mutation analysis of *STRC* should be implemented as part of routine differential diagnostics for NSHL. Unfortunately, targeted NGS of deafness genes or exome sequencing does not reliably detect *STRC* mutations. As the prevalence of heterozygous deletion carriers at this locus is high, incidental CNVs could be detected in diagnostic and prenatal cases requiring microarray analysis. Initiation of mutational screening in *STRC* should be indicated in these cases for the detection of possible mutations in trans. The presentation of our sequencing assay allows the full disclosure of *STRC* mutations that will translate to improved NSHL diagnostics.

Supporting Information

The following Supporting information is available for this article:

Fig. S1. Long-range primer selection based on divergent nucleotides existing between *pSTRC* (top sequence) and *STRC* (bottom sequence). Dots represent deleted nucleotides; vertical dashes identical nucleotide bases. Primer sequences are boxed in red; divergent nucleotides due to deletions or divergent sequences are boxed in black. The upper part presents the long-range primers amplifying exons 1–19; the lower part, the primers amplifying exons 12–29.

Fig. S2. Conservation of STRC residues in mutated positions. Human wild-type residues are aligned against those of 36 species. Blosum62 coloring was used to notate conservation levels. The analyzed residue is highlighted in dark blue. If residue and consensus sequences match, they are colored in medium blue. If they do not match but they have a positive Blosum62 score indicating weaker conservation, then they are colored in light blue. Gaps are marked with a dot. Annotation tracks were obtained from PolyPhen-2.

Table S1. Primers for *STRC* long-range PCR, nested PCR, and Sanger sequencing

Table S2. PCR cycling information

Table S3. Patients with *STRC* deletions or copy neutral LOH

Table S4. *STRC* sequence changes with in silico predictions

Table S5. Summary of patients with biallelic *STRC* mutations (DFNB16) listed in publications to date

Additional Supporting information may be found in the online version of this article.

Acknowledgements

The authors would like to express the gratitude to the patients and their families for participation in this study. We would like to acknowledge Dr Wolfram Kreß, Dr Erdmute Kunstmann, and Dr Simone Rost from the University of Würzburg for clinical information and sequence analysis assistance. We thank Dr Tom Muller from the University of Arizona, Dr Ian Krantz and Dr Lauren Francey from the Children's Hospital of Philadelphia for their constructive discussion. This study was supported by a research grant (HA 1374/7-2) from the German Research Foundation.

References

1. Morton CC, Nance WE. Newborn hearing screening - a silent revolution. N Engl J Med 2006: 354: 2151–2164.
2. Tranebjaerg L. Genetics of congenital hearing impairment: a clinical approach. Int J Audiol 2008: 47: 535–545.
3. Bitner-Glindzicz M. Hereditary deafness and phenotyping in humans. Br Med Bull 2002: 63: 73–94.
4. Verpy E, Masmoudi S, Zwaenepoel I et al. Mutations in a new gene encoding a protein of the hair bundle cause non-syndromic deafness at the DFNB16 locus. Nat Genet 2001: 29: 345–349.
5. Hackney CM, Furness DN. Intercellular cross-linkages between the stereociliary bundles of adjacent hair cells in the guinea pig cochlea. Cell Tissue Res 1986: 245: 685–688.
6. Tsuprun V, Santi P. Structure of outer hair cell stereocilia side and attachment links in the chinchilla cochlea. J Histochem Cytochem 2002: 50: 493–502.
7. Verpy E, Weil D, Leibovici M et al. Stereocilin-deficient mice reveal the origin of cochlear waveform distortions. Nature 2008: 456: 255–258.
8. Hoppman N, Aypar U, Brodersen P, Brown N, Wilson J, Babovic-Vuksanovic D. Genetic testing for hearing loss in the United States should include deletion/duplication analysis for the deafness/infertility locus at 15q15.3. Mol Cytogenet 2013: 6: 19.
9. Francey LJ, Conlin LK, Kadesch HE et al. Genome-wide SNP genotyping identifies the stereocilin (STRC) gene as a major contributor to pediatric bilateral sensorineural hearing impairment. Am J Med Genet Part A 2012: 158A: 298–308.
10. Knijnenburg J, Oberstein SA, Frei K et al. A homozygous deletion of a normal variation locus in a patient with hearing loss from non-consanguineous parents. J Med Genet 2009: 46: 412–417.
11. Colella S, Yau C, Taylor JM et al. QuantiSNP: an Objective Bayes Hidden-Markov Model to detect and accurately map copy number variation using SNP genotyping data. Nucleic Acids Res 2007: 35: 2013–2025.
12. Rozen S, Skaletsky H. Primer3 on the WWW for general users and for biologist programmers. Methods Mol Biol 2000: 132: 365–386.
13. Sim NL, Kumar P, Hu J, Henikoff S, Schneider G, Ng PC. SIFT web server: predicting effects of amino acid substitutions on proteins. Nucleic Acids Res 2012: 40: W452–W457.
14. Adzhubei IA, Schmidt S, Peshkin L et al. A method and server for predicting damaging missense mutations. Nat Methods 2010: 7: 248–249.
15. Avidan N, Tamary H, Dgany O et al. CATSPER2, a human autosomal nonsyndromic male infertility gene. Eur J Hum Genet 2003: 11: 497–502.
16. Zhang Y, Malekpour M, Al-Madani N et al. Sensorineural deafness and male infertility: a contiguous gene deletion syndrome. J Med Genet 2007: 44: 233–240.
17. Liu P, Carvalho CM, Hastings PJ, Lupski JR. Mechanisms for recurrent and complex human genomic rearrangements. Curr Opin Genet Dev 2012: 22: 211–220.
18. Kumar S, Dudley JT, Filipski A, Liu L. Phylomedicine: an evolutionary telescope to explore and diagnose the universe of disease mutations. Trends Genet 2011: 27: 377–386.

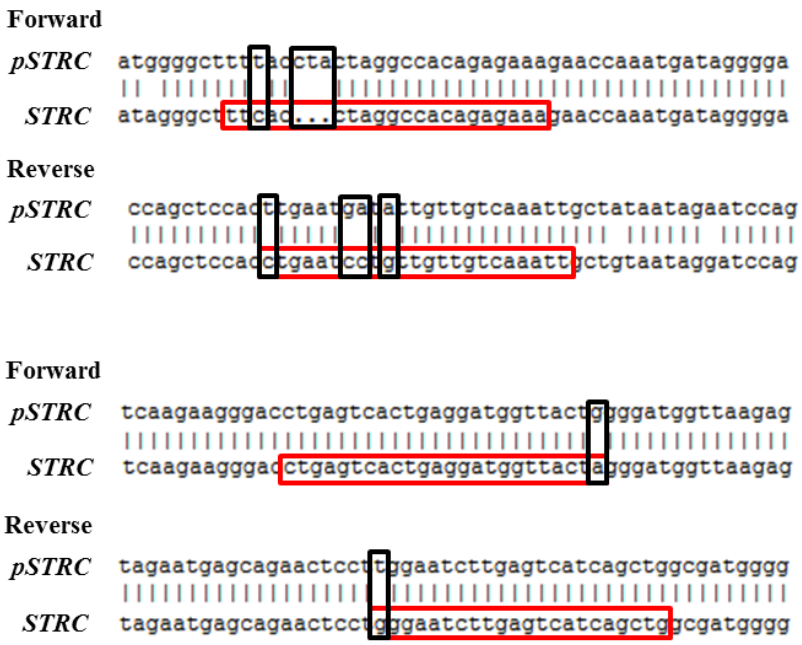

Supplementary Figure S1. Long-range primer selection based on divergent nucleotides existing between *pSTRC* (top sequence) and *STRC* (bottom sequence). Dots represent deleted nucleotides; vertical dashes identical nucleotide bases. Primer sequences are boxed in red; divergent nucleotides due to deletions or divergent sequences are boxed in black. The upper part presents the long-range primers amplifying exons 1-19; the lower part, the primers amplifying exons 12-29.

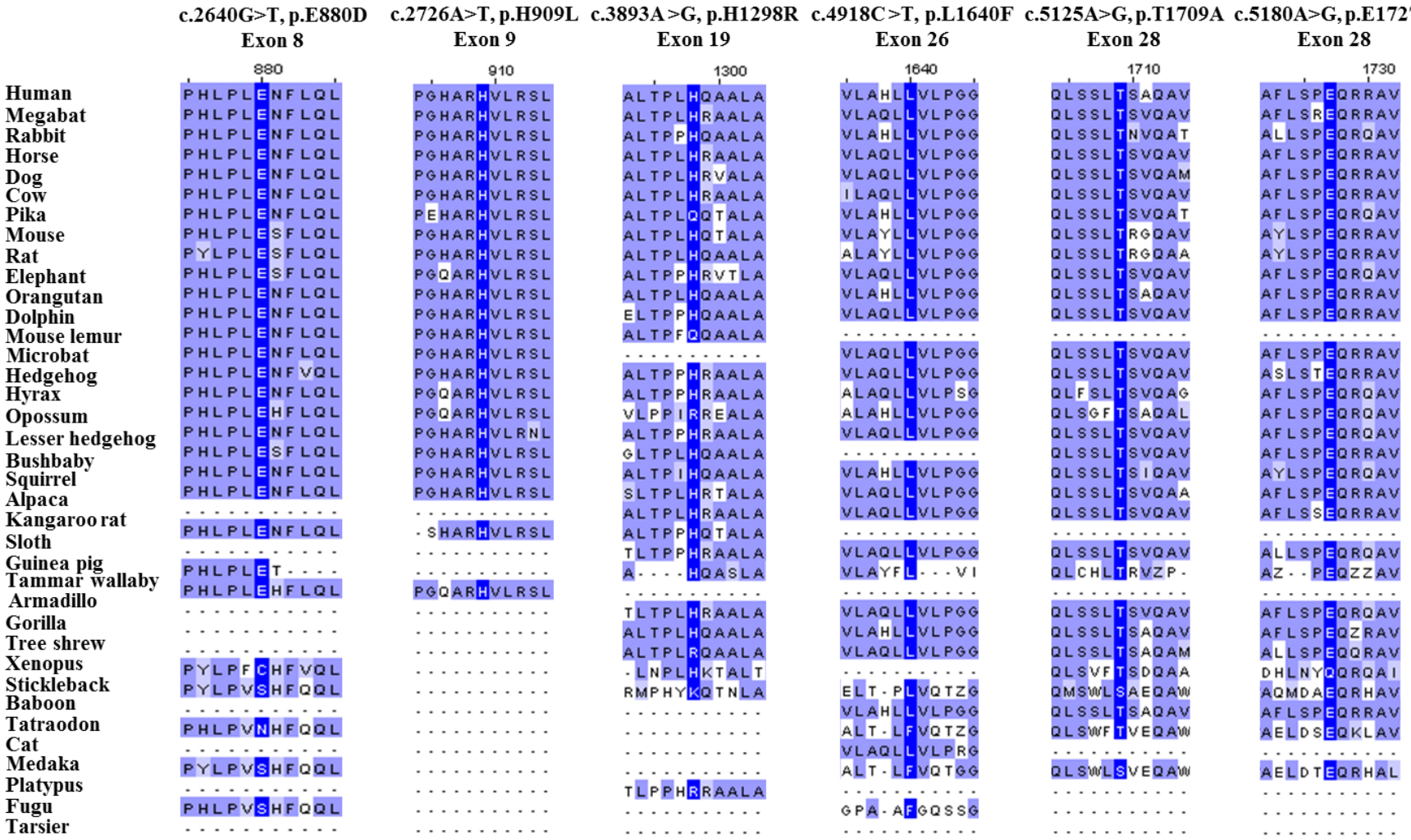

Supplementary Figure S2. Conservation of *STRC* residues in mutated positions. Human wild-type residues are aligned against those of 36 species. Blosum62 coloring was used to notate conservation levels. The analyzed residue is hightlighted dark blue. If residue and consensus sequences match, they are coloured medium blue. If they do not match but they have a positive Blosum62 score indicating weaker conservation, then they are coloured light blue. Gaps are marked with a dot. Annotation tracks were obtained from PolyPhen-2.

Supplementary Table S1. Primers for *STRC* long-range PCR, nested PCR, and Sanger sequencing

Primer name	Forward Sequence (5'-3')[a]	Reverse Sequence (5'-3')[a]	Size (bp)	Purpose
Exon 1-19	TTCACCTAGGCCACAGAGAAA	AATTTGACAACAACAGGATTCAG	14,036	long-range PCR
Exon 12-29	CTGAGTCACTGAGGATGGTTACTA	CAGCTGATGACTCAAGATTCCC	12,365	long-range PCR
Intron 18	CCTCTGATTTCGGGTAAAAGG	GAAATTCGAGACCACCCTGA	267	PCR, sequencing (long-range control)
Exon 1	GTGTCAGTGGAGCCTCAGGT	ATCCCCAGTTCTGCTCACTG	131	PCR, sequencing
Exon 1_Seq[b]		AGGGGCCAGAGGCTGAGA		sequencing
Exon 2_1	GATCCAGGTAGGGAACTGTG[c]	ACACAGTCAGACGGCCC[c]	535	PCR, sequencing
Exon 2_2	GCTGGGAGCCTTAGCTCCTG	CCCTCAGAACTGGTCTCCTG	560	PCR, sequencing
Exon 3	CTGGGACTGGGATGTGG[c]	TGCTCAAGGTCATATGGCTAG[c]	277	PCR, sequencing
Exon 4_1	TCAGGGTCAGAATCTTCAGC[c]	AGCAGGCCAGCACAGAG[c]	543	PCR, sequencing
Exon 4_2	CACGACCAGTTTCCTGATG[c]	GGATGGTCCCAGTGGTG[c]	525	PCR, sequencing
Exon 4_3	CAGGCCAATGCAGGATAAGT	TTCTAGGAGCTTTCCCTCTGG	503	PCR, sequencing
Exon 4_4	CACGCCTACACTATCTCCTC	TCTAGAGCTGTGTGCTTCAA	396	PCR, sequencing
Exons 5-6	GACAAGCATCCCAGCAAG[c]	CCTCCTCCCACTAAAGCAAG[c]	450	PCR, sequencing
Exon7	TGGAGCCTAGTGTTCAGAGG[c]	GCACATTGCCTATCTGGC[c]	398	PCR, sequencing
Exons 8-9	GACAGCAGGGCTACAGAGG[c]	TCTTCCTAGAACACCGACCC[c]	610	PCR, sequencing
Exon 10	TGTACCCATACCATCTGCTG[c]	CAAGTTGACACAATGGGAAAG[c]	295	PCR, sequencing
Exon 11	GGGAAATTCAGATGTGGGATTA	ATTCTCTTGACTGGGGCTCA	329	PCR, sequencing
Exons 12-13	GCCTTAGGAACCCACTTAGG[c]	AAGATGCCTTCCTCCCAAC[c]	532	PCR, sequencing
Exon 14	AGGGAAGGCCTTTCATACC[c]	AGGGTAGTGTGGGAGGTAGC[c]	232	PCR
Exon 14_Seq[b]	CACAACCAATTCTCATGCAG			sequencing
Exon 15	TTTGGTCCCTTTCCACC[c]	AGGGCTAAGGGATAGGTAAAG[c]	296	PCR, sequencing
Exon 16	TCGAGAGAAGAGTGGGCAT	GTCCTTTGGCTCTAGTCAGG	422	PCR
Exon 16_Seq[b]	TTGGACAGTGTCTCTTCTGG			sequencing
Exons 17-18	TTACGGTGGATGAACATCTG[c]	AAACTACCTCCTCCAGGGC[c]	537	PCR, sequencing
Exon 19	GCTGCGGACTGTGGGGTTT[c]	CTTCCTTAAGCAATGAGCCCAG[c]	498	PCR, sequencing
Exon 20	TCTGGGCTCATTGCTTAAGG	ACACAGGGCTCCAGGGGA	470	PCR, sequencing
Exon 21	TCCATATTCTTAAGGTCCCC	CCTGTCTCTGTTTTGCAGTC	342	PCR, sequencing
Exon 22	GGAGACTGCAAAACAGAGAC[c]	AACTCCCAGAACTACAGAATTC[c]	429	PCR, sequencing
Exon 23	CAGTGCTACCATTAAATCTCTGAAT	GGTAACCACTGCTTTCGTC[c]	628	PCR, sequencing
Exon 24	GAGGAAACTAAAGAAAAGGCAAA	AATTCCTTGGGCTTTAGATGAT	372	PCR, sequencing
Exon 25	CCTTCTTTCTATCTTTTGTTG	CTTCCTCCATGGGACCAGAC	511	PCR, sequencing
Exon 26	GAAAGAAGGATCATGAAGGTCTG	TAAACACCCTCAGGCCCC[c]	391	PCR, sequencing
Exons 27-28	CTTTGGGAGTAGTTAGAGAAGGTC[c]	TCTAAGAGCCAGACAGCACC[c]	503	PCR, sequencing
Exon 29	ACAGGCAGAGCGCTAATTTC[c]	TCAGGATGCACTTCTGTTTG[c]	254	PCR, sequencing

[a]All primers are tagged with universal M13 sequences with the exception of exon 16 forward primer.

[b]Primers designed specifically for sequencing due to nucleotide repeats in the targeted region.

[c]Primers originating from Francey et al., 2012 (reference 9).

Supplementary Table S2. PCR cycling information

Step	Temperature	Time	Cycle repeats
Long-range PCR for exons 1-19			
1	93°C	hold	
2	93°C	3 min	
3	93°C	15 sec	
4	62°C	30 sec	
5	68°C	17 min	go to step 3, 37x
6	68°C	5 min	
7	4°C	hold	
Long-range PCR for exons 12-29			
1	93°C	hold	
2	93°C	3 min	
3	93°C	15 sec	
4	64°C	30 sec	
5	68°C	17 min	go to step 3, 37x
6	68°C	5 min	
7	4°C	hold	
Nested PCR			
1	94°C	hold	
2	94°C	2 min	
3	94°C	30 sec	
4	70°C	30 sec	
5	72°C	30 sec	go to step 3, 2x
6	94°C	30 sec	
7	67°C	30 sec	
8	72°C	30 sec	go to step 6, 2x
9	94°C	30 sec	
10	65°C	30 sec	
11	72°C	30 sec	go to step 9, 33x
12	72°C	5 min	
13	4°C	hold	

Supplementary Table S3. Patients with *STRC* deletions or copy neutral LOH

Patient no.	Coordinates on chr. 15 (bp)[a]	Size[b]	Chromosomal change	Technique
1	43,888,976-43,919,081	30.1 kb	homozygous deletion	Illumina Omni1-Quad
2	43,888,976-43,919,081	30.1 kb	homozygous deletion	Illumina Omni1-Quad
95	43,888,727-43,933,874	45.1 kb	homozygous deletion	Agilent 4x180K
3	43,888,976-43,933,724	44.7 kb	heterozygous deletion	Illumina Omni1-Quad
4	43,888,976-43,933,895	44.9 kb	heterozygous deletion	Illumina Omni1-Quad
5	43,888,976-43,933,895	44.9 kb	heterozygous deletion	Illumina Omni1-Quad
6	43,852,043-43,933,724	81.7 kb	heterozygous deletion	Illumina Omni1-Quad
7	43,852,043-43,933,724	81.7 kb	heterozygous deletion	Illumina Omni1-Quad
94	43,896,021-43,896,449	429 bp	heterozygous deletion	qPCR
8	42,913,470-44,046,092	1.1 Mb	copy neutral LOH	Illumina Omni1-Quad
9	42,679,480-43,923,019	1.2 Mb	copy neutral LOH	Illumina Omni1-Quad
10	42,977,116-45,001,901	2.0 Mb	copy neutral LOH	Illumina Omni1-Quad
11	42,615,492-44,120,559	1.5 Mb	copy neutral LOH	Illumina Omni1-Quad
12	42,439,376-44,509,500	2.1 Mb	copy neutral LOH	Illumina Omni1-Quad
13	42,615,492-43,923,018	1.3 Mb	copy neutral LOH	Illumina Omni1-Quad
14	42,550,353-43,972,109	1.4 Mb	copy neutral LOH	Illumina Omni1-Quad
15	43,831,923-45,001,900	1.2 Mb	copy neutral LOH	Illumina Omni1-Quad
16	42,913,470-43,923,018	1.0 Mb	copy neutral LOH	Illumina Omni1-Quad
17	42,948,647-44,046,092	1.1 Mb	copy neutral LOH	Illumina Omni1-Quad

[a]Coordinates listed using the Ensembl hg 19 genome assembly.

[b]Minimum size of the deleted region.

Table S4. *STRC* sequence changes with in silico predictions

Patient number	Sequence change	Exon	PolyPhen-2 prediction[a]	SIFT prediction[b]
3	c.2726A>T, p.H909L	9	probably damaging (0.99)	deleterious (0.00)
4	c.4918C>T, L1640F	26	probably damaging (0.95)	deleterious (0.00)
6	c.4402C>T, p.R1468X	23	stop codon[c]	stop codon[c]
16	c.5180A>G, p.E1727G	28	probably damaging (1.00)	deleterious (0.02)
24	c.2303_2313+1del12, p.G768Vfs*77	6	stop codon[c]	stop codon[c]
24	c.5125A>G, p.T1709A	28	probably damaging (0.99)	deleterious (0.00)
25	c.2640G>T, p.E880D	8	possibly damaging (0.95)	deleterious (0.00)
5, 22, 23, 25, 26	c.3893A>G, p.H1298R	19	benign (0.00)	deleterious (0.00)

[a]PolyPhen-2 operates on a scale from 0 to 1.0, with 1.0 having the highest probability of being a damaging substitution.

[b]SIFT values <0.05 predict substitutions that are deleterious, whereas values >0.05 predict tolerated substitutions.

[c]Programs do not predict the damaging nature of stop codons.

Supplementary Table S5. Summary of patients with biallelic *STRC* mutations (DFNB16) listed in publications to date

Reference	No. of patients	Age of onset	Allele 1	Allele 2	Phenotype
16	n = 4♂ (family D_SM)	prelingual	*STRC* gene deletion	*STRC* gene deletion	SNHL, DIS (MIM: 611102)
16	n = 1♂, 2♀ (family L709)	prelingual	*STRC* gene deletion	*STRC* gene deletion	SNHL
16	n = 2♂, 1♀ (family L1014)	prelingual	*STRC* gene deletion	*STRC* gene deletion	SNHL, DIS
15	n = 3♂ (one family)	before infancy	*STRC* gene deletion	*STRC* gene deletion	moderate SNHL, DIS, CDAI (MIM: 224120)
10	n = 1♂	before 10 years	*STRC* gene deletion	*STRC* gene deletion	moderate SNHL, mental retardation, facial anomalies, brachydactyly
8	n = 1♀	1 year	*STRC* gene deletion	*STRC* gene deletion	mild to moderate SNHL, macrocephaly
9	n = 4	pediatric[a]	*STRC* gene deletion	*STRC* gene deletion	SNHL
This study	n = 1♂, 1♀	♂: 2 years, ♀: childhood	*STRC* gene deletion	*STRC* gene deletion	SNHL
This study	n = 1♂	♂: newborn	*STRC* gene deletion	*STRC* gene deletion	SNHL, facial anomalies, atrial spetal defect, hydroxylysinuria/lysinemia, recurrent infections

9	n = 2	pediatric[a]	*STRC* gene deletion	c.3795-?_5125+?del (exons 19-28)	SNHL
9	n = 1	pediatric[a]	*STRC* gene deletion	c.4171C>G, p.R1391G	mild to moderate SNHL
9	n = 1	pediatric[a]	*STRC* gene deletion	c.2667G>C, p.Q889H	SNHL
9	n = 1	pediatric[a]	*STRC* gene deletion	c.1873C>T, p.R625C[b]	SNHL
This study	n = 1♂	5 years	*STRC* gene deletion	c.2726A>T, p.H909L	mild to moderate SNHL, bipartite uvula
This study	n = 1♂	3 years	*STRC* gene deletion	c.4918C>T, p.L1640F	mild to moderate SNHL
This study	n = 1♂	newborn	*STRC* gene deletion	c.4402C>T, p.R1468X	mild to moderate SNHL, hypothyroidism
9	n = 3	pediatric	c.3540-?_5125+?del (exons 16-28)	c.3540-?_5125+?del (exons 16-28)	SNHL
9	n = 1	pediatric	c.3540-?_5125+?del (exons 16-28)	c.1021C>T, p.R341C[b]	SNHL
9	n = 1	pediatric	c.3540-?_5125+?del (exons 16-28)	c.326T>A, p.M109K[b]	SNHL
9	n = 1	pediatric	c.4171C>G, p.R1391G	c.4171C>G, p.R1391G	mild to moderate SNHL
9	n = 1	pediatric	c.3436G>A, p.D1146N[b]	c.4433C>T, p.T1478I)	severe to profound SNHL
9	n = 1	pediatric	c.2303_2313+1del[b]	c.2303_2313+1del[b]	severe to profound SNHL
This study	n = 1♀	6 years	c.2303_2313+1del12, p.G768Vfs*77	c.5125A>G, p.T1709A	moderate SNHL

CDAI, congenital dyserythropoietic anemia type I; DIS, sensorineural deafness and male infertility syndrome; SNHL, sensorineural hearing loss.
[a]The age of the studied pediatric patients ranged from newborn to 18 years with an average of 3-4 years at the time of enrollment.
[b]Variant not confirmed as *STRC* copy specific.

14.4 Attachment 4

Confirmation of *GRHL2* as the gene for the DFNA28 locus.

CLINICAL REPORT

AMERICAN JOURNAL OF medical genetics PART A

Confirmation of *GRHL2* as the Gene for the DFNA28 Locus

Barbara Vona,[1] Indrajit Nanda,[1] Cordula Neuner,[1] Tobias Müller,[2] and Thomas Haaf[1]*

[1]Institute of Human Genetics, Julius Maximilians University, Würzburg, Germany

[2]Department of Bioinformatics, Julius Maximilians University, Würzburg, Germany

Manuscript Received: 14 February 2013; Manuscript Accepted: 14 April 2013

More than 10 years ago, a c.1609_1610insC mutation in the grainyhead-like 2 (*GRHL2*) gene was identified in a large family with nonsyndromic sensorineural hearing loss, so far presenting the only evidence for *GRHL2* being an autosomal-dominant deafness gene (DFNA28). Here, we report on a second large family, in which post-lingual hearing loss with a highly variable age of onset and progression segregated with a heterozygous non-classical splice site mutation in *GRHL2*. The c.1258-1G>A mutation disrupts the acceptor recognition sequence of intron 9, creating a new AG splice site, which is shifted by only one nucleotide in the 3′ direction. cDNA analysis confirmed a p.Gly420Glufs*111 frameshift mutation in exon 10. © 2013 Wiley Periodicals, Inc.

Key words: autosomal dominant hearing impairment; DFNA28; *GRHL2*; haploinsufficiency; postlingual hearing impairment; progressive hearing loss

How to Cite this Article:
Vona B, Nanda I, Neuner C, Müller T, Haaf T. 2013. Confirmation of GRHL2 as the gene for the DFNA28 locus.
Am J Med Genet Part A.

INTRODUCTION

Autosomal dominant nonsyndromic hearing impairment accounts for approximately 20% of hereditary hearing loss. To date, there are 54 autosomal dominant loci with 27 associated causative genes identified [Van Camp and Smith, 2012]. The DFNA28 (OMIM: 608641) locus is comprised of *GRHL2* (OMIM: 608576) with the alias *TFCP2L3* (transcription factor cellular promoter 2-like 3), which is a widely expressed transcription factor in human epithelial tissues [Werth et al., 2010]. *GRHL2* spans approximately 177 kb on chromosome 8q22.3 (NCBI 37/hg19) and contains 16 exons, which translate into a 625 amino acid protein. It was first associated with the DFNA28 locus through mapping studies involving a five-generation North American family affected with mild to moderate post-lingual progressive bilateral sensorineural hearing loss. In this family, affected members had a heterozygous c.1609_1610insC mutation in exon 13 [Peters et al., 2002]. In addition, several single nucleotide polymorphisms (SNPs) in *GRHL2* have been associated with marginal significance with age-related hearing impairment susceptibility [Van Laer et al., 2008]. Considering that a second disease-causing mutation has not been reported, one might begin to suspect that *GRHL2* is not a bonafide deafness gene.

The expression and function of *GRHL2* have previously been investigated in animal studies. Northern blot and in situ hybridization studies in the mouse demonstrated high *Grhl2* expression in the cochlear duct at embryonic day 18.5 and postnatal day 5 [Peters et al., 2002; Wilanowski et al., 2002]. $Grhl2^{-/-}$ knockout mice were embryonic lethal, displaying split face and neural tube defects. $Grhl2^{+/-}/Grhl3^{+/-}$ compound heterozygotes were viable and exhibited neural tube defects of varying severity. Evidently, coordinated expression of GRHL transcription factors in the non-neural ectoderm is important for neural tube closure [Rifat et al., 2010]. Unfortunately, hearing was not tested in heterozygous animals. *Tol2* transposon-mediated insertional mutagenesis in zebrafish produced offspring with enlarged otocysts, reduced or absent otoliths, malformed semicircular canals, insensitivities to sound stimulation, and abnormal swimming position despite the normal appearance of hair cells in the inner ear. Upon wild type human *GRHL2* mRNA injection, the inner ear defects in the zebrafish were rescued, whereas injection with mutant human *GRHL2* was unable to rescue otic defects [Han et al., 2011]. This suggests a conserved structure and function of GRHL2 in vertebrate inner ear development.

Conflict of interest: none.
Grant sponsor: German Research Foundation; Grant number: HA 1374/7-2.
*Correspondence to:
Professor Thomas Haaf, Institute of Human Genetics, Julius-Maximilians-Universität Würzburg, Biozentrum, Am Hubland, 97074 Wuerzburg, Germany.
E-mail: thomas.haaf@uni-wuerzburg.de
Article first published online in Wiley Online Library (wileyonlinelibrary.com): 00 Month 2013
DOI 10.1002/ajmg.a.36017

MATERIALS AND METHODS

The study was approved by the Ethics Committee of the University of Würzburg.

Mutation Analysis

Genomic DNA was extracted from whole blood using a standard salt extraction method, and was submitted to Otogenetics Corporation (Norcross, GA) for exome capture (targeting 80 known deafness genes) and next generation sequencing (NGS) on a HiSeq2000 (Illumina, San Diego, CA). Paired-end reads of 90–100 bp were analyzed for quality, exome coverage, and exome-wide SNP/InDels using the platform provided by DNAnexus (Mountain View, CA), to which we applied our systematic analysis beginning with the removal of calls that did not meet certain quality and confidence thresholds. Intronic variants not predicted to affect splicing or regulation were also removed, since they are not likely to impact protein structure and function. As we expected the causative dominant mutation to be absent in the healthy population, it is unlikely to be reported in variant databases such as dbSNP and SwissVar. We also used SIFT [Ng and Henikoff, 2001], PolyPhen-2 [Adzhubei et al., 2010], and MutationTaster [Schwarz et al., 2010] to predict the impact of any identified amino acid substitution on the protein structure and function and to predict disease causing potential resulting from sequence alterations.

To validate the identified mutation, an amplicon containing the *GRHL2* c.1258-1G>A mutation was PCR amplified from genomic DNA using standard PCR cycling conditions with forward primer 5′-GGATTTCACTGGTTTAGGG-3′ and reverse primer 5′-AGCG-TAGACTTCAAGTGAGC-3′ (Metabion, Martinsried, Germany). PCR products were sequenced with an ABI 3130xl 16-capillary sequencer (Life Technologies, Carlsbad, CA).

RNA Analysis

RNA samples were isolated from saliva using a standard protocol from the Oragene RNA collection kit (DNA Genotek, Ottawa, ON, Canada). RNA quality and quantity were assessed with a NanoDrop spectrophotometer (NanoDrop Technologies, Wilmington, DE). cDNA was produced using the SuperScript III First-Strand Synthesis SuperMix RT-PCR kit (Invitrogen, Karlsruhe, Germany). The *GRHL2* region of interest was amplified using standard PCR cycling conditions from the synthesized cDNA with forward primer 5′-GGAAA-TACTGGCACTCTCG-3′ and reverse primer 5′-ACCTTCTCGTTC-ATCATCC-3′. A second round nested PCR continued with inner forward primer 5′-CCGTGAATTGCTTGAGCACA-3′ and reverse primer 5′-GGTTTGCAAAGTGAACATCAG-3′ in order to shorten the amplicon length for Sanger sequencing and enhance the product on the agarose gel.

RESULTS

Pedigree Analysis

The index patient (IV:4) developed type I diabetes at the age of 10 and bilateral progressive hearing loss at the age of 32. He does not show any syndromic features and maintains an academic position.

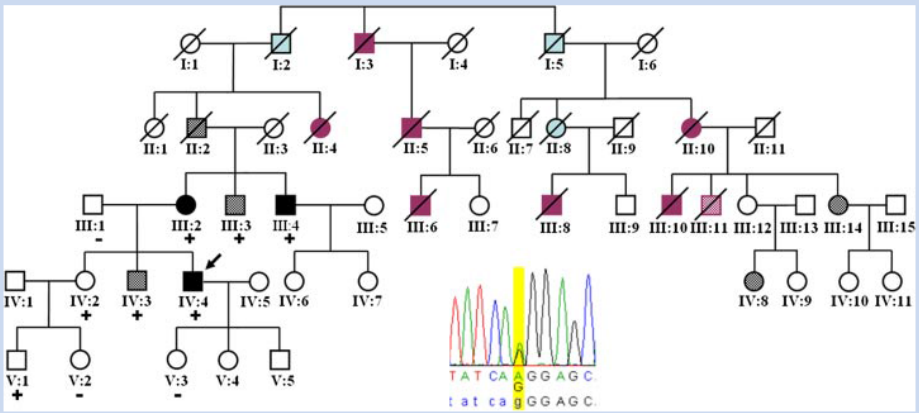

FIG. 1. Pedigree of the family. Black and purple filled symbols indicate family members with bilateral hearing impairment, light blue symbols individuals with an unclear hearing status. Approximate time of onset is denoted by black color, representing middle to late adulthood onset, and purple color, representing childhood onset. Completely filled symbols indicate severe hearing loss and squared symbols mild to moderate hearing loss for each onset group. Individuals who were tested positively and negatively for the heterozygous *GRHL2* mutation are indicated by a "+" or "−", respectively. The index patient IV:4 is marked by an arrow. His 44-year-old sister IV:2 who also carries the mutation has normal hearing thresholds with exceptions at higher frequencies in the right ear. The inset shows the sequence chromatogram of parts of *GRHL2* intron 9 and exon 10 of our index patient, containing the c.1258-1G>A substitution (highlighted in yellow).

The family history allowed for the tracing back of hearing status over five generations (Fig. 1). Ten family members representing the last three generations were available for genetic analysis.

The hearing loss in the family members with detailed clinical examination is characterized as bilateral and progressive, usually beginning in the fifth decade of life (III:2, III:4, and IV:3) with the earliest documented age of diagnosis being 32 years of age in the index patient (IV:4) and latest diagnosis at age 65 (III:3). However notably, several more distantly related individuals without detailed clinical records (I:3, II:4, II:5, II:10, III:6, III:8, III:10, and III:11) had post-lingual childhood onset reported. Apart from childhood onset hearing loss, III:6 had a reduced IQ and severe epilepsy, which were thought to represent comorbidities contributing to his early death at approximately 40 years of age. Individuals III:8, III:10, and III:11 presented with varying spectrums of communication disorders in addition to childhood onset hearing loss and died prematurely at approximately 50 years of age. III:8 was described as having profound hearing impairment beginning from childhood and had infantile seborrhoeic dermatitis. III:10 was reported as having profound hearing loss that made it nearly impossible to communicate with him. III:11 was able to communicate orally with others, but overcompensated for his hearing loss by utilizing stilted speech.

Although great care was taken to record the hearing statuses of distantly related family members, there were three individuals having ambiguous hearing classifications. I:2 died at approximately 50 years of age at a time when his affection status was not clear. I:5 was reported as being hearing impaired; however, detailed information about onset and severity was unknown. Both these individuals lived in the 19th century, limiting clinical information to what members of the family collected. II:8 had normal hearing early in life but adult onset hearing loss cannot be excluded. III:12 was reported to hear normally, while his daughter IV:8 had mild hearing impairment at approximately 50 years of age. Thus, III:12 may be a non-penetrant mutation carrier. Unfortunately, III:14 and IV:8 were not available for genetic analysis and, thus, we could not test whether the same form of hearing loss segregates in the left and the right side of the pedigree.

Age of Onset and Progression of Hearing Loss

Figure 2 shows the bilateral pure-tone air conduction audiograms for family members III:2, III:3; III:4, IV:2, and IV:4. Hearing loss in all frequencies was observed for III:2, III:3, and III:4. Upward sloping profiles in these individuals indicate a greater affection in higher frequencies, particularly at 6 and 8 kHz, as compared to the lower and middle frequencies. IV:2 had only one recorded audiogram from age 44 and had normal hearing thresholds with exceptions at 6 and 8 kHz in the right ear. While IV:4 followed a predictable trend of hearing loss, he displayed an earlier and more severe onset, and was the only affected family member with type I diabetes.

Excluding individual IV:2, there was a positive correlation of hearing loss progression and advancing age exceeding what can be expected by normal aging (Fig. 3). We performed a linear regression analysis using the R statistical package [R Development Core Team, 2012] to estimate the progression of hearing loss. Figure 3A shows three of the five mutation carriers clustering linearly, two of which, namely III:2 and III:3, have closely matching

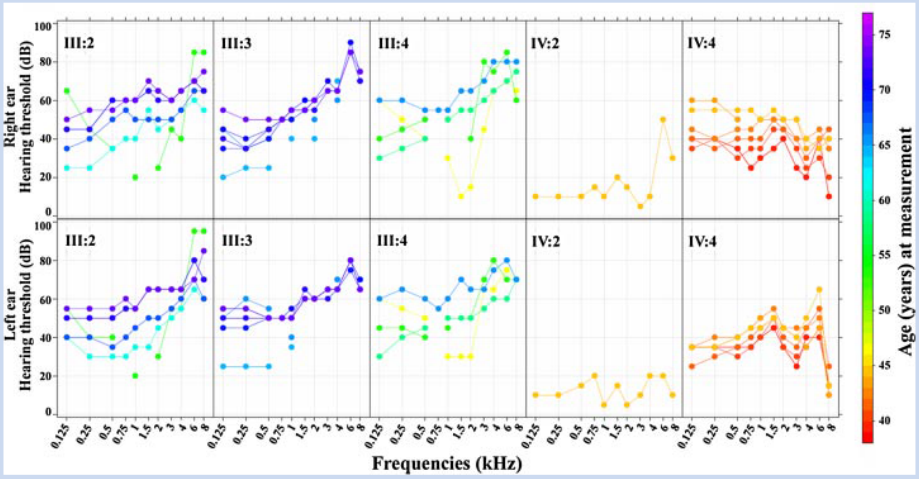

FIG. 2. Bilateral pure-tone audiogram data of five mutation heterozygotes [III:2, III:3, III:4, IV:2, and IV:4]. The diagrams were constructed with the R Lattice Package [Sarkar, 2008]. The top panels represent measurements of the right ear; the bottom panels of the left ear. Audiograms are scaled by color according to the age at measurement.

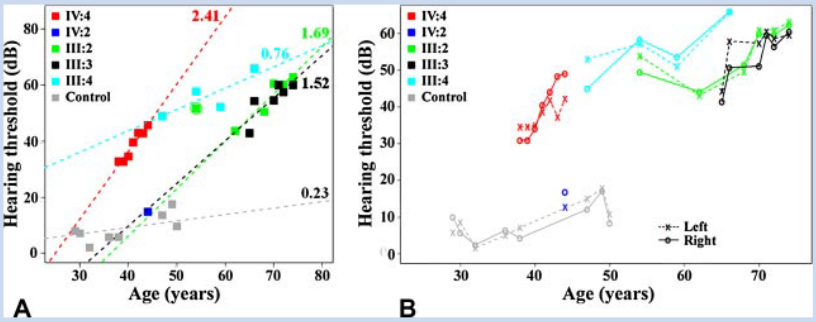

FIG. 3. Air conduction pure-tone audiometry analysis from five mutation heterozygotes and one normal hearing control individual. A: The correlation of hearing threshold and age. Linear regression modeling of averaged left and right hearing thresholds across averaged frequencies was performed to obtain ATD values [dB/year] as indicated in the top right portion of each dotted line. An outlier not fitting the linear regression [III:2] is circled and excluded from the statistical analysis. A single plotted square represents one measurement. B: Plot of left and right thresholds [dB] averaged over all frequencies to assess the presence of a left/right difference in hearing loss with increasing age [in years]. Each point represents a separate measurement for right [denoted by open circles] and left [denoted by crosses] ears.

annual threshold deterioration (ATD) rates of 1.69 and 1.52 dB/year, respectively, when comparing hearing loss over age after averaging left and right ear thresholds and all frequencies. One outlier measurement was excluded for ATD calculation in III:2 at 54 years of age. Individual III:4 demonstrated greater hearing loss with his initial measurement and had a reduced ATD compared to his other family members with a value of 0.76 dB/year. The index patient IV:4 had an earlier and more severe hearing loss, with an ATD of 2.41 dB/year and when comparing the left and right thresholds averaged across all frequencies, he demonstrated greater hearing loss in his right ear compared to his left as seen in his last three measurements (Fig. 3B). When assessing lateralization of hearing loss using averaged frequencies, we were able to infer from individuals III:2, III:3, and III:4 that there was not a consistent lateral bias between left and right sided hearing loss (Fig. 3B). Apart from IV:2, affected individuals showed a mild (20–40 dB) to moderate (40–55 dB) sensorineural hearing loss in the fourth to seventh decade of life that progressed to moderately severe (55–70 dB) levels in higher frequencies by the seventh and eighth decade.

Mutation Identification and Characterization

The index patient was negative for mutations in the *GJB2* (OMIM: 121011) gene. He was included in a microarray screen of 50 *GJB2* mutation-negative non-syndromic hearing loss patients, which did not identify any potentially pathogenic copy number variations (data not shown). We then used targeted deafness gene enrichment sequencing (Otogenetics Corporation) to screen for mutations in 80 known deafness genes including 23 DFNA genes, 32 DFNB genes, and 2 DFN genes (with a number of genes being classified as being both dominant and recessive). Syndromic deafness genes were also included. The analysis strategy we employed filtered out apparently non-pathogenic variants, disclosing a single heterozygous c.1258-1G>A substitution in the *GRHL2* gene as pathogenic. The average coverage of *GRHL2* in the analyzed data set was 195x. It is worth emphasizing that mutations in the gene responsible for Wolfram syndrome (*WFS1*), which is characterized by juvenile diabetes mellitus, optic atrophy and progressive hearing loss, were excluded, as *WFS1* is also covered in the NGS deafness panel. To date, we have analyzed 24 additional *GJB2* mutation-negative hearing loss patients and eight normal hearing controls using targeted deafness gene sequencing and did not find any additional mutation in *GRHL2* (data not shown).

Sanger sequencing of genomic DNA (accession: NG_011971.1) showed that the mutation was detected in five family members (III:2, III:3, III:4, IV:3, and IV:4) with middle to late adulthood onset of hearing loss and absent in the normal hearing father (III:1) of the index patient (Fig. 1). Individual IV:2 who was also heterozygous for the *GRHL2* mutation did not report hearing loss at the age of 44. In the youngest generation, we identified one heterozygous individual (V:1) and two individuals (V:2 and V:3) without the mutation. Hearing was normal in all three of these individuals, which was expected, considering their young age.

We initially predicted that the c.1258-1G>A substitution in the acceptor site of *GRHL2* intron 9 would result in the skipping of exon 10. To test this, we extracted RNA from saliva samples from the index patient and a normal hearing control, synthesized cDNA (accession: NM_024915.3), and amplified a region spanning exons 9 and 11. Comparing the product size of the patient and control through gel electrophoresis, it was demonstrated that the exon 10 was not skipped (Fig. 4A). Instead, Sanger sequencing of the cDNA product showed that a new 3′ AG splice site was shifted by only one nucleotide in the 3′ direction, causing a heterozygous deletion of the first guanine in exon 10 (Fig. 4B). This mutation thus predicts a p.Gly420Glufs*111 in exon 13 (Fig. 4C).

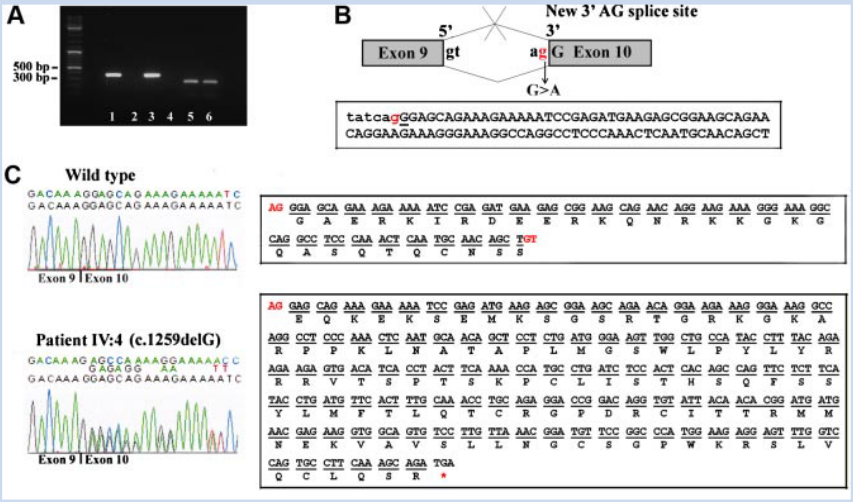

FIG. 4. RNA analysis and splice site illustration. A: An agarose gel image shows the RT PCR of the index patient and healthy hearing control cDNA using *GRHL2* primers flanking exons 9 and 11, amplifying a 360 bp product. Human β-actin primers amplified a 250 bp product. Lanes 1, *GRHL2* RT-positive patient cDNA; 2, *GRHL2* RT-negative patient cDNA; 3, *GRHL2* RT-positive control; 4, *GRHL2* RT-negative control; 5, β-actin RT-positive patient; 6, β-actin RT-positive control. B: The *GRHL2* c.1258-1G>A heterozygous mutation introduces a new 3′ AG splice site that causes a deletion in the first nucleotide of exon 10. The splice site is composed of the mutant A and the wild type G in the first position of exon 10. The red nucleotide represents the G>A mutation in intron 9. Partial intron 9 and exon 10 sequence is boxed and depicted in lowercase and capital letters, respectively. The mutated position is highlighted in red and the deleted nucleotide is underlined. C: Chromatograms show cDNA sequencing of the exon 9 and 10-spanning region of interest in the normal hearing control (top) and index patient IV:4 (bottom). The forward cDNA sequence of the index patient shows a heterozygous single nucleotide deletion and a frameshift in exon 10. Encoded amino acid residues are boxed to the right of each chromatogram, with the AG and GT splice recognition sequences depicted in red. A premature stop codon in exon 13 of the index patient is represented with a red asterisk.

DISCUSSION

We report on a second DFNA28-causing mutation and the first splice site mutation in *GRHL2* in a family affected with non-syndromic hearing loss. Previously, only one mutation in *GRHL2* has been associated with hearing loss [Peters et al., 2002]. The mutation described here confirms that mutations in *GRHL2* cause postlingual progressive hearing loss. In this light, it may also be worth following up the marginally significant association of presbycusis with *GRHL2* variants [Van Laer et al., 2008], using larger cohorts.

This newly identified *GRHL2* mutation constitutes a type IV nonclassical (intronic) splicing mutation, which could have been misinterpreted as a classic (type I) splice defect if cDNA was not analyzed [Eng et al., 2004]. In the index patient, the heterozygous c.1258-1G>A mutation activates a cryptic 3′ splice site in genomic DNA. The first nucleotide in exon 10 is a G, and the consequence of the G>A mutation is a one nucleotide shift of the splice site consensus sequence resulting in a deletion of the first nucleotide in exon 10 and a frameshift ending in an in-frame stop codon. Given the cDNA sequence data, it is predicted that this mutation negatively impacts the protein. There are several hypothesized outcomes as a consequence of mutations leading to a frameshift and premature termination, namely nonsense-mediated decay, loss of protein function via protein truncation, and alteration of protein-folding kinetics leading to proteolysis [Gregersen et al., 2000; Williams et al., 2003]. Additionally, they may act as dominant-negative mutations [Schell et al., 2002].

The maximum entropy model called MaxEntScan by Yeo and Burge [2004] provides a splice site prediction algorithm that assesses the relative strengths of new splice sites. High MaxENT scores indicate an increased efficiency in splicing. When considering the impact of a mutation in a splice consensus region on exon inclusion or exclusion, the contributions of both the 3′ and 5′ splice site MaxENT scores should be taken into consideration [Shepard et al., 2011]. The wild type *GRHL2* exon 10 MaxENT score of the 3′ site is 10.1 and the 5′ is 7.4. The cryptic 3′ splice site generated by the c.1258-1G>A mutation has a strong MaxENT score of 9.5. A 6% decrease compared to the wild-type is most likely not sufficient to cause exon skipping or other aberrant splicing, especially since MaxENT scores become increasingly negative as splicing becomes less likely to occur. This further substantiates our cDNA sequence analysis.

GRHL2 participates in the differentiation and maintenance of epithelial cells throughout life [Werth et al., 2010]. Impaired

epithelial cell integrity is the most reasonable pathological explanation as to its involvement in late-onset hearing impairment [Peters et al., 2002; Van Laer et al., 2008]. Considering a number of factors that are useful for predicting haploinsufficiency such as temporal expression, proximity to other haploinsufficiency genes, interaction partners, and genetic implication in disease [Huang et al., 2010], *GRHL2* is predicted to have a high probability of exhibiting haploinsufficiency. It is plausible to assume that the hearing loss in the present family and the previously reported family [Peters et al., 2002] is due to *GRHL2* haploinsufficiency.

The results show that the heterozygotes for the c.1258-1G>A mutation in *GRHL2* have progressive, bilateral hearing loss with a typical onset in middle to late adulthood. The variability in the onset of hearing loss and audiometric profiles in heterozygotes argue for the interplay of other genetic or environmental factors in determining the events leading to hearing loss. Comorbidities independent of hearing loss such as epilepsy, reduced IQ, and type I diabetes may influence the onset and severity of hearing loss and explain this variation. Alternatively, given the enormous genetic heterogeneity of hearing loss and the high rate of marriage among hearing-impaired individuals, it is possible that the family members with a documented childhood onset in the right branch of the pedigree, who were not available for genetic diagnostics and detailed clinical examination, suffer from a distinct form of dominant deafness.

ACKNOWLEDGMENTS

The authors express their sincere gratitude to the family who has actively participated in this study. We also thank Dr. Andrea Gehrig for helping with the mutation analyses, Dr. Jörg Schröder for helping with the collection of audiograms, and Claus Steinlein for technical assistance. The authors greatly appreciate the journal editor's and reviewers' support and helpful comments to the original manuscript. T.H. was supported by a grant (HA 1374/7-2) from the German Research Foundation.

REFERENCES

Adzhubei IA, Schmidt S, Peshkin L, Ramensky VE, Gerasimova A, Bork P, Kondrashov AS, Sunyaev SR. 2010. A method and server for predicting damaging missense mutations. Nat Methods 7:248–249.

Eng L, Coutinho G, Nahas S, Yeo G, Tanouye R, Babaei M, Dörk T, Burge C, Gatti R. 2004. Nonclassical splicing mutations in the coding and noncoding regions of the ATM gene: Maximum entropy estimates of splice junction strengths. Hum Mutat 23:67–76.

Gregersen N, Bross P, Jørgensen MM, Corydon TJ, Andersen BS. 2000. Defective folding and rapid degradation of mutant proteins is a common disease mechanism in genetic disorders. J Inherit Metab Dis 23:441–447.

Han Y, Mu Y, Xiaoquan L, Xu P, Tong J, Liu Z, Ma T, Guodong Z, Yang S, Du J, Meng A. 2011. Grhl2 deficiency impairs otic development and hearing ability in a zebrafish model of the progressive dominant hearing loss DFNA28. Hum Mol Genet 20:3213–3226.

Huang N, Lee I, Marcotte EM, Hurles ME. 2010. Characterising and predicting haploinsufficiency in the human genome. PLoS Genet 6: e1001154.

Ng PC, Henikoff S. 2001. Predicting deleterious amino acid substitutions. Genome Res 11:863–874.

Peters LM, Anderson DW, Griffith AJ, Grundfast KM, San Agustin TB, Madeo AC, Friedman TB, Morell RJ. 2002. Mutation of a transcription factor, *TFCP2L3*, causes progressive autosomal dominant hearing loss, DFNA28. Hum Mol Genet 11:2877–2885.

R Development Core Team. 2012. R: A language and environment for statistical computing. Vienna, Austria: R Foundation for Statistical Computing.

Rifat Y, Parekh V, Wilanowski T, Hislop NR, Auden A, Ting SB, Cunningham JM, Jane SM. 2010. Regional neural tube closure defined by the grainy head-like transcription factors. Dev Biol 345:237–245.

Sarkar D. 2008. Lattice: Multivariate data visualization with R. New York: Springer.

Schell T, Kulozik AE, Hentze MW. 2002. Integration of splicing, transport and translation to achieve mRNA quality control by the nonsense-mediated decay pathway. Genome Biol 3: Reviews1006.1-1006.6.

Schwarz JM, Rödelsperger C, Schuelke M, Seelow D. 2010. MutationTaster evaluates disease-causing potential of sequence alterations. Nat Methods 7:575–576.

Shepard PJ, Choi EA, Busch A, Hertel KJ. 2011. Efficient internal exon recognition depends on near equal contributions of the 3′ and 5′ splice sites. Nucleic Acids Res 39:8928–8937.

Van Camp G, Smith RJH. 2012. Hereditary hearing loss homepage. http://hereditaryhearingloss.org/.

Van Laer L, van Eyken E, Fransen E, Huyghe JR, Topsakal V, Hendrickx JJ, Hannula S, Maki-Torkko E, Jensen M, Demeester K, Baur M, Bonaconsa A, Mazzoli M, Espeso A, Verbruggen K, Huyghe J, Huygen P, Kunst S, Manninen M, Konings A, Diaz-Lacava AN, Steffens M, Wienker TF, Pyykkö I, Cremers CWRJ, Kremer H, Dhooge I, Stephens D, Orzan E, Pfister M, Bille M, Parving A, Sorri M, van de Heyning PH, van Camp G. 2008. The grainyhead like 2 gene (*GRHL2*), alias *TFCP2L3*, is associated with age-related hearing impairment. Hum Mol Genet 17:159–169.

Werth M, Walentin K, Aue A, Schönheit J, Wuebken A, Pode-Shakked N, Vilianovitch L, Erdmann B, Dekel B, Bader M, Barasch J, Rosenbauer F, Luft FC, Schmidt-Ott KM. 2010. The transcription factor grainyhead-like 2 regulates the molecular composition of the epithelial junctional complex. Development 137:3835–3845.

Wilanowski T, Tuckfield A, Cerruti L, O'Connell S, Saint R, Parekh V, Cunningham JM, Jane SM. 2002. A highly conserved novel family of mammalian developmental transcription factors related to Drosophila grainyhead. Mech Dev 114:37–50.

Williams RS, Chasman DI, Hau DD, Hui B, Lau AY, Glover JNM. 2003. Detection of protein folding defects caused by BRCA1-BRCT truncation and missense mutations. J Biol Chem 278:53007–53016.

Yeo G, Burge CB. 2004. Maximum entropy modeling of short sequence motifs with applications to RNA splicing signals. J Comput Biol 11:377–394.

14.5 Attachment 5

Targeted deafness gene next generation sequencing of hearing impaired individuals uncovers unformative mutations.

Targeted deafness gene next generation sequencing of hearing impaired individuals uncovers informative mutations

Short title: Targeted deafness gene next generation sequencing

Barbara Vona, MSc[1], Tobias Müller, PhD[2], Indrajit Nanda, PhD[1], Cordula Neuner[1], Michaela A. H. Hofrichter, MSc[1], Jörg Schröder, MD[1], Oliver Bartsch, MD[3], Anne Läßig, MD[4], Annerose Keilmann, MD[4], Sebastian Schraven, MD[5], Fabian Kraus, MD[5], Wafaa Shehata-Dieler, MD[5], and Thomas Haaf, MD[1]

From the [1]Institute of Human Genetics, Julius Maximilians University, Würzburg, Germany; [2]Department of Bioinformatics, Julius Maximilians University, Würzburg, Germany; [3]Institute of Human Genetics, University Medical Centre of the Johannes Gutenberg University, Mainz, Germany; [4]Division of Communication Disorders, Department of ORL, University Medical Centre of the Johannes Gutenberg University, Mainz, Germany; and [5]Comprehensive Hearing Center, Department of ORL, Plastic, Aesthetic and Reconstructive Head and Neck Surgery, Würzburg, Germany.

Correspondence to: Professor Thomas Haaf, Institute of Human Genetics, Julius-Maximilians-Universität Würzburg, Biozentrum, Am Hubland, 97074 Würzburg, Germany.

Tel.: +49 931 3188738; Fax: +49 931 3187398; Email: thomas.haaf@uni-wuerzburg.de

Purpose: Targeted next generation sequencing (NGS) provides remarkable opportunity to identify variants in known disease genes, particularly in extremely heterogeneous disorders, such as non-syndromic hearing loss (NSHL). Our study attempts to shed light on the complexity of hearing impairment. **Methods:** Using one of two NGS panels containing 80 or 129 deafness genes, we screened 30 NSHL individuals (from 23 unrelated families) and analyzed nine normal hearing controls. **Results:** Overall, we found an average of 3.7 variants (in 80 genes) with deleterious prediction outcome, including a number of novel variants, in NSHL individuals and 1.4 in controls. By NGS alone, 12 of 23 (52%) probands were diagnosed with monogenic forms of NSHL; one individual displayed a DNA sequence mutation together with a microdeletion. Two (9%) probands have Usher syndrome. In the unsolved individuals (10/23; 43%) we detected a significant enrichment of potentially pathogenic variants, compared to controls. **Conclusion:** NGS combined with microarrays provide the diagnosis for approximately half of the *GJB2*-mutation negative individuals. Usher syndrome is more frequent in our cohort than anticipated. A proportion of NSHL individuals, particularly in the unsolved group may be caused/modified by an accumulation of unfavourable variants across multiple genes.

Key Words *Deafness gene panel, mutational load, non-syndromic hearing loss (NSHL), sensorineural hearing loss (SNHL), targeted next generation sequencing (NGS)*

Hereditary hearing loss (HL) is one of the most common birth defects with an approximate incidence of one to two per one thousand newborns presenting bilateral sensorineural hearing loss (SNHL) at the time of newborn hearing screening. In developed countries, HL stems from both environmental and genetic etiological factors, with the genetic contribution comprising 50 to 60 percent of cases.[1,2]

Because of the Mendelian nature of NSHL, the search for new genes has witnessed profound achievement, particularly in the past decade. NSHL demonstrates extreme genetic heterogeneity with over 54 autosomal dominant (DFNA), 75 autosomal recessive (DFNB) and five X-linked (DFN) loci with 27, 44 and three causative genes identified to date, respectively (http://hereditaryhearingloss.org). A fraction of these genes have been associated with both dominant and recessive HL. Furthermore, mitochondrial mutations can also underlie NSHL. NGS technologies are causing a paradigm shift in how clinical geneticists and medical researchers investigate genetic disorders[3] and provide powerful application not only to molecular diagnostics but also to the discovery of new genes and further characterization of already known disease-associated genes.[4-6] Of particular interest to clinicians is target capture NGS involving a subset of disease-relevant genes in the form of gene panels that accommodate sequencing of dozens or hundreds of genes in parallel, with a clear advantage over conventional polymerase chain reaction (PCR)-based Sanger sequencing approaches by achieving faster results at a fraction of the cost.[7]

A further application of NGS is learning the variation landscape of the minor allele load on a gene-by-gene, exome- or genome-wide basis in affected and unaffected individuals. Understanding the concept of mutational load in human disorders will provide insight on the potential role of rare non-synonymous single nucleotide polymorphisms (SNPs), their maintenance throughout human evolution and their predication underlying human disease. By

shifting emphasis away from individual frequencies of deleterious variants toward cumulative frequencies, explanations for common disorders with complex inheritance become plausible.[8]

In this study, we employed one of two gene panels consisting of either 80 or 129 deafness genes using NGS to detect damaging variants in 30 individuals from 23 unrelated families with a broad range of HL onset and severity, with an initial goal of HL diagnostics. The remaining unsolved cohort (14 probands from 10 unrelated families) was carefully compared against nine normal hearing controls for enrichment of deleterious variants.

MATERIALS AND METHODS

Case evaluation, classification and controls

Thirty individuals with hearing impairment were recruited over a number of years from Würzburg and Mainz, Germany for targeted deafness gene sequencing after genetic counselling was initiated. All of the probands except one (R5) had been pre-screened by conventional Sanger sequencing for mutations in *GJB2*. All parents and participants provided informed written consent. This study was approved by the Ethics Committee of the University of Würzburg.

Upon diagnosis of HL, patients routinely undergo kidney and thyroid sonography, urinalysis, electrocardiogram, neurological examination, blood profile analysis, serological examination for infectious disease, as well as ophthalmological examination and magnetic resonance imaging of brain, inner ear and temporal bones for the assessment HL in conjunction with a syndrome. Clinical test results, age of onset and age of enrollment are summarized in Table S1. Pure-tone audiometry (PTA) and auditory brainstem response (ABR) were used to assess degree and

progression of HL. The following guideline was used to determine severity of HL: 0 to 20 dB normal, 20 to 40 dB mild, 40 to 55 dB moderate, 55 to 70 dB moderately severe, 70 to 90 dB severe, and >90 dB profound. Seven of the 30 individuals were family members of affected probands who were included to aid with analysis but not considered for statistics and success rate calculation. When possible, additional family members were also recruited for follow-up co-segregation analysis.

Seventeen of the 23 probands had pre-lingual HL, which is either present at birth or begins before the age of five in the critical time interval for language acquisition. Six individuals had postlingual HL with onset between age 6 and 10 years. From pedigree analysis and familial information, we were able to characterize hearing impairment types into three subgroups: dominant (two or more generations affected or mutations detected in genes conferring dominant HL without opportunity for co-segregation analysis; represented by families D1 through D8), recessive (parents are normal hearing, possible consanguinity known; indicated by families R1 through R5), and unsolved (which could be consistent with dominant or recessive HL but based on lack of familial involvement, inheritance category was unconfirmed; as shown in families U1 through U10). In total, we had eight dominant, five recessive and ten unsolved individuals. The majority of our probands are of European descent, except for D7 and U5 with Turkish, and R2 and U8 with Arab ethnicity. We also included nine unrelated healthy controls with normal hearing and without a family history of HL in our study to investigate the prevalence of pathogenic variants in subjectively normal hearing individuals and to aid variant filtering.

Microarray screen

For the exclusion of pathogenic copy number variation (CNV) in the genome of all hearing impaired individuals before undergoing target enrichment sequencing, we performed either a

SNP array or array CGH using genomic DNA prepared from peripheral blood by a standard salt extraction method. SNP array CNV detection was performed with an Illumina Omni1-Quad v1.0 chip (Illumina, San Diego, CA, USA) according to the manufacturer's specifications. Array data were analyzed using GenomeStudio version 2011.1 (Illumina) and QuantiSNP 2.2 copy number detection algorithm.[9] Array CGH was performed using a Roche NimbleGen CGX v1 315K array (Roche NimbleGen, Madison, WI, USA) per manufacturer's recommendations using healthy pooled male and female reference DNA (Promega, Madison, WI, USA) and arrays were analyzed using Genoglyphix software (Signature Genomics, Spokane, WA, USA).

Target enrichment sequencing, alignment and variant detection

Genomic DNAs from 30 individuals with hearing impairment and nine normal hearing individuals were subjected to one of two possible gene panels containing 80 or 129 genes that are listed in Table S2. Both panels shared the same 80 genes, with the 129 gene panel containing additional genes. These panels included non-syndromic HL genes with a DFN locus annotation, syndromic HL genes, as well as a limited number of strong candidate HL genes (i.e. from animal experiments). Exome capture and NGS on a HiSeq2000 (Illumina) were performed by Otogenetics Corporation (Norcross, GA, USA). A total of 5 µg genomic DNA at a concentration of 20-500 ng/µl in TE was used as input material for NimbleGen capture methods to generate 2x100 paired-end reads. High-quality sequence reads were mapped to the human genome reference (NCBI build 37, hg19), as well as to the reference sequences of the targeted genes in each of the panels using DNAnexus cloud-based data analysis (Mountain View, CA, USA) for variant calling.

Because we did not want to risk losing variants impacting splice sites, pathogenic dbSNP (https://www.ncbi.nlm.nih.gov/SNP) entries and synonymous variants potentially affecting splice

sites, we filtered data conservatively in three areas: (i) mean depth and read counts ≥10, (ii) removal of 3'UTR, 5'UTR, downstream, upstream, and non-coding exon transcript variants, and (iii) removal of non-coding change types. We then referenced dbSNP, Exome Sequencing Project (http://evs.gs.washington.edu/EVS) and 1000 Genomes Project (http://browser.1000genomes.org/index.html) to screen rare variants with minor allele frequencies residing around or under 1% of available population frequency data. SIFT,[10] PolyPhen-2,[11] MutationTaster,[12] and Alamut (Interactive Biosoftware, Rouen, France) predicted the consequence of an identified amino acid substitution on protein structure/function and pathogenic potential, and rapidly assessed nucleotide and amino acid conservation, potential protein domain involvement and nucleotide variation impact on splice site. The Human Gene Mutation Database (HGMD)[13] was also used to determine whether variants were novel or already associated with a phenotype. As a final step, these variants were screened against the control group and were removed unless already established as a deafness-associated damaging mutation. When potentially pathogenic variants were detected, familial co-segregation analysis ensued when possible and comparisons between proband and published audiogram and clinical data followed to substantiate which variants are likely underlying HL in the affected individual.

Sanger sequencing

Candidate variations that remained after filtering were amplified by PCR using primer pairs designed from Primer3 software[14] for validation. We sequenced all the control variants and damaging mutations in Figures 1 and 2, as well as additional case variants with less than 50-fold coverage. Primer sequences are available upon request. PCR products were bidirectionally sequenced with an ABI 3130xl 16-capillary sequencer (Life Technologies, Carlsbad, CA, USA). Sequence reactions were completed with 5x sequencing buffer and big dye terminator (Applied

Biosystems). DNA sequence analysis was performed using Gensearch software (Phenosystems, Lillois Witterzee, Belgium).

Statistical analysis

As there were two different panel types in this study, we excluded all genes from the 129 gene panel that were not included in the 80 gene panel. On the basis of these 80 common genes, we analyzed variant distribution. The pairwise Wilcoxon test followed by a Benjamini-Hochberg multiple testing correction was used to determine whether there was a significant difference in the number of variants in the control versus case groups. Multidimensional-scaling plots were generated to analyze the gene variant distribution patterns between the unsolved and control groups using the statistical framework R (http://www.R-project.org) and the vegan statistical package.[15]

RESULTS

Hearing loss and clinical summaries

Audiometric information from the 23 probands revealed a spectrum of severity: three each had mild and severe hearing loss, respectively, four presented moderate, nine had moderately severe, and four reported profound hearing loss. With one exception (proband U2), the individuals we include have no indication of syndromic background. The Usher syndrome probands disclosed are currently younger than the age of onset for retinitis pigmentosa, which is why we do not currently consider these individuals as syndromic. The most common clinical

indication was speech delay that was present in seven of the probands (D1, D3, R3, R5, U2, U5, and U6), but this is a common occurrence in children with HL, as hearing and speaking are complementary processes. A complete summary of clinical indications and audiograms from available family members is included in Table S1.

Variant analysis

With one notable exception, our probands did not exhibit pathogenic CNVs in the microarray screen. Using a SNP array, the index case of family R4 presented a heterozygous deletion in *USH2A* spanning exons 58-64. This deletion was validated with quantitative real-time PCR in exons 61, 63 and 64 (data not shown).

Targeted deafness gene sequencing of 30 HL individuals (from 23 unrelated families) and nine normal hearing controls was performed with one of two panel types consisting of known and suspected HL genes. Twenty-two out of 30 individuals (16 out of 23 index probands) and eight out of nine controls were sequenced with the 80 gene panel, and eight individuals (seven probands) and one control with the 129 gene panel. The 80 gene panel produced 222.8 kb of targeted sequence, covering 1258 exons and flanking sequence and yielded an average of 8.2 ±1.5 million reads per sample, with approximately 86% mapping to the targeted regions. The average mean depth for the targeted regions was 311.8 ±86.3; 98.4% ±2.9% of the exons had a coverage ≥10 reads. The 129 gene panel achieved a total of 313.0 kb of targeted sequence, covering 1902 exons and flanking sequence. An average of 6.8 ±0.5 million reads per sample was acquired with approximately 88% mapping to their targets. The average mean depth for the targeted regions was 246.2 ±14.9; 98.7% ±0.1% of the covered exons had ≥10 reads. The run statistics from both panel types per individual are presented in Table S3. Missed or low-coverage exons were shared in common among samples.

Analysis of both panel types yielded a total of 89 variants in probands and 14 variants in controls (Table S4). The affected individuals had a total of 68 missense, 10 frameshift, three indels, five nonsense, and three splice variants. Controls had 11 missense, one frameshift and two indel variants.

Variant spectrum and solved individuals

Applying conservative filtering strategies to the genes common in both panels, 42 of the 80 target genes did not show a single pathogenic variant in 23 probands and nine controls. Fourteen genes (*ACTG1*, *COL9A3*, *EYA4*, *GATA3*, *KCNJ10*, *LHFPL5*, *MARVELD2*, *MYO1F*, *MYO3A*, *MYO6*, *OTOA*, *TCF21*, *TMC1*, and *TMIE*) displayed a single variant, six (*ERCC2*, *ESPN*, *OTOR*, *TMPRSS5*, *USH1C*, and *WSF1*), two variants, seven (*GJB3*, *DSPP*, *MYH9*, *MYO1C*, *PCDH15*, *SPINK5*, and *TECTA*), three variants, seven (*CCDC50*, *CDH23*, *GJB2*, *MYO1A*, *MYO15A*, *SLC26A4*, and *TRIOBP*), four variants, three (*GJB4*, *MYO7A* and *OTOF*), five variants, and one (*MYH14*), seven variants that met the criteria for potential pathogenicity, evolutionary conservation, and additional filtering criteria such as depth and quality (Table S4). A correspondence analysis of the identified variants in the entire data set with 23 probands and nine controls did not reveal any clustering, in particular there was no split between affected individuals and controls (data not shown). In this context, it is important to emphasize that all these potentially pathogenic variants represent in silico predictions and usually additional information is needed to identify the disease-causing mutation(s) in a particular case and family. For example, improper segregation of a variant in a dominant family or detection of the same variant in a recessive family or control clearly argues against its pathogenicity. In three probands, we found two damaging variants in a gene conferring recessive HL, i.e. in *GPR98* and twice in *OTOF*, but both were inherited on the same allele from a normal hearing parent. Also, if clinical

features and audiograms were not in agreement with the typical hearing loss of a mutated candidate gene, the individual remained in the unsolved group.

In eight out of the 23 probands, targeted NGS identified a pathogenic mutation in a gene associated with dominant HL (*ACTG1*, *CCDC50*, *EYA4*, *MYH14*, *MYO6*, *TCF21*, and twice in *MYO1A*). Table 1 describes the pathogenic variants with characteristic hearing impairment for each variant. All pathogenic variants were confirmed by Sanger sequencing. The pedigrees of D1, D2, D4, D6, D7, and D8 were consistent with dominant HL (Fig. 1). Segregation of the mutation with HL could be analyzed in families D1, D4, D7, and D8. In family D2, only the affected child was available for analysis, but given that both parents are hearing impaired, it is likely that one of them has this mutation as well. To our knowledge, D3 and D5 had normal hearing parents and no family history of HL, suggesting de novo mutation and/or reduced penetrance. However, in each case, clinical information and audiograms were in agreement with typical HL for the affected genes (Table 1, Table S1) and the mutations occurred in highly conserved amino acids or were predicted to affect gene splicing.

Five probands presented homozygous or compound heterozygous mutations in a gene resulting in recessive HL (*MYO15A*, *MYO7A*, *GJB2*, and twice in *USH2A*) (Table 1). The pedigrees were consistent with recessive HL (Fig. 2). Interestingly, two of the 23 probands were referred to our clinics with NSHL but were diagnosed with a mild form of Usher syndrome (type 2A). Neither of the patients had signs of retinitis pigmentosa at the time of diagnosis. Individual R3 and his affected sister were compound heterozygous for a splice site and a nonsense mutation, whereas individual R4 displayed a microdeletion (of exons 58-64) in combination with a missense mutation (Table 1). Notably, individual R5, who had been pre-screened for mutations in *OTOF* because of suspected auditory neuropathy, was homozygous for the classic c.35delG mutation in *GJB2*.

Unsolved individuals and controls

Considering only the 80 genes that were screened in all individuals, we detected an average of 4.5 (36/8) potentially damaging variants in probands with dominant HL, 3.6 (18/5) in individuals with recessive HL, 3.0 (30/10) in the unsolved group, and 1.4 (13/9) in controls (Table S5). The median number of variants was four for individuals with dominant HL, three each for the recessive and unsolved groups, and one for controls (Fig. 3). Pairwise Wilcoxon tests with multiple testing correction revealed significant differences between probands and controls (dominant group versus control, p=0.003; recessive group versus control, p=0.01; and unsolved group versus control, p=0.01), but not between different case groups.

One individual from the unsolved group and two controls did not display any variant at all. Most (8 of 10; 80%) unsolved probands had three or more potentially pathogenic rare variants, whereas most controls (5 of 9; 56%) had less than two (Table S5). In the control group, we detected damaging variants in *GJB3*, *GJB4*, *MYO1C*, *MYO1F*, *MYO7A*, *PCDH15*, *TMC1*, *TRIOBP*, and *WFS1*, as well as two variants each in *CDH23* and *SPINK5* (Table S4). Only one of these variants was in *WFS1*, a gene responsible for dominant HL and all variants in genes responsible for recessive HL were heterozygous. The individual with the *WSF1* variant describes having episodes of tinnitus under stress, but does not report hearing impairment. A multidimensional scaling analysis[16] of these two groups revealed a clustering of primarily the control group near zero and an extensive heterogeneity of probands from the unsolved group (Fig. S1). In other words, individuals from the unsolved group show a large variety of different variants resulting in the extensive heterogeneity in the multidimensional scaling plot. The controls show only a few variants, resulting in a much higher similarity of these individuals and a homogeneous cluster around zero.

DISCUSSION

Enrichment of deleterious variants in HL individuals

Studies investigating heterogeneous sensorineural disorders such as intellectual disability and macular degeneration have uncovered the complex variation landscape underlying these phenotypes and detected an accumulation of rare deleterious variants in probands versus controls.[17-19] Consistent with several studies suggesting digenic inheritance of HL,[20,21] the concept of a mutational load, whereby an excess of deleterious variants scattered across multiple genes[22] impeding the proper functioning of auditory processes, is an interesting perspective to a typically Mendelian disorder. The enormous complexity of the auditory system suggests elaborate gene interactions may render vulnerable to accumulation of deleterious variants otherwise tolerable in the context of a neutral genetic environment. Since the majority of missense substitutions with a frequency <1% are deleterious in humans, low allele frequency alone can serve as a predictor of functional significance.[23] Furthermore, the number of affected genes harbouring these rare, deleterious variants could also impact phenotypic consequence.

Evolutionary genetic models predict a cumulative effect of rare, possibly pathogenic variants scattered across the genome increasing susceptibility to disorders.[23] Our observation that individuals in the unsolved group harbour significantly more damaging variants in HL genes than controls supports this hypothesis. We propose a polygenic or multifactorial form of inheritance in the unsolved group, whereby affected genes in combination with other adverse genetic and/or environmental factors may exceed a critical threshold for phenotypic manifestation. However, we cannot exclude that increased numbers of deleterious variants in probands is coincidental. Given the extensive genetic heterogeneity of HL and high marriage rate among hearing impaired

individuals, it is expected that variants accumulate in certain families. Additionally, we cannot negate that HL in the unsolved group is due to monogenic forms of deafness caused by highly penetrant variants in novel genes. Follow-up whole exome sequencing of these individuals could provide clarity to this question.

Application of targeted NGS in routine diagnostics

The great heterogeneity comprising NSHL undoubtedly contributes to molecular diagnostic challenges. In the pre-NGS era, the identification of damaging mutations was dependent on labour- and cost-intensive Sanger sequencing. Routine screening is typically initiated with *GJB2* analysis, since 30-40% of NSHL probands with European ancestry have mutations in this gene.[1] Unless additional clinical symptoms hint to specific genes (i.e. goiter to *SLC26A4* or auditory neuropathy to *OTOF*), the vast majority of *GJB2*-mutation negative probands remain without genetic diagnoses. The development and optimization of NGS gene panels expand the spectrum of disease-relevant genes simultaneously screened in affected individuals with the potential to translate into better case outcomes and support when rare pathogenic mutations are liable.

Through targeted NGS, the most likely causative gene mutations in eight dominant and five recessive individuals were detected, for a success rate of 13 (57%) out of 23 probands. Two (9%) individuals displayed compound heterozygous mutations in the *USH2A* gene, which is a higher frequency rate compared to a previous study,[24] reporting 11% of *GJB2*-mutation negative children with HL carrying single Usher syndrome mutations. An early diagnosis of Usher syndrome may benefit these children to delay vision loss with basic interventions such as adhering to certain diets and lifestyles,[25] as well as using eye UV protection with sunglasses[26] to slow photoreceptor degeneration. Early diagnosis is especially relevant in our Usher syndrome probands since they are below the age of onset for vision loss. While it is undeniably important

for familial co-segregation analysis for accurate and definitive variant interpretation, we could not always obtain familial DNAs. More specifically, individual D3 presented characteristic flat audiometric thresholds for *TCF21* c.63C>T mutation. Furthermore, this mutation is associated with adult-onset cardiomyopathy, but since he is a child, periodic cardiac monitoring is recommended to detect early signs of dysfunction.[27,28] Similarly, individual D5 has an audiometric profile with high-frequency HL. Secondary to this audiometric hallmark, *MYO1A* is a gene with variable penetrance.[29] Furthermore, this variant resides in a myosin motor domain. The *EYA4* variant in family D8 creates a stronger mutated 3' splice acceptor position compared to the wild type based on four splice in silico predictor programs. We consider the described mutations (Table 1) as diagnostic benchmarks for HL characterization and clarification. In agreement with the success rate of previous studies,[30,31] our diagnostic yield supports application of this technique for routine diagnostics. However, to enhance the diagnostic potential of NGS, deeper knowledge about population frequencies and pathogenicity of sequence variants is required.

The potential to correct clinical misdiagnosis by broadly screening a pre-defined gene panel has been previously demonstrated in isolated individuals using exome sequencing without family pedigree information available.[32] We detected a common *GJB2* c.35delG homozygous mutation in the available affected members of family R5 with profound HL and suspected auditory neuropathy. At the time of clinical evaluation, haplotype analysis was compatible with *OTOF* mutation; however, *OTOF* was negative for mutations and no further sequencing was completed until inclusion in this study. The proband in family R4 was previously included in CNV analysis and presented a heterozygous deletion of exons 58-64 in the 72 exon gene, *USH2A*. Sanger sequencing of this gene for the detection of a second mutation would have been a time- and cost-

intensive procedure; however, the NGS panel provided rapid insight into a second *USH2A* mutation.

As *GJB2* is a single exon gene accounting for a disproportionate number of HL cases, Sanger sequencing is still recommended for first-line diagnostics. Recent studies[33,34] showed that besides *GJB2* (DFNB1), *STRC* (DFNB16) is a major contributor to congenital HL, particularly in children with mild to moderate high-frequency HL. A pseudogene with 99.6% coding sequence identity makes it impossible to rely on NGS for *STRC* screening and a Sanger sequencing protocol excluding the pseudogene is recommended.[34] We propose targeted NGS deafness gene screening in the remaining unsolved individuals. Since CNVs in not only *STRC* but also other deafness genes may significantly contribute to the mutational load, targeted NGS is most powerful in combination with microarray analysis.

Conclusions

While a major limitation of our study was small sample size, we employed conservative statistics not to overstate our findings. Recent studies have only begun discovering genetic complexities unknown before the advent of NGS technologies. It is noteworthy that all 13 probands diagnosed with a monogenic form of deafness exhibited additional pathogenic variants in other HL genes. It is tempting to speculate these additional variants having a modifying phenotypic effect, explaining variability in age of onset and progression. As NGS becomes an increasingly conventional method for approaching the genotype-phenotype puzzle, future more comprehensive surveys will help elucidate the complexities of HL.

ACKNOWLEDGMENTS

The authors are indebted to the patients and their families for making this work possible. We thank Dr. Wolfram Kress and Dr. Erdmute Kunstmann for mutation consultation and case information, and Jens Gräf for sequencing work. This work was supported by the German Research Foundation (HA 1374/7-2).

REFERENCES

1. Morton CC, Nance WE. Newborn hearing screening—a silent revolution. *N Engl J Med* 2006;354:2151-2164.
2. Smith RJ, Bale JF, Jr., White KR. Sensorineural hearing loss in children. *Lancet* 2005;365:879-890.
3. Majewski J, Schwartzentruber J, Lalonde E, Montpetit A, Jabado N. What can exome sequencing do for you? *J Med Genet* 2011;48:580-589.
4. Shearer AE, DeLuca AP, Hildebrand MS, et al. Comprehensive genetic testing for hereditary hearing loss using massively parallel sequencing. *Proc Natl Acad Sci USA* 2010;107:21104-21109.
5. De Keulenaer S, Hellemans J, Lefever S, et al. Molecular diagnostics for congenital hearing loss including 15 deafness genes using a next generation sequencing platform. *BMC Med Genomics* 2012;5:17.
6. Tang W, Qian D, Ahmad S, et al. A low-cost exon capture method suitable for large-scale screening of genetic deafness by the massively-parallel sequencing approach. *Genet Test Mol Biomarkers* 2012;16:536-542.
7. Lin X, Tang W, Ahmad S, et al. Applications of targeted gene capture and next-generation sequencing technologies in studies of human deafness and other genetic disabilities. *Hear Res* 2012;288:67-76.
8. Howrigan DP, Simonson MA, Kamens HM, et al. Mutational load analysis of unrelated individuals. *BMC Proc* 2011;5 Suppl 9:S55.
9. Colella S, Yau C, Taylor JM, et al. QuantiSNP: an Objective Bayes Hidden-Markov Model to detect and accurately map copy number variation using SNP genotyping data. *Nucleic Acids Res* 2007;35:2013-2025.

10. Kumar P, Henikoff S, Ng PC. Predicting the effects of coding non-synonymous variants on protein function using the SIFT algorithm. *Nat Protoc* 2009;4:1073-1081.
11. Adzhubei IA, Schmidt S, Peshkin L, et al. A method and server for predicting damaging missense mutations. *Nat Methods* 2010;7:248-249.
12. Schwarz JM, Rodelsperger C, Schuelke M, Seelow D. MutationTaster evaluates disease-causing potential of sequence alterations. *Nat Methods* 2010;7:575-576.
13. Stenson PD, Mort M, Ball EV, et al. The Human Gene Mutation Database: 2008 update. *Genome Med* 2009;1:13.
14. Untergasser A, Cutcutache I, Koressaar T, et al. Primer3—new capabilities and interfaces. *Nucleic Acids Res* 2012;40:e115.
15. Oksanen J, Blachet FG, Kindt R, et al. Vegan: community ecology package. R package version 2.0-7. Oulu, Finland: University of Oulu 2013.
16. Gower JC. Some distance properties of latent root and vector methods used in multivariate analysis. *Biometrika* 1966;53:325-328.
17. Najmabadi H, Hu H, Garshasbi M, et al. Deep sequencing reveals 50 novel genes for recessive cognitive disorders. *Nature* 2011;478:57-63.
18. Rauch A, Wieczorek D, Graf E, et al. Range of genetic mutations associated with severe non-syndromic sporadic intellectual disability: an exome sequencing study. *Lancet* 2012;380:1674-1682.
19. Fritsche LG, Fleckenstein M, Fiebig BS, et al. A subgroup of age-related macular degeneration is associated with mono-allelic sequence variants in the ABCA4 gene. *Invest Ophthalmol Vis Sci* 2012;53:2112-2118.

20. Zheng QY, Yan D, Ouyang XM, et al. Digenic inheritance of deafness caused by mutations in genes encoding cadherin 23 and protocadherin 15 in mice and humans. *Hum Mol Genet* 2005;14:103-111.

21. Kooshavar D, Tabatabaiefar MA, Farrokhi E, et al. Digenic inheritance in autosomal recessive non-syndromic hearing loss cases carrying GJB2 heterozygote mutations: assessment of GJB4, GJA1, and GJC3. *Int J Pediatr Otorhinolaryngol* 2013;77:189-193.

22. Neale BM, Rivas MA, Voight BF, et al. Testing for an unusual distribution of rare variants. *PLoS Genet* 2011;7:e1001322.

23. Kryukov GV, Pennacchio LA, Sunyaev SR. Most rare missense alleles are deleterious in humans: implications for complex disease and association studies. *Am J Hum Genet* 2007;80:727-739.

24. Kimberling WJ, Hildebrand MS, Shearer AE, et al. Frequency of Usher syndrome in two pediatric populations: Implications for genetic screening of deaf and hard of hearing children. *Genet Med* 2010;12:512-516.

25. Chiu CJ, Klein R, Milton RC, et al. Does eating a particular diet alter the risk of age-related macular degeneration in users of the Age-Related Eye Disease Study supplements? *Br J Ophthalmol* 2009;93:1241-1246.

26. Cideciyan AV, Jacobson SG, Aleman TS, et al. In vivo dynamics of retinal injury and repair in the rhodopsin mutant dog model of human retinitis pigmentosa. *Proc Natl Acad Sci USA* 2005;102:5233-5238.

27. Schönberger J, Levy H, Grünig E, et al. Dilated cardiomyopathy and sensorineural hearing loss a heritable syndrome that maps to 6p23-24. *Circulation* 2000;101:1812-1818.

28. Arbustini Eloisa AE, Diegoli M, Pasotti M, et al. Gene symbol: CMD1J. Disease: SensoriNeural Hearing Loss (SNHL). *Hum Genet* 2005;117:297.

29. Donaudy F, Ferrara A, Esposito L, et al. Multiple mutations of MYO1A, a cochlear-expressed gene, in sensorineural hearing loss. *Am J Hum Genet* 2003;72:1571-1577.

30. Choi BY, Park G, Gim J, et al. Diagnostic application of targeted resequencing for familial nonsyndromic hearing loss. *PLoS ONE* 2013;8:e68692.

31. Mutai H, Suzuki N, Shimizu A, et al. Diverse spectrum of rare deafness genes underlies early-childhood hearing loss in Japanese patients: a cross-sectional, multi-center next-generation sequencing study. *Orphanet J Rare Dis* 2013;8:172.

32. Leidenroth A, Sorte HS, Gilfillan G, Ehrlich M, Lyle R, Hewitt JE. Diagnosis by sequencing: correction of misdiagnosis from FSHD2 to LGMD2A by whole-exome analysis. *Eur J Hum Genet* 2012;20:999-1003.

33. Francey LJ, Conlin LK, Kadesch HE, et al. Genome-wide SNP genotyping identifies the stereocilin (STRC) gene as a major contributor to pediatric bilateral sensorineural hearing impairment. *Am J Med Genet A* 2012;158A:298-308.

34. Vona B, Hofrichter M.A.H., Neuner C, et al. DFNB16 is a frequent cause of congenital hearing impairment: implementation of STRC mutation analysis in routine diagnostics. *Clin Genet*. 2014; doi 10.1111/cge.12332.

35. Bernal S, Ayuso C, Antinolo G, et al. Mutations in USH2A in Spanish patients with autosomal recessive retinitis pigmentosa: high prevalence and phenotypic variation. *J Med Genet* 2003;40:e8.

36. Rivolta C, Sweklo EA, Berson EL, Dryja TP. Missense mutation in the USH2A gene: association with recessive retinitis pigmentosa without hearing loss. *Am J Hum Genet* 2000;66:1975-1978.

37. Zelante L, Gasparini P, Estivill X, et al. Connexin26 mutations associated with the most common form of non-syndromic neurosensory autosomal recessive deafness (DFNB1) in Mediterraneans. *Hum Mol Genet* 1997;6:1605-1609.

FIGURE LEGENDS

Figure 1. Pedigrees and sequence chromatograms of the autosomal dominant families D1 through D8. Asterisks denote those who were available for sequencing. All mutations are heterozygous. (D1) *MYO6* c.884_893delGCAAAAGTCC (p.Arg295Leufs*13). The deleted sequence under segregation analysis is boxed. The affected index patient (II:2) transmitted the frameshift mutation to one of her two sons (III:1) who was enrolled before the typical age of onset for DFNA22 and is not yet affected. (D2) *ACTG1* c.974T>A (p.Met325Lys). (D3) *TCF21* c.63C>G (p.Asp21Glu). (D4) *CCDC50* c.227G>A (p.Arg76His). (D5) *MYO1A* c.2032A>T (p.Ile678Phe). (D6) *MYH14* c.5008C>T (p.Arg1670Cys). (D7) *MYO1A* c.2390C>T (p.Ser797Phe). (D8) *EYA4* c.1341-19T>A predicted 3' splice site mutation.

Figure 2. Pedigrees and sequence chromatograms of the autosomal recessive families R1 through R5. Asterisks denote those who were available for sequencing. (R1) Compound heterozygous *MYO15A* c.1137delC (p.Tyr380Metfs*65) (left) and c.7124_7127delACAG (p.Asp2375Valfs*29) (right) mutations. The deleted sequence under segregation analysis is boxed. (R2) Homozygous *MYO7A* c.3935T>C (p.Leu1312Pro) mutation in a consanguineous family. (R3) Compound heterozygous *USH2A* c.1841-2A>G (left) and c.2440C>T (p.Gln814*) (right) mutations. (R4) Heterozygous *USH2A* c.2276G>T (p.Cys759Phe). (R5) Homozygous *GJB2* c.35delG (p.Gly12Valfs*2).

Figure 3. The distribution of variants in the case and control groups among 80 deafness genes. The median number of variants in controls (C) is 1.0, while the median number is 4.0 in the dominant (D) group, and 3.0 each in the recessive (R) and unsolved (U) groups. This represents a significantly higher number of variants in the case groups compared to the controls.

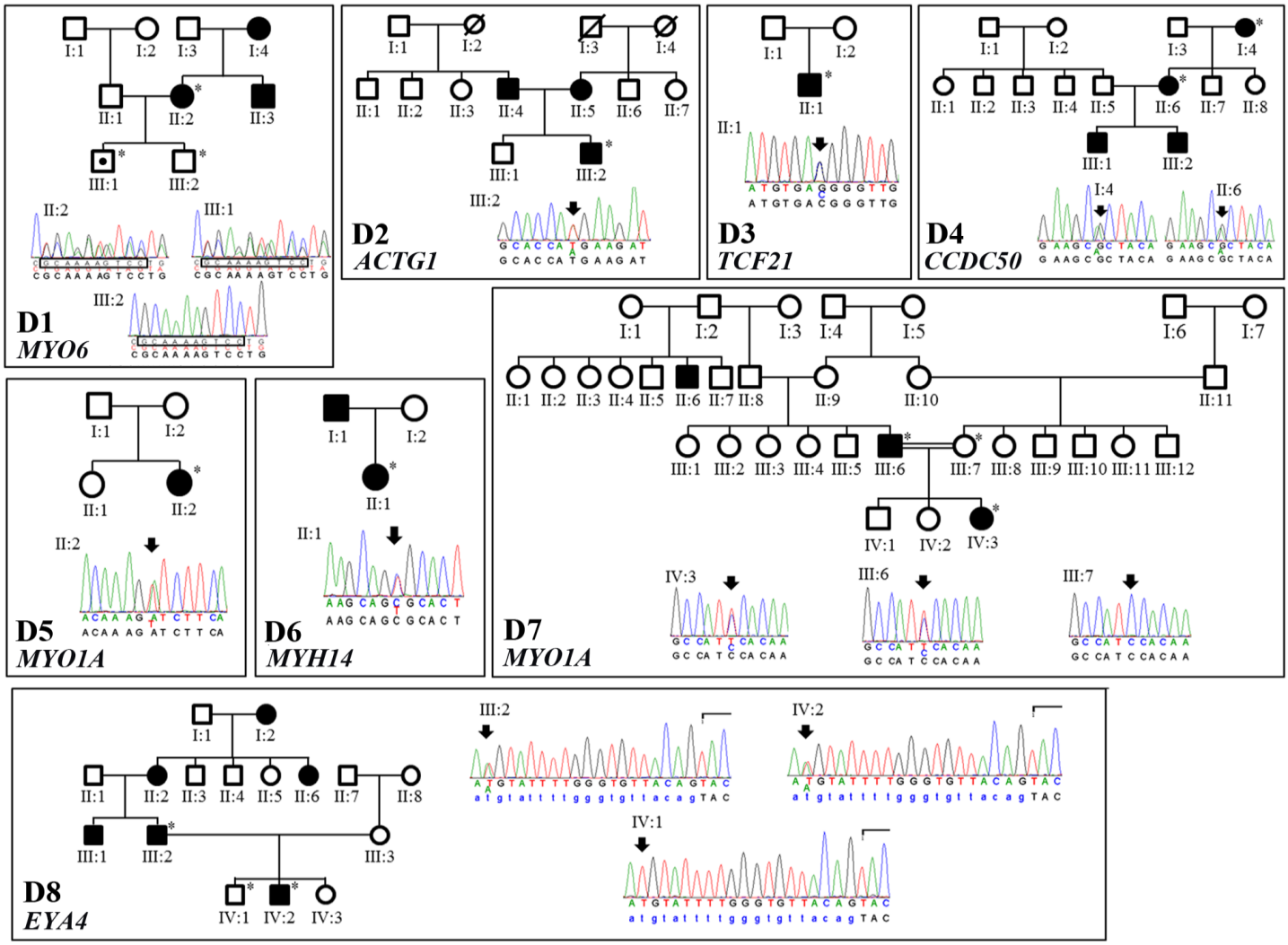
D1
MYO6
D2
ACTG1
D3
TCF21
D4
CCDC50
D5
MYO1A
D6
MYH14
D7
MYO1A
D8
EYA4

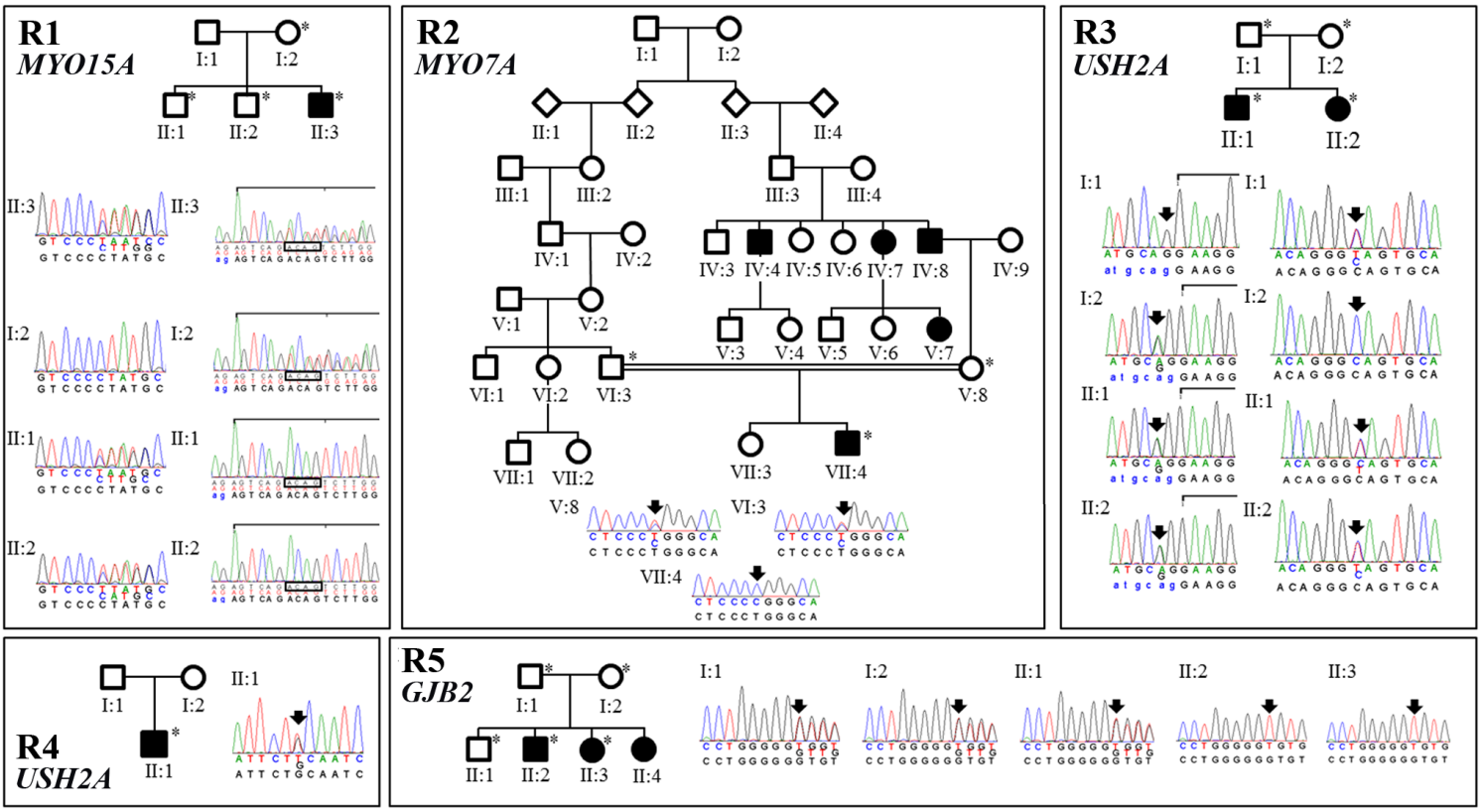
R1
MYO15A
I:1
I:2
II:1
II:2
II:3
R2
MYO7A
III:1
III:2
III:3
III:4
IV:1
IV:2
IV:3
IV:4
IV:5
IV:6
IV:7
IV:8
IV:9
V:1
V:2
V:3
V:4
V:5
V:6
V:7
V:8
VI:1
VI:2
VI:3
VII:1
VII:2
VII:3
VII:4
R3
USH2A
R4
USH2A
R5
GJB2

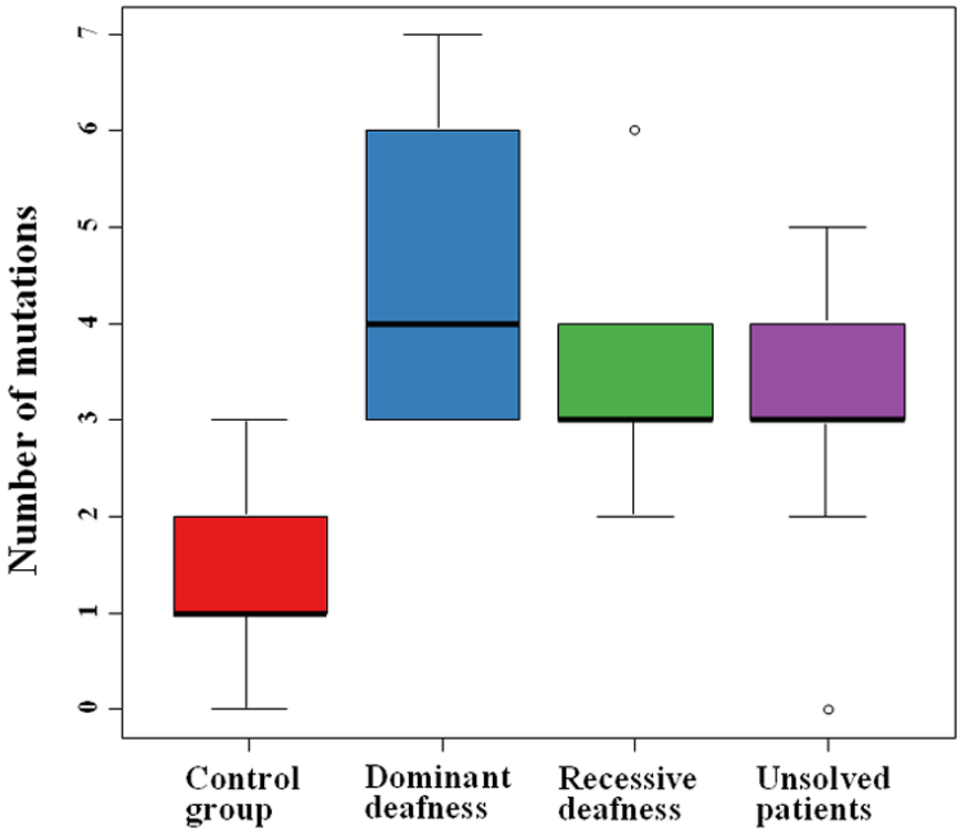
Number of mutations
0
1
2
3
4
5
6
7
Control group
Dominant deafness
Recessive deafness
Unsolved patients

Table 1 Clinical descriptions and characteristic hearing loss of each dominant or recessive hearing loss patient

Family ID	Gene	DFN Locus	Nucleotide	Protein	Chr	Exon/ Intron	Novel or HGMD	MAF[1]	Audiological information[2]
Dominant									
D1 (II.2)	*MYO6*	DFNA22	c.884_893delGC AAAAGTCC	p.Arg295Leufs*13	6	Exon 10	Novel	-	HL across all frequencies with flat PTA between 30 and 60 dB
D2 (III:2)	*ACTG1*	DFNA20/26	c.974T>A	p.Met325Lys	17	Exon 5	Novel	-	Gently sloping pure tone audiometric thresholds indicating HL across all frequencies, moderate HL between 0.125 kHz and 0.5 kHz; severe HL between 1 and 8 kHz
D3	*TCF21*	-	c.63C>G	p.Asp21Glu	6	Exon 1a	Arbustini et al.[28]	0.0078	Flat pure tone audiometric thresholds across all frequencies between 45 and 80 dB; diagnosed with high-grade SNHL at the age of 10 months
D4 (I:4; II:6)	*CCDC50*	DFNA44	c.227G>A	p.Arg76His	3	Exon 3	Novel	0.0005	Moderate mid-grade HL since birth
D5	*MYO1A*	DFNA48	c.2032A>T	p.Ile678Phe	12	Exon 19	-	0.0031	Normal hearing until 2 kHz, sloping to profound SNHL to 8 kHz
D6	*MYH14*	DFNA4A	c.5008C>T	p.Arg1670Cys	19	Exon 36	Novel	-	All frequencies mildly affected until 1 kHz; right ear mid-grade SNHL sloping to severe 8 kHz; left ear, moderate to mild low-grade SNHL at 8 kHz
D7	*MYO1A*	DFNA48	c.2390C>T	p.Ser797Phe	12	Exon 23	Donaudy et al.[29]	0.0073	Mild HL until 1 kHz; moderately severe between 2 and 8 kHz right; moderately severe between 2 and 6 kHz left sloping to 8 kHz; middle-grade hightone SNHL
D8 (III:2; IV:2)	*EYA4*	DFNA10	c.1341-19T>A	-	6	Intron 15	Novel	-	Mild SNHL across all frequencies, particularly in the middle frequency range with PTA between 40 and 50 dB with cookie bite audiogram profile
Recessive									
R1 (II:3)	*MYO15A*	DFNB3	c.1137delC; c.7124_7127del ACAG	p.Tyr380Metfs*65; p.Asp2375Valfs*2 9	17	Exon 2; Exon 35	Novel[3] Novel	0.0004 0.0032	Normal audiometric thresholds between 0.125 and 0.25 kHz, then steeply sloping to severe HL between 0.5 and 8 kHz; HL is progressive
R2 (VII:4; V:8)	*MYO7A*	DFNA11/ DFNB2	c.3935T>C; 3935T>C	p.Leu1312Pro; p.Leu1312Pro	11	Exon 31; Exon 31	Novel	-	Severe to profound SNHL; no responses to high frequencies
R3 (II:1)	*USH2A*	USH2A	c.1841-2A>G; c.2440C>T	-; p.Gln814*	1	Intron 10; Exon 13	Bernal et al.[35] Novel	- -	Flat audiometric profiles indicating mild to moderate mid-grade SNHL across all frequencies; HL in proband and sibling is reported in the first year of life; no family history of HL
R4 (II:1)	*USH2A*	-	c.2276G>T; CNV	p.Cys759Phe -	1	Exon 13; Exon 58-64	Rivolta et al.[36] Novel	0.0021	Normal hearing between 0.25 and 1 kHz, moderate to moderately severe HL between 1 and 8 kHz
R5 (II:1)	*GJB2*	DFNB1A	c.35delG	p.Gly12Valfs*2	13	Exon 1	Zelante et al.[37]	0.0108	Severe HL with signs of auditory neuropathy since birth; no prior family history indicated; out of four children, three are affected

[1]Minor allele frequency (MAF) data are from the European American population of the Exome Variant Server from the Exome Sequencing Project.
[2]All patients had bilateral hearing loss.
[3]The HGMD reference for the *MYO15A* c.1137delC mutation should be c.1134delC. On this basis, we label this mutation novel.

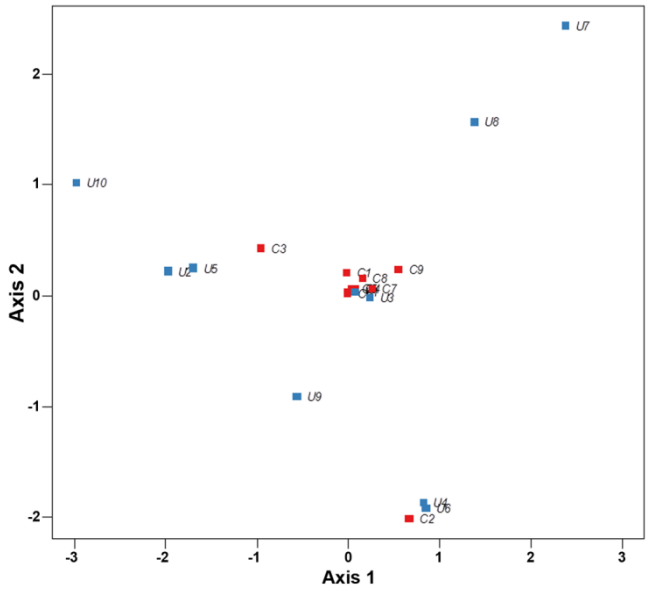

Figure S1. Multi-dimensional-scaling plot depicting distribution patterns between control (C) and unsolved (U) groups.

Table S1 Clinical information from each proband.

Case	Age of onset (in years)	Age at enrollment	Clinical Testing					Other clinical information/ audiograms from additional family members
			Kidney	Ophthalmological	Thyroid	ECG	MRI (inner ear/ temporal bone)	
D1	1	1	Normal	Normal	Normal	Normal	Normal	Speech delay; mother has HL across all frequencies with flat PTA between 30 and 60 dB
D2	At birth	23	Normal	Normal	Normal	Normal	Normal	Father is completely deaf; mother has profound HL
D3	1	10	Normal	Normal	Normal	Normal	Normal	Behavioural problems; ADHD; severe speech delay; intermodular perceptual disturbance (cognition and fine motor function); no evidence of cardiac phenotype but proband is recommended for regular cardiac evaluation
D4	At birth	44	Normal	Normal	Normal	Normal	Normal	Grandmother was deaf since birth and mother has profound HL since birth
D5	7	11	Normal	Normal	Normal	Normal	Normal	Head trauma (right mastoid fracture at one year of age); hearing test was normal at time of fracture
D6	6	14	Normal	Optic neuritis at five years of age	Normal	Normal	Normal	Otosclerosis; keratosis pilaris; alopecia; irregular EEG waveforms since childhood; father's audiogram indicates HL with profile similar to his daughter
D7	5	10	Normal	Normal	Normal	Normal	Normal	Parents are first degree cousins; father's audiogram also sloping in higher frequencies
D8	6	7	Normal	Normal	Normal	Normal	Normal	Father has similar cookie bite audiogram profile
R1	3	5	Normal	Normal	Normal	Normal	Normal	Two brothers tested with normal audiogram results; HL was initially thought to be due to one of three reasons: (1) post-partum hypoxic event, (2) acute vasculitis, or (3) herpes infection at six months of age, but the *MYO15A* segregating mutation challenges these hypotheses
R2	1-2	2	Normal	Normal	Normal	Normal	Normal	The proband is from a consanguineous union; nuclear family has no indication of HL but has a family history of severe HL
R3	1-2	1	Normal	Normal	Normal	Normal	Normal	Speech delay, orofacial sensorimotor muscle coordination difficulties, but responding well to phonetic training
R4	3	3	Normal	Normal, but wears glasses since four years of age	Normal	Normal	Normal	N.a.
R5	At birth	4	Normal	Normal	Normal	Normal	Normal	Speech delay
U1	At birth	3	Normal	Eyes lasered (retinopathy of prematurity), wears glasses	Normal	Normal	Normal	Delivered 14 weeks prematurely with patent ductus arteriosus; hernia surgery was performed at one year of age
U2	At birth	6	Normal	Normal	Normal	Normal	Normal	Failure to thrive, developmental delay, small and low set ears, small hands and feet, motor developmental delay, scoliosis, obstructive sleep apnea, narrowing of tympanic cavity, speech delay, dental malocclusion
U3	7	7	Normal	Normal	Normal	Normal	Normal	Sudden HL, incomplete simple syndactyly of the second and third proximal phalanges
U4	5	47	Normal	Normal	Normal	Normal	Normal	N.a.
U5	1	2	Normal	Normal	Normal	Normal	Normal	Speech delay, oral motor hypotonia, dysphagia, born four weeks prematurely, audiogram from mother was normal
U6	6	7	Normal	Normal	Normal	Normal	Normal	Speech delay, born five weeks prematurely, audiograms from two other brothers shows one with normal hearing and one with HL
U7	5	6	Normal	Normal	Normal	Normal	Normal	Grandfather has HL since childhood
U8	4	4	Normal	Normal	Normal	Normal	Normal	Parents are first degree cousins
U9	5	11	Normal	Normal	Normal	Normal	Normal	Father has suspected noise exposure HL
U10	5	41	Normal	Normal	Normal	Normal	Normal	Audiogram of daughter indicates mild HL at the age of six years

Abbreviations: ADHD, attention deficit hyperactivity disorder; EEG, electrocardiogram; EEG, electroencephalogram; HL, hearing loss; MRI, magnetic resonance imaging; N.a., not available; PTA, pure tone audiometry

Table S2 Analyzed genes

Gene symbol	Gene description	Deafness locus	Chromo-some	mRNA length	OMIM	Reference
80 gene panel						
ACTB	Actin, beta	-	7p22.1	1852	102630	Procaccio et al. (2006)
ACTG1	Actin, gamma-1	DFNA20/26	17q25.3	1919	102560	Zhu et al. (2003)
ATP6V1B1	ATPase, H+ transporting, lysosomal, 56/58-KD, V1 subunit B, isoform 1	-	2q13.3	1956	192132	Karet et al. (1999)
BCS1L	BCS1, S. cerevisiae, homologue-like	-	2q35	1663	603647	Hinston et al. (2007)
BSND	Bartter syndrome, infantile, with sensorineural deafness (Barttin)	DFNB73	1q32.3	1396	606412	Riazuddin et al. (2009)
CATSPER2	Cation channel, sperm-associated 2	-	15q15.3	1948	607249	Zhang et al. (2007)
CCDC50	Coiled-coil domain-containing protein 50	DFNA44	3q28	2454	611051	Modamio-Hoybjor et al. (2003)
CDH23	Cadherin 23	DFNB12	10q22.1	11073	605516	Borck et al. (2001)
CLDN14	Claudin 14	DFNB29	21q22.13	1943	605608	Wilcox et al. (2001)
COCH	Coagulation factor C homology	DFNA9	14q12	2534	603196	Robertson et al. (1998)
COL11A2	Collagen, type XI, alpha-2	DFNA13; DFNB53	6p21.32	6414	120290	McGuirt et al. (1999); Chen et al. (2005)
COL9A3	Collagen, type IX, alpha-3	-	20q13.33	2485	120270	Asamura et al. (2005)
CRYM	Crystallin, mu	DFNA40	16q12.2	1303	123740	Abe et al. (2003)
DFNA5	Deafness, autosomal dominant 5	DFNA5	7p15.3	2230	608798	Van Laer et al. (1998)
DFNB31	Deafness, autosomal recessive 31	DFNB31	9q32	4022	607084	Mustapha et al. (2002)
DIAPH1	Diaphanous, Drosophila, homolog 1	DFNA1	5q31.3	5662	602121	Lynch et al. (1997)
DSPP	Dentin sialophosphoprotein	DFNA39	4q22.1	4187	125485	Xiao et al. (2001)
ERCC2	Excision repair, complementing defective, in Chinese hamster 2	-	19q13.32	2568	126340	Flores-Alvarado et al. (2010)
ERCC3	Excision repair, complementing defective, in Chinese hamster 3	-	2q14.3	2751	133510	Flores-Alvarado et al. (2010)
ESPN	Espin	DFNB36	1q36.31	3542	606351	Naz et al. (2004)
ESRRB	Estrogen-related receptor, beta	DFNB35	14q24.3	2193	602167	Ansar et al. (2003)
EYA4	Eyes absent 4	DFNA10	6q23.2	3077	603550	Wayne et al. (2001)
FGF3	Fibroblast growth factor 3	-	11q13.3	1548	164950	Tekin et al. (2008)
GATA3	GATA-binding protein 3	-	10p14	3067	131320	Van Esch et al. (2000)
GJA1	Gap junction protein, alpha-1	DFNB38	6q22.31	3130	121014	Liu et al. (2001)
GJB1	Gap junction protein, beta-1	-	Xq13.1	1623	304040	Bergoffen et al. (1993)
GJB2	Gap junction protein, beta-2	DFNA3A;	13q12.11	2263	121011	Kelsell et al. (1997);

		DFNB1A				Carrasquello et al. (1997)
GJB3	Gap junction protein, beta-3	DFNA2B	1p34.3	1777	603324	Xia et al. (1998)
GJB4	Gap junction protein, beta-4	-	1p34.2	2840	605425	Lopez-Bigas et al. (2002)
GJB6	Gap junction protein, beta-6	DFNA3B; DFNB1B	13q12.11	1805	604418	Grifa et al. (1999)
GRHL2	Grainyhead-like 2	DFNA28	8q22.3	5231	608576	Peters et al. (2002)
GSTP1	Glutathione S-transferase, pi	-	11q13.2	986	134660	Ateş et al. (2005)
JAG1	Jagged 1	-	20p12.2	5988	601920	Le Caignec et al. (2002)
KCNE1	Potassium channel, voltage-gated, Isk-related subfamily, member 1	-	21q22.12	3338	176261	Van Laer et al. (2006)
KCNJ10	Potassium channel, inwardly rectifying, subfamily J, member 10	-	1q23.2	5323	602208	Yang et al. (2009)
KCNQ4	Potassium channel, voltage-gated, KQT-like subfamily, member 4	DFNA2A	1p34.3	2335	603537	Kubisch et al. (1999)
LHFPL5	Lipoma HMGIC fusion partner-like 5	DFNB66/67	6p21.31	2162	609427	Kalay et al. (2006)
LHX3	LIM homeobox gene 3	-	9p34.3	2376	600577	Rjab et al. (2008)
LRTOMT	Leucine-rich transmembrane and O-methyltransferase	DFNB63	11q13.4	2332	612414	Ahmed et al. (2008)
MARVELD2	MARVEL domain-containing protein 2	DFNB49	5q13.2	2385	610572	Riazuddin et al. (2006)
MTAP	Methylthioadenosine phosphorylase	-	9p21.3	4937	156540	Williamson et al. (2007)
MYH14	Myosin, heavy chain 14, nonmuscle	DFNA4A	19q13.33	6786	608568	Donaudy et al. (2004)
MYH9	Myosin, heavy chain 9, nonmuscle	DFNA17	22q12.3	7474	160775	Lalwani et al. (2000)
MYO1A	Myosin IA	DFNA48	12q13.3	3624	601478	Donaudy et al. (2003)
MYO1C	Myosin IC	-	17p13.3	4973	606538	Zadaro et al. (2009)
MYO1F	Myosin IF	-	19p13.2	4173	601480	Chen et al. (2001)
MYO3A	Myosin IIIA	DFNB30	10p12.1	5597	606808	Walsh et al. (2002)
MYO6	Myosin VI	DFNA22; DFNB37	6q14.1	5278	600970	Melchioda et al. (2001); Ahmed et al. (2003)
MYO7A	Myosin VIIA	DFNA11; DFNB2	11q13.5	7465	276903	Liu et al. (1997)
MYO15A	Myosin XVA	DFNB3	17p11.2	11876	602666	Wang et al. (1998)
NR2F1	Nuclear receptor subfamily 2, group F, member 1	-	5q15	3210	132890	Brown et al. (2009)
OTOA	Otoancorin	DFNB22	16p12.2	3625	607038	Zwaenepoel et al. (2002)
OTOF	Otoferlin	DFNB9	2p23.3	7173	603681	Yasunaga et al. (2000)
OTOR	Otoraplin	-	20p12.1	1477	606067	Rendtorff et al. (2011)
PAX3	Paired box gene 3	-	2q36.1	3359	606597	Baldwin et al. (1992)
PCDH15	Protocadherin 15	DFNB23	10q21.1	7022	605514	Ahmed et al. (2003)
PDZD7	PDZ domain-containing 7	-	10q24.31	2072	612971	Schneider et al. (2009)
PJVK	Pejvakin	DFNB59	2q31.2	1415	610219	Delmaghani et al. (2006)

PMP22	Peripheral myelin protein 22	-	17p12	1828	601097	Boerkoel et al. (2002)
POU3F4	POU domain, class 3, transcription factor 4	DFNX2	Xq21.1	1491	300039	De Kok et al. (1995)
POU4F3	POU domain, class 4, transcription factor 3	DFNA15	5q32	1017	602460	Vahava et al. (1998)
RDX	Radixin	DFNB24	11q22.3	4498	179410	Khan et al. (2007)
SLC4A11	Solute carrier family 4 (sodium borate transporter), member 11	-	20p13	3110	610206	Desir et al. (2007)
SLC17A8	Solute carrier family 17 (sodium phosphate cotransporter), member 8	DFNA25	12q23.1	3983	607557	Ruel et al. (2008)
SLC26A4	Solute carrier family 26, member 4	DFNB4	7q22.3	4930	605646	Li et al. (1998)
SLC26A5	Solute carrier family 26, member 5	DFNB61	7q22.1	2671	604943	Liu et al. (2003)
SOX2	SRY-box 2	-	3q26.33	2518	184429	Kelberman et al. (2006)
SPINK5	Serine protease inhibitor, Kazal-type 5	-	5q32	3655	605010	Chavanas et al. (2000)
STRC	Stereocilin	DFNB16	15q15.3	5516	606440	Verpy et al. (2001)
TBL1X	Transducin-beta-like 1, X-linked	-	Xp22.3-p22.2	5586	300196	Yan, et al. (2005)
TCF21	Transcription factor 21	-	6q23.2	3249	603306	Schonberger et al. (2005)
TECTA	Tectorin, alpha	DFNA8/12; DFNB21	11q23.3	6469	602574	Verhoeven et al. (1998); Mustapha et al. (1999)
TIMM8A	Translocase of inner mitochondrial membrane 8, yeast homolog A	-	Xq22.1	1459	300356	Tranebjaerg et al. (2000)
TMC1	Transmembrane channel-like protein 1	DFNA36; DFNB7/11	9q21.13	3201	606706	Kurima et al. (2002)
TMIE	Transmembrane inner ear-expressed gene	DFNB6	3p21.31	1646	607237	Naz et al. (2002)
TMPRSS3	Transmembrane protease, serine 3	DFNB8/10	21q22.3	2468	605511	Scott et al. (2001)
TMPRSS5	Transmembrane protease, serine 5	-	11q23.2	2233	606751	Guipponi et al. (2008)
TRIOBP	TRIO- and F-actin binding protein	DFNB28	22q13.1	10024	609761	Shahin et al. (2006)
USH1C	Usher syndrome, type 1C	DFNB18A	11p15.1	2228	605242	Verpy et al. (2000)
WFS1	Wolframin	DFNA6/14/38	4p16.1	3640	606201	Baspalova et al. (2001)
Additional genes in 129 gene panel						
ATP6V1B2	ATPase, H+ transporting, lysosomal, 56/58-KD, V1 subunit B, isoform 2	-	6p21.3	3054	606939	Lee et al. (1995)
CEACAM16	Carcinoembryonic antigen-related cell adhesion molecule 16	DFNA4B	19q13.32	1692	614591	Zheng et al. (2011)
CLRN1	Clarin 1	-	3q25.1	2359	606397	Ness et al. (2003)
COL9A2	Collagen, type IX, alpha-2	-	1p34.2	2831	120260	Baker et al. (2011)
ECE1	Endothelin-converting enzyme 1	-	1p36.12	5114	600423	Albertin et al. (1996)
EDNRA	Endothelin receptor, type A	-	4q31.22	4168	131243	Tzourio et al. (2001)
EDNRB	Endothelin receptor, type B	-	13q22.3	4296	131244	Puffenberger et al. (1994)

FAS	Tumor necrosis factor receptor superfamily, member 6	-	10q23.31	2755	134637	Rieux-Laucat et al. (1995)
FGFR3	Fibroblast growth factor receptor 3	-	4p16.3	4304	134934	Toydemir et al. (2006)
FOXI1	Forkhead box I1	-	5q35.1	2296	601093	Hulander et al. (1998)
GIPC3	GIPC PDZ domain-containing family, member 3	DFNB15	19p13.3	4317	608792	Charizopoulou et al. (2011)
GPR98	G protein-coupled receptor 98	-	5q14.3	19333	602851	Weston et al. (2003)
GPSM2	G protein signaling modulator 2	DFNB82	1p13.3	3039	609245	Walsh et al. (2010)
GRXCR1	Glutaredoxin, cysteine-rich 1	DFNB25	4p13	1003	613283	Schraders et al. (2010)
HAL	Histadine ammonia-lyase	-	12q23.1	3927	609457	Kawai et al. (2005)
HGF	Hepatocyte growth factor	DFNB39	7q21.11	2820	142409	Schultz et al. (2009)
ILDR1	Immunoglobulin-like domain-containing receptor 1	DFNB42	3q13.33	2908	609739	Borck et al. (2011)
KCNQ1	Potassium channel, voltage-gated, KQT-like subfamily, member 1	-	11p15.5	3262	607542	Reardon et al. (1993)
KIAA1199	KIAA1199 protein	-	15q25.1	7080	608366	Abe et al. (2003)
LOXHD1	Lipoxygenase homology domain-containing 1	DFNB77	18q21.1	6854	613072	Grillet et al. (2009)
MIR96	Micro RNA 96	DFNA50	7q32.2	78	611606	Mencia et al. (2010)
MIR182	Micro RNA 182	-	7q32.2	110	611607	Weston et al. (2006)
MIR183	Micro RNA 183	-	7q32.2	110	611608	Weston et al. (2006)
MITF	Microphthalmia-associated transcription factor	-	3p13	4815	156845	Tassabehji et al. (1994)
MSRB3	Methionine sulfoxide reductase B3	DFNB74	12q14.3	4307	613719	Waryah et al. (2009)
MT-TD	Transfer RNA, mitochondrial, aspartic acid	-	Mito.	68	590015	Seneca et al. (2005)
MT-TH	Transfer RNA, mitochondrial, histidine	-	Mito.	69	590040	Crimi et al. (2003)
MT-TI	Transfer RNA, mitochondrial, isoleucine	-	Mito.	69	590045	Corona et al. (2002)
MT-TK	Transfer RNA, mitochondrial, lysine	-	Mito.	70	590060	Silvestri et al. (1992)
MT-TL1	Transfer RNA, mitochondrial, leucine 1	-	Mito.	75	590050	Mosewich et al. (1993)
MT-TL2	Transfer RNA, mitochondrial, leucine 2	-	Mito.	71	590055	Fu et al. (1996)
MT-TM	Transfer RNA, mitochondrial, methionine	-	Mito.	68	590065	Jones et al. (2008)
MT-TQ	Transfer RNA, mitochondrial, glutamine	-	Mito.	72	590030	Finnila et al. (2001)
MT-TS1	Transfer RNA, mitochondrial, serine 1	-	Mito.	69	590080	Reid et al. (1994)
MT-TS2	Transfer RNA, mitochondrial, serine 2	-	Mito.	59	590085	Mansergh et al. (1999)
NDP	Norrin	-	Xp11.3	2058	300658	Rehm et al. (1997)
P2RX2	Purinergin receptor P2X, ligand-gated ion channel 2	-	12q24.33	1945	600844	Yan et al. (2013)
PRPS1	Phosphoribosylpyrophosphate synthetase 1	DFNX1	Xq22.3	2156	311850	Liu et al. (2010)
PTPRQ	Protein-tyrosine phosphatase receptor-type Q	DFNB84A	12q21.31	8066	603317	Schraders et al. (2013)
SERPINB6	Serpin peptidase inhibitor, clade B (ovalbumin), member 6	DFNB91	6p25.2	1932	173321	Sirmanci et al. (2010)
SIX1	Sine oculis homeobox, drosophila, homolog 1	DFNA23	14q23.1	2687	601205	Ruf et al. (2004)
SIX5	Sine oculis homeobox, drosophila, homolog 5	-	19q13.32	3352	600963	Hoskins et al. (2007)
SMPX	Small muscle protein, X-linked	DFNX4	Xp22.12	951	300226	Schraders et al. (2011)
SNAI2	Snail, drosophila, homolog 2	-	8q11.21	2112	602150	Sanchez-Martin et al. (2002)
TFCP2	Transcription factor CP2	-	12q13.12-q13.13	3715	189889	Swendeman et al. (1994)
TJP2	Tight junction protein 2	DFNA51	9q21.11	4725	607709	Walsh et al. (2010)
TPRN	Taperin	DFNB79	9q34.3	2641	613354	Rehman et al. (2010)
USH1G	Usher syndrome 1G	-	17q25.1	3568	607696	Bashir et al. (2010)
USH2A	Usher syndrome 2A	-	1q41	18883	608400	Van Wijk et al. (2004)

Table S3 Run statistics and target coverage information from human deafness gene panel sequencing

Individual	Number of reads*	Mapped reads*	Mean depth (x)	% of exons with Depth ≥10x
D1[a]	6,325,660	4,815,197	176	95.4
D2[a]	13,618,872	11,778,140	409	99.7
D3[a]	7,318,278	5,560,271	197	95.7
D4[a] (I:4)	10,945,026	9,427,871	309	99.5
D4[a] (II:6)	12,107,818	10,763,523	345	99.6
D5[b]	6,313,548	5,797,322	242	99.4
D6[a]	5,318,288	4,909,669	396	99.6
D7[b]	7,463,506	6,822,238	282	99.6
D8[a] (III:2)	5,741,568	5,215,973	437	99.5
D8[a] (IV:2)	5,019,068	4,556,298	352	99.5
R1[a]	4,792,488	4,410,058	377	99.7
R2[a] (VII:4)	5,479,774	4,211,942	147	95.4
R2[a] (V:8)	6,768,524	5,029,245	177	95.5
R3[b]	7,314,120	6,658,222	284	99.7
R4[b]	6,814,618	6,202,347	261	99.5
R5[b] (II:2)	6,931,570	6,438,225	204	92.5
U1[a]	7,561,986	5,752,732	207	95.8
U2[a]	7,114,584	5,376,162	195	95.6
U3[a]	5,131,806	4,716,270	408	99.7
U4A[b]	6,331,630	5,843,843	198	99.1
U4B[b]	6,916,206	6,378,414	230	99.3
U5A[a]	4,635,632	4,270,323	326	99.5
U5B[a]	4,356,056	3,972,174	318	99.6
U6A[a]	14,706,372	13,247,035	474	99.5
U6B[a]	12,850,352	11,452,294	410	99.5
U7[a]	7,377,024	5,536,805	199	99.4
U8[b]	6,092,050	5,585,863	252	99.4
U9A[a]	6,858,184	5,198,277	181	95.5
U9B[a]	6,791,602	5,211,423	195	95.8
U10[a]	7,142,816	5,156,676	191	95.6
Control 1[a]	13,844,186	12,470,109	447	99.5
Control 2[a]	14,257,838	12,318,824	433	99.5
Control 3[a]	10,985,596	9,618,643	322	99.5
Control 4[a]	12,704,104	11,408,390	408	99.5
Control 5[a]	12,590,204	11,087,703	375	99.5
Control 6[a]	3,875,190	3,589,027	280	99.5
Control 7[a]	4,680,476	4,295,677	366	99.7
Control 8[a]	4,211,518	3,891,516	298	99.5
Control 9[b]	6,971,952	6,493,175	263	99.5

*Number of reads and number of mapped reads are in bp.
[a]80 gene panel; [b]129 gene panel.

Table S4 Summary of all damaging variants and mutations per patient according to group

Cases	Gene[1]	DFN Locus	Nucleotide	Protein	Mutat.Taster[2]	PolyPhen2[2]	SIFT[3]	Zyg.[4]	Depth	MAF	dbSNP
Patients with dominant forms of deafness											
D1	***MYO6***	DFNA22	c.884_893delGCAAAAGTCC	p.Arg295Leufs*13	DC (1.0)	NA	NA	0/1	44	-	-
D1	*DSPP*	DFNA39	c.691C>A	p.Pro231Thr	B (1.0)	PoD (0.90)	D (0.00)	0/1	306	A = 0.010	rs61738509
D1	*DSPP*	DFNA39	c.802G>T	p.Gly268Trp	B (1.0)	PrD (1.0)	D (0.00)	0/1	298	T = 0.010	rs61738508
D1	*KCNJ10*	-	c.811C>T	p.Arg271Cys	DC (1.0)	PrD (1.0)	D (0.02)	0/1	287	A = 0.023	rs1130183
D1	*OTOF*	DFNB9	c.1393-1G>C	-	NA	NA	NA	0/1	208	-	-
D1	*OTOF*	DFNB9	c.5558G>A	p.Arg1853Gln	DC (1.0)	PrD (0.98)	D (0.00)	0/1	80	T = 0.006	rs111033329
D1	*TRIOBP*	DFNB28	c.3089C>G	p.Pro1030Arg	B (0.96)	PrD (1.0)	D (0.00)	0/1	110	G = 0.005	rs193013234
D2	***ACTG1***	DFNA20/26	c.974T>A	p.Met325Lys	DC (1.0)	B (0.00)	D (0.00)	0/1	181	-	-
D2	*ESPN*	DFNB36	c.752G>A	p.Gly251Asp	DC (1.0)	PrD (1.0)	B (0.29)	0/1	354	-	rs200602012
D2	*SLC26A4*	DFNB4	c.2326C>T	p.Arg776Cys	DC (1.0)	PrD (1.0)	D (0.01)	0/1	183	T = 0.001	rs111033255
D2	*MYO1C*	-	c.859G>A	p.Val287Ile	DC (1.0)	PrD (0.98)	B (0.05)	0/1	143	T = 0.001	rs117696188
D2	*USH1C*	DFNB18	c.1823C>G	p.Pro608Arg	DC (0.98)	NA	B (1.00)	0/1	212	-	rs41282932
D3	***TCF21***	-	c.63C>G	p.Asp21Glu	DC (1.0)	B (0.15)	D (0.00)	0/1	374	G = 0.006	rs61729591
D3	*CDH23*	DFNB12	c.2001C>A	p.Asn667Lys	DC (1.0)	PrD (1.0)	D (0.00)	0/1	10	-	-
D3	*OTOR*	-	c.2T>C	p.Met1Thr	DC (1.0)	PoD (0.96)	D (0.00)	0/1	108	C = 0.029	rs17686437
D4	***CCDC50***	DFNA44	c.227G>A	p.Arg76His	DC (0.99)	B (0.21)	D (0.01)	0/1	80	A = 0.001	rs138443787
D4	*CCDC50*	DFNA44	c.157C>T	p.Gln53*	DC (1.0)	NA	NA	0/1	107	-	-
D4	*GATA3*	-	c.231_238delGACCCACC	p.Thr78Argfs*223	DC (1.0)	NA	NA	0/1	202	-	-
D4	*MYO1C*	-	c.319G>A	p.Val107Ile	DC (1.0)	PoD (0.62)	B (0.28)	0/1	101	T = 0.001	rs140549082
D4	*SPINK5*	-	c.3134G>A	p.Gly1045Asp	DC (0.99)	PrD (1.0)	D (0.00)	0/1	309	-	-
D5	***MYO1A***	DFNA48	c.2032A>T	p.Ile678Phe	DC (1.0)	PrD (0.99)	D (0.00)	0/1	46	A = 0.003	rs151269703
D5	*DSPP*	DFNA39	c.974G>C	p.Ser325Thr	B (0.99)	PrD (0.97)	D (0.00)	0/1	315	C = 0.001	rs145481275
D5	*OTOR*	-	c.2T>C	p.Met1Thr	DC (1.0)	PoD (0.96)	D (0.00)	0/1	176	C = 0.029	rs17686437
D6	***MYH14***	DFNA4A	c.5008C>T	p.Arg1670Cys	DC (1.0)	PrD (1.0)	D (0.00)	0/1	330	-	-
D6	*CCDC50*	DFNA44	c.1396C>T	p.Arg466Trp	B (1.0)	NA	D (0.05)	0/1	75	T = 0.006	rs147604673
D6	*GJB4*	-	c.384G>A	p.Trp128*	DC (1.0)	NA	NA	0/1	398	A = 0.002	rs149110828
D7	***MYO1A***	DFNA48	c.2390C>T	p.Ser797Phe	DC (0.89)	PrD (0.71)	D (0.00)	0/1	73	A = 0.003	rs113470661
D7	*MYH14*	DFNA4A	c.483G>A	p.Met161Ile	DC (1.0)	PoD (0.76)	D (0.00)	1/1	351	A = 0.013	rs34773557
D7	*LHFPL5*	DFNB67	c.169C>T	p.Pro57Ser	DC (1.0)	PrD (1.0)	B (0.28)	0/1	380	-	-
D8	***EYA4***	DFNA10	c.1341-19T>A	-	NA	NA	NA	0/1	351	-	-
D8	*CDH23*	DFNB12	c.1096G>A	p.Ala366Thr	DC (1.0)	PrD (1.0)	D (0.00)	0/1	255	A = 0.004	rs143282422
D8	*GJB3*	DFNB91	c.94C>T	p.Arg32Trp	DC (1.0)	PrD (1.0)	D (0.00)	0/1	401	T = 0.015	rs1805063
D8	*GJB4*	-	c.155_158delTCTG	p.Val52Alafs*55	DC (1.0)	NA	NA	0/1	333	-	-
D8	*MYH9*	DFNA17	c.193G>A	p.Val65Met	DC (0.93)	B (0.37)	D (0.01)	0/1	257	-	-

D8	*MYO3A*	DFNB30	c.2387T>G	p.Phe796Cys	DC (1.0)	PrD (1.0)	D (0.00)	0/1	36	-	-
D8	*TECTA*	DFNB21	c.4355T>A	p.Phe1452Tyr	DC (0.98)	PrD (0.99)	B (0.11)	0/1	172	-	-
Patients with recessive forms of deafness											
R1	***MYO15A***	DFNB3	c.1137delC	p.Tyr380Metfs*65	DC (1.0)	NA	NA	0/1	306	-	-
R1	***MYO15A***	DFNB3	c.7124_7217delACAG	p.Asp2375Valfs*29	DC (1.0)	NA	NA	0/1	89	-	-
R1	*MYH9*	DFNA17	c.7C>G	p.Gln3Glu	DC (0.98)	PoD (0.53)	D (0.00)	0/1	315	C = 0.001	rs56200894
R2	***MYO7A***	DFNB2	c.3935T>C	p.Leu1312Pro	DC (1.0)	PrD (1.0)	D (0.00)	1/1	87	-	-
R2	*TMIE*	DFNB6	c.191C>T	p.Ser64Leu	DC (1.0)	PrD (0.99)	D (0.02)	0/1	183	T = 0.001	rs189895472
R3	***USH2A***	-	c.1841-2A>G	-	NA	NA	NA	0/1	393	-	-
R3	***USH2A***	-	c.2440C>T	p.Gln814*	NA	NA	NA	0/1	144	-	-
R3	*MYH14*	DFNA4A	c.1150G>T	p.Gly384Cys	DC (1.0)	PrD (1.0)	D (0.00)	0/1	389	T = 0.003	rs119103280
R3	*MYH14*	DFNA4A	c.3805C>T	p.Gln1269*	DC (1.0)	NA	NA	1/1	342	-	-
R3	*GJB2*	DFNB1A	c.35delG	p.Gly12Valfs*2	DC (1.0)	NA	NA	0/1	429	-	rs80338939
R3	*TMPRSS5*	-	c.393G>A	p.Trp131*	DC (1.0)	NA	NA	0/1	240	-	-
R3	*TRIOBP*	DFNB28	c.1617_1619delCTC	p.Ser540del	DC (0.61)	NA	NA	0/1	331	-	-
R4	***USH2A***	-	c.2276G>T	p.Cys759Phe	DC (1.0)	PrD (1.0)	D (0.00)	0/1	130	A = 0.001	rs80338902
R4	*MARVELD2*	DFNB49	c.466C>T	p.Arg156Trp	B (1.0)	PrD (0.97)	D (0.05)	0/1	128	-	rs142099889
R4	*MYH14*	DFNA4A	c.483G>A	p.Met161Ile	DC (1.0)	PoD (0.76)	D (0.00)	0/1	349	A = 0.013	rs34773557
R5	***GJB2***	DFNB1A	c.35delG	p.Gly12Valfs*2	DC (1.0)	NA	NA	1/1	205	-	rs80338939
R5	*ERCC2*	-	c.1381C>G	p.Leu461Val	DC (1.0)	PrD (0.98)	B (0.13)	0/1	53	-	rs121913016
R5	*TECTA*	DFNB12	c.5012C>T	p.Ser1671Leu	DC (1.0)	B (0.172)	D (0.05)	0/1	189	T = 0.001	rs142948530
R5	*USH2A*	-	c.1663C>G	p.Leu555Val	DC (1.0)	PrD (1.0)	D (0.00)	0/1	217	C = 0.001	rs35818432
Unsolved cases											
U2	*GJB4*	-	c.155_158delTCTG	p.Val52Alafs*55	DC (1.0)	NA	NA	0/1	468	-	-
U2	*MYO1A*	DFNA48	c.1985G>A	p.Gly662Glu	DC (0.10)	B (0.00)	D (0.04)	0/1	89	T = 0.015	rs33962952
U2	*PCDH15*	DFNB23	c.2252C>A	p.Ala751Asp	DC (1.0)	PrD (0.98)	D (0.02)	0/1	121	-	-
U2	*SLC26A4*	DFNA4	c.760A>G	p.Ile254Val	DC (0.70)	PoD (0.94)	B (0.11)	0/1	128	-	-
U2	*TMPRSS5*	-	c.1187G>A	p.Gly396Glu	DC (1.0)	PrD (1.0)	D (0.00)	0/1	10	-	-
U3	*CCDC50*	DFNA44	c.1396C>T	p.Arg466Trp	B (1.0)	NA	D (0.05)	0/1	86	T = 0.006	rs147604673
U3	*COL9A3*	-	c.753C>G	p.Phe251Leu	DC (0.99)	PoD (0.96)	B (0.12)	0/1	346	-	-
U3	*MYH9*	DFNA17	c.5143G>A	p.Gly1715Ser	DC (0.99)	B (0.02)	D (0.04)	0/1	108	T = 0.001	rs148109368
U4	*ESPN*	DFNB36	c.786C>G	p.His262Gln	DC (0.98)	PoD (0.47)	B (0.41)	0/1	25	-	-
U4	*MYO7A*	DFNB2	c.2476G>T	p.Ala826Ser	DC (0.98)	B (0.15)	D (0.05)	0/1	22	-	-
U5	*SLC26A4*	DFNB4	c.1003T>C	p.Phe335Leu	DC (1.0)	PrD (1.0)	D (0.00)	0/1	130	C = 0.001	rs111033212
U5	*OTOF*	DFNB9	c.2464C>T	p.Arg822Trp	DC (0.98)	PrD (1.0)	D (0.00)	0/1	99	A = 0.009	rs80356570
U5	*OTOF*	DFNB9	c.3247G>C	p.Ala1083Pro	DC (0.60)	PoD (0.62)	D (0.04)	0/1	76	G = 0.009	rs80356574
U5	*WFS1*	DFNA6/14/38	c.2393_2394insACG	p.Val798_Thr799insArg	DC (0.67)	NA	NA	0/1	74	-	-

U6	*ERCC2*	-	c.1726G>A	p.Glu576Lys	DC (1.0)	PrD (1.0)	D (0.00)	0/1	148	T = 0.001	rs201165309
U6	*MYO7A*	DFNB2	c.5227C>T	p.Arg1743Trp	DC (0.99)	PoD (0.91)	D (0.01)	0/1	151	-	rs111033287
U6	*USH1C*	DFNB18	c.1591C>T	p.Arg531Cys	DC (0.99)	PrD (1.0)	B (0.08)	0/1	219	-	rs140528164
U7	*GJB2*	DFNB1A	c.457G>A	p.Val153Ile	DC (0.82)	B (0.00)	D (0.05)	0/1	346	T = 0.002	rs111033186
U7	*MYO15A*	DFNB3	c.7885G>A	p.Gly2629Ser	DC (0.56)	PoD (0.90)	B (0.09)	0/1	140	-	-
U7	*TECTA*	DFNB21	c.764A>C	p.Asp255Ala	DC (0.99)	PoD (0.94)	D (0.00)	0/1	203	-	-
U8	*GJB3*	DFNB91	c.94C>T	p.Arg32Trp	DC (1.0)	PrD (1.0)	D (0.00)	0/1	337	T = 0.015	rs1805063
U8	*GJB4*	-	c.155_158delTCTG	p.Val52Alafs*55	DC (1.0)	NA	NA	0/1	325	-	-
U8	*GPR98*	-	c.1849G>A	p.Val617Met	DC (0.87)	PrD (1.0)	D (0.03)	0/1	226	A = 0.001	rs199988872
U8	*GPR98*	-	c.6994A>T	p.Ile2332Phe	DC (1.0)	PrD (0.99)	D (0.02)	0/1	284	T = 0.001	rs193030567
U8	*MYO15A*	DFNB3	c.8782G>A	p.Asp2928Asn	DC (1.0)	PrD (1.0)	D (0.00)	0/1	100	-	-
U8	*P2RX2*	DFNA41	c.118C>T	p.Arg40Cys	DC (1.0)	PrD (1.0)	D (0.00)	0/1	103	-	-
U8	*TJP2*	DFNA51	c.116C>T	p.Thr39Met	DC (1.0)	PoD (0.74)	D (0.05)	0/1	226	T = 0.002	rs138241615
U9	*MYH14*	DFNA4A	c.483G>A	p.Met161Ile	DC (1.0)	PoD (0.76)	D (0.00)	0/1	159	A = 0.013	rs34773557
U9	*MYO1A*	DFNA48	c.1985G>A	p.Gly662Glu	DC (0.10)	B (0.00)	D (0.04)	0/1	84	T = 0.015	rs33962952
U9	*SLC26A4*	DFNB4	c.1766A>C	p.Gln589Pro	DC (1.0)	B (0.41)	D (0.03)	0/1	134	-	-
U9	*TRIOBP*	DFNB28	c.1617_1619delCTC	p.Ser540del	DC (0.61)	NA	NA	0/1	508	-	rs146565844
U10	*OTOA*	DFNB22	c.970A>C	p.Thr324Pro	DC (1.0)	PrD (1.0)	D (0.02)	0/1	106	-	-
U10	*OTOF*	DFNB9	c.3572A>C	p.Asp1191Ala	DC (1.0)	PrD (1.0)	D (0.00)	0/1	95	-	-
U10	*PCDH15*	DFNB23	c.5308_5315delGCTCCTCT	p.Ala1770Cysfs*5	DC (1.0)	NA	NA	0/1	179	-	-
Controls											
1	*MYO1C*	-	c.2596G>A	p.Glu866Lys	DC (1.0)	PoD (0.62)	D (0.00)	0/1	115	T = 0.005	rs61753655
2	*MYO7A*	DFNA11/ DFNB2	c.1960C>T	p.Arg654Cys	DC (1.0)	PrD (1.0)	D (0.00)	0/1	96	-	rs201928014
2	*TRIOBP*	DFNB28	c.6736G>A	p.Glu2246Lys	DC (1.0)	PrD (1.0)	D (0.00)	0/1	71	A = 0.005	rs138139146
3	*PCDH15*	DFNB23	c.3832C>A	p.Gln1278Lys	DC (1.0)	PrD (0.99)	B (0.1)	0/1	248	-	-
3	*TMC1*	DFNA36/ DFNB7	c.1141T>A	p.Tyr381Asn	DC (1.0)	PrD (1.0)	B (0.46)	0/1	152	T = 0.001	rs111033363
4	*CDH23*	DFBN23	c.2239C>T	p.Arg747Cys	DC (1.0)	PrD (1.0)	D (0.00)	0/1	233	-	rs200649500
4	*SPINK5*	-	c.1322G>A	p.Arg441His	B (1.0)	PoD (0.87)	D (0.00)	0/1	367	A = 0.004	rs34393923
4	*SPINK5*	-	c.2094_2096delTGG	p.Gly699del	DC (1.0)	NA	NA	0/1	430	-	rs111662216
5	*MYO1F*	-	c.3080G>A	p.Arg1038Gln	DC (1.0)	PrD (0.99)	B (0.34)	0/1	103	-	rs200864651
6	*WFS1*	DFNA6/14/ 38	c.1597C>T	p.Pro533Ser	DC (1.0)	PrD (1.0)	D (0.00)	0/1	126	T = 0.001	rs146132083
7	*CDH23*	DFNB12	c.3986G>A	p.Gly1329Asp	DC (0.98)	PrD (1.0)	D (0.00)	0/1	265	-	rs201877610
9	*GJB3*	DFNA2B/ DFNB2B	c.94C>T	p.Arg32Trp	DC (1.0)	PrD (1.0)	D (0.00)	0/1	236	T = 0.015	rs1805063
9	*GJB4*	-	c.155_158delTCTG	p.Val52Alafs*55	DC (1.0)	NA	NA	0/1	196	-	-
9	*KIAA1199*	-	c.4078_4080AAG	p.Lys1360del	DC (0.83)	NA	NA	0/1	185	T = 0.009	rs200201338

[1]The quality score of all analyzed sequences was 35, which is the highest quality. The gene underlying hearing impairment in a given patient is presented in bold.
[2]MutationTaster and PolyPhen-2 operate on a scale from 0 to 1.0, with 1.0 having the highest probability of being a damaging substitution. DC=disease-causing; B=benign; NA=not analyzed; PoD=possibly damaging; PrD, probably damaging.
[3]SIFT values <0.05 predict substitutions that are deleterious (D), whereas values >0.05 predict benign (B) substitutions.
[4]Zyg, Zygosity; 1/1, homozygous, 0/1, heterozygous.

Table S5 Variant counts of patients and controls

		In silico predicted pathogenic mutations*				
	Total number	**Dominant**	**Recessive**	**Dominant and/or recessive**	**Syndromic**	**Candidate genes**
Patients with dominant HL						
D1	7	3	3	0	0	1
D2	5	1	3	0	0	1
D3	3	1	1	0	0	1
D4 (I:4)	5	2	0	0	2	1
D5	3	2	0	0	0	1
D6	3	2	0	0	0	1
D7	3	2	1	0	0	0
D8 (III:2)	7	2	4	0	0	1
All	36	15 (42%)	12 (33%)	0	2 (6%)	7 (19%)
Patients with recessive HL						
R1	3	1	2	0	0	0
R2 (VII:4)	3	0	3	0	0	0
R3	6	3	2	0	0	1
R4	2	1	1	0	0	0
R5	4	0	3	0	1	0
All	18	5 (28%)	11 (61%)	0	1 (6%)	1 (6%)
Unsolved cases						
U1	0	0	0	0	0	0
U2	5	1	2	0	0	2
U3	3	2	0	0	0	1
U4	2	0	2	0	0	0
U5	4	1	3	0	0	0
U6	3	0	2	0	1	0
U7	3	0	3	0	0	0
U8	3	0	2	0	0	1
U9	4	2	2	0	0	0
U10	3	0	3	0	0	0
All	30	6 (20%)	19 (63%)	0	1 (3%)	4 (13%)
Controls without HL						
C1	1	0	0	0	0	1
C2	2	0	2	0	0	0
C3	2	0	1	1	0	0
C4	3	0	1	0	2	0
C5	1	0	0	0	0	1
C6	1	1	0	0	0	0
C7	1	0	1	0	0	0
C8	0	0	0	0	0	0
C9	2	0	1	0	0	1
All	13	1 (8%)	6 (46%)	1 (8%)	2 (15%)	3 (23%)

*Patients with the 129 gene panel were reduced to the same overlapping 80 genes contained in the 80 gene panel.

15. Curriculum vitae

My CV is not included in the online version of this dissertation for data protection reasons.

16. Co-author Signatures

Vona B, Nanda I, Neuner C, Schröder J, Kalscheuer VM, Shehata-Dieler W, Haaf T.

Terminal chromosome 4q deletion syndrome: a case report and mapping of critical intervals for associated phenotypes.

BMC Medical Genetics. 2014 (submitted).

Barbara Vona was responsible for the microarray analysis, qPCR deletion confirmation, parent-of-origin determination, literature review, and writing the manuscript.

Co-author	Signature
Indrajit Nanda	
Cordula Neuner	
Jörg Schröder	
Vera M. Kalscheuer	
Wafaa Shehata-Dieler	
Thomas Haaf	

Vona B, Nanda I, Neuner C, Schröder J, Kalscheuer VM, Shehata-Dieler W, Haaf T.

Terminal chromosome 4q deletion syndrome: a case report and mapping of critical intervals for associated phenotypes.

BMC Medical Genetics. 2014 (submitted).

Barbara Vona was responsible for the microarray analysis, qPCR deletion confirmation, parent-of-origin determination, literature review, and writing the manuscript.

Co-author	Signature
Indrajit Nanda	
Cordula Neuner	
Jörg Schröder	
Vera M. Kalscheuer	
Wafaa Shehata-Dieler	
Thomas Haaf	

Vona B, Neuner C, El Hajj N, Schneider E, Farcas R, Beyer V, Zechner U, Keilmann A, Poot M, Bartsch O, Nanda I, Haaf T.

Disruption of the *ATE1* and *SLC12A1* genes by balanced translocation in a boy with non-syndromic hearing loss.

Mol Syndromol. 2014 Jan;5:3-10.

Barbara Vona was responsible for the targeted deafness NGS panel analysis, sequence confirmation, and writing the manuscript.

Co-author	Signature
Cordula Neuner	
Nady El Hajj	
Eberhard Schneider	
Ruxandra Farcas	
Vera Beyer	
Ulrich Zechner	
Annerose Keilmann	
Martin Poot	
Oliver Bartsch	
Indrajit Nanda	
Thomas Haaf	

Vona B, Neuner C, El Hajj N, Schneider E, Farcas R, Beyer V, Zechner U, Keilmann A, Poot M, Bartsch O, Nanda I, Haaf T.

Disruption of the *ATE1* and *SLC12A1* genes by balanced translocation in a boy with non-syndromic hearing loss.

Mol Syndromol. 2014 Jan;5:3-10.

Barbara Vona was responsible for the targeted deafness NGS panel analysis, sequence confirmation, and writing the manuscript.

Co-author	Signature
Cordula Neuner	
Nady El Hajj	
Eberhard Schneider	
Ruxandra Farcas	
Vera Beyer	
Ulrich Zechner	
Annerose Keilmann	
Martin Poot	
Oliver Bartsch	
Indrajit Nanda	
Thomas Haaf	

Vona B, Neuner C, El Hajj N, Schneider E, Farcas R, Beyer V, Zechner U, Keilmann A, Poot M, Bartsch O, Nanda I, Haaf T.

Disruption of the *ATE1* and *SLC12A1* genes by balanced translocation in a boy with non-syndromic hearing loss.

Mol Syndromol. 2014 Jan;5:3-10.

Barbara Vona was responsible for the targeted deafness NGS panel analysis, sequence confirmation, and writing the manuscript.

Co-author	Signature
Cordula Neuner	
Nady El Hajj	
Eberhard Schneider	
Ruxandra Farcas	
Vera Beyer	
Ulrich Zechner	
Annerose Keilmann	
Martin Poot	
Oliver Bartsch	
Indrajit Nanda	
Thomas Haaf	

Vona B, Neuner C, El Hajj N, Schneider E, Farcas R, Beyer V, Zechner U, Keilmann A, Poot M, Bartsch O, Nanda I, Haaf T.

Disruption of the *ATE1* and *SLC12A1* genes by balanced translocation in a boy with non-syndromic hearing loss.

Mol Syndromol. 2014 Jan;5:3-10.

Barbara Vona was responsible for the targeted deafness NGS panel analysis, sequence confirmation, and writing the manuscript.

Co-author	Signature
Cordula Neuner	
Nady El Hajj	
Eberhard Schneider	
Ruxandra Farcas	
Vera Beyer	
Ulrich Zechner	
Annerose Keilmann	
Martin Poot	
Oliver Bartsch	
Indrajit Nanda	
Thomas Haaf	

Vona B, MAH Hofrichter, Neuner C, Schröder J, Gehrig A, Hennermann JB, Kraus F, Shehata-Dieler W, Kolpocki E, Nanda I, Haaf T.

DFNB16 is a frequent cause of congenital hearing impairment: implementation of *STRC* mutation analysis in routine diagnostics.

Clin Genet. 2014 (in press); DOI: 10.1111/cge.12332

Barbara Vona was responsible for the microarray analysis and confirmation of deletions, design and analysis of the Sanger sequence assay, and writing the manuscript.

Co-author	Signature
Michaela Hofrichter	
Cordula Neuner	
Jörg Schröder	
Andrea Gehrig	
Julia B. Hennermann	
Fabian Kraus	
Waafa Shehata-Dieler	
Eva Klopocki	
Indrajit Nanda	
Thomas Haaf	

Vona B, MAH Hofrichter, Neuner C, Schröder J, Gehrig A, Hennermann JB, Kraus F, Shehata-Dieler W, Kolpocki E, Nanda I, Haaf T.

DFNB16 is a frequent cause of congenital hearing impairment: implementation of *STRC* mutation analysis in routine diagnostics.

Clin Genet. 2014 (in press); DOI: 10.1111/cge.12332

Barbara Vona was responsible for the microarray analysis and confirmation of deletions, design and analysis of the Sanger sequence assay, and writing the manuscript.

Co-author	Signature
Michaela Hofrichter	
Cordula Neuner	
Jörg Schröder	
Andrea Gehrig	
Julia B. Hennermann	
Fabian Kraus	
Wafaa Shehata-Dieler	
Eva Klopocki	
Indrajit Nanda	
Thomas Haaf	

Vona B, MAH Hofrichter, Neuner C, Schröder J, Gehrig A, Hennermann JB, Kraus F, Shehata-Dieler W, Kolpocki E, Nanda I, Haaf T.

DFNB16 is a frequent cause of congenital hearing impairment: implementation of *STRC* mutation analysis in routine diagnostics.

Clin Genet. 2014 (in press); DOI: 10.1111/cge.12332

Barbara Vona was responsible for the microarray analysis and confirmation of deletions, design and analysis of the Sanger sequence assay, and writing the manuscript.

Co-author	Signature
Michaela Hofrichter	
Cordula Neuner	
Jörg Schröder	
Andrea Gehrig	
Julia B. Hennermann	
Fabian Kraus	
Wafaa Shehata-Dieler	
Eva Klopocki	
Indrajit Nanda	
Thomas Haaf	

Vona B, Nanda I, Neuner C, Müller T, Haaf T.

Confirmation of *GRHL2* as the gene for the DFNA28 locus.

Am J Med Genet Part A. 2013 Aug;161A(8):2060-2065.

Barbara Vona was responsible for the targeted deafness NGS panel analysis, sequence confirmation and analysis, design of the cDNA experiment, and writing the manuscript.

Co-author	Signature
Indrajit Nanda	
Cordula Neuner	
Tobias Müller	
Thomas Haaf	

Vona B, Müller T, Nanda I, Neuner C, Hofrichter MAH, Schröder J, Bartsch O, Läßig A, Keilmann A, Schraven S, Kraus F, Shehata-Dieler W, Haaf T.

Targeted deafness gene next generation sequencing of hearing impaired individuals uncovers informative mutations.

Genet Med. 2014 (in press)

Barbara Vona was responsible for the next generation sequencing analysis of all patients and control individuals, design, analysis and performing of the Sanger sequencing assays for mutational confirmation, acquisition and analysis of clinical records, and writing the manuscript.

Co-author	Signature
Tobias Müller	
Indrajit Nanda	
Cordula Neuner	
Michaela Hofrichter	
Jörg Schröder	
Oliver Bartsch	
Anne Läßig	
Annerose Keilmann	
Sebastian Schraven	
Fabian Kraus	
Wafaa Shehata-Dieler	
Thomas Haaf	

Vona B, Müller T, Nanda I, Neuner C, Hofrichter MAH, Schröder J, Bartsch O, Läßig A, Keilmann A, Schraven S, Kraus F, Shehata-Dieler W, Haaf T.

Targeted deafness gene next generation sequencing of hearing impaired individuals uncovers informative mutations.

Genet Med. 2014 (in press)

Barbara Vona was responsible for the next generation sequencing analysis of all patients and control individuals, design, analysis and performing of the Sanger sequencing assays for mutational confirmation, acquisition and analysis of clinical records, and writing the manuscript.

Co-author	Signature
Tobias Müller	
Indrajit Nanda	
Cordula Neuner	
Michaela Hofrichter	
Jörg Schröder	
Oliver Bartsch	
Anne Läßig	
Annerose Keilmann	
Sebastian Schraven	
Fabian Kraus	
Wafaa Shehata-Dieler	
Thomas Haaf	

sch
k
Mainz

Vona B, Müller T, Nanda I, Neuner C, Hofrichter MAH, Schröder J, Bartsch O, Läßig A, Keilmann A, Schraven S, Kraus F, Shehata-Dieler W, Haaf T.

Targeted deafness gene next generation sequencing of hearing impaired individuals uncovers informative mutations.

Genet Med. 2014 (in press)

Barbara Vona was responsible for the next generation sequencing analysis of all patients and control individuals, design, analysis and performing of the Sanger sequencing assays for mutational confirmation, acquisition and analysis of clinical records, and writing the manuscript.

Co-author	Signature
Tobias Müller	
Indrajit Nanda	
Cordula Neuner	
Michaela Hofrichter	
Jörg Schröder	
Oliver Bartsch	
Anne Läßig	
Annerose Keilmann	
Sebastian Schraven	
Fabian Kraus	
Wafaa Shehata-Dieler	
Thomas Haaf	

Vona B, Müller T, Nanda I, Neuner C, Hofrichter MAH, Schröder J, Bartsch O, Läßig A, Keilmann A, Schraven S, Kraus F, Shehata-Dieler W, Haaf T.

Targeted deafness gene next generation sequencing of hearing impaired individuals uncovers informative mutations.

Genet Med. 2014 (in press)

Barbara Vona was responsible for the next generation sequencing analysis of all patients and control individuals, design, analysis and performing of the Sanger sequencing assays for mutational confirmation, acquisition and analysis of clinical records, and writing the manuscript.

Co-author	Signature
Tobias Müller	
Indrajit Nanda	
Cordula Neuner	
Michaela Hofrichter	
Jörg Schröder	
Oliver Bartsch	
Anne Läßig	
Annerose Keilmann	
Sebastian Schraven	
Fabian Kraus	
Wafaa Shehata-Dieler	
Thomas Haaf	

Vona B, Müller T, Nanda I, Neuner C, Hofrichter MAH, Schröder J, Bartsch O, Läßig A, Keilmann A, Schraven S, Kraus F, Shehata-Dieler W, Haaf T.

Targeted deafness gene next generation sequencing of hearing impaired individuals uncovers informative mutations.

Genet Med. 2014 (in press)

Barbara Vona was responsible for the next generation sequencing analysis of all patients and control individuals, design, analysis and performing of the Sanger sequencing assays for mutational confirmation, acquisition and analysis of clinical records, and writing the manuscript.

Co-author	Signature
Tobias Müller	
Indrajit Nanda	
Cordula Neuner	
Michaela Hofrichter	
Jörg Schröder	
Oliver Bartsch	
Anne Läßig	
Annerose Keilmann	
Sebastian Schraven	
Fabian Kraus	
Wafaa Shehata-Dieler	
Thomas Haaf	

17. Acknowledgements

Seldomly have I ever described an experience as profoundly life changing. My time at the Department of Human Genetics has been a life altering milestone and I am unbelievably appreciative for the opportunity to have completed my “Doktorarbeit” here.

There are many people to whom I am indebted and could never express enough thanks for the support over the past years. Firstly, I would like to thank Prof. Thomas Haaf for allowing me to work in his lab on this project and the members of AG Haaf for their tremendous support. I would also like to thank Prof. Manfred Schartl for serving as my “Zweitgutachter” and for the encouragement over the years. Additionally, I would like to express many thanks to Dr. Jörg Schröder, Dr. Erdmute Kunstmann, and Prof. Shehata-Dieler, as well as for the great collaboration from Prof. Oliver Bartsch and Prof. Annerose Keilmann from the University of Mainz for patient recruitment and information. Many thanks to Dr. Simone Rost and Dr. Andrea Gehrig for the assistance with mutation analysis software and mutation questions. I thank the excellent input and mutation interpretation assistance from Dr. Kreß, who always found time to answer my many questions. I especially thank Ruth Walther and Alex Rais for their kindness and assistance.

I would like to thank many talented TAs who have helped me throughout the years. Firstly, I would like to thank Cordula Neuner for her excellent technical work. Without her, this work would have never have developed the way it had. I would also like to thank Jens Gräf and Birgit Halliger-Keller for technical support.

I am fortunate to have worked with an excellent bioinformatics team. Dr. Tobias Müller and Dr. Marcus Dittrich have both been invaluable mentors and a lot of fun to work with.

I would never be able to find the right words to thank Dr. Indrajit Nanda for believing in me throughout the many highs and lows and for taking me under his wing from the first day I began and guiding me until the very end. Thank you to Michaela Hofrichter, my partner-in-crime, for the excellent teamwork, putting up with my Denglisch and having the same sense of humour that I do. Thanks to Prof. Eva Klopocki for being an enduring source of support.

This work would never have been possible without the altruism of the patients who engaged in this study. To the many families who have participated, I extend my greatest thanks and appreciation.

Finally, I thank my closest friends and family for being an unwavering support system and providing continuous encouragement to follow my dreams no matter where they end up taking me. I especially thank my parents for believing in me and teaching me that there are no shortcuts to any place worth going.

You have brains in your head.

You have feet in your shoes.

You can steer yourself in any direction you choose.

You're on your own.

And you know what you know.

You are the guy who'll decide where to go.

--Dr. Seuss